

The Design and Fabrication of a Biomimetic Lifting Aid

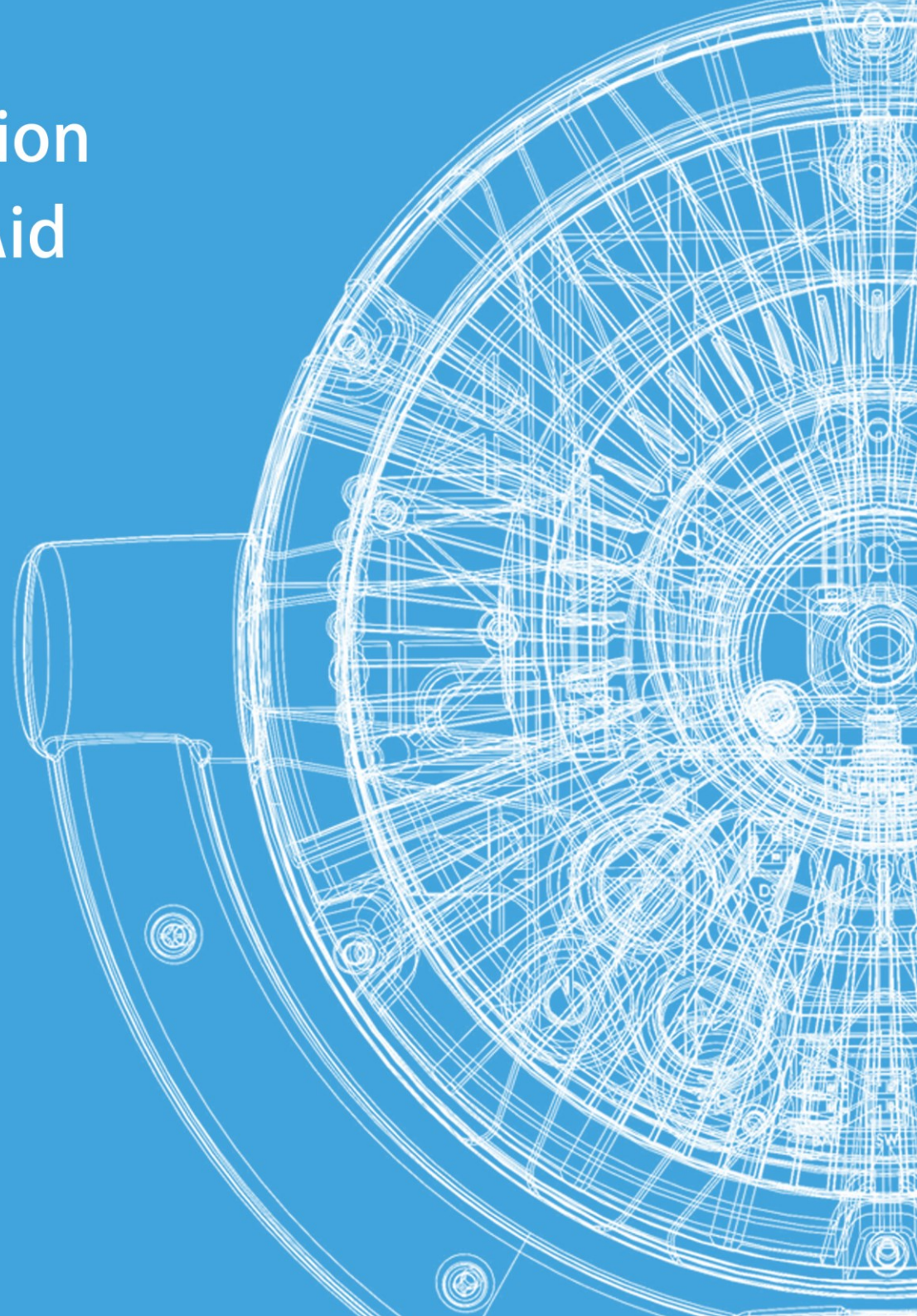
by Tjitte de Wolff

A master's thesis presented to the faculty of
Engineering Technology

in partial fulfilment of
the requirements for the degree of
Industrial Design Engineer

at the
University of Twente

Enschede, January 2017



The design and fabrication of a biomimetic lifting aid

Publication date: 27 January

Name: Tjitte de Wolff

Student number: s1127640

Master: Industrial Design Engineering

Master track: Emerging Technology Design

Specialization: Product and surfaces

Tutors: M.B. de Rooij, E. van der Heide

Supervisor: J.A. Garde

Contact: University of Twente

Faculty of Engineering Technology

Building de Horst, number 20

PO Box 217

7500 AE Enschede

The Netherlands

tel: +31 53 4892547

Abstract

The report that lies in front of you shows the development and fabrication of a lifting aid based on natural suction adhesion systems. The deeper laying goal for this undertaking is to find a way to translate information that is available regarding biological systems into an innovative product that is both usable and compatible with nature. It is felt that such a method is deeply necessary to reduce the gap between the technological and biological world. Technology should improve the stability of the environment instead of destroying it by becoming more efficient and by using better materials.

To obtain the information upon which the lifting aid is based 16 species that use suction adhesion are analysed. By comparing the characteristics of their suckers a number of patterns can be observed. Since the species have evolved independent from each other it is likely that these strategies have a positive impact on the functioning of their suction organ. In total there are 12 suction adhesion strategies, of which a conforming sealing rim and an inherent resistance against shear force seem to be the most important.

To find a suitable application for the knowledge gained in the literature study, the strategies are compared to solutions found in science, industry and the consumer market. From the comparison can be derived that scientists that have attempted to develop a bio-inspired sucker, did not fare well. Their suction cups lack the characterizing traits found in natural suction adhesion systems and have a disappointing level of performance. Industrial suction adhesion systems on the other hand follow the suction adhesion strategies much more closely. This is possibly the result from trying to attain the same goals, which are efficiency, reliability and suitability. The significant developments made in the industrial sector however have not been translated to the consumer market. It could be that this is due to the low cost applications for which suction cups are used nowadays. Because of this reason a new application has been devised. A powertool-like device with a suction cup helps people to lift difficult items outside of the industrial setting. In these circumstances the bulky and energy intensive solutions found in the industry cannot be used. The device is aimed at the prosumer market and it intended to provide a helping handle for people working in the furniture moving business.

Three concepts which are created to fulfil this same application are a hand powered suction handle, an automatic handle that can be used with a lifting harness and a lifting trolley that uses suction cups instead of securing straps. After rating, the concepts based on keydrivers for the application it has been decided to further develop the harness concept.

The first step in developing the suction adhesion device has been the design of a suction cup that can meet the requirements. Finite element analyses in combination with an assembled set of equations and online tools predict that the suction cup should be able to attach itself to very rough substrates and generate a pulling resistance of around 1250 N on glass. Next the final concept is supplemented by a vision of the rest of the powertool is and the functionality of the device is further discussed. In addition a framework is sketched to produce the suction adhesion device in a circular way. This is felt necessary in order to fulfil the deeper lying goal of making technological and biological systems more compatible.

In the final design the predictions of the theoretical model are put to the test by making a prototype version of the suction cup. This prototype is able to perform the most basic functions of the envisioned device. Valuable information is subsequently gathered by reading out a vacuum sensor and by pulling the suction cup with a tensile strength tester from a set of substrates. The results show that the suction cup generates more adhesion than estimated (1291 N) but a lot less friction (617 N). This discrepancy is likely due to flaws in the production process and it is expected that difference between these values reduces as the suction cup wears in. On rougher substrates the performance of the suction cup remains relatively stable as long as good seal can be achieved. In general it can be stated that friction increases on rougher substrates, while the amount of adhesion decreases. The Achilles heel of the sealing rim seems to be on substrates with a roughness of around 10-20 μm .

Based on the performance shown by the prototype it can be concluded that the developed technology has a lot of potential. However more work is required to simplify the design and to create a more durable sealing rim. Also use tests will be necessary in order to determine how the user interacts with this type of device.

Introduction

Some technology philosophers, like Kevin Kelly, state that humankind is so strongly interwoven with technology that our species cannot exist without it (“Kevin Kelly: Technology’s”, 2009). After all, most modern people would not be able to survive in the wild when robbed of their technological aides. Even survival experts resort to the use of knives, spears and fire making equipment in order to stay alive. You could thus imagine technology as a twig on the tree of life that emerges from the human branch and that interacts with us all the time.

With the help from technology humans have become the most dominant force on the planet. This has allowed for a large increase in the world’s population and has given rise to many great societies. However in the last century it seems as though a gap has emerged between the technological and the natural world. Some twigs on the technological branch are becoming toxic for the rest of the tree and have started to eat into the shared pool of resources that this planet offers. Clean water fresh air and fertile soil have become a scarce commodity.

Since technology originates from the human mind, it is our duty to trim these toxic twigs down or to improve them in such a way that they live in better harmony with the planet. To find the rotten parts and to be able to see how they need to be improved it is important to understand the differences between natural and technological systems. These differences lie at the root of the problems but some may also contribute to solving them. As can be seen in Table 1, almost all differences can be considered in favour of natural systems. They are better in tune with their environment, require low amounts of energy to function and use abundantly available materials.

The last difference listed however may be the key to bring natural and technological systems closer together. Whereas nature has taken billions of years to evolve into the beautiful and diverse system we see today, technology is able to develop much faster. This is because nature uses a trial and error method to come up with new solutions and lets the environment judge which of those solutions is good enough for the next generation. Depending on the harshness of the environment species can remain unchanged for millions of years or take evolutionary leaps. Survival of the fittest can therefore better be phrased as survival of the fit enough.

Technology on the other hand is subjected to the judgement of human consciousness. The ability to reflect upon our creations and to make new designs based on the lessons learned from previous generations, causes technology to improve exponentially. This exponential growth of performance was first demonstrated by Moore, who has become famous for his prediction that the amount of transistors on a chip doubles every two years. In addition to Moore’s law also other technologies have shown exponential performance growth, like for example magnetic data storage, genetic sequencing, the internet and nano-manufacturing (“The accelerating power”, 2007).

It is believed by the author that using the power of exponential performance increase, technology can close the gap with nature. However this requires a new approach towards design. In addition to including goals regarding sustainability during the design process, more lessons should be taken from the methods used by nature. This is because natural systems have lived in harmony with each other for billions of years.

Natural systems	Technological system
Adapt to the environment	Generalized solutions
Complex interactions across many scientific disciplines	Repeated interactions based on basic principles
Low energy intensity	High energy intensity
Low amount of scarce materials	High amount of scarce materials
Bio-degradable and re-usable	Non-degradable and single use
Self-maintaining and self-healing	Subjective to wear and dependable on maintenance
Increase environmental stability	Negative impact on environmental stability
Slow performance increase due to evolution	Exponential performance increase

Table 1 - Differences between natural and technological systems.

Introduction



Figure 1 - The Northern Clingfish lifting a rock.

Extracting the knowledge from these systems means taking advantage of the free research and development that is embedded in them and can be used to design new products that are better in tune with the planet.

The goal of this thesis is therefore to analyse some of the solutions offered by nature and develop an innovative biomimetic product. The process that is used to create this design can then be boiled down into a design approach that can be applied to design other biomimetic products.

The choice for developing a suction adhesion system was made after stumbling upon an article published on Wired.com, a popular online magazine. The article showed the amazing capabilities of the Northern clingfish. This fish was shown lifting a large encrusted boulder even though it was no longer alive. It is believed that the efficiency and versatility displayed by this biological sucker cannot yet be found in any technological system. Another reason to focus on natural suction adhesion systems is that, unlike other bio-inspired tribological topics such as self-cleaning surfaces and gecko-inspired adhesion, suction adhesion seems to have been somewhat overlooked. This is probably due to the fact that most creatures that use this strategy are tucked away beneath the surface of the sea. They are thus harder to study in a laboratory.

The effort needed to bring the knowledge behind biological suckers to the surface is furthermore justified since it can expand the capabilities of reversible adhesion systems. This type of adhesive is able to attach to a surface, transmit forces across the interface and detach without leaving any scars on the object. Improving the capabilities of this branch of technology can give rise to new types of flexible mounting systems, ergonomic lifting devices, robotic grasping tools and climbing gear.

To add structure to the thesis a number of research questions have been postulated. These questions coincide with the chapters in this report.

1. *For what purpose do organisms use suction adhesion and how do these suction solutions work?*
2. *How does suction adhesion found in nature compare to existing suction adhesion systems?*
3. *What innovative application can be derived from the comparison and what requirements need to be fulfilled?*
4. *What design can fulfil the application and fits the requirements?*
5. *How does a prototype of the design perform and how can the differences with the predicted performance be explained?*
6. *Is the created design a viable solution for the selected application?*

The work done to answer these questions, in turn provide an answer for the main research question.

How can information regarding biological suction adhesion be leveraged to design a useful biomimetic product?

To make it easy to find the important sections in this extensive report a system has been adopted to highlight the most relevant information. This is done by varying the colour of the chapter number that is present on the top of each page. A dark grey square means that the information provided on that page is very relevant to the report, while a light grey box indicates less relevant information. It was chosen not to leave these sections out since they contain the building blocks upon which more important chapters rely. It is also felt that leaving out certain sections harms the structure of the report and therefore the coherency of the biomimetic design approach.

- Relevant information
- Less relevant information

Content

Abstract	3	4.1 Keydrivers	43	Appendix B: Consumer market solutions	146
Introduction	4	4.2 System behaviour	44	Appendix C: Market research	149
1. Suction adhesion in nature	7	4.3 Concept generation	46	Appendix D: Use environment analysis	151
1.1 Clingfish	8	4.4 Concept selection	57	Appendix E: Pressure differential curves	156
1.2 Abalone	12	4.5 Suction cup design	57	Appendix F: Pressure drop calculator	163
1.3 Garra	15	4.6 System architecture	95	Appendix G: Suction cup design parameters	164
1.4 Octopus	20	4.7 Design embodiment	97	Appendix H: Cost and weight estimation	166
1.5 Conclusion	23	4.8 Use and interface design	104	Appendix I: Prototype components	169
2. Existing suction adhesion solutions	30	4.9 Conclusion	108	Appendix J: Wiring diagram	170
2.1 Existing solutions in literature	31	5. Prototype design and performance testing	109	Appendix K: Prototype suction cup	171
2.2 Conclusion	35	5.1 Prototype design	110	Appendix L: Prototype suction cup	172
3. Application and requirements	36	5.2 Prototype fabrication	114	Appendix M: Prototype suction cup	175
3.1 Stakeholders	38	5.3 Performance testing	120	References	177
3.2 Ergonomics	39	5.4 Conclusion	131		
3.3 Conclusion	40	6.0 Requirements check and final conclusion	132		
4. Conceptual design and design embodiment	42	Appendix A: Industrial suction solutions	139		

Suction adhesion in nature

This chapter contains an investigation of various examples of suction adhesion found in nature. The species that are discussed have been selected based on the uniqueness of their sucker and the availability of credible scientific work that explains their functioning. The goal of the analysis is to find the strategies that are used by these organisms to increase the performance of their suction organs. Care has been taken to make the analysis an inspiration source that is accessible for engineers and designers and that can be understood without any background in biology. To achieve this, common names and layman's terms will be used to translate the information found in literature to a format that is easier to understand.

The choice to analyse multiple species was made for a number of reasons. First of all it allows the formation of a detailed mental image about the structure and functioning of suction adhesion systems found in nature. This is not possible by analysing just one species, as in many cases there are holes in the knowledge provided by literature. By looking at more than one species these holes can be filled by carefully combining the pieces of information with each other.

The second reason is that the adhesion strategies used by each species can be compared with others. This allows an estimation of the benefits provided by each strategy by looking at the performance of the suckers and the occurrence of the same strategy in other species. Such a comparison can sift out strategies that may seem significant at first, but do not actually provide any real benefits. These features could for example be vestigial remnants that have lost their functionality. On the other hand the occurrence of similar features in unrelated species can highlight strategies that have a positive impact on adhesion. These instances of convergent or parallel evolution decrease the chance that the features are just a fluke of evolution.

The final reason for opting for a broad analysis is its scientific relevance. There are multiple examples of researchers that have analysed suction adhesion in one species and that have created a biomimetic suction cup based on these

findings. Tramacere et al. (2014) designed a suction cup based on the octopus sucker, Feng et al. (2014) translated the sucker of a leech into an artificial suction cup and the same conversion was done for the squid (Hou et al., 2012) and the remora (Rutkowski, 2014). However neither of these designs, except the system based on the remora, seems to have succeeded in fulfilling a practical application. This might be due to their sole focus on only one species, as it restricts the freedom of the design. Some biological features like muscles and intricate microstructures also do not translate well into technical solutions. Copying them without paying attention to these restrictions can result in sucker designs with sub-optimal performance. The use of an analysis based upon suction systems from multiple species should be able to circumvent this problem, as it allows for a larger choice between adhesion strategies in the design phase. Strategies from different organisms that translate well into technical solutions can then be combined to create a viable high performance suction cup design.

In the following sections 4 natural suckers are analysed. These are only a selection of the 16 species that have been investigated. Although each sucker has provided useful information, the four species in this printed version of the report are considered the most relevant for the final design. The remaining analyses performed for the other biological suction adhesion can be found in the digital version of this report. Each section contains information about the habits of the organism that has led to the formation of the sucker. In addition a review of the most important anatomical features of the suction organ is included and when available an oversight of its performance characteristics is provided. It was chosen to list the maximum values of each parameter as they are the ones most frequently mentioned in literature. It should be noted that these maximum values do not correspond with one specimen. In many cases the largest animals do not create the highest tenacities for example.

Clingfish

Clingfishes (Gobiesocidae) are a family of fishes that is frequently seen in tropical and warm waters in the Atlantic, Pacific and Indian Ocean. A distinguishing feature of the family is its abdominal suction organ, which consists of multiple chambers that are loosely interconnected. A typical example of the suction disc possessed by clingfish can be found on the Northern Clingfish (*Gobiesox maeandricus*). This is a small fish that lives in the coastal waters of the eastern shorelines of America. Millions of years of evolution have given the fish a peculiar structure on the bottom of its stomach. In this spot its pelvic fins and part of the pectoral fins have merged to create a suction disc (Wainwright et al., 2013). The fish utilizes a muscular structure around the disc to create a low pressure area which presses its belly against the sea floor. This allows the fish to pin itself to a rock and prevent it from being swept away amidst the crashing waves. Once the tides have receded the Clingfish scours the tide pools that are left behind for limpets, peeling them from the rocks with its suction disc (Ditsche et al., 2014).

This predator-prey relationship has contributed to the development of a suction disc that differs in a number of ways from other pelvic suckers. The suction disc of the clingfish is for example much more flexible (Arita, 1967) and consists out of two suction chambers instead of one (Figure 2) (Gibson 1969). The round and grooved surface topography of the limpet shell could be one of the reasons behind these modifications.

The high amount of flexibility of the suction organ of the Northern Clingfish can be explained by looking at the anatomy that lies behind it. The study of Arita (1967) contains a treasure trove worth of information about this aspect of the clingfish sucker. The frontal area of the suction cup is supported by two triangular bones that form the pelvis (Figure 5). These are joined in the middle by sturdy



Figure 3 - A Northern clingfish and its prey (Ditsche, 2015).



Figure 2 - The anterior and posterior suction chambers of the Northern Clingfish divided by a sideways cleft (Porter, 2015).

connective tissue. Towards the sides, the pelvis is surrounded by a pair of Y-shaped pelvic spines and 4 pairs of rays. These rays are less ossified than the rays of the lumpsucker (see digital version) and become cartilaginous towards the end. Another aspect that increases their flexibility is that the rays branch into two paired halves called lepidotrichs, which are fused at their end by collagenous tissue. This segmentation is a feature that can be found in the rays in most bony fish and seems to have been retained in the suction organ of the Northern clingfish. The reason for this, in addition to the increase of flexibility, is that the paired rays in combination with their associated musculature can be used to actively control the functions of the suction cup. The skeletal structure of the clingfish sucker is completed by two pair of bones that support the rear portion of the suction cup. These are called the distal postcleithrum and the proximal postcleithrum (Arita, 1967).



Figure 4 - Suction disc of the Northern clingfish (Ma, 2015)

Clingfish

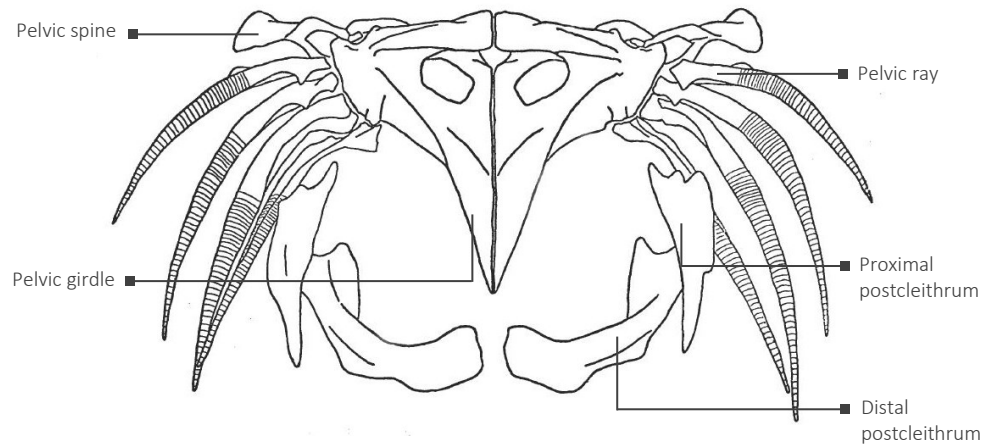


Figure 5 - Skeletal structure from the sucker of the Northern clingfish (Arita, 1967).

As the skeleton of the Northern Clingfish is not set up to be very sturdy it requires multiple layers of muscles in order for the fish to be able to control it and to give it structural coherency. These layers have been peeled off by Arita (1969) which has revealed how they do their job. In a similar way as the lumpsucker the clingfish has a set of counteracting muscles for each movement of the suction cup. This means that the pelvis, rays, spines and cleithra are moved with respect towards each other by a set of adductor and abductor muscles. To explain the function of these muscles the sequence of actions performed by the Northern clingfish to attach and detach is discussed.

To attach the suction cup the fish first needs to make sure that the cleft that separates the two halves of the suction disc is closed. This is achieved by contracting the adductor muscles of the fourth ray which is connected to the postcleithrum (adductor I of postcleithrum). In contrast to the other rays the fourth ray is rotated 90 degrees with respect to the pelvic girdle. This means that when one the two lepidotrichs is abducted

towards the postcleithrum the whole ray will bend towards the rear. The reason for this modification lies in the fact that the fourth ray is connected to a flap that is part of the pectoral fin. By rotating the fourth fin towards the cup, the flap is pushed against the cleft and consequently the suction cup is sealed. This part of the attachment sequence has been proven to be crucial for the functioning of the clingfish sucker. Specimens in which the rays of the pectoral fins were removed lost their ability to adhere to a substrate (Arita, 1967).

Other actions undertaken by the clingfish to prepare its sucker are the contraction of the arrector dorsal and ventralis. These muscles spread the pelvic spine together with the first two rays, and push them against the substrate. Simultaneously other abductor muscles also bend the second and third rays downward. Observations of the behaviour of the clingfish in combination with adhesion measurements performed with dead animals indicate that the fish is able to generate most of its adhesion in a passive way. The fish for example almost never leaves the substrate, which means that it needs a very energy efficient adhesion mechanism. It also has been shown that dead animals retain almost 96% of its suction capabilities (Arita, 1967). It is theorized that this high percentage of passive suction is due to the flexibility and the structure of the rays. By bending them downward they store energy in the same way as a bow and arrow. When the pressure caused by the contraction of the abductor muscle is released, the energy stored in the rays is converted into negative pressure underneath the suction cup.

To detach itself the clingfish equalizes the internal pressure with its surrounding by pushing the pectoral flap away from the body using the extensor proprius muscle. This allows water to flow back into the suction chamber through the sideways clefts. The fish is then able to use its adductor muscles to peel the rim of the substrate. The amazing thing about the clingfish suction disc is that it seems to adhere better to rough surfaces than to very smooth ones. This ability of clinging onto to rough surfaces increases with the size of the fish. The largest analyzed specimens of about 12 cm are able to stick themselves to a surface with a grain size of 2-4 mm. A general rule presented in a study by Ditsche et al. (2014) is that the suction cup can adhere to surfaces with a grid size that is 2-9% of the width of the suction cup. According to them

Clingfish

the ability of the fish to adhere to rough surfaces is caused by four hierarchical mechanisms. On the macro scale the clingfish uses the flexibility of the suction disc rim to conform to larger surface irregularities. To adjust to smaller features in the range of a few 100 μm the rim contains numerous papillae which each make contact with the substrate (Figure 4 and Figure 8). When zooming in on the papillae the third hierarchical mechanism becomes visible. Hundreds of small hairs on every papilla make contact with surface features of a few micrometers in size. The seal is perfected by microscopic rods at the end of each hair, which are able to conform to asperities that are a few 100 nm in diameter. Such a hierarchical structure is quite similar to the one found on the adhesive pads of gecko's and serves to maximize the contact area between the adhesive surface and the substrate. It is still under discussion whether the

clingfish uses the same weak intermolecular forces as the gecko to generate adhesion (Wainwright et al., 2013 and Elizabeth Pennisi, 2012). However it is clear that the microstructure helps to generate extra friction that prevents the rim from slipping inward when a detachment force is applied.

Another impressive feat of suction that originates from the edges of the suction disc of the clingfish is that it is able to adhere to fouled and algae covered rocks. This means that the suction cup has to make a seal on a heterogeneous and slippery biofilm that acts as a lubricant. Despite a decrease of about 35% in adhesion strength, the clingfish is still able to carry 150 times its own bodyweight on these challenging substrates (Ditsche et al., 2014).

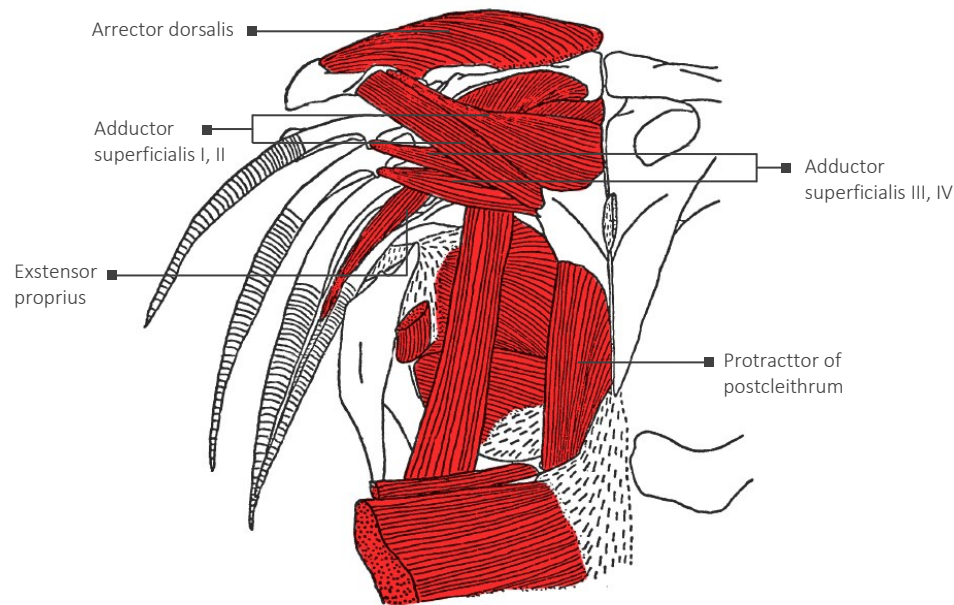


Figure 6 - Topview of the musculature of the suction disc of the Northern clingfish (Arita, 1967)

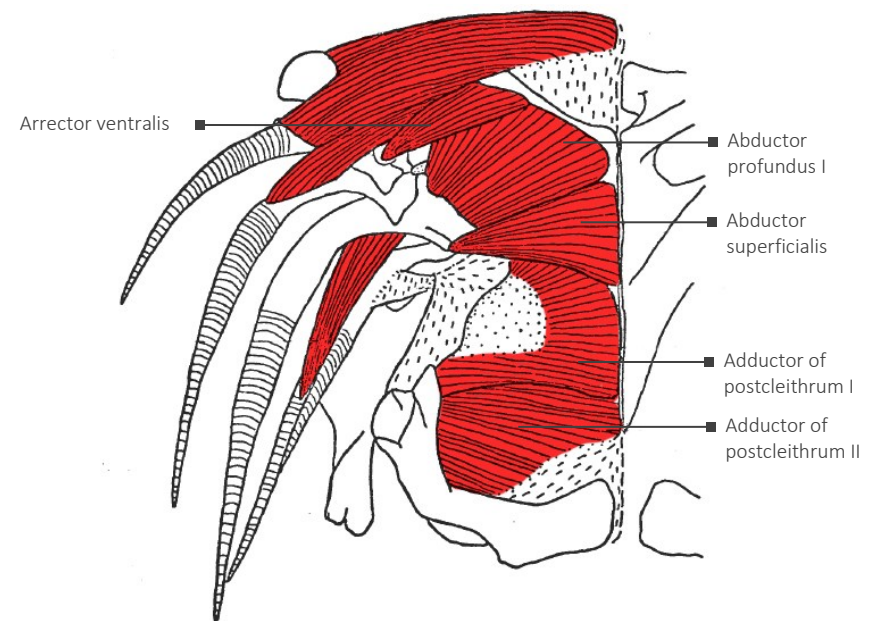


Figure 7 - Bottom view of the musculature of the suction disc of the Northern clingfish (Arita, 1967)

Clingfish



Image source: Murch, n.d.

The performance characteristics of the sucker of the Northern Clingfish (*Gobysox maeandricus*) have been abstracted from the study of Arita (1967). Due to the flexible nature of its suction disc the clingfish cannot create the same tenacities as seen in lumpfish (see digital report version). However the species still manages to generate a respectable 4.5 N/cm^2 . A figure that stands out is the large amount of negative pressure recorded underneath the sucker of the clingfish. According to Arita these high values are due to the flexibility of the disc that allows it to bulge upwards. This results in a pressure spike just before detachment.

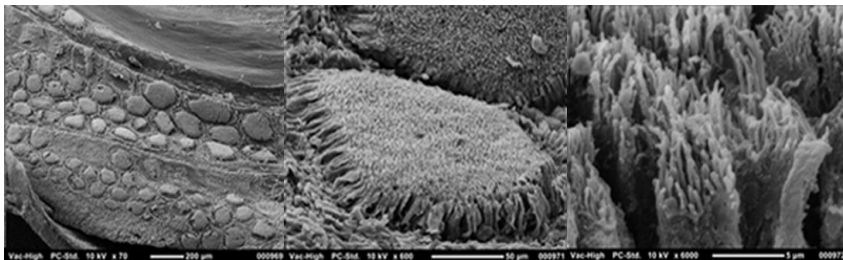


Figure 8 - SEM images of the papillae of the Northern clingfish (Tiethbohl, 2014).

<i>Gobysox maeandricus</i>	
Max. length (cm)	10.2
Max. weight (g)	?
Max. sucker size (cm^2)	8.2
Max. ΔP (kPa)	91
Max. tenacity (N/cm^2)	4.5
Max. force (N)	33

Abalone

Abalone is a common name for a family of sea snails known by its scientific name Haliotidae. This group of species has been an important source of income for fisherman since prehistoric times. Their meat is considered a delicacy and the beautiful pearlescent inside of their shells is used for all kinds of jewellery (Cox, 1962). A feature that has not aroused much interest over the years, but that could still prove to be valuable in the future, is the sticky underside of the abalone. The species in the abalone family use this part of their body to fix themselves to the rocky bottom of their habitat when they are threatened by predators, or when the currents try to wash them ashore. If there is no apparent danger, the abalone uses a sit-and-wait strategy to catch algae with its large shell (Donovan and Tailor, 2008). However when it becomes necessary for the abalone to reposition itself it uses wave-like contractions of its underside to move about.

The adhesion organ of the abalone works in the same basic way as the limpet's suction cup (see digital version). The epidermis secretes slightly adhesive mucus that in combination with suction provides the necessary adhesion force to stay attached. The amount of adhesion is controlled by contractions of a large columellar muscle (Figure 9) that connects the shell with the epidermis (Donovan and Tailor, 2008). Adducting the centre of the epidermis causes a pressure differential that pushes the abalone hard against the sea floor.

Figure 9 - Dorsal view of an abalone with its shell removed (Tailor, 2008).

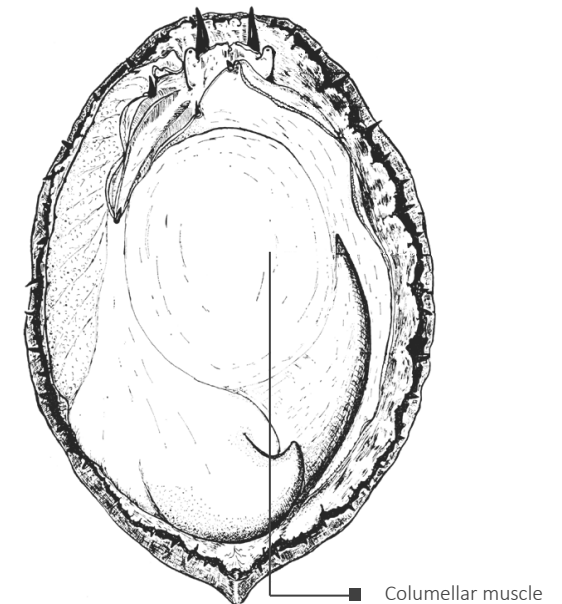




Figure 10 - Frontal view of the South African abalone ("THINGS WE LIKE", 2014).

Abalone

One of the features that emerges from literature and that makes the abalone sucker different from the limpet suction cup is described by Lin et al. (2009). Scanning Electron Microscope images made from the wrinkled surface of the suction organ of the red abalone (*Haliotis rufescens*) show that it is covered with an intricate microstructure (Figure 12) that is very reminiscent of the features on the papillae of the clingfish. The millions of hairs that grow on the surface have two hierarchical levels. The bottom part of the texture is constructed out of 2 μm wide fibres that are about 100 μm long. These branch out into dozens of smaller hairs that are approximately 200 nm in diameter. The fact that similar microstructures have appeared on the suction organs of two unrelated aquatic species suggests that they provide them with a large evolutionary benefit. It is therefore very unlikely that these textures are a fluke of evolution.

The resemblance of the two aquatic microstructures with the hairs on the sole of the gecko once again comes to mind as well as the question whether it is possible that the textures on aquatic suction cups utilize van der Waals forces to generate adhesion. Although a number of scientists believe that so-called dry adhesion cannot occur in wet environments (Wainwright et al., 2013 and Tracamere et al., 2014) direct evidence for the opposite comes from the study from Lin et al. (2009). In addition to the demonstration of the adhesive capabilities of the abalone seen in Figure 11, they also performed force measurements on a single hair taken from its micro structure. By varying the humidity and by testing on both hydrophilic and hydrophobic surfaces they worked out whether the hair is able to generate dry adhesion and how large the contribution of capillary adhesion is.

Using the cantilever on an Atomic Force Microscope they measured a pull off force of 558 nN in high humidity in combination with a hydrophilic substrate and 294 nN on hydrophobic surfaces. This means that about half of the force measured in hydrophilic conditions is due to capillary adhesion and the other half is the result of dry adhesion. The study also shows that a single microfiber can generate a pull-off force of about 5 nN in hydrophobic conditions. This number lies in the same ballpark as the spatula from the gecko microstructure. Work done by Huber et al. (2005), shows that these features with a similar size can produce 11 nN worth of dry adhesion. The difference in adhesion

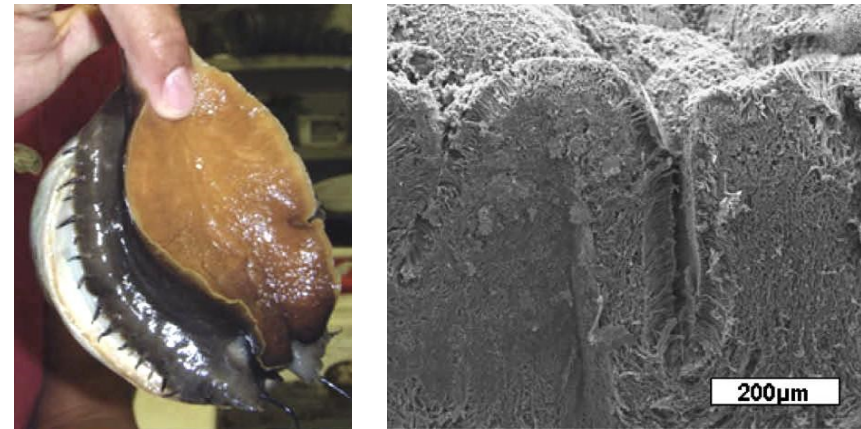


Figure 11 - Left: abalone sticking to a finger. Right: Folds that allow wave-like locomotion (Lin et al., 2009).

strength is probably due to the difference in the shape of the tip of both features. The flattened end of the spatula has a larger area of contact than the rounded ends of the microfibers found on abalone (Figure 12). However when taking the density of the microstructure into account it is well possible that abalones can generate more dry adhesion than geckos. When it is assumed that the observed 25 active microfibers per μm^2 (Lin et al., 2009) is true for the entire contact area the abalone is theoretically able to create a 12.5N of dry adhesion for each square centimetre. This is more than the 9.1N observed in for example the Tokay Gecko (Irschick et al., 1996).

Because the abalone also has to use some of its adhesion area to create suction, the theoretical tenacity due to dry adhesion is not reached under normal circumstances. Lin et al. (2009) determined that the mean tenacity of *Haliotis rufescens* (red abalone) is about 11.5 N/cm².

Abalone



Haliotis rufescens	
Max. length (cm)	?
Max. weight (g)	?
Max. sucker size (cm ²)*	55
Max. ΔP (kPa)**	115
Max. tenacity (N/cm ²)*	11.5
Max. force (N)***	633

* Average sucker size and tenacity.
 ** Assuming that all adhesion is caused by suction and 100% efficient use of sucker surface.
 *** Based on sucker size and tenacity.
 Image source: Weisburger, 2016

Unfortunately they did not make any pressure measurements which could have shed light on how much the microstructure contributes directly to the adhesion of the total system. However as the mean tenacity is higher than the theoretical maximum pressure differential, the abalone has to be able to create pressures below 0 Pa or use its microstructure to create the additional adhesion.

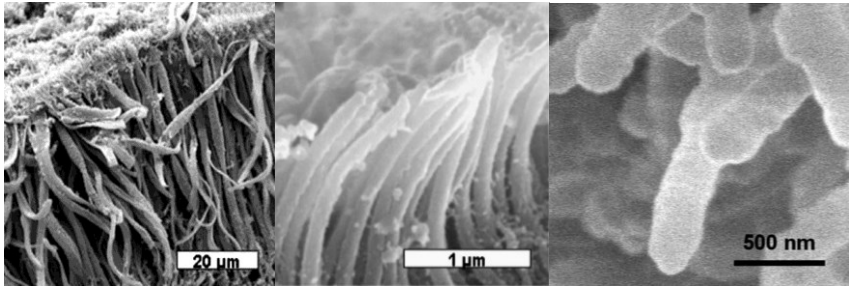


Figure 12 - SEM images of the microstructure of Haliotis rufescens (Lin et al., 2009).

Garra

Every summer thousands of tourists pamper their feet by putting them in an aquarium that contains a dedicated team of doctor fish. These fin-rayed fish belonging to the genus Garra feast on dead skin cells by scraping them off with their oral sucker (Figure 15). Supposedly this alleviates the symptoms of skin diseases like psoriasis (Grassberger and Hoch, 2007) although no conclusive evidence exists that this treatment can cure any of them.

The reason that doctor fish have become such a tourist attraction is the suction organ that is formed by adhesive pads surrounding their mouth. A feature that can be found on most species of Garra, performs best in fishes that inhabit fast flowing mountain streams. The anatomy of the sucker from Garra mullya that lives in the torrential streams of India and Nepal has been described by Saxena (1959) and gives a good understanding of the basic mechanisms of the Garra sucker.

The oral sucker is formed by heavy tuberculated lips which encircle the ventrally positioned mouth (Figure 14 and Figure 13). The lips are able to protrude and retract to attach to the surface and connect with each other in the corners where the front lip is thickened. A thin groove separates the rear lip from the suction disc, which is bordered by another tuberculated region.

At first sight it seems that the suction disc is controlled by the respiratory system in the same way as the tadpole (see digital version).

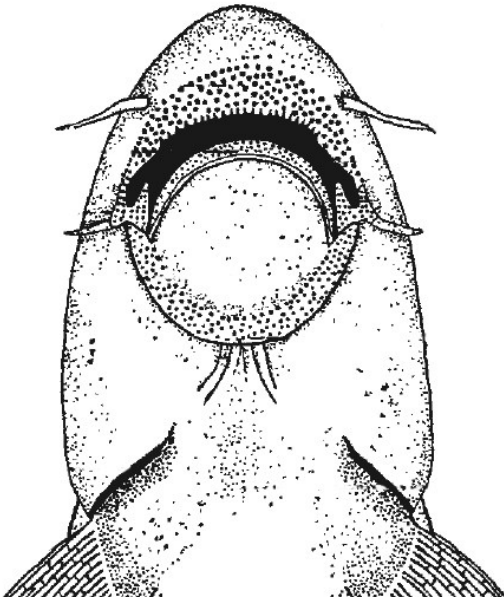


Figure 13 - External morphology of the oral area of Garra mullya (Saxena, 1959).



Figure 14 - Underside of the panda garra (*Garra flavatra*) ("Panda Garra").

Garra



Figure 15 - Docter fish (*Garra ruffa*) giving a pedicure (Hamid, 2007).

However Saxena (1959) reports that the respiratory system of *Garra mullya* is unable to create any long lasting suction as the mouth forms the single aperture through which water can flow towards the gills. This means that the only possible contribution of the mouth to suction adhesion is temporary at best and requires the garra to hold its breath. It also explains why the suction disc is sealed off by the rear lip from the mouth area.

The main source of sustainable suction is created by a set of muscles that is connected to the hardened centre of the suction disc and pulls it towards the tongue bone. A seal is formed around the disc using a combination of tubercles with mucus from a large array of mucus glands. Because the rear half of the disc is separated from the body it is unlikely that the garra can generate pressure differentials that come close to some of the stronger suckers discussed in previous chapters. A lack of mechanisms for creating

passive suction also indicates that pressures beneath the disc will not be significantly below the ambient pressure, as this would have a high metabolic cost.

Despite the high chance that the *Garra* is not creating any interesting amounts of pressure differences, most species of the genus do have a curious and well-documented microstructure on their lips. Images made using a Scanning Electron Microscope by Massar (2015) show numerous tubercles that are each covered by 12 to 16 horny spines (Figure 16). These protrusions help the *Garra* to scrape of algae from rocks but also provide resistance against shear forces as they interlock with the substrate. The study by Saxena (1959) contains a comprehensive analysis of the underlying tissue of the tubercles, which sheds more light on how these kinds of microstructures are created and how they function. A good overview of the morphology of the cell types involved in the mouth and suction disc area can be seen in Figure 17. It shows the three tuberculated regions and the arrangement of the supporting cell layers. When zooming in a row of tubercles on the posterior lip, the structure of Figure 18 emerges. In this image two types of

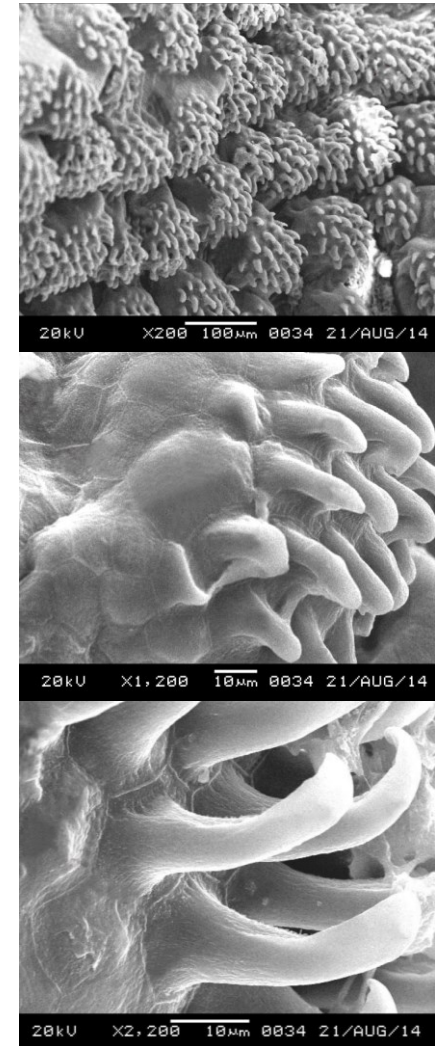


Figure 16 - Horny spines on the tubercles of *Garra lissorhynchus* (Massar, 2015).

Garra

tubercles can be seen. One type of tubercles bears spikes while the other is bald and contains mucus and sensory cells. The second type of tubercles is more prominent in young specimens, which suggests that the amount of grip Garras require increases during growth.

The top layer of the tubercles consists of stratum corneum, which forms knobs on the surface of the skin. These outer cells have morphed into pointy spikes that are fully solidified and do not contain a cell nucleus anymore. During use the spikes wear and sometimes break off. Therefore they constantly need to be replaced to maintain the functionality of the microstructure. The replacement cells are sourced from the underlying epithelial cells. One of these layers forms the core of the tubercles. This cell type consists of large polygonal cells with big nuclei that solidify when a spike breaks off. To reinvigorate the upper layers of the dermis a number of rows of stratum basale underneath the tubercles act as stem cells, by slowly developing into stratum corneum or core cells.



Figure 17 - Longitudinal cross-section of the oral area of *Garra mullia* (Saxena, 1959).

Layers of flattened cells called the stratum compactum connect the epidermis with deeper laying tissue. These deeper layers of tissue provide support by means of a sturdy structure consisting out of compact connective tissue cells, which are knit together by collagen fibres (Saxena, 1959). The collagen fibres do not stay bounded to this layer but also travel deeper into the body where they probably secure the suction rim to the fish's skeleton. However they could also be used to store energy passively. In order to give back some flexibility to the rim the tough backing sits upon a number of layers of fatcells. These allow the top layers of the skin to move slightly to conform to the surface.

No sucker performance characteristics for the *Garra* genus could be found in literature. However as stated before it is unlikely that they perform anywhere near as good as the suckers of lumpfish or limpets (see digital version). The main function of the adhesive disc of *Garra* fish therefore seems to be to provide resistance against shear forces due to mountain stream currents.

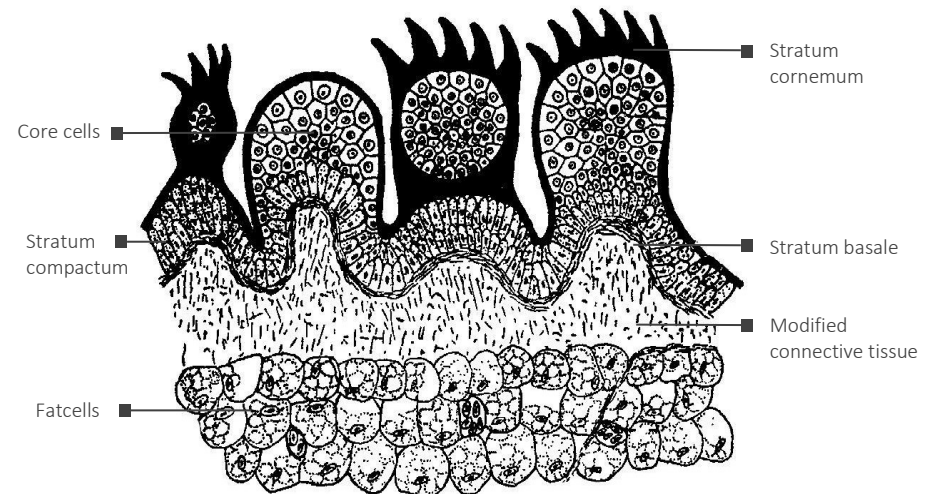


Figure 18 - Transverse section of the tubercles of anterior lip (Saxena, 1959).



Figure 19 - Close-up of octopus suckers (species unknown) (Chong, 2013).

Octopus

The suction cups on the arms of an octopus (Octopoda) are by many considered the archetype for natural suckers. This is probably because of their well-defined cup shape, their high performance and the way they are used by the octopus. Many divers have experienced firsthand how difficult it can be to remove an arm from a curious octopus once its suckers have gripped onto their diving gear. Normally an octopus uses this firm grip to reel in prey so that it can inject it with paralyzing venom coming from its mouth. This ruthless way of hunting has been a source of inspiration for a number of legendary sea creatures like the kraken and Akkorokamui, which are usually depicted as giant ship devouring octopuses.

Also during locomotion the octopus makes good use of its sucker arms. Its soft and pliable body allows it to pull itself through small nooks and crannies by attaching its arms to the substrate. This gives it an edge over predators as they have to abort their chase. In combination with other inventive defense strategies like camouflaging, mimicry and the use of ink sacs the octopus can prove to be quite a challenge to catch (Klappenbach, 2015). This is probably one of the reasons for their success, as the Octopoda order consists of more than 300 species that can be found in most parts of the ocean.

The interesting behavior displayed by octopus species and their suction cup archetype status has led to a large number of scientific studies that include detailed descriptions about the structure and biomechanics of the octopus sucker. A stepwise reconstruction of the attachment and detachment cycle has been made by abstracting information from work by Tracamere et al. (2015) and Kier and Smith (2002). The proposed attachment detachment cycle is a summary based on the characteristics of multiple octopus species, namely: *Octopus vulgaris*, *Octopus joubini*, *Octopus maya*, *Octopus bimaculoides*, *Octopus aegina*, *Thaumoctopus mimicus*, *Eledone moschata* and *Eledone cirrosa*.

In the first step of the attachment process the suction cup approaches the surface. Sensory receptors in the infundibulum and epithelium (Figure 20) feel when contact is made and smell what type of surface they are in contact with. This ability to determine the surface composition of the substrate comes in handy as it prevents the octopus

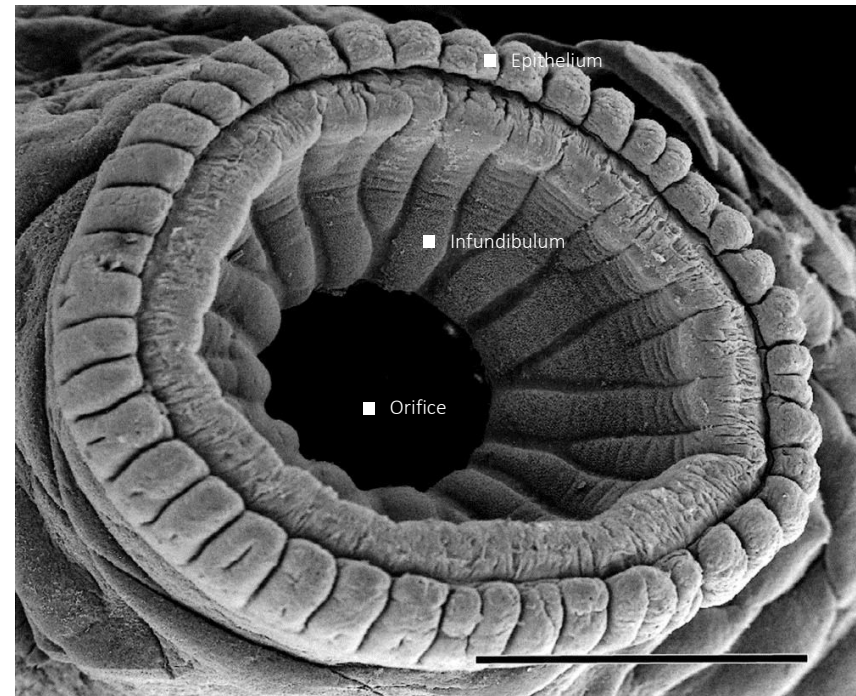


Figure 20 - SEM image from the suction cup the California two-spot octopus (*Octopus bimaculoides*). Scale bar = 1mm (Kier and Smith, 2002).

from adhering to its own body. When a suitable surface has been found to adhere to, the octopus can adjust the shape of the rim until a good seal has been achieved. It does this by using a muscular hydrostat structure, which consists of a combination of radial, circular and meridional muscles. By selectively contracting some of these muscles the octopus can change the shape of the rim anyway it likes.

When enough of the mechanoreceptors feel that contact is made with the substratum a signal is sent to the nerve system that the suction cup is ready to be used. These

Octopus

signals do not travel all the way to the brain but stay in the large decentralized nerve system of the arm, which allows the octopus to react fast on incoming stimuli.

During the second step the suction cup prepares for providing suction. The evolutionary solution developed by the octopus entails a second suction chamber behind the infundibulum called the acetabulum. The two chambers are connected with each other through an orifice that is strengthened using two sphincter muscles. Just as the infundibulum the acetabulum contains a combination of radial, circular and meridional muscles, which allows it to contract in various directions. During suction preparation the circular and meridional muscles contract which due to the fixed volume of the hydrostat results in a thickening of the acetabulum wall. This decreases the internal volume of the acetabulum and pushes water into the groove structure (Figure 20) of the infundibulum and eventually out of the cup.

To attach the suction cups to the substratum the octopus relaxes the tension in the circular and meridional muscles of the acetabulum. This is followed by a passive elastic force coming from tension that has been build up in crossed connective tissue fibres (Figure 21). These collagenous fibres act as a large array tiny tensile springs that want to restore the shape of the suction cup. However because water has a fixed volume a negative differential pressure inside the cup is created. This negative pressure differential is distributed across the entire surface of the infundibulum through a groove structure covered with chitinous denticles (Figure 22) and tries to suck water back into the acetabulum. Due to the close proximity of the suction rim to the substratum however the suction force results in viscous adhesion that pushes the soft rippled surface of the epithelium towards the ground. The tiny holes that the epithelium tissue cannot fit in are filled up by mucus that is distributed over the rim by numerous glands. This results in a watertight seal that continues to become stronger as the negative differential pressure inside the cup rises.

After a short while equilibrium is reached between the elastic forces in the acetabulum and the negative pressure differential inside the suction cup. During the equilibrium phase the infundibulum is pushed firmly against the substratum. This allows the tips of the denticles to penetrate the liquid layer in between the interface and come into

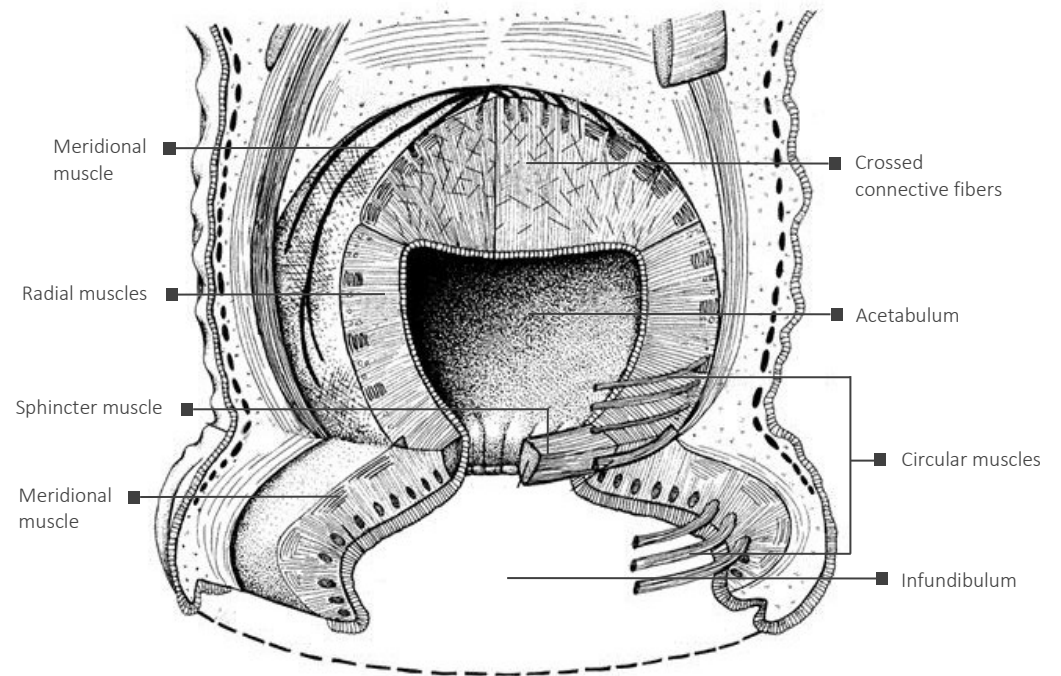


Figure 21 - Schematic cutaway of an octopus sucker (Kier and Smith, 2002).

contact with the substrate Figure 22). The contact made by the microstructure with the substratum results in three types of adhesion. Interlocking can occur as the denticles get stuck behind the asperities of the substrate. This results in a ratcheting mechanism that provides resistance against shear forces. The microstructure furthermore creates adsorption adhesion because of the intermolecular forces that form between the tips of the denticles and the adhering surface. This provides additional adhesion in both the perpendicular direction and the direction along the surface.

Octopus



Octopus vulgaris	
Max. length (cm)	?
Max. weight (g)	?
Max. sucker size (cm ²)	?
Max. ΔP (kPa)*	271
Max. tenacity (N/cm ²)	18.2
Max. force (N)	?

* On a hydrophilic surfaces.

** Based on the assumption that all adhesion is due to suction and the maximum fraction reported to be subjected to the suction pressure.

Image source: ("Octopus vulgaris, 2011")

The presence of a thin layer of water around the denticles furthermore forms a perfect stage for Stefan adhesion to occur. When the denticles are pulled away from the substrate a thin layer of water needs to move into the newly created space, resulting in shear forces that produce a net attractive force.

To detach the suction cup the octopus once again contracts the circular and meridional muscles in its acetabulum. This causes the pressure inside and outside the cup to equalize. Suction is lost and water can once again travel through the grooves towards the inside of the pressure chamber, resulting in a fast detachment of the suction cup.

From the structure of the octopus sucker can be concluded that it is unable to compensate for leaks beyond a certain point. When the hydrostat muscles in the acetabulum have returned to their normal shape and the tension in the crossed connective tissue fiber is released, the suction cup stops producing adhesion and detaches. This might be one of the reasons why octopus arms are covered by so many suckers. Their large number provides redundancy and prevents that a prey can escape when one of the suction cups fails.

The performance of the octopus suction cup has been determined by Smith (1995). He measured the pressure generated underneath the suction cup using a fully hydrophilic test set-up which allowed him to record pressures differentials higher than 100 kPa. His data shows that the common octopus (*Octopus vulgaris*) is capable of generating 271 kPa. In many cases this performance is not available at sea-level because of cavitation, but can be fully utilized on very hydrophilic surfaces or at depths lower than 10 meter.

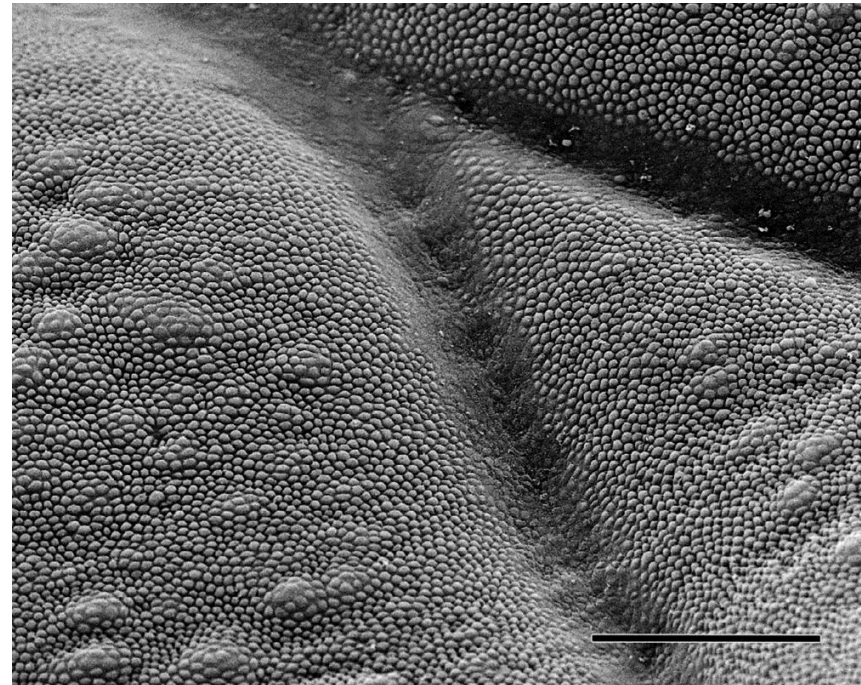


Figure 22 - SEM image of the infundibulum of *Octopus vulgaris*. Scale bar = 100 μm (Kier and Smith, 2002).

Conclusion

The analysis of the various examples of suction adhesion has shown a wide variety of solutions that have emerged through evolution. Each species has selected a different approach to achieve more or less the same goal, which is to adhere itself to a surface using suction. However when zooming out a bit, it becomes clear that there are also a lot of similarities between the different solutions. These similarities are best described as strategies used for improving the functioning of the suction organ and can be divided over three main goals.

1. Efficiency

The first goal that the strategies aim to achieve is efficiency. Each organism has only a limited supply of energy available, which needs to be divided over all of its vital functions. It is therefore necessary to make energy intensive activities such as creating suction as efficient as possible in order to reduce its metabolic cost. Analysis of the organisms discussed in chapter 1.1 – 1.4 and the additional suckers found in the digital version has revealed the following four strategies with respect to this goal.

1.1 Passive suction

Passive suction comprises the storage of muscular forces in elastic deforming structures. This strategy can be seen in nearly all high performance suckers that are able to provide long term adhesion. The advantage of passive suction is that energy only has to be expended during attachment and detachment, which greatly reduces the metabolic cost of prolonged adhesion.

Energy storage is achieved by using three types of structures. The first type encompasses the use of skeletal features as a passive energy buffer. A clingfish for example stores energy in its skeleton by bending the flexible rays in its pelvic sucker. Other animals like the octopus and the garra use connective tissue fibres to achieve this same objective. The third type of storage is only used by the limpet. Its sucker stores energy directly in the muscles by using the catch muscle mechanism. Although there are three distinct ways to store energy for passive suction, some organisms may use two or even three of these mechanisms simultaneously in order to achieve the best results.

1.2 Detachment force conversion

The automatic conversion of attachment forces into additional suction is a powerful strategy to increase sucker performance. Two of the best performing suction solutions that were analysed use this mechanism, albeit in quite a different way. The remora transforms drag into additional grip using a ratchet mechanism, while the squid uses a piston to convert the force of a struggling prey into suction. Efficiency is increased by this method as the additional adhesion is created by external energy. This means that the animal itself only needs to contribute a small part of the total energy expenditure.

1.3 Pressure distribution texture

The use of a pressure distribution texture was spotted in a number of animals like the octopus, the leach and the goby. This strategy increases the area affected by suction by creating a network of pressure distributing grooves. It is a simple way to improve the performance of a suction system, as the amount of suction adhesion has a direct correlation with the suction area. An additional advantage of distributing the pressure over the suction rim is that the areas in between the grooves are pressed against the substrate more evenly and with more force. Efficiency is improved by this strategy as the sucker can create more adhesion using the same pressure differential.

1.4 Smart detachment

Smart detachment is a strategy used by animals that use passive suction. Normally such an animal would have to reduce the volume of its suction chamber and counteract the passive forces that are stored in the suction cup to be able to detach. This is quite an energy intensive operation, and has led some species to develop other ways to equalize the pressure within their sucker. The clingfish for example uses flaps on its pectoral fins to open the furrows in between its suction clefts. This mechanism functions as a reverse pressure release valve and allows water to flow into the suction chamber. Another type of smart detachment system was found in animals that use respiratory pumps. Tadpoles use hyper expiration to reverse the flow in their buccal pump. This results in a rapid increase of the pressure in their oral chamber and causes fast detachment. The hyper expiration method probably does not increase efficiency as it

Conclusion

requires more energy than their usual detachment mechanism. It was probably developed to provide a quick getaway in the event of an approaching predator.

2. Reliability

The reliability of its suction organ is a main concern for the organism that uses it. If the sucker were to fail it could result in bodily harm, reduced chances of reproduction and even death. The animals discussed before therefore have developed a number of strategies that aim to increase the reliability of their suction solution.

2.1 Conforming rim shape

Every animal that was analysed in this chapter has adapted its sucker in such a way that the shape of the sealing rim can conform to the intended substrate as best as possible. This improves the reliability of the suction organ as a tightly conformed suction rim significantly reduces the amount of leakage.

In general the sucker rim achieves the right pliability by using structures that adept to the typography of the substrate on multiple hierarchical levels. A good example of such a sequence can be found on the abalone and the clingfish. Their flexible rim drapes over the substrate while microscopic hairs covered by a nano-textures bridge the remaining gaps.

2.2 Segmented rim

Segmentation of the suction cup rim has been witnessed in several organisms and allows it to expand during attachment. In some species these folds also provide spare sucker surface for locomotion purposes. However an even more important purpose for strategy is to prevent peel forces from breaking the seal. The gap in between the segments provides resistance against this as they dissipate energy. In this way cracks are stopped from propagating and reliability is increased. Segmentation can be seen on the macro level in the form of the segmented adhesive pads in the snailfish but also occurs on the micro level. Each small hair that is present on the surface of the abalone sucker for example can be considered a separate segment.

2.3 Rim strengthening

One of the common methods of failure for natural suction cups is when their rim moves inwards. This is due to the translation of the perpendicular detachment force into forces at the rim that are aimed towards the centre of the cup. The rim starts to slide inward when these forces overcome the static friction generated by the sucker, which usually results in leak formation and detachment. Therefore organisms have developed ways to strengthen the circumference of their sucker. Two strengthening methods were observed. The first method entails the use of skeletal features to support the suction ring segments. This is most obvious in the pelvic suckers which use thick calcified rays to support their sealing rim. The second type of strengthening was seen in species that do not have skeletal features in their sucker. To acquire the needed strength they use a support structure of hydrostatic muscles. A good example of such a hydrostat muscle structure can be seen in the sucker of the octopus.

2.4 Secretion sealing

Mucus secretion can reduce wear and helps to promote the strength of the seal by filling up small cavities in between the rim and the substrate by expelling water from between the interface. Some secretions also contribute directly to adhesion due to their stickiness. All these functions help to stabilize suction performance and therefore have a positive influence on the sucker's reliability.

The exact benefits of this strategy however are hard to estimate as many animals have mucus glands over their entire body. This means that it is hard to distinguish between normal skin secretion and secretion that is specially intended to increase the performance of the suction organ. Another aspect that makes it hard to judge this strategy is the fact that the animal actively changes the composition of the mucus according to the circumstances. The limpet for example has two distinct types of mucus that help it adhere in different ways. A final remark regarding secretion sealing is that it appears that some animals purposefully choose to devoid some areas of its suction rim from mucus. This is most clear in the lumpfish. The entire body of this species is covered in skin secretion except for the adhesive pads on its pelvic sucker. It could be

Conclusion

that the anti-skid function of these pads is hindered by secretion, as the mucus starts to act as a lubricant.

2.5 Leak compensation

Most powerful suction cups shy away from using respiratory pumps, as their strength is limited by the valves that are used. However the use of such a pump does carry along with it the possibility to actively compensate for leaks during adhesion. This strategy provides a large benefit because it allows the animal to retain suction for as long as it pleases. This is in contrast with most pelvic suckers which from time to time have to shortly detach in order to push the excess water from underneath their sucker. A way to compensate for leaks gives the animal more suction reliability as it can maintain a more stable pressure differential underneath its sucker.

3. Suitability

Every organism at some point in evolution started with the same basic suction structure. A rudimentary enclosure that could generate and hold a negative pressure differential. However natural and sexual selection has forced adaptations onto these structures to make them perform better. The evolutionary pathway that was followed for these adaptations depends heavily on the purpose for which the sucker is used. This means that the choices that are made can have an adverse effect in conditions outside of the normal use situation. The suction cup of the Humboldt squid for example is impractical for adhering to hard substrates because of its protruding teeth and the clingfish seems to have sacrificed performance to be able to adhere better to rough and uneven surfaces. The modifications witnessed in nature go quite far as some species, like the remora even base their growth patterns on the surface they intend to adhere to. All this effort is directed at making sure that the suction organ is suitably equipped for its intended purpose. Suitability is therefore an important goal for a natural sucker and is achieved through one of the following strategies.

3.1 Shear force resistance

Simple suction cups do not provide a lot of resistance against shear forces. Suction cups in the shower for example keep sliding away because their rim loses its grip on the

shower wall. As organisms that live in the aquatic environments have to deal with forces from all directions they have developed ways to convert the perpendicular suction tenacity in more omnidirectional grip.

In general the animal uses the proximity of the rim to the substrate to promote other adhesion mechanisms, like interlocking and adsorption adhesion to take place. This conversion depends on the use situation. Species that have to face a lot of head-on currents usually opt for rows of teeth that interdigitate with the substrate. This method generates a lot of grip but does require that the teeth face in the correct way with respect to the detachment force. Animals that require resistance against unpredictable forces that can come from any direction therefore use a different method. Two types of omnidirectional textures were found in literature. Gecko-like microstructures were found on the adhesive pads of the clingfish and abalone, and are mainly used to create adsorption adhesion. The second type can be seen on the sucker of the octopus and the rays of the hillstream loach. These species have horny projections on their skin that increase friction through a combination of interlocking, adsorption adhesion and Stefan adhesion.

3.2 Active adjustment

Active adjustment is used by animals in times of distress to compensate for a temporary increase in detachment forces. This strategy therefore makes sure that the sucker's performance suits the circumstances of its environment. Different types of active adjustment can be seen in the analysed suction solutions. These are closely related to the way the animal creates the initial pressure differential. Pelvic suckers from the lumpfish and snailfish for example use active muscular activity to support the passive suction forces that are stored in their skeleton, while animals with a respiratory pump use more vigorous inhalations to increase the pressure differential underneath their sucker.

3.3 Decentralized suction cup control

In systems with multiple suction cups it is important that each sucker responds in a suitable way to maximize adhesion and to prevent unnecessary sucker activation. When for example an octopus grips its prey, not all suction cups will make a good seal with the

Conclusion

substrate. Each sucker is therefore equipped with an array of sensors that can detect whether it can be engaged. To prevent overloading the central brain, suction cups are largely governed by reflexes that do not travel all the way the central nervous system. The large amount of autonomy furthermore allows for a fast and suitable reaction on incoming stimuli.

Strategy/performance matrix

To give a good overview of the strategies that are used by the various species, they have been summarized in Table 2. Combining this matrix with the sucker performances that were found in literature allows an indicative importance factor to be assigned to them. Due to the holes in the knowledge provided by literature and the incompatibility of the various performance measurements methods, it is not possible to base any hard conclusion in these factors. An example of such a hole in knowledge is the lack of any passive suction features found in the abalone. Based on the behaviour of the abalone it is obvious that this animal should have such a mechanism. However there is no mention of it in the analysed studies.

Despite the lack of credibility of the importance factor at this point the matrix does provide a good insight in the knowledge gaps that need to be filled and could therefore function as a guideline for future research. If it were to be complemented with the required additional knowledge and reliable performance measurements the matrix could also be used as a powerful design tool that highlights the most important strategies for bio-based artificial suckers.

Suction adhesion and the aquatic environment

Why do all species that use suction adhesion live in an aquatic environment?

This is an important question that arises from the analysis made in this chapter. Although it is a simple question, the answer to it is not as straightforward and consists out of multiple arguments. Some of these arguments come from a study by Ditsche and Summers (2014) about the differences in terrestrial and aquatic attachment, while others come from own observations.

1. It is easier to create large pressure differentials in water than in air.

Water is non-compressible just like solids. This means that it also resists tensile stresses, as hydrogen bonds hold the water molecules together. Animals living in aquatic environments can therefore create large pressure differentials without having to move their sucker a lot. Air in contrast behaves like a gas and can be compressed or expanded. When a lumpsucker for example uses its suction cup in a terrestrial environment, it would find that it produces a disappointing amount of suction adhesion. This is because according to Boyle's law even a large expansion that results in a 100% increase of the internal volume of the sucker only results in a pressure decrease of 50% with respect to the ambient environment.

The second reason for the occurrence of larger differential pressures in aquatic environments is that there is usually more pressure to start with. Atmospheric air pressure is quite constant and maxes out at around 101 kPa at ground level. This means that the maximum amount of suction adhesion in terrestrial application is 10.1 N/cm^2 . Under water however the ambient pressure starts to increase rapidly due to the higher density of water. The weight of the water column pushes down on the objects below and results in an additional pressure increase of 100 kPa for every 10 meter. Sucker species that live at a depth of 100 meter are therefore allowed to generate 11 times more suction adhesion than is possible at sea level.

Multiple studies have shown that suction adhesion in animals like the limpet and the octopus can be even stronger than the ambient pressure normally allows. Negative pressures in liquids are a phenomenon that allows them to sustain pressures below 0 kPa. Many people get confused by this as their intuition tells them that pressures can never get below the absolute vacuum. This is because they mix up the behaviour of gas with liquids. A vacuum pressure in a liquid is not the same as the absolute vacuum of a gas in the sense that it doesn't require that all the molecules are removed from the pressure chamber. 0 kPa simply means that the liquid no longer produces a net force on the walls of its enclosure. A negative pressure inside a liquid can therefore be visualized as the liquid producing a force that pulls the walls of the container inward. The tensile strength of the liquid keeps it together, as long as there are no nucleation sites for

Conclusion

bubbles to form. In this way the pressure in natural suction cups can decrease down to -100 kPa.

2. It is easier to create a watertight seal than an airtight seal.

To maintain suction adhesion it is necessary to prevent the expelled gas or liquid from leaking back into the sucker. There are two reasons why it is easier to prevent this in the aquatic environment than in terrestrial applications. First of all water in its liquid form consists out of much larger molecules than its chemical formula H_2O suggests. The hydrogen atoms form a networks of atoms held together by hydrogen bonds. These bonds are constantly rearranged and result in a higher viscosity that makes it more difficult for water to enter small cavities. This makes it less likely that water travels through small gaps underneath the suction rim. Air on the other hand has little coherency and can therefore leak into the suction cup molecule for molecule. This means that it is almost impossible to create an airtight seal when the substrate has some roughness.

The second aspect of water that plays a role is its high surface tension. A water molecule likes to surround itself with as many other water molecules as possible. This is because of the forces that are generated by hydrogen bonding. For a molecule in the middle of the liquid these forces are distributed equally over all directions. A molecule at the surface in contrast only experiences attractive forces coming from the water underneath it. This produces a net force towards the bulk of the liquid and results in a stretched membrane effect at the surface. A body of water will therefore always try to minimize its surface area to abide to the principle of minimum energy. The geometric shape with the smallest area compared to its volume is the sphere. This is why small amounts of water tend to morph into spherical droplets. For suction systems the surface tension of water means that it costs energy to form leaks underneath the suction rim as the liquid has to increase its surface area. Very small leaks will therefore close automatically if the energy needed to create the additional surface area is larger than the energy potential between the inside and the outside of the cup. Once again air molecules are not hindered by surface energy and therefore leak easier into the suction chamber.

3. The detachment forces in aquatic environments are less predictable and stronger.

When looking at the forces that terrestrial and aquatic animals have to cope with during attachment, it becomes clear that there are large differences between them. The gecko, which has become the archetype of natural adhesion in terrestrial situations, can always count on the strength and direction of gravity. It therefore has developed an adhesion system around the characteristics of this force. However if a prying moment is applied to the gecko's toes they immediately lose their grip as the mechanism is not designed to handle this kind of moments. This is a handy detachment method for the gecko itself but unacceptable for any aquatic organism that lives in the intertidal zone. In these places the strength of the currents varies greatly and flow induced drag forces and moments can come from any direction. These animals consequently need an attachment mechanism that is less susceptible to the variations in detachment force. They therefore usually opt for a glue-like adhesive in stationary applications and suction adhesion in situations where reversible adhesion is required. This is because these mechanisms are inherently better in resisting strong omnidirectional forces.

To get a better understanding of the quantitative differences between the detachment forces on land and under water, their strength has been calculated for both environments for a specimen from the *Liparis florae* species. For the drag calculations it has been assumed that the body of the fish can be modelled as a streamlined body. This means that the drag coefficient is 0.04 and that the cross-sectional area is represented by a circle. The diameter of the circle has been estimated by using a photo from a *Liparis florae* specimen and its maximum length (Figure 23). This method assumes that the species grows in an isometric way.

Conclusion

The relative speed has been obtained from work from done by Jones and Demetropoulos (1968), who measured water flow velocities of the coast from Wales.

This same flow speed has been used to determine the amount of drag in air to be able to make a useful comparison. The flow rate of 15 m/s equals a moderate gale (force 7 on the Beaufort scale). From the data it becomes clear that the large density of water compared to air greatly increases the strength of its flow. Currents can generate about 800 times more force than its terrestrial counterpart, the wind, for a creature the size of a tidepool snailfish. Also gravity, the main detachment force in terrestrial environments, only generates about a tenth of the force that is produced by a powerful wave.



Length L	0.167 m
Cross-sectional area A	$1.36 \cdot 10^{-3} \text{ m}^2$
Weight m	$2.67 \cdot 10^{-2} \text{ kg}$

Density of water ρ_w	1000 kg/m^3
Density of air ρ_a	1.225 kg/m^3
Relative speed v	15 m/s
Drag coefficient C_D	0.04

Drag in water	$F_a = 0.5 \rho_w v^2 C_D A$	2.4 N
Drag in air	$F_w = 0.5 \rho_a v^2 C_D A$	$3.0 \cdot 10^{-3} \text{ N}$
Gravity	$F_g = mg$	0.26 N

Figure 23 - Measurements and calculations on *Liparis florum*

4. Water hinders the functioning of terrestrial adhesion mechanisms.

Beneath the water level the effects of gravity become unnoticeable as water has about the same density as the animal itself. This is why astronauts train in large swimming pools to get a sense of weightlessness. The lack of influence from gravity is one of the aspects of the aquatic environment that hinders adhesion mechanisms that are used a lot by terrestrial species. Animals that climb trees for example need gravity to push their claws into the grooves of the bark. Another type of adhesion that is popular among terrestrial species but that cannot be used on its own underwater is adsorption

adhesion. This is because it requires a preload to come into close contact with the substrate. Gravity is not available underwater and thus the mechanism depends on other adhesion methods to provide this force. This is why gecko-like microstructures have been seen a number of times in combination with suction cups. The sucker provides the initial attachment force that allows adsorption adhesion to occur. This force needs to be significantly larger than gravity as all the water needs to be pressed out from between the interface in order for adsorption adhesion to occur. Even when an animal succeeds in doing that, adsorption adhesion probably does not play a prominent role. This is because most objects in water are covered by a crust of slimy algae and bacteria that do not provide a lot of grip. It is therefore plausible that adsorption adhesion is only useable to improve the seal of the rim as its adhesive pull closes small gaps at the interface.

5. The energy costs to operate and develop a sucker are high.

The final reason why all analysed suction organs are used in aquatic environments has to do with the metabolic costs to grow and power a sucker. An actively controlled suction cup is only worth the investment when it makes the difference between survival and extinction and when no other adhesion mechanism can do the job. This is because a sucker requires a dedicated skeleton and/or muscular system to power it. In addition to this it requires maintenance in the form of mucus production and microstructure renewal. Also powering it costs quite a lot of energy compared to terrestrial adhesion system. The gecko for example only has to lightly push its toes onto the substrate, while a clingfish needs to contract numerous muscles before it is ready to use its sucker. Finally the development of a suction adhesion cup bears with it extra energy costs for locomotion as the flattened round shape on the exterior of the animal increases drag. Although drag is not the reason why terrestrial organisms have abandoned the idea of developing an adhesive sucker, the other mentioned energy expenditures probably are. Therefore it is only logical that no elaborate suction adhesion systems can be found on land animals as there are far more viable alternatives available.

Conclusion

	Tenacity N/cm ²	1.1 Passive	1.2 Conversion	1.3 Distribution	1.4 Detachment	2.1 Conforming	2.2 Segmented	2.3 Strengthen	2.4 Secretion	2.5 Compensate	3.1 Resistance	3.2 Adjustment	3.3 Decentralize
Goby	0.3			x		x		x				x	
Snailfish	5.5	x			x	x	x	x			x	x	
Lumpsucker	8.5	x			x	x	x	x			x	x	
Clingfish	4.5	x	x		x	x	x	x	x		x	x	
Hillstream loach	?					x	x	x	x	x	x	x	
Limpet	23	x				x		x	x		x	x	
Abalone	11.5	?		x		x	x	x	x		x	x	
Tadpole	1.7	x			x	x	x	x	x	x	x	x	
Garra	?	x				x	x	x	x	x	x	x	
Pleco	?	x				x	x	x		x	x	x	
Leech	5.8	x		x		x			x	x		x	
Lamprey	6.2	x				x	x		x	x	x	x	
Remora	9.3	x	x			x		x			x		
Octopus	18.2	x		x		x	x	x	x		x	x	x
Squid	83	x	x			x		x			x	x	?
Diving beetle	2.1	x	x			x		x	x				
Importance		167.8	98.9	34.8	16.2	177.5	44.6	163.5	73.0	13.7	171.4	168,2	18.2
Importance indexed		94.5	55.7	19.6	9.1	100	25.1	93.2	41.1	7.7	96.6	95.8	10.3

Table 2 - Suction adhesion strategies and their importance based on performance. X= strategy is used by this particular species. ?= knowledge gap

Existing suction solutions

To determine how the knowledge gained in chapter 1 can be transformed into a useful application; a comparison is made with existing suction adhesion solutions. This chapter therefore contains an inventory of all relevant solutions that are gathered from multiple sources.

First an investigation is made to see how researchers that set themselves the goal to develop a bionic suction adhesion system have fared. The aim of this investigation is to learn from the methods which they use to translate insights from natural suckers into a technical design. The results from the studies can also provide valuable information about the performance benefits gained by applying the lessons learned from nature.

The second source of information is gained from analysing systems that are used in the industry. Useful techniques for creating efficient, reliable and suitable suction adhesion can be abstracted from this, as well as possible applications for the biomimicry strategies. Since this section is just an inventory of what is available it has been attached to this report as an appendix (Appendix A).

Finally market research provides an overview of the suction adhesion solutions that are already available on the consumer market. The aim of this section is to see which strategies are already incorporated into consumer products, but even more important which strategies are not yet used. These unused strategies could form the basis of a competitive advantage. All information gathered during the market research can be found in Appendix B.

To conclude the chapter all information is reviewed and a direction for the biomimetic sucker design is chosen.



Figure 24 - Tanker docking system based on the remora adhesion mechanism.

Existing solutions in literature

Artificial octopus sucker

Tramacere et al. have written numerous articles to unearth the workings of the octopus suction cup. Their aim is to develop a bionic sucker that uses some of the clever mechanisms used by this animal. After determining the characteristic of the suction cup they made two different prototypes that mimic some of the octopus sucker's features.

Their first attempt is described in an article from 2014, in which they combined a silicone casting shaped like an octopus suction cup with a dielectric elastomer actuator. This allows the sucker to work under water with a minimum amount of components. A dielectric elastomer is a thin layer of a non-conductive polymer that is sandwiched in

between two flexible electrodes. When a voltage is applied over the electrodes the electrostatic pressure will squeeze the elastomer causing a deformation. To create an actuator with this effect the researchers combined two dome-shaped membranes. One of the membranes was a dielectric elastomer and the other passive.

The activated dielectric elastomer on top deforms in such a way that it wants to increase the volume in between the membranes (Figure 25). As this void is filled with water, which is non-compressible, the pressure is transmitted through the passive membrane to the suction chamber. The resulting pressure differential results in suction adhesion and pushes the cup against the substrate. By increasing the voltage in between the conductive layers the amount of adhesion can easily be adjusted. The maximum amount of pressure that this method is able to generate is 8 kPa at a voltage of 2500 V. This is rather low compared to the 271 kPa generated by natural



Figure 26 - Suction cup with pressure distribution grooves (Tramacere et al., 2014).

octopus suction cups. Another downside of this method is that a continuous voltage needs to be applied in order to keep the suction cup attached. Although the energy consumption of a dielectric elastomer is quite low, the method cannot be called passive.

The second study by Tramacere et al. from 2015 focusses on another strategy used by the octopus. The pressure distribution grooves on the infundibulum and its mechanical properties were measured, and the findings translated into an artificial sucker. A soft silicon rubber was used to mimic the infundibulum and grooves were engraved into it with a laser cutter. The scientists compared multiple groove patterns by varying the amount of grooves and their dimensions. Unsurprisingly they found that the suction cup with the most grooves and the largest width has the highest pull-off strength. This is because a larger area underneath the cup is subjected to the pressure differential. It would have been more interesting to know how the amount of lateral grip depends on the groove pattern and if there is an optimum ratio between groove and friction surface.

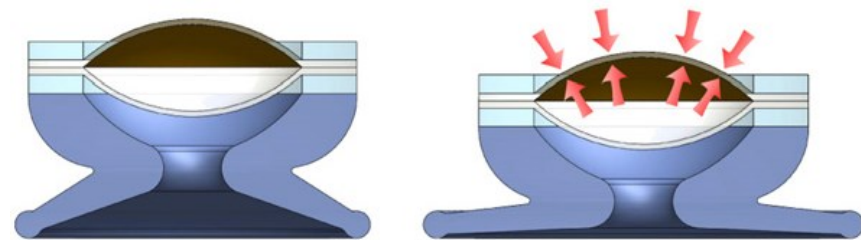


Figure 25 - Artificial sucker with dielectric elastomer actuator (Tramacere et al., 2015)

Existing solutions in literature

Artificial octopus suction cup array

To lift difficult to handle shapes that have a lot of curvature Kessens and Dessai (2010) developed small 3D printable suction cups that can be individually activated (Figure 27). This allows them to be coupled into series using a simple vacuum system that operates without any complicated control system.

The cups work by converting the preload force into a hinging movement that unplugs the vacuum tube (Figure 28). Essentially the rim functions as a crude mechanoreceptor that senses when the suction cup can be activated. It is therefore in good agreement with strategy 3.3, decentralized suction cup control. A large disadvantage of this system however is that although the cups can be activated individually, they cannot be summoned to stop adhering. This means that the vacuum in the entire array has to be equalized before the sucker can detach. Such a requirement is not in accordance with natural suction systems. If the octopus would use a similar system its prey would have no problem escaping from its grasp. Also for handling complex objects this is a large downside.

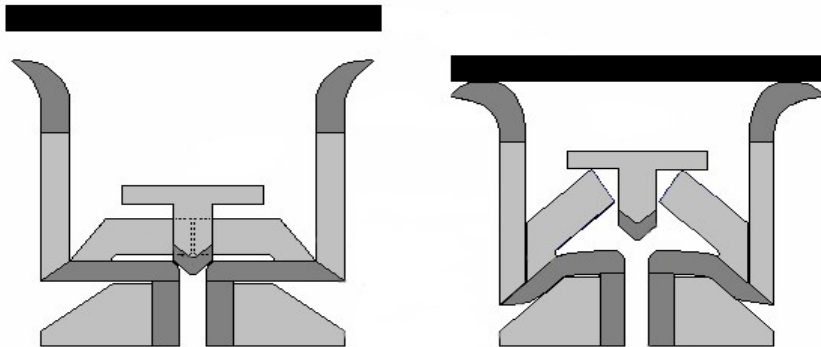


Figure 28 - Self-selecting valve mechanism (Kessens and Dessai, 2010).

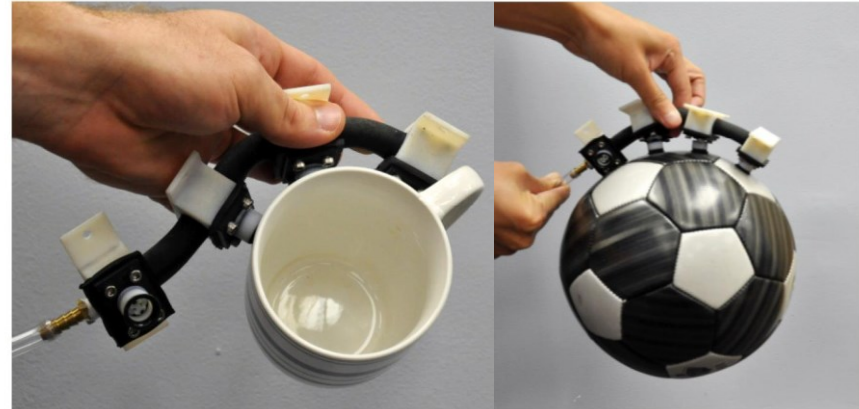


Figure 27 - Suction adhesion capabilities of a suction cup array (Kessens and Dessai, 2010).

Biomimetic squid suction cup (Hou et al.)

Hou et al. (2012) attempted to copy the suction adhesion capabilities of the squid by coming up with three bionic suction cup concepts. Although their intentions were good, they completely failed to capture the unique detachment force conversion mechanism of the squid. Their first concept, which according to them is a direct copy of the squid sucker, is made by encapsulating a nylon ring made from stockings in a casting of silicone rubber. By pulling on the ring the enclosed volume of the suction cup wants to increase and therefore a negative pressure differential is generated. However no piston-like motion is used. Calling the concept a copy of the squid sucker is thus an overstatement. The second and third concept look even less like a squid sucker and are essentially just columns of silicone rubber with a hole in their middle. By putting a lot of them together on a strip the impression of a squid tentacle is created (Figure 29). However they are unsuitable for any form of active adhesion.

Existing solutions in literature

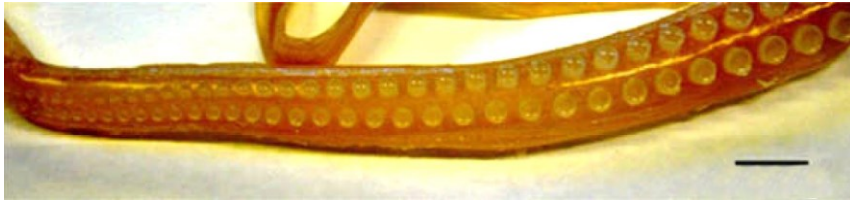


Figure 29 - Artificial squid tentacle (Hou et al., 2010).

Artificial leech suction cup

Feng et al. (2014) used the rear sucker of the leech as a source of inspiration for developing a biomimetic suction device. After an analysis of the suction organ of the leech they developed the suction that can be seen in Figure 30. The device uses a clever actuator that is embedded in a silicon cup shape. The actuator is made from an ionic polymer–metal composite that flexes when a voltage is applied across it. This is caused by the migration of the ions due to the attractive and repulsive forces generated by the electrodes. By alternating the voltage the suction cup can be flattened or curved. This allows the cup to be actively attached and detached.



Figure 30 - Bionic leech sucker with ionic polymer–metal composites actuator Feng et al., 2014).

A downside of this type of actuation is that the IPMC artificial muscle only produces a small force. A suction cup of this type with a diameter of 10 mm produces 2N of suction adhesion, which is 6 times less than the maximum tenacity of *Hirudo nipponica*. In addition to this downside it is questionable whether the design can be called biomimetic, as it does not really incorporate any distinguishing trait of the leech sucker.

Remora suction system

The HiLoad DP1 is a dynamic docking system for floating oil platforms. It allows a normal tanker to remain stationed at a safe distance from the production ship by acting as a set of moveable bow thrusters (Figure 24). This requires a tight grip between the tanker and the HiLoad system that can transfer several tons worth of force. The developers of the HiLoad DP1 have therefore developed a suction system that is based on the remora adhesion pad.

The system works by manoeuvring the attachment pads underneath the tanker and then pressing them against its hull by increasing the buoyancy of the HiLoad. This creates a watertight seal around the pads and allows the suction system to be activated. Suction adhesion is created by pumping out the water in between the tanker and the HiLoad which leaves behind a negative pressure that can be compensated for leaks. This means the system can adhere reliably to the tanker for long periods of time. The amount of friction at the interface is greatly increased by rubber friction elements

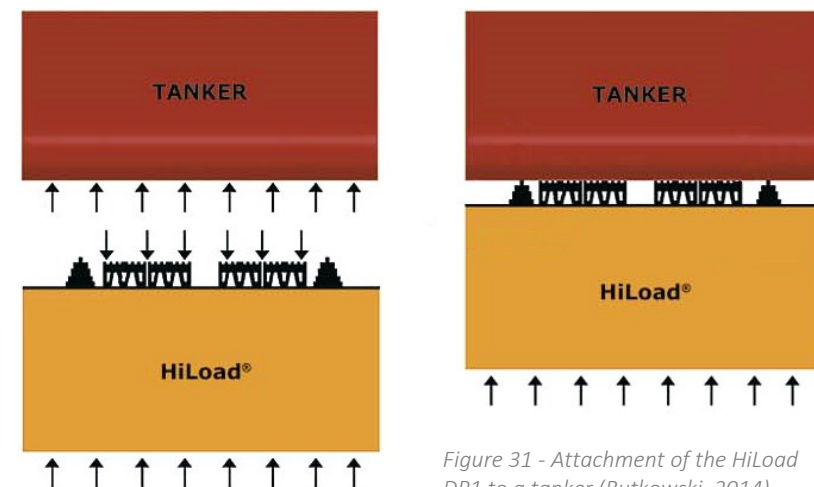


Figure 31 - Attachment of the HiLoad DP1 to a tanker (Rutkowski, 2014).

Existing solutions in literature

that are indeed reminiscent of the spiny ridges of the remora. However from the crisscross positioning of the rubber elements it can be concluded that these do not contain a detachment force conversion mechanism. This is a missed opportunity as it is the feature that makes the remora's suction pad different from all other natural suction adhesion systems.



Figure 33 - Attachment elements of the Highload DP1 (Diederichsen and Olsen, 2012).)

Biomimetic suction cup

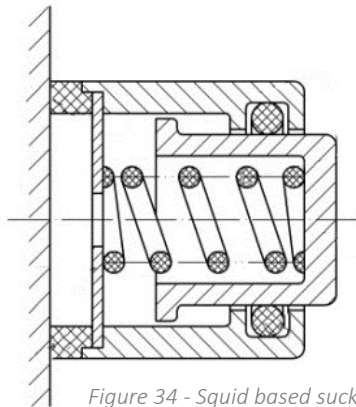
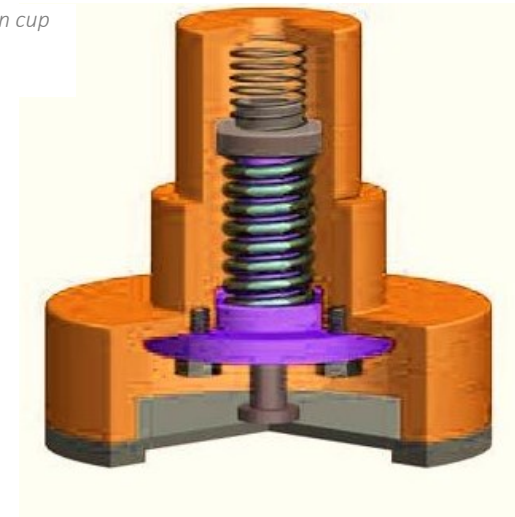


Figure 34 - Squid based sucker (Bing-shan et al., 2009).

Bing-shan et al. (2009) did not choose one sucker species to base their suction cup device on but used features from multiple organisms as an inspiration source. This resulted in two concepts that are quite similar and that, with some creativity, can be seen as an artificial version of a squid and an octopus sucker. Both concepts use a shape memory alloy as an actuator which is a type of material that remembers its original shape. After it has deformed it returns to the pre-deformed shape when it is heated. This phenomenon has many applications but

can be used as an actuator by forming the shape memory alloy into a spring. Figure 34 shows a design that uses the two-way shape memory effect to achieve both contraction and extension with the same spring. The two cylinders slide into each other and allow the sealed space in between them to expand and shrink. When the spring is heated by running a current through it the actuator extends and pushes the internal tube towards the rear. This creates a pressure differential and engages the sucker. When the spring is allowed to cool down again, the spring contracts and the suction cup detaches. The second design does not shrink when its heat is dissipated and has therefore only a one-way shape memory. A second spring has therefore been added to push the piston back into its position after activation (Figure 32). Shape memory alloys generate more force than ionic polymer-metal composites and do not require high voltages like the dielectric elastomers. However a downside to these actuators is that they consume a lot of power and also require a significant amount of time to heat up. Fully extending the spring of the octopus prototype takes 20 seconds at a current of 4.75A and a voltage of 5 volt.

Figure 32 - Octopus inspired suction cup (Bing-shan et al., 2009)



Conclusion

In this chapter numerous suction adhesion solutions that were found in literature, used in industry or sold on the consumer market have been analysed.

From the analysis of the bionic suckers that were found in literature can be concluded that they do not really comply with the suction strategies found in chapter 1. The researchers generally focus on mimicking muscle structures, but fail to develop a truthful technical translation of the natural sucker they are studying. It is also suspected that in a number of cases the researchers add the words bio-inspired and biomimetic to their work to give it extra élan. The hype surrounding bio-based designs helps to get their articles published. To overcome this pitfall in the future, suction adhesion devices should only take inspiration from natural suckers but not try to directly copy them. This is because nature and technology are inherently different and have their own set of strengths and weaknesses.

The review of suction adhesion solutions used in the industry has revealed many interesting ways to create, govern and apply a vacuum. Numerous vacuum pump designs that each have their advantages and disadvantages were found as well as a large array of suction cups for almost any kind of substrate. Also the analysis of the components used to govern vacuum systems has yielded valuable insights. Many of the solutions found in the industry moreover bear large similarities with natural suckers. A good example is the resemblance of the suction cups used to pick up thin sheets and the sucker of the whip lash squid (see digital version). It is unknown whether the designers used the squid's suction cup as a source of inspiration or that the

resemblance is the result of having similar goals and requirements. In this case the similarity lies in the fact that both solutions try to prevent material from buckling into the suction chamber. Also in general it can be concluded that suction adhesion solutions in the industry are a good translation of the principles behind natural suckers. This might be because they have comparable goals. Both try to achieve an efficient, reliable and suitable form of suction adhesion.

In contrast to the industrial sector not many consumer products incorporate natural suction adhesion strategies. Most companies focus on making their suction cup easy to attach and detach but use very basic suction cup designs. This has probably to do with the fact that the price that a producer can command for his suction adhesion product is lower than in the industrial sector. Therefore companies are not induced to develop more advanced products. The lack of any products using natural suction adhesion however could also be a possible market opportunity. It seems that there is room for a more high tech solution that creates a not yet fulfilled application for suction adhesion. The findings of this chapter have been summarized in Table 3. It shows which natural suction adhesion strategies are already in use for each category. From the table can be seen that industrial suction adhesion solutions follow the strategies most closely, followed by literature and the consumer market. The table is a useful tool to determine the subject of future development. Any strategy that has not been fulfilled could be leveraged to come up with innovative new solutions.

	1.1 Passive	1.2 Conversion	1.3 Distribution	1.4 Detachment	2.1 Conforming	2.2 Segmented	2.3 Strengthen	2.4 Secretion	2.5 Compensate	3.1 Resistance	3.2 Adjustment	3.3 Decentralize
Literature	x	x	x	x			x			x		x
Industry		x	x	x	x	x	x		x	x	x	x
Consumer	x			x	x		x					
Nature	x	x	x	x	x	x	x	x	x	x	x	x

Table 3 - Usage of strategies in the different solution categories

Application and requirements

In Chapter 2 it was established where the knowledge about natural suction adhesion can best be applied. Based on Table 3 the choice is made to develop a product for the higher segments of the consumer market. The 'prosumer' market was chosen as it allows for the incorporation of not yet fulfilled natural suction adhesion strategies, which could form the basis of a competitive advantage.

To command a higher price that allows a more advanced suction adhesion system, the product will not be aimed at the average consumer. It is chosen to develop a product for small businesses and professionals that can help them during their daily jobs. The product therefore has a higher intrinsic value than normal consumer suction adhesion products by making their occupation safer, more efficient and healthier.

The purpose of the product will be to help people to handle difficult to lift items in circumstances where no bulky and complex lifting aids (Figure 36) are available. Furniture movers for example frequently need to lift heavy closets that do not have any handles to hold on to. Also on construction sites, building components like doors and windows need to be placed manually. Having a handle that can grab onto these objects makes lifting a lot more ergonomically responsible.

The choice for a high tech consumer product is furthermore motivated by the fact that the knowledge that is available in industry can be leveraged. This sector has already developed much of the required components needed for such a device. Suction cups that can grab onto a wide variety of substrates are already available for example. Using the knowledge embedded in these solutions prevents reinventing the wheel.

In contrast to natural suckers the application chosen does not take place in the aquatic environment. This is because the number of applications and the market size for underwater suction adhesion devices is rather small. When developing a device for the selected application the differences between terrestrial and aquatic environments therefore need to be kept in mind. These differences can be found in the conclusion of Chapter 1.

In order for the suction adhesion device to be able to fulfil the application it needs to comply with a certain set of requirements. These requirements are determined by analysing a number of aspects that have an influence on the design of the device.

First a stakeholder analysis is made to determine their requirements and preferences. Subsequently market research is done to determine which competing products are already on the market. Then an analysis of the use environment provides information about the circumstances under which the device has to function. Since the market research is just an inventory of the available products it can be found in Appendix C. The same decision was made for the use environment analysis which forms Appendix D. The final part of this chapter contains an analysis of the ergonomic aspects that the device has to take into account.

All the information gathered in this chapter is summarized in a list of requirements. This list is used as a guideline against which the design can be evaluated.



Figure 36 - The struggle of moving large and heavy objects ("Não há nada").



Figure 37 - Professional movers carrying a cabinet ("Pollards Removals")

Stakeholders

The use of the portable lifting device affects a number of stakeholders. To make sure that the designed solution takes into account all the demands from these various stakeholders, an analysis of their requirements has been made. In order to do this all stakeholders have been inventoried in Figure 38. Based on this diagram the demands for each stakeholder for the portable lifting device are listed.

User

The user of the portable lifting device is anybody who frequently has to lift items that are difficult to handle. This includes people working as furniture movers and construction workers, but also less obvious occupations like people who build up stages for a living. The things they all have in common are the requirements they will have for the device. As stated before the portable lifter is meant to make their jobs safer, more efficient and healthier. This requires the following things from the device. The lifter has to be fast at attaching and detaching and should to be easy and intuitive to operate. Secondly the device needs to communicate in a clear way with the user in order to be

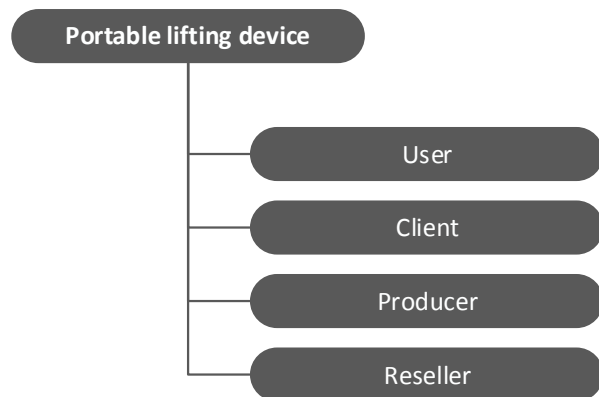


Figure 38 - Stakeholder analysis of the portable lifter.

able to lift an object safely. This requires the user to have insight in how much adhesion the device is creating and how long it will be able to do its job. A feature that warns the user when the device is struggling to stay attached would also be very useful. To increase the healthiness of heavy lifting jobs, the device has to make a large difference in the effort it takes to lift an object. Because the lifter is portable it cannot offer the same lifting performance as fixed devices. It therefore has to make smart use of the energy provided by the user.

Client

The client is the person or organisation whose objects are lifted and moved. These objects could be very valuable and may not be damaged by the lifting device in any way. This means the suction adhesion device distributes the lifting force over a sufficiently large surface area and does not contaminate the substrate. The suction cup should therefore be made from a material that does not leave marks, but it also requires that the cup can be cleaned after a number of uses.

Producer

The producer of the portable lifting device wants to make a high quality device that meets the requirements at the lowest possible costs. In this way the company's profits are maximized and the reputation of the brand is increased. To achieve this, the device should contain a modular platform with fixed interfaces. The use of a modular approach allows the use of standardized components and outsourcing of components that are outside the producers expertise. A modular platform furthermore makes it easier to produce multiple versions of the device that can be sold in different market segments.

Reseller

Most of the portable lifting devices will not be sold directly to a customer but through a reseller. These could be wholesalers, DIY stores or webshops. For these parties it is of interest whether they can make a decent margin on the device and if the device is appealing for their customers. To achieve this, the device should be affordable, of high quality and have an attractive appearance.

Ergonomics

In order to be able to design a lifting aid for heavy objects it is crucial to understand what forces are allowed to be transmitted to the human body during use. Therefore an analysis is made to determine the best way for lifting heavy objects and how much this object is allowed to weigh. In addition to being safe and healthy, lifting with the device should also be comfortable. An effort is therefore made to find guidelines that specify how much stress on a particular body part is allowed before the user experiences discomfort.

Lifting heavy objects

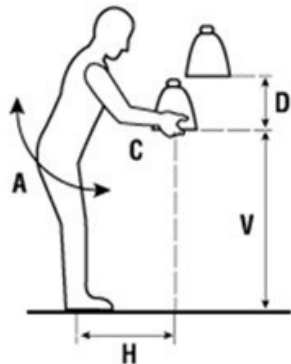


Figure 39 - Variables for calculating RWL (Middlesworth, n.d.).

Guidelines for heavy lifting have been around for a while and are aimed to reduce the risk of musculoskeletal disorders. Of these tools the NIOSH lifting equation is the most comprehensive. The equation around which the method is build can be used to calculate the maximum allowable weight and gives a score that indicates how much risk an average healthy employee has on developing an injury.

The equation is based on a lifting constant of 23 kg, which represents the maximum amount of weight a person is allowed to lift under ideal circumstances (Middlesworth, n.d.). This number is multiplied with a number of weighing coefficients (M) that can be determined by measuring the aspects listed below (Figure 39).

$$LC (51) \times HM \times VM \times DM \times AM \times FM \times CM = RWL$$

- H = Horizontal location of the object relative to the body
- V = Vertical location of the object relative to the floor
- D = Distance the object is moved vertically
- A = Asymmetry angle or twisting requirement
- F = Frequency and duration of lifting activity
- C = Coupling or quality of the workers grip on the object

The recommended weight limit (RWL) that comes out of the equation can be converted in the lifting index (LI) by dividing it by the 23. A number larger than 1, signals that the average employee runs the risk of developing an injury, while a number smaller than 1 means that the job can be accomplished without any health hazards.

A quick analysis whether furniture movers abide the NIOSH lifting equation shows however that this is not the case in all situations. Table 4, which lists the average weights of a number of household items, shows that some objects are too heavy even when lifted with two persons. This discrepancy has already led to a high number of health issues amongst professional furniture movers. Silverstein and Adams (2007) for example found that furniture moving companies belong to the top 5 of sectors with the most applications for worker's compensation due to work related musculoskeletal disorders of the neck, back and upper extremities.

Item description	Average weight (kg)
Bookcase	21
Large desk	27
Dining table	29
3-seater sofa	42
Fridge-freezer	51
Double wardrobe	55
Large cabinet	77

Table 4 - Average weight of furniture and appliances (FRN, 2009).

Design guidelines for comfortable lifting

Comfort is not only determined by the amount of weight that is lifted but, also by how the force is transmitted onto the body. Although there are no stringent rules about this, a number of design guidelines should be kept in mind.

When designing an ergonomic handle for an application that requires a firm grip a number of design guidelines need to be followed. These where abstracted from a checklist developed by Patkin (2001).

The length of the handle should be at least 10-15 centimetres to fit the width of the palm. The thickness of the handle has to be such that the thumb can just cover the

Ergonomics

index and middle fingers. For adult males this means the handle should have a diameter of around 3-4 cm. The shape of the handle can be slightly flattened and thickened in the middle to prevent sliding. To increase grip further the handle should have smooth grooves that fit the fingers (Figure 40). Sharp edges and protruding shapes should be avoided to prevent stress hotspots. Surface roughness may help to prevent sliding but should not be overdone.

In addition to handles for lifting, chapter 3.2 has shown that harnesses can be used to transfer forces to areas of the body that can handle more stress. Figure 41 shows such a harness in more detail. This particular harness has been designed by a team of scientists from the University of California to reduce neck, shoulders and back injuries sustained by heavy lifting. The harness features padded straps and supports that transfer the lifting force evenly over the shoulder and the lower back. According to Paskiewicz and Fathallah (2007) this reduces the probability of developing lower back disorder by about 40%.



Figure 40 - Ergonomic handle ("Backyard Gardening").



Figure 41 - Ergonomic lifting harness ("Grip System").

Conclusions

A number of things have been learned from the work done in this chapter. The stakeholder analysis has provided insight in the requirements that the user, client and reseller will demand from the suction adhesion device. What catches the eye when looking at this first set of requirements, is the importance of the device's ability to communicate the status of the adhesion process. This improves trust in the device's capabilities and makes the user more comfortable with lifting big and expensive items.

In section 3.2, market research showed what competing solutions are already available. It can be concluded that there are a couple of low-tech solutions that cost less than €50,-, but also a lot of high-tech devices that require an investment of thousands of euros. In between these two segments however no solutions could be found. It is therefore a good idea to design a device that fills this hole in the market.

The analysis of the use environment yielded important parameters that act as boundaries in between which the suction adhesion device has to function. It can be concluded that all substrates have more or less a similar amount of surface free energy. This value usually lies between 30-50 mJm⁻². Typical roughness on the other hand varies a lot more. Glass is by far the smoothest with a roughness of only 0.0006 µm, while the roughness of plaster can be as high as 400 µm.

The ergonomics surrounding heavy lifting have revealed a couple of interesting things. People working in the furniture industry have to frequently lift items that are heavier than what is considered safe. This leads to health issues by overloading the neck, shoulder and lower back. The ergonomic solutions found for this problem generally do not reduce the amount of force, but transmit it to the body in a better way. In this way the NIOSH limit, which assumes that items are lifted by hand, can be safely exceeded. Especially the use of lifting harnesses seems to be promising in order to reduce lifting related health issues.

All requirements that were encountered during the analysis of the problem have been concluded in the table on the next page. This list of requirements is used as a guideline for the design of the suction adhesion device and as a checklist to validate whether it meets all the demands.

Conclusion

Analysis section	Requirement	Specifications
1.	1. The suction adhesion device mimics natural suction adhesion systems	The suction adhesion device uses the 12 suction adhesion strategies.
3.1 and 3.4	2. The suction adhesion device significantly lowers the effort needed to lift difficult to handle objects.	Attachment and detachment within 5 seconds and no straps required. Provides stable attachment point. Abides to NIOSH lifting guideline and design guidelines for comfortable lifting.
	3. The suction adhesion device is easy and intuitive to operate.	Maximum of 5 buttons and no double functions.
	4. The suction adhesion device communicates the remaining adhesion time.	Using an interface that specifies the amount of adhesion time left in minutes.
	5. The suction adhesion device communicates the adhesion strength.	Using an interface that specifies the adhesion strength in kg.
	6. The suction adhesion device warns the user when it is about to let go.	Using clear audible and visible warning signals.
3.1 and 3.4	7. The suction adhesion device is mobile and easy to handle.	The device is cordless and has a maximum weight of 2.3 kg.
	8. The suction adhesion device is rugged and reliable.	The device survives drop from 2 meters, uses high quality components and is not susceptible to wear.
	9. The suction adhesion device does not require a lot of maintenance.	No lubricants or sealants that need to be refreshed and easy to clean.
	10. The suction adhesion device does not damage or contaminate the handled objects.	Does not leave behind any residue and distributes the adhesion force over the attachment area.
	11. The suction adhesion device has a modular platform with fixed interfaces and uses standardized components when possible.	-
	12. The suction adhesion device has an attractive appearance that fits the preferences of the target group.	-
3.1 and 3.2	13. The suction adhesion device should be affordable for the target group.	Retail price should be between €150,- and €800,-.
3.2 and 3.4	14. The suction adhesion device has to deliver a competitive level of performance.	The suction adhesion device has to be able to produce an isotropic adhesion force that is enough to lift 80 kg.
3.3	15. The suction adhesion device is able to adhere under all use circumstances.	Can adhere to surfaces with surface free energies between 30 and 169 mJm ⁻² , surface roughness between 0.0006 and 400 µm and maximum permeance of 1.67 µmPa ⁻¹ s ⁻¹ . Can deal with water, grease and dust. Functions under temperatures between -6 and 40 °C, humidity up to 49.8 g of water per kg of air and atmospheric pressures between 80 and 106 kPa.

Table 5 - List of requirements.

Conceptual design and design embodiment

In this chapter a design is created that fits the list of requirements that was developed in chapter 3. In order to determine the best design direction, first a number of conceptual designs are created. These are evaluated and the best design is elaborated into the final concept.

The conceptual designs are a result of an investigation that determines the functional structure of the suction adhesion device and the keydrivers behind the device. Together with the biomimicry strategies from chapter 1 these ideas are formed into three concepts. The concepts each tackle the problem from a different angle but use the same functional structure.

The concepts are rated based on the keydrivers, and the best concept is chosen for further elaboration. A large part of this elaboration consists out of the design and characterisation of the suction cup. A model is created that predicts the pulling resistances of the suction cup. In addition to this the pressure-drop underneath the suction cup and the sealing capabilities of the sealing rim are determined.

Although the suction cup design takes up a large portion of this chapter also effort is put into developing the system behind it. An impression of the final product is generated by determining what components are used, how they look like and what method is used to make or obtain them. This information is subsequently used to give a rough approximation of the costs to produce such a device. Also a proposal of a business plan around the suction cup device is presented to show that it can be made according to the requirements of the new circular economy paradigm.



Keydrivers

To get a deeper understanding of what the list of requirements asks from the suction adhesion device they are converted into keydrivers. These are the motives that lie behind the requirements and are a more abstract representation of what the stakeholders want from the device. Having a set of keydrivers makes it easier to create and evaluate concepts that have not yet been fully developed. This is because many requirements cannot be tested until after the system has been fully specified.

Total costs of ownership (TCO)

The total costs of ownership are an important keydriver that comprises all the monetary costs the owner has to make to buy and use the device. To make the device an interesting option for the potential buyers the TCO should be as low as possible. However other stakeholder, like the manufacturer and reseller will want to maximize profit by increasing the TCO. Therefore it is better to strive for a high ratio between the total benefits of ownership and the total costs of ownership.

Examples of costs that are associated with the ownership of the suction adhesion device are listed below.

Purchasing costs

The purchasing costs of the suction adhesion device will make up most of the TCO and is the amount of money that needs to be spent in order to obtain the suction adhesion device and all its required ancillaries.

Operational costs

The operational costs are all the costs associated with using the device. These are for example the costs of supplying the device with energy and the cost for maintenance and replacement of parts that have worn out.

Total benefits of ownership (TBO)

The total benefits of ownership need to be as high as possible to make sure that the user is satisfied with the device and that the manufacturer can ask a good price for his product. Tangible benefits that make an important contribution to the total benefits of ownership are the increase in efficiency, healthiness and safety during heavy lifting.

A furniture mover can expect that device allows him to work faster and more efficient. Another advantage that the device offers is its ability to make lifting more ergonomically responsible and safe, which translates into a lowering of the costs associated with work related injuries.

Performance (Pe)

Performance is where it all comes down to in the end. When the device is unable to perform at its intended level it becomes useless. A number of parameters are important when it comes down to performance. The device should for example provide enough adhesion and friction to lift the items that a furniture mover encounters during his work. A second important performance parameter is the time the device takes to attach and detach. When this takes too long the furniture mover is not able to work as efficiently as he wants.

Reliability (Re)

Just as in the animals discussed in chapter 1, the reliability of the generated adhesion is a key aspect of the device. This means that the user needs to be able to rely on the information that the device communicates at all times. When for example an estimated amount of adhesion is displayed, it has to be guaranteed that the device can provide this under all use circumstances.

Comfort (Co)

Most of the benefits listed under TBO only prove their worth after a longer period of use. Lifting injuries, like a hernia for example take time to develop. To make sure that the lifting device has a pleasurable use experience it should therefore also provide the user with an immediate advantage. This advantage is the increased comfort that the device offers over lifting with ones bear hands. The device therefore has to make sure that lifting forces are transmitted to the body in a comfortable manner.

Keydrivers

Ease of use (EoU)

Ease of use lowers the threshold for a user to be able to benefit from the advantages that the suction adhesion device offers. As the users of the device are often practically minded, the steps needed to use the device should be intuitive and few in number. Furthermore the device should provide the user with feedback in an understandable way that uses real world units like kilograms and minutes.

Universality (Un)

Even if the lifting device provides the ultimate use experience and makes lifting extremely comfortable it is worth only a small amount when its use is limited to a few applications. When for example only a quarter of all heavy household items can be lifted, it diminishes the value of the device greatly. Therefore the design of the device has to cater for as many applications as possible to make it worth the investment.

System behaviour

Before the concepts can be generated it is important to know what functions the device has to perform to comply with the list of requirements. Because these requirements are the same for all concepts they also share the same function structure. A schematic representation of this structure can be seen in Figure 43.

1. Attachment

The first phase in the function structure contains all the functions required for the suction cup to attach to the substrate.

1.1 Perform start-up check

A start-up check has to be incorporated into the suction adhesion device to make sure that it can be turned on and off while being attached to the substrate. If this is the case the system should automatically fetch the last pressure setting and compensate for any pressure losses during the period in which the device was switched off. Integrating a start-up check makes it possible for the user to switch the energy supply whilst the device is in use and allows the device to recover after a power outage.

1.2 Let user set required amount of adhesion

To increase the speed at which the device attaches and to prevent unnecessary energy consumption the user has to be able to set the required amount of adhesion. This setting is based on an estimation made by the user of the weight that has to be lifted. The function therefore makes use of the expertise of the user for determining the optimal settings for the device.

1.3 Calculate and remember required pressure

Because requirement 5 dictates that the interface is specified in kg, the device first has to translate the specified amount of adhesion into the required pressure differential. This pressure difference can be determined through controlled experiments and has to be such that enough adhesion is created under all use circumstances.

System behaviour

1.4 Detect when a seal is made

To prevent the suction adhesion device from switching on in situations where it is impossible to form a seal with the substrate, a function has to be incorporated that detects when the rim is in good contact with the substrate. Such a feature makes the suction cup self-selecting and diminishes unnecessary energy use.

2. Monitoring

Once the suction cup is attached to the substrate the device switches into monitoring mode. During this period the device keeps an eye out for any disturbances of the pressure differential and compensates for this accordingly.

2.1 Create the required pressure differential

At the onset of the monitoring phase the system has to create the pressure differential calculated in function 1.3.

2.2 Monitor the pressure differential

Once the set pressure has been achieved the device has to constantly keep watch and give a signal when either the pressure differential is too high or too low.

2.3 Calculate the amount of adhesion

This function calculates the amount of adhesion that is being generated in real-time by sensing the pressure differential underneath the suction cup and matching it to the amount of adhesion.

2.4 Communicate the amount of adhesion

To provide the user with feedback about the suction adhesion process the device has to communicate the amount of adhesion that is generated as a percentage of the set pressure. This means that at the beginning of function 2.1 the device is at 0% and climbs until it reaches 100% of the set pressure differential.

2.5 Detect when the device is about to let go

To ensure the safety of the user and the goods that are carried the device needs to give a signal when it detects that it loses its grip on the object. This is most likely preceded by a pressure spike or drop that cannot be attributed to the functioning of the device. By keeping an eye out for these events the device should be able to alert the user a few seconds before the suction cup falls off the substrate

2.6 Warn the user

When function 2.5 or 2.8 has detected a risk of detachment the user needs to be warned in a clear and unambiguous way. According to requirement 6 the warning signal has to be both audible and visible. This is to make the warning signal perceivable in situations with a high amount of ambient noise or when there is no clear line of sight between the user and the device.

2.7 Compensate for pressure loss

When the adhesion device is attached to rough or porous substrates pressure losses will accumulate over time as air re-enters the suction cup. The system therefore has to actively compensate to keep providing the set amount of adhesion.

2.8 Monitor the battery charge

When a user wants to move a piece of furniture it is important for him to know whether the device has enough energy on board to provide the required adhesion for the duration of the lift. Therefore the device has to monitor its own battery charge level to determine how much energy it still has in stock.

2.10 Calculate the remaining adhesion time

To calculate the remaining adhesion time and to comply with requirement 4 the device has to calculate the remaining adhesion time using data gathered in function 2.8. To do so the device will need to sample battery charge levels over a period of time and work out the rate of descent. The amount of adhesion time is determined by the speed at which the charge level drops and the minimum voltage at which the device is able to operate.

System behaviour

2.11 Communicate remaining adhesion time

This function makes sure that the user is informed about the remaining adhesion time and can act accordingly.

3. Detachment

The final phase of the function structure results in the detachment of the suction adhesion device.

3.1 Let the user detach the device

When the lift is completed the user will want to detach the device from the substrate. The device should therefore give the user this option using a clear and intuitive interaction.

3.2 Equalize the pressure differential

After the user has ordered to device to detach, the system needs to equalize the pressure underneath the suction cup. This will stop any suction adhesion from taking place.

3.3 Detach the suction cup

Even after the pressure differential has been reduced to zero there is bound to be some adhesion left due to molecular interactions between the suction cup surface and the substrate. Therefore the device has to create a positive pressure differential in order to pry the device from the substrate.

Concept generation

In this section multiple concepts are generated that explore the amount of freedom that is still possible within the constraints of the list of requirements and the function structure. To visualize the different starting points for the concepts a strategic space has been drawn in Figure 42. This figure shows the positions fulfilled by the concepts in a graph with two axes that correspond with important keydrivers. The horizontal axis represents the keydriver 'total costs of ownership' while the vertical axis represents the amount of automation used by the system. This corresponds to the keydrivers 'total benefits of ownership', 'performance', 'reliability', 'comfort' and 'ease of use'. To expand the strategic space some of the functions described in 4.2 are siphoned over from the device to the user, which makes the device less complex and reduces its cost.

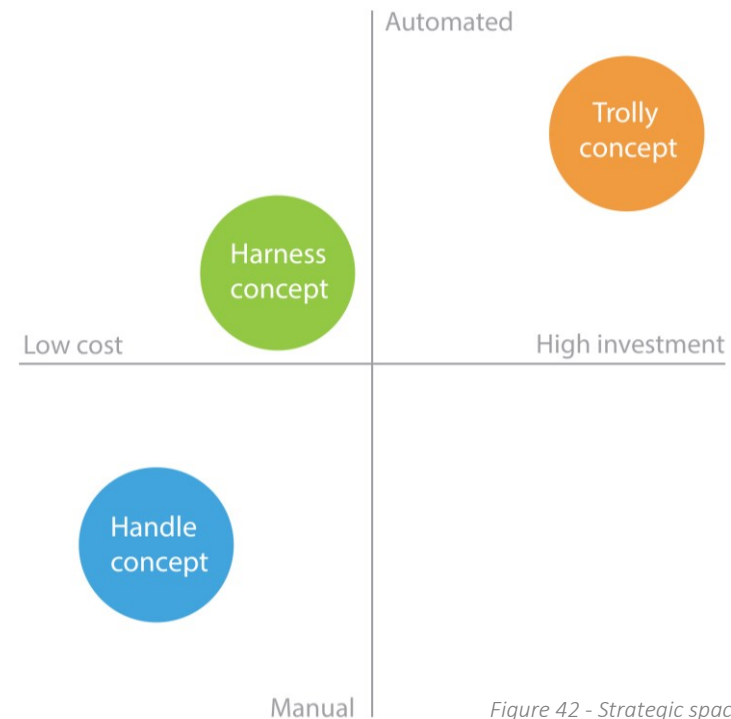


Figure 42 - Strategic space

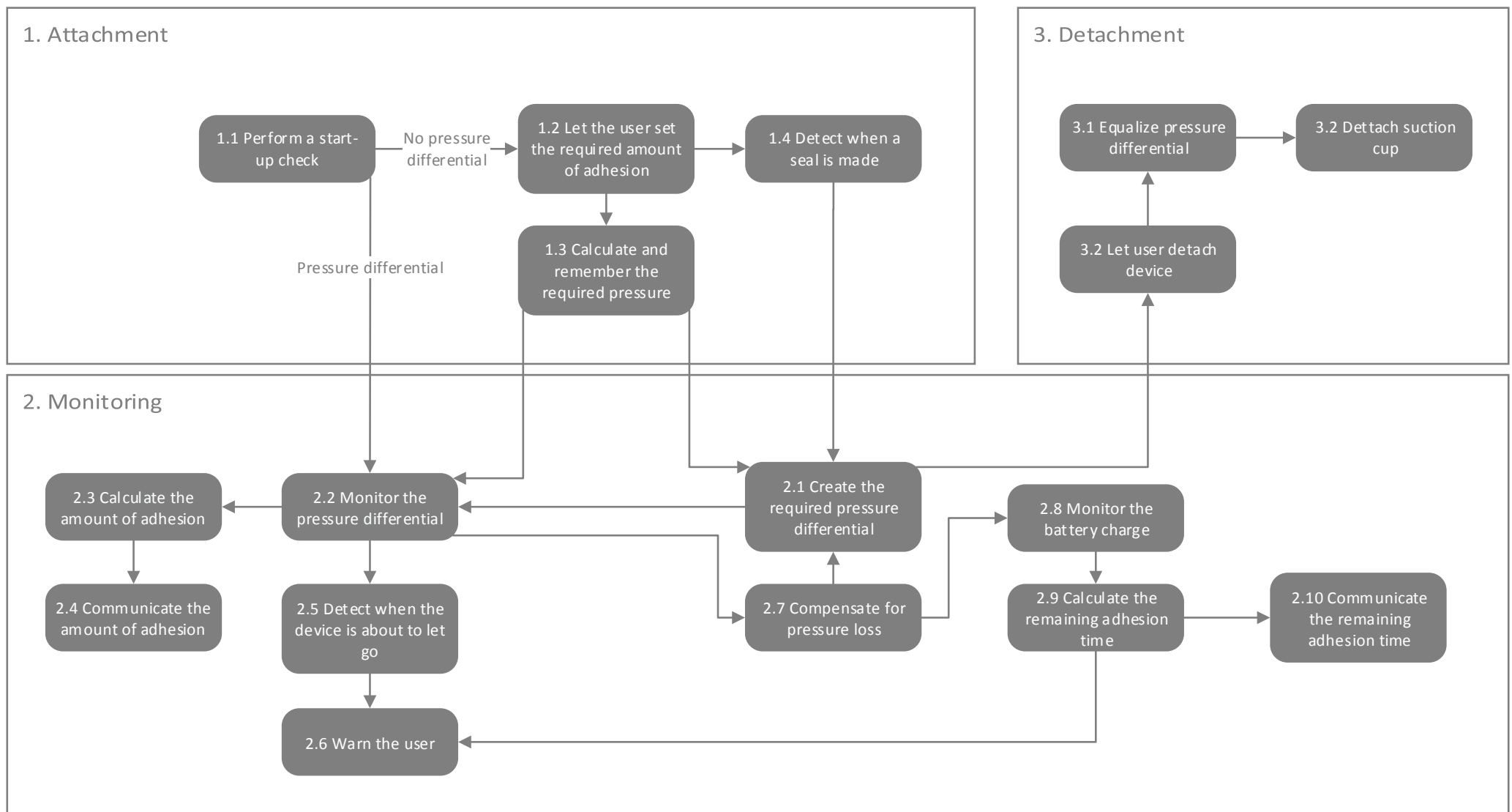


Figure 43 - Functional Block Diagram

Concept generation

Use scenarios

Conceptual designs can best be explained by imagining how they will interact with the environment and the user. Therefore each of the concepts is first placed in a scenario that explores the use of the suction adhesion device. These scenarios are complemented by a Functional Component Diagram and drawings of the product and its functionality. Together they form a comprehensive image of the envisioned concept.

Handle concept

The handle device is a concept that tries to minimize the investment costs by assigning some of the functions seen in Figure 43 to the user. In this case the user is responsible for function 1.4, 2.1, 2.7 and 3.2. As a result of this there is no need for the device to execute function 2.9 and 2.10, as most of the energy that is needed for the device to operate is provided by the user. Scrapping the mentioned functions means that the device only requires a simple system (Figure 45) from which the most expensive parts can be left out.

Today is the big day. Chris is finally moving to his new newly build house. However before he can enjoy his new dwelling he has to move his beloved furniture to its new location. As some of the pieces are quite heavy Chris has borrowed two pairs of suction cups from his local DIY store. These were recommended to him by a friend who had to move a few weeks before him. 'They make moving a breeze' he recalled him saying. Time to put that to the test then. Chris switches on the suction cup by sliding down the on/off button (Figure 44). The device comes to life and shows the amount adhesion that the last user entered into its memory. LEDs above the screen also light up and then fade out again to indicate that the device is ready to use. All devices are set to 12 kg which Chris estimates should be enough to lift the sideboard. He places one of the suction cups on the side of the closet and starts to pump the air out from underneath by pushing a few times on the hand pump that sticks out of the side of the device. One by one the LEDs above the adhesion display turn on to let Chris know how much he still has to pump to reach the required level of adhesion. After a few more pumps all LEDs are brightly lit up. Chris decides to give it a try. Together with his brother, who has attached another set of suction cups at the other side of the sideboard, Chris lifts the

closet from the ground. 'That is a lot heavier than I thought' Chris shouts at his brother. Fortunately the rubberized grips are very comfortable and give him more than enough grip to keep the sideboard from the ground. As they start to move however the sideboards starts to rock gently and one of the suction cups has decided that it might not generate enough adhesion to keep itself attached to the closet. A loud beep fills the room, which Chris intuitively understands is a sign that he needs to increase the pressure underneath suction cup. He presses a few times on the handpump which silences the alarm. To display the effect of the extra pumps the device has changed its setting from 12 to 18 kg and the LEDs give a rough estimation of the percentage of this reading that is currently being generated. To make sure that the alarm doesn't trip again Chris pumps the suction handles all the way to 15 kg. After that the lift goes according to plan and they reach the moving lorry without any problems. Once in place Chris detaches the suction cups by pushing a big button on the bottom of the device. This equalizes the pressure underneath the suction cup and makes it easy to detach the suction cup from the closet. 'Let's tackle the next lifting job.'

After a day of hard work all Chris's furniture has traded places from his old apartment to his new home. Time for a well-deserved beer. These are well worth the few quid in rent Chris's brother remarks. I don't feel as shot as I normally do after a day of moving.

■ HANDLE CONCEPT

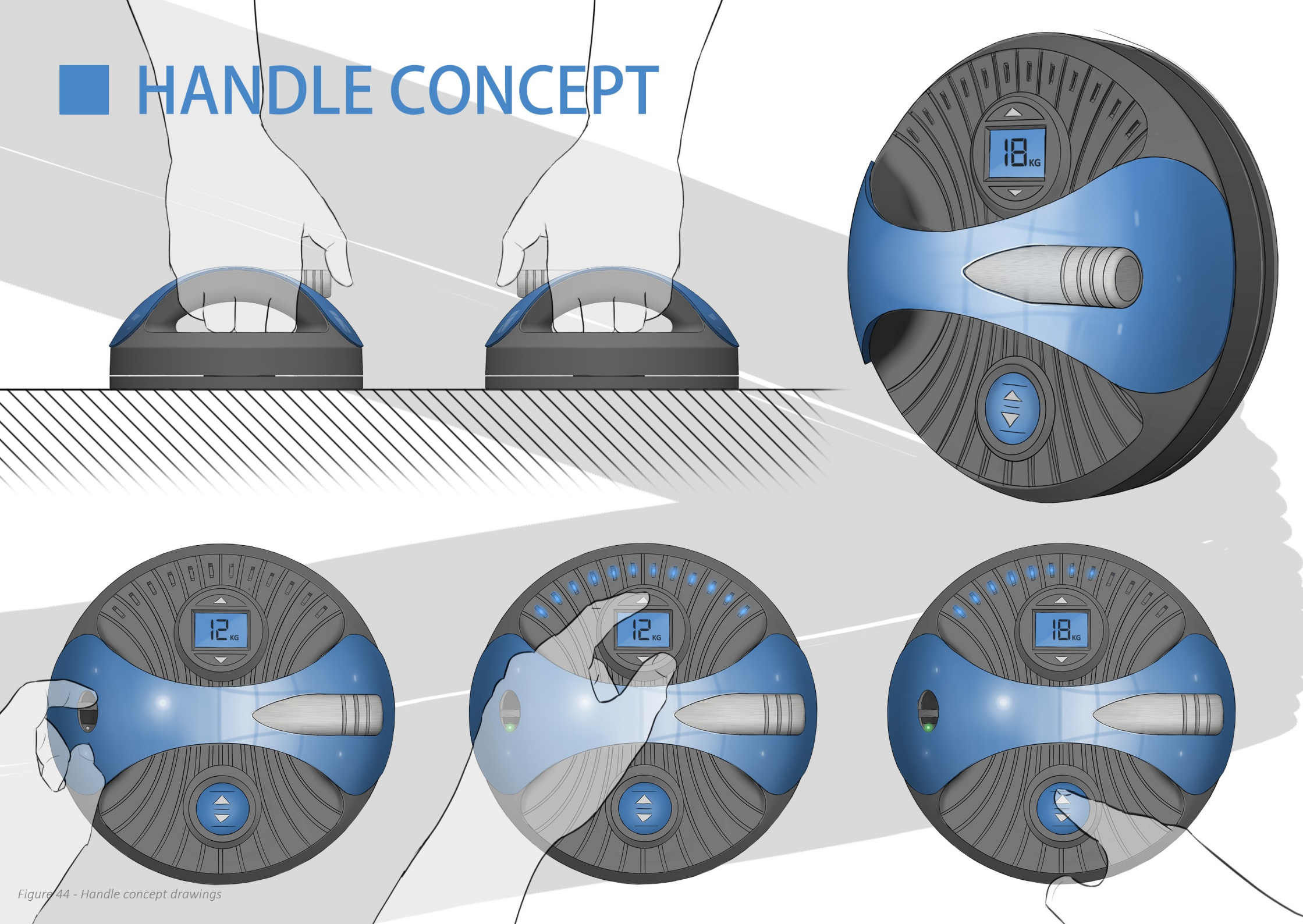


Figure 44 - Handle concept drawings

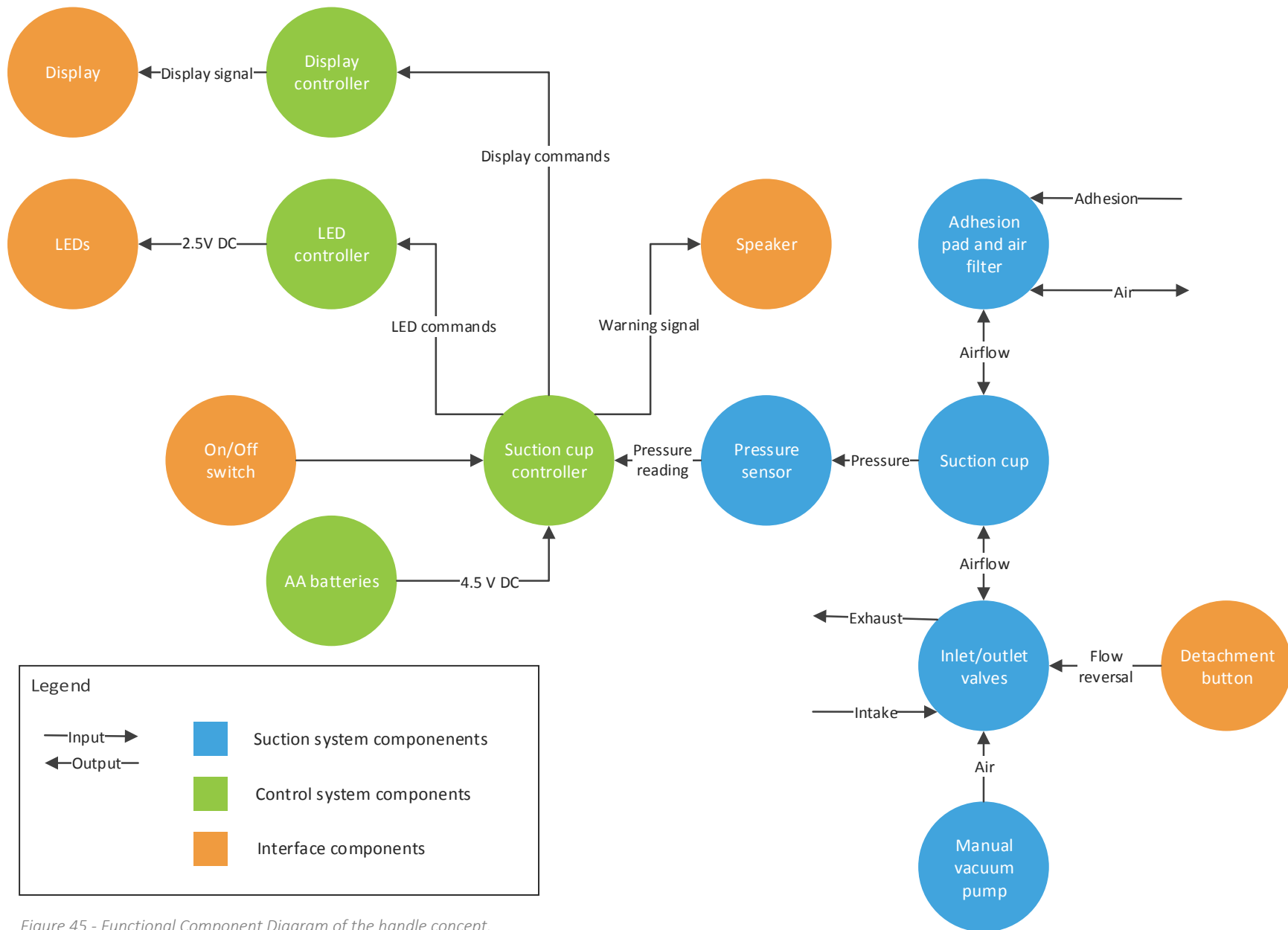


Figure 45 - Functional Component Diagram of the handle concept.

Concept generation

Harness concept

The harness concept is aimed at creating a mobile device that fulfils all the functions seen in Figure 43. This means that the concept requires a higher investment as it is inherently more complex (Figure 45), but also delivers better performance, safety and use comfort. To justify the higher total costs of ownership the device is aimed at professionals since they can use it more frequently. This increases the benefits associated with the system. Another strategy to improve the benefits of ownership is the incorporation of a lifting harness in the concept which is similar to the one shown in chapter 3.4. The use of a harness allows the user to lift objects that are above the NIOSH weight limit more safely by transferring the load to stronger areas of the body. The following scenario explains how the device is used and how it is able to provide the benefits mentioned in section 4.1.

Peter has been a self-employed furniture mover for almost 20 years. During this period his business has steadily grown. He now employs about 10 to 15 people depending on how much work is available. Throughout his career the moving business has been more or less the same. Although some furniture pieces like televisions have gotten lighter and smaller it is still a matter of bringing heavy pieces of furniture from point A to point B without damaging them. A few years ago Peter used to help his guys out during large jobs but due to a hernia he now manages his business from the office. Furniture moving is a back-breaking job and most of his employees have to stop doing it way before they reach their retirement age. This is a costly problem and it has forced Peter to look for ways to reduce injuries amongst his personnel.

Peter therefore decided to buy a set of powertools from a company that claims they can alleviate the problem. The kit consists out of a two self-powered suction cups and lifting harnesses. Today is the first time his team will use them and therefore Peter has decided to come along. After a short drive they arrive with their lorry at their client's apartment. The apartment is on the third floor, which means they will have to carry all the objects through a narrow stairwell.

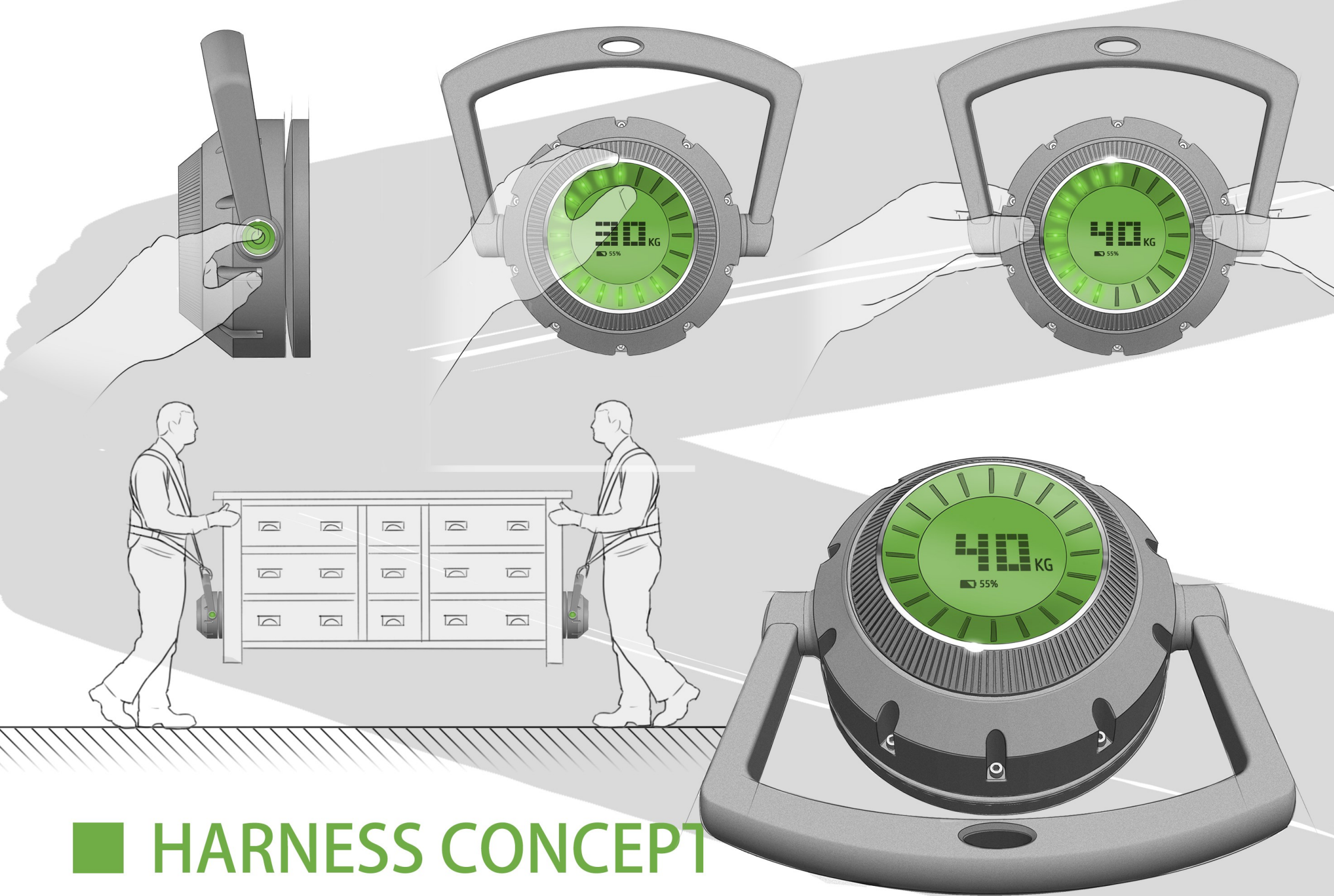
After introducing themselves to their client they quickly get going. First a medium sized wardrobe needs to be lifted. Two of Peter's employees strap on their lifting harness

while Peter explains how the suction cup works. 'First you turn this ring to set the device to how much you think the object weighs and then you push the suction cup onto the closet. If you place it correctly the suction cup will automatically start to suck itself against the surface. These LEDs show you how long it takes until the device reaches your required setting, but from what I've been told that shouldn't take too long.

When Peter's employee has finished putting on his vest he turns on his suction cup by pushing the on/off button, which is located on the side of the suction cup. When the device comes to life he turns it up to 40 kg by sliding the ring that surrounds the display. A number he thinks should be more than enough for this type of closet. 'How do you turn it on Peter?' the employee asks. 'Just push it onto the closet and it will turn on automatically' Peter replies. Peter's employee pushes the suction cup onto a flat section of the closet and the cup immediately begins to hum. Quickly the LED's around the display start the light up and after a few seconds the device has reached the intended pressure differential. 'I think we're good to go'. Both movers attach their lifting harnesses to the handle of the suction cup which requires them to squat down. When they rise again they lift the closet with their leg muscles and only have to use their hands to keep the object balanced. This gives the movers the freedom to unlock doors, give non-verbal directions with their hands and wave at attractive female passer-by's. A big advantage for any well respected mover.

After making their way down the stairwell, Peter's employees reach the van with the wardrobe and detach themselves from it by pushing the pressure settings ring downward (Figure 46). This releases the suction cup by pumping air back into the suction cavity. With their first successful lift completed, Peter's men move back to the apartment to tackle the next lifting job. For carrying light objects they use the suction cup's handgrips while heavier items are more convenient to carry by using the harness.

At the end of the day all items have been successfully moved to the clients' new home and on their way back Peter and his employees talk about their experiences with the device. 'I still feel as fresh as a daisy', one of Peter's employees remarks. 'These things really take the strain out of lifting.'



■ HARNESS CONCEPT

Figure 46 - Harness concept drawings

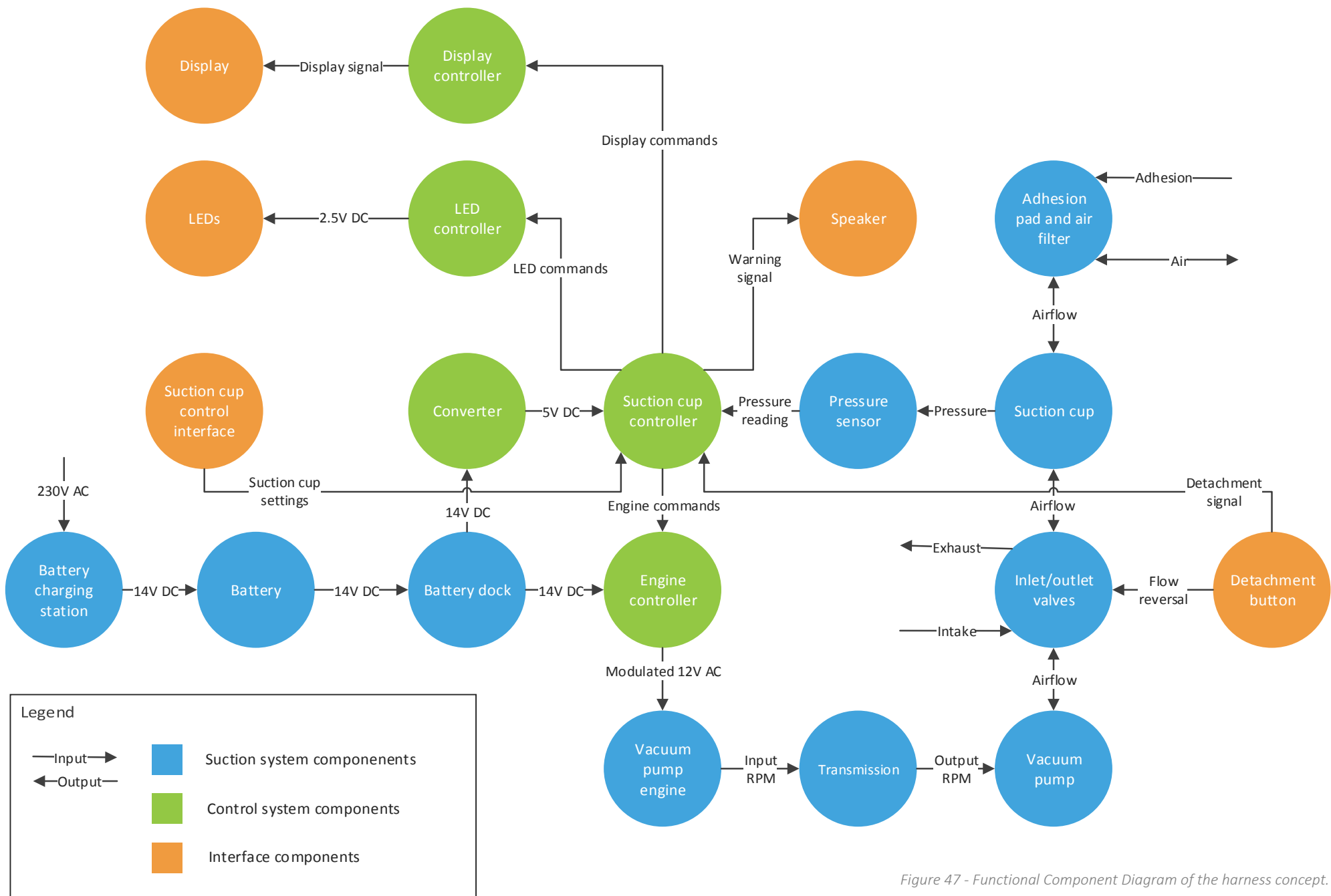


Figure 47 - Functional Component Diagram of the harness concept.

Concept generation

Trolley concept

The trolley system is intended to significantly reduce the stress of heavy lifting by taking over all physically demanding tasks from the user. The solution for this comes in the form of a lifting trolley that is similar to the Liftkar SAL and Stairmobil, but is outfitted with two suction cups. These suction cups produce a tight grip on the object that needs to be lifted and replace the troublesome task of wiggling spades underneath the object and securing it with straps. All this convenience does come at a price however as the trolley requires a complex system with many interacting parts (Figure 49). To show in which setting such a high investment can be justified the following scenario has been written.

Mary just started working at a distribution centre from a company that sells household appliances online and delivers them to their customers the next day. This means the company has had to set up their own distribution network that is able to efficiently deliver the heavy machines to customer's kitchens and utility rooms. In the early days the company had to send a delivery crew consisting out of two employees as the products were too heavy to be carried singlehanded. Now however the company has invested in top of the line lifting trolleys that can deliver the appliances anywhere the customer wants without any back breaking lifting. They also allow the company to reduce the amount of personnel needed as the trolley can be operated by a single person.

When she was hired, Mary never expected that she would be assigned to deliver the heavy household appliances sold by the company, as she didn't consider herself to be particularly strong. Her manager however convinced her that with their new trolleys this wouldn't be a problem and after a day of training Mary is able to move out for her for delivery.

The van Mary drives had been loaded up with a dozen washing machines and her lifting trolley. After having found a parking spot Mary climbs out of the cab and unloads the trolley. To grab the washing machine she is intended to deliver she moves the suction cups upwards by means of a winching system that is incorporated in the trolley. Then she pushes the cups against the side of the washing machine. As soon as the cups make

a good seal a valve opened and the air is sucked into one of the two vacuum storage tanks, which are incorporated into the suction cups. This storage allows the cups to attach instantly and therefore reduces attachment time. After the display on the handlebar of the trolley tells Mary that the suction adhesion has risen to the correct level, she lifts the washing machine with one push of a button and backs it out of the delivery van.

During the short walk to the customer's front door Mary notices that the large wheels smooth out any imperfections and make it easy to overcome small ridges. The next obstacle however will be a bit more challenging as the washing machine has to be delivered to an apartment on the second floor. Luckily the trolley has been equipped with a stairclimbing mechanism that helps her to traverse the stairs. After being greeted by a customer that is happy to receive his washing machine in such short notice, she starts the climbing engine. This moves a small wheel on the rear of the device downward, pushing the trolley upwards as it goes (Figure 48).

After having successfully delivered the washing machine to the clients utility space Mary is ready to head to her next address. This means she has to conquer one last obstacle which is to descend the stairs with the trolley. As the device contains a lot of heavy components, such as batteries and electric motors, the system is equipped with a feature that helps Mary to safely move downward. This is accomplished by using the stair climber as a brake that slows down the trolley during each step. This feature enables the trolley descent at a steady and controlled pace.

Pleased at how smooth her first delivery went Mary quickly starts up the van and heads toward the next address on her list.

TROLLEY CONCEPT

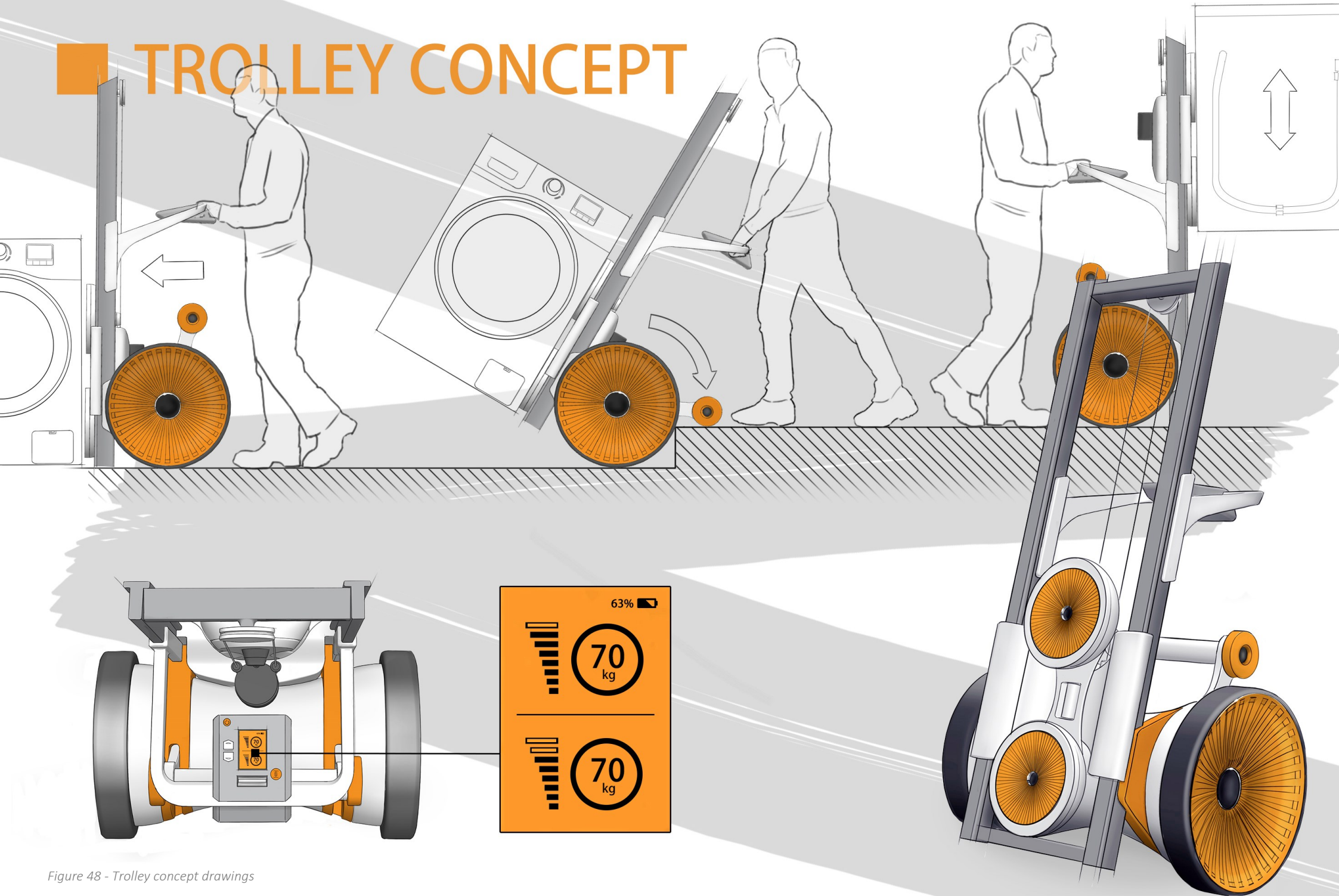


Figure 48 - Trolley concept drawings

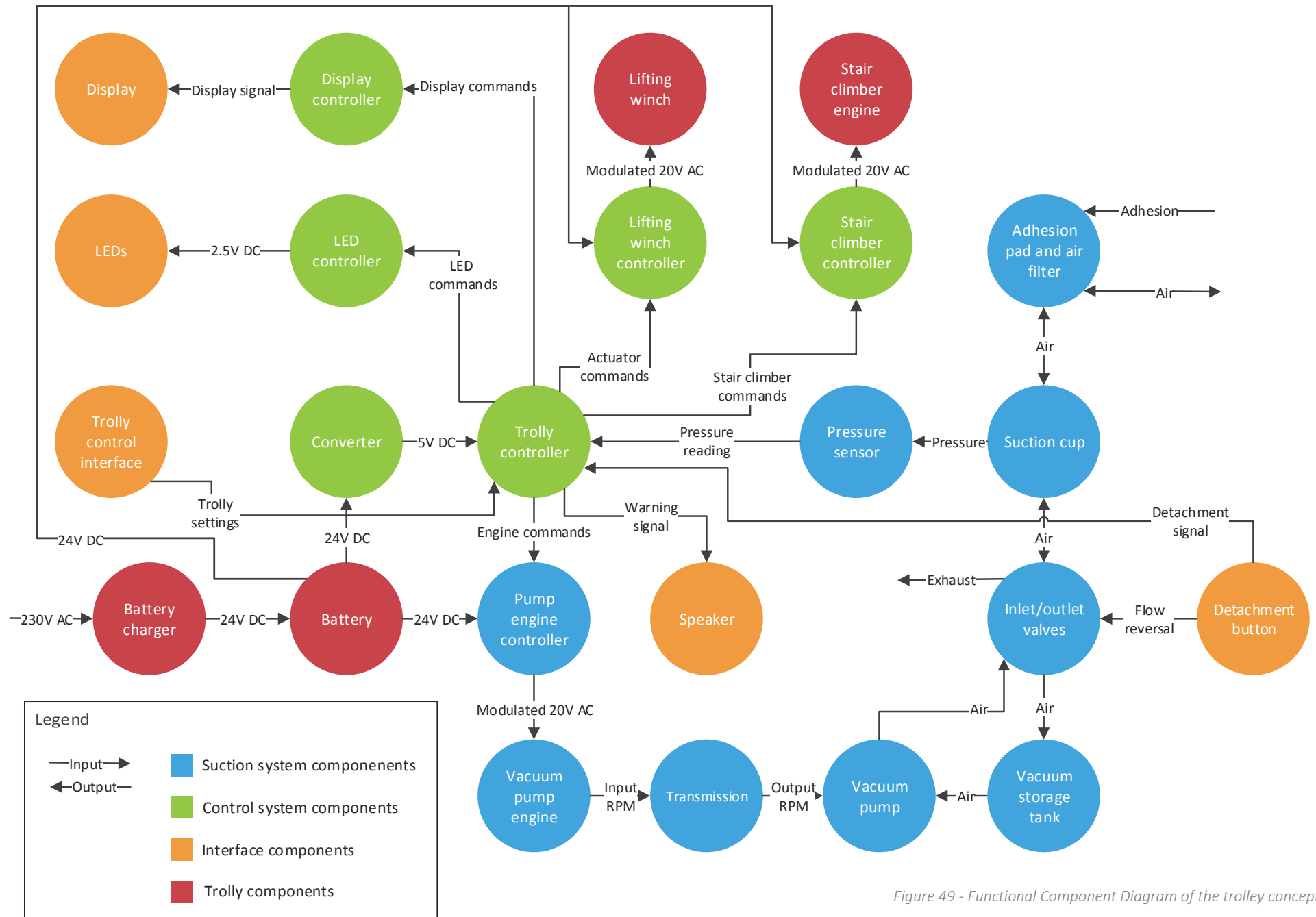


Figure 49 - Functional Component Diagram of the trolley concept.

Concept selection

Despite the fact that all the designed concepts show potential, only one of them is chosen for further development. To determine which of the concepts justifies this additional effort the most, they are rated using the keydrivers from chapter 4.1. The rating consists out of a score between 1 and 5. A five means that the concept complies fully with the keydriver, while a low score means that the concept lacks in this area.

When comparing the scores from the concepts with each other a number of conclusions can be made. Although the handle concept is an affordable device that due to its mobility can be used in a lot of different situations, it lacks in the area of performance and use comfort. This is because too many tasks are assigned to the user itself. The trolley concept on the other hand scores excellent on use related aspects, but loses points on total costs of ownership and universality. The trolley can only be used for heavy devices with a restricted footprint. A wardrobe for example would be too wide to lift with this kind of system. The high production costs will furthermore limit the market size for this concept to a handful of specialized businesses.

From the comparison it becomes clear that the harness concept is the most viable option for further development. The concept has a solid score on every keydriver and represents the best compromise between total costs of ownership and the degree of automation. The concept possesses the strength of being universally applicable and delivers excellent performance and reliability at a moderate amount of costs. It is therefore believed that the market size for this type of device is larger than for the other two concepts.

	TCO	TBO	Pe	Re	Co	EoU	Un	Total
Handle concept	5	3	2	2	2	2	5	21
Harness concept	4	4	5	5	4	4	5	31
Trolley concept	1	5	5	5	5	5	2	28

Table 6 - Concept rating: TCO= Total Costs of Ownership, TBO= Total Benefits of Ownership, Pe= Performance, Re= Reliability, Co= Comfortability, EoU= Ease of Use, Un= Universality.

Suction cup design

The first step in creating the final concept is to design the business-end of the device. This involves creating a suction cup that fits the list of requirements. To achieve this goal, a number of steps have to be taken. First a schematic design of the suction cup is created and the parameters that govern its design are declared. Secondly two free body diagrams are created. These give insight in the forces that the suction cup has to cope with. Subsequently a number of aspects of the suction cup are analysed. These subjects are based on the requirements that were declared in chapter 3.

The isotropic pulling resistance is determined to see whether the design can comply with requirement 14 and 15. Under all use circumstances the suction should be able to resist a pulling force of 80 kg. The impact of wear is furthermore investigated to make sure that requirement 8 is fulfilled. The reliability of the performance of the device should not be affected when wear sets in. Subsequently an analysis of the pressure drop underneath the suction cup is made to see whether to performance of the device is not negatively affected by air flow resistance in the system. This gives an important indication whether the device meets requirement 2. To verify that the design meets requirement 15, the sealing capabilities of the rim are studied. Finally the effects of a peel force on the suction cup are explored and an analysis of the strength of the suction cup is made. These last two sections do not belong to a particular requirement but are still a prerequisite for the device to function correctly.

Schematic design and design parameters

The schematic design is created based on the lessons learned in chapter 1. To illustrate this, the inspiration sources for each of the components of the suction cup are listed.

Soft sealing layer

The soft sealing layer (Figure 50) forms a seal with the substrate by conforming to its surface typography. In order to do this the polymer has to behave the same as the epithelium ring found on octopus suction cups. The parameters that govern this behaviour are listed in Appendix C.

Suction cup design

Adhesion and friction pad

The adhesion and friction pads are based on the infundibulum of the octopus suction cup and feature radial and circumferential grooves that distribute the pressure differential over the surface of the suction cup (Tramacere et al., 2014). The area in between the grooves is used to generate friction and adsorptive adhesion by conforming to the substrate. The design parameters that determine the behaviour of this component can be found in Appendix E.

Textile backing

To be able to resist the shear forces that are exerted on the adhesion and friction pad and the soft sealing layer they have a textile backing. This solution is inspired by work from King et al. (2014) who developed a simple but elegant reversible adhesive that is inspired by the gecko foot. They combined a soft elastomer that drapes over the substrate with a stiff fabric backing that absorbs the shear forces that are exerted on it. This solution can not only be seen in the gecko but is also found in natural suction adhesion systems. The Garra suction cup for example has a layer of connective tissue

just underneath its epidermis, which is anchored to the skeleton by a network of tendons (Saxena, 1959). In the schematic suction cup design the tendons are formed by the fabric itself which is anchored to a central base by clamping it down in a cup-shaped cylinder.

Closed foam ring

The backing of the sealing layer is bonded to a layer of closed cell foam that helps it to adjust its shape to the larger scale geometry of the substrate. In addition to keeping the air out from underneath the suction cup the foam layer also distributes the rim pressure evenly over the soft sealing layer. This layer therefore mimics the functionality of adipose tissue that can be found underneath the Garra suction cup (Saxena, 1959).

Supporting foam

The supporting foam is bonded to the adhesion and friction pad backing and fulfils the same task as the closed foam ring. It distributes the suction pressure evenly over the adhesion and friction pad.

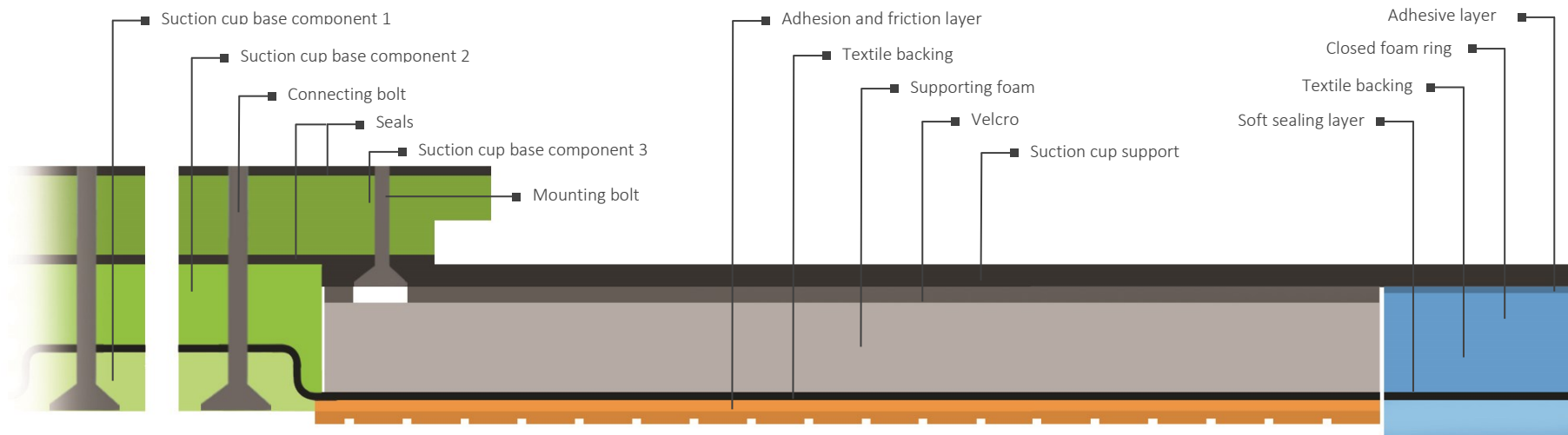


Figure 50 - Cross-section of the suction cup design.

Suction cup design

Velcro

To be able to replace and clean the adhesion and friction pad the supporting foam is bonded to a Velcro layer. Velcro was chosen because it is a reversible adhesive that is water resistant. Velcro is furthermore a great example of a reversible adhesive that is inspired by nature and therefore fits well with the intention of the suction adhesion device. A relatively weak adhesive like Velcro is possible since the connection between the layers is not loaded with any pull force during the functioning of the device. This is because the textile backing transfers any shear forces away from the adhesion and friction layer to the suction cup base. Forces perpendicular to the Velcro on the other hand are countered by the force that is the result of the differential in pressure between the atmosphere and the underside of the suction cup.

Adhesive layer

Just as the adhesion and friction pad the soft sealing layer has to be replaceable when it wears out. Therefore the closed foam ring is bonded to an adhesive tape. Tape was chosen as Velcro cannot be used in this instance due to its air permeability.

Suction cup base

The suction cup base forms the anchor for the textile backing and transmits all the friction and adhesion that is generated to the body of the suction adhesion device. The suction cup base is constructed out of three components. The bottom two components form a cup shaped clamp that locks the textile backing in place. The third component of the suction cup base connects this contraption to the housing of the device and is separated from the other two components by a seal. This makes sure that an airtight connection is created between the top and bottom halve of the suction cup base.

Suction cup support

The suction cup support prevents the closed foam ring from buckling in or outward but still allows it to flex up and down. The combination of these constraints is inspired by the skeletal structures that can be found in pelvic suction cups. The flexibility of the suction cup support furthermore gives the cup the ability to convert a detachment force into additional suction. This conversion mechanism is similar to the mechanism found in clingfish, as it allows for partial detachment without breaking the seal of the

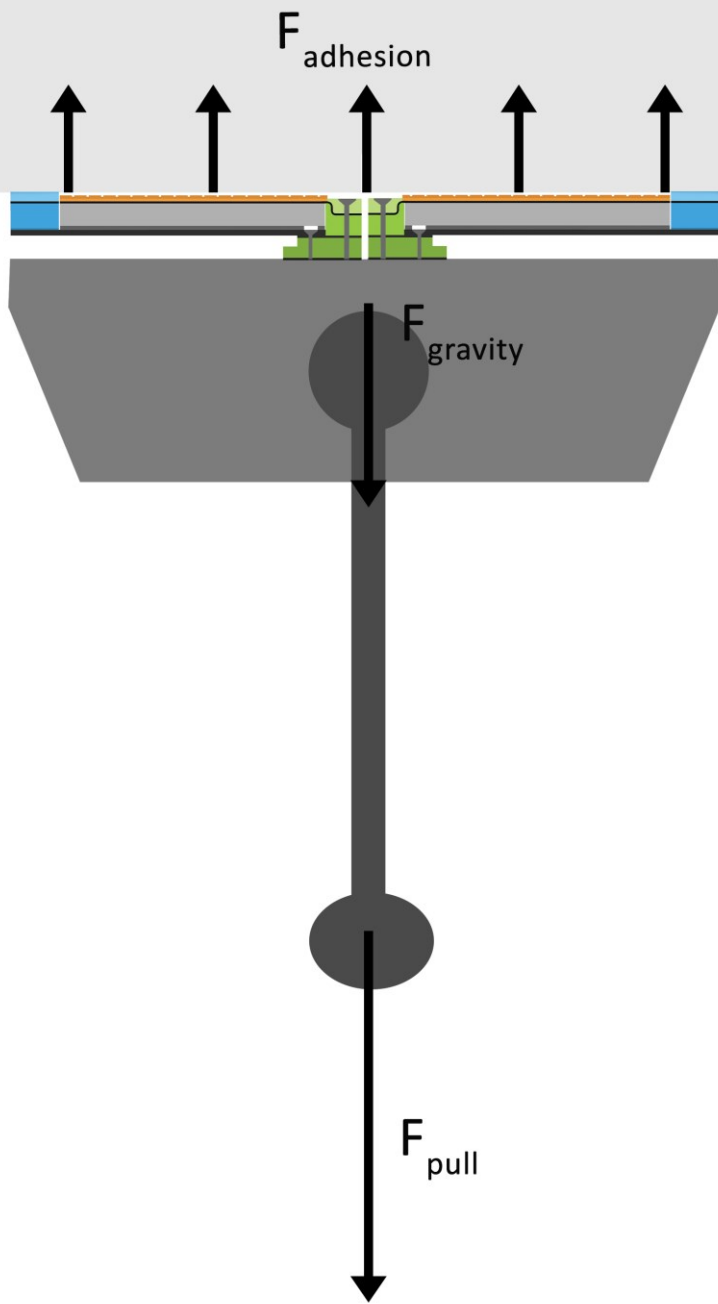
rim. The resulting increase in volume translates in a pressure spike that prevents full detachment.

Seals

Two seals at the top and bottom of suction cup base component 3 make sure that an airtight connection can be achieved between the suction cup base, the suction cup device and the suction cup support. Having a seal in between these components makes it possible to replace the entire suction cup or just the adhesion and friction pad.

Connecting bolts

The connecting bolts create a sturdy connection between the top and bottom halve of the suction cup base. These bolts need to be undone in order to replace a worn adhesion and friction pad.



Free body diagrams and force equations

To get an idea of the forces acting upon the suction cup two free body diagrams have been constructed. The scenarios chosen for these diagrams are based on requirement 14, which states that the suction cup has to produce an isotropic lifting force. Therefore the device has to be able to resist the same pulling force coming from both the perpendicular (Figure 51) and parallel (Figure 54) direction. All situations in between these pulling directions can be determined by projecting the pulling force vector on the x and y axis.

From Figure 51 the following force equations for perpendicular pulling can be derived.

$$(1) \quad \sum F_y = F_{adhesion} - F_{pull} - F_{gravity} = 0 \rightarrow F_{adhesion} = F_{pull} + F_{gravity}$$

Doing the same for Figure 54 yields the equation below for the parallel pulling situation.

$$(2) \quad \sum F_y = F_{friction} - F_{pull} - F_{gravity} = 0 \rightarrow F_{friction} = F_{pull} + F_{gravity}$$

$$(3) \quad \sum M_A = M_{peel} - \int_A^{l_2} l_2 F_{adhesion} dx = 0 \rightarrow \frac{1}{2} l_2 F_{adhesion} = l_3 F_{gravity} + l_4 F_{pull}$$

From the parallel pulling equations can be seen that in addition to forces in the Y direction also moments around the suction cup edge play a role. This is because the mounting point for the handle is not positioned straight above the friction pad. A peel moment is therefore generated which needs to be countered by the adhesion forces generated by the suction pad. The maximum peel force that the adhesion and friction pad needs to overcome is felt by the edge of the pad and depends on the ratio between l_4 , l_2 , l_3 and the magnitude of the forces.

Isotropic pulling resistance

To meet requirement 14 it is important that the suction pad generates equal amounts of friction and adhesion when placed in the situations sketched in Figure 51 and Figure 54. This can be tuned by varying the ratio (R) between the total contact surface ($A_{contact}$) and the surface area exposed to reduced pressure ($A_{pressure}$).

Figure 51 - Free body diagram with perpendicular pulling

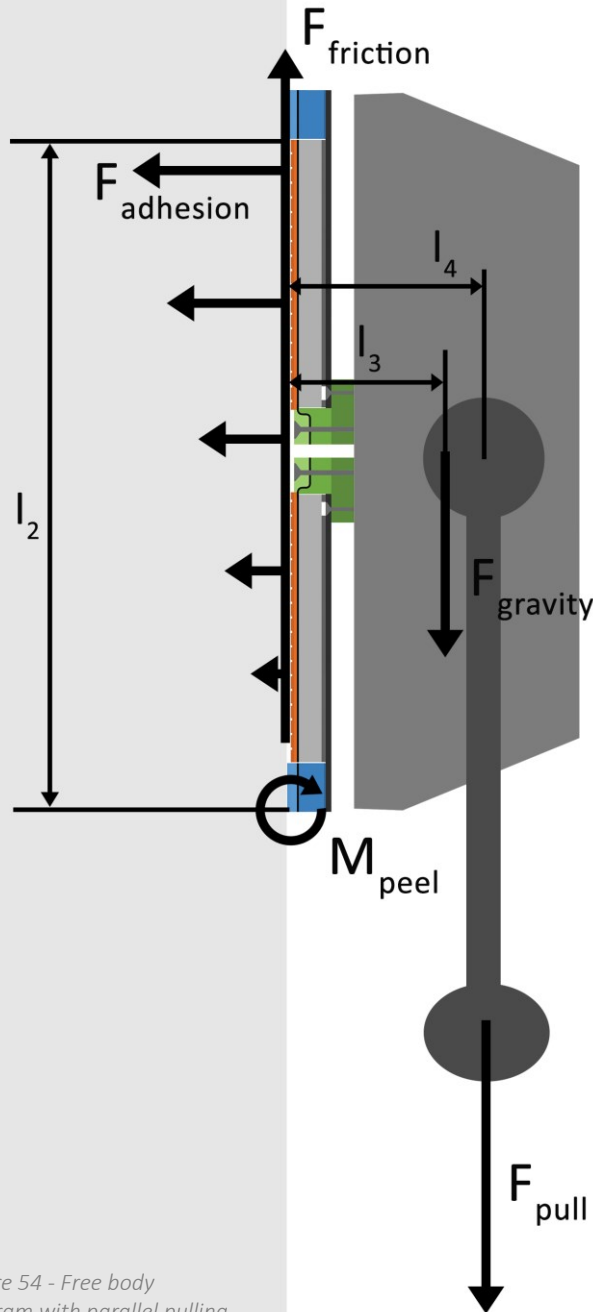


Figure 54 - Free body diagram with parallel pulling

For a suction cup with a structure as seen in Figure 50 the following equations can be used.

$$(4) R = \frac{A_{\text{contact}}}{A_{\text{pressure}}}$$

$$(5) A_{\text{total}} = A_{\text{pressure}} + A_{\text{contact}}$$

This means that the surface of the adhesion and friction pad is always used optimally. Surface area that is not in direct contact generates suction adhesion, while surfaces that are in contact contribute to friction and adhesion via intermolecular interactions. To determine the isotropic pulling resistance the formulas for both adhesion and friction need to be specified.

The adhesion force generated by the adhesion and friction pad consists out of two components. These are the adhesion forces generated by the pressure differential (F_{suction}) and adhesion forces due to adsorptive interactions between the pad and the substrate ($F_{\text{adsorptive}}$). In this model any adsorptive adhesion generated

by the sealing ring is not taken into account, as it is most likely negligible.

$$(6) F_{\text{adhesion}} = F_{\text{suction}} + F_{\text{adsorptive}}$$

The force generated by suction adhesion can be calculated using the simple formula below, in which ' Δp ' is the pressure differential relative to the atmospheric pressure.

$$(7) F_{\text{suction}} = \Delta p A_{\text{pressure}}$$

Calculating the amount of adsorptive adhesion created by the adhesion and friction pad is more complicated and requires detailed information about the pad's geometry. As stated before the aim of the adhesion and friction pad is to mimic the functionality of the infundibulum of the octopus sucker. To achieve this, the pad needs to at least contain the radial and circumferential grooves that are characteristic of the octopus sucker. An easy method of creating such features is with the help of a laser engraving system. These systems have become widely available in recent years and are able to create low cost moulds with highly detailed patterns.

For the production of the adhesion and friction pad a CO2 laser engraving system is used to carve a pattern of grooves into a sheet of acrylic glass.

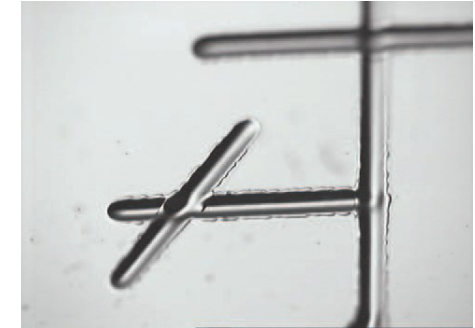


Figure 52 - Grooves in acrylic glass created with CO2 laser engraving system.

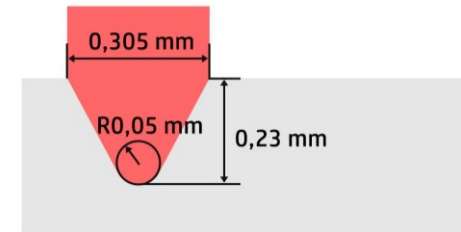


Figure 53 - First pass of the laser.

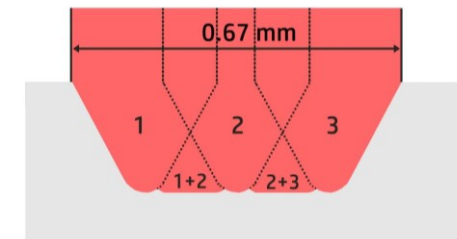


Figure 55 - Cross-section after three passes

(PMMA). The combination of using a CO2 laser engraving system and acrylic glass was chosen because it results in very smooth grooves (Figure 52). This is due to the fact that acrylic glass is one of the few polymers that vaporize instead of melt when engraved with a laser (Snakenborg and Kutter, 2003).

Using information provided by a study from Snakenborg and Kutter (2003) the following strategy for creating a grooved adhesion and friction pads was developed.

To create areas of contact multiple passes by the laser create flat debossed areas as seen in Figure 56. The flat areas in the cross-section are due to the irradiance distribution of the laser beam. Where the beams overlap the depth of the individual cuts can be added together (Figure 55). To vary the ratio between contact and pressure surface the space in between the debossed areas can be varied, or the debossed areas can be widened by using more laser passes.

In an attempt to keep the distance between the radial grooves more or less constant, they split near the middle into two separate grooves (Figure 57). The size of these grooves before and after they split is determined on page 82 and depends on the pressure drop they create due to their resistance to air flow.

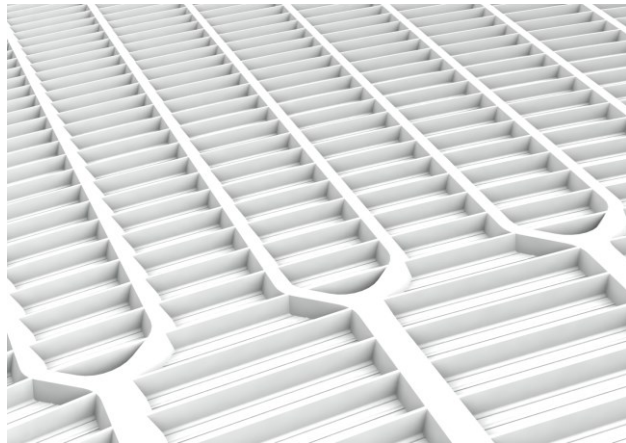
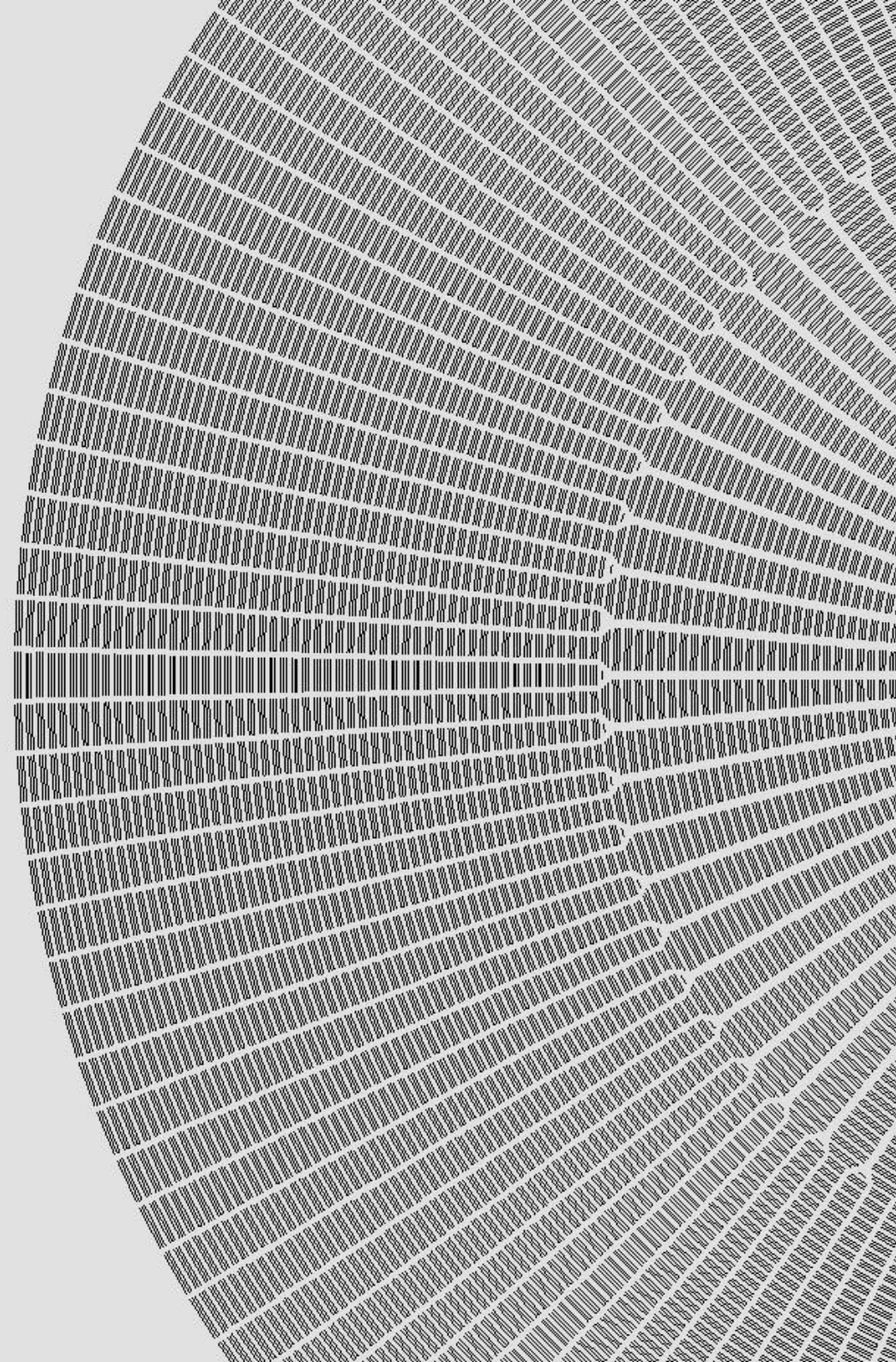


Figure 57 - The paths required to make the textured mould.

Figure 56 - Close-up of the mould's groove structure.



Suction cup design

Now that the geometry of the adhesion and friction pad is known an attempt can be made to estimate the adsorptive adhesion that can be created using this pattern. For this attempt the JKR method of predicting adhesion is used. This method was chosen as it is specifically developed to calculate the amount of adhesion between large and soft surface features. The cross-section seen in Figure 55 however is not a shape for which JKR equations exist. It therefore needs to be decomposed in a number of sections. By calculating the amount of adhesion for each section, a prediction can be made for the total adhesion generated by the pattern. A downside to this strategy is that interactions between the different sections are not taken into account.

In Figure 58 can be seen how the cross-section of the pattern can be decomposed in JKR eligible shapes. It was chosen to approximate the shape of the pattern with three half- space cylinders (C1, C2, C3) and two flat planes (P1, P2). By adding the adsorptive adhesion of all elements, the total adsorptive adhesion force generated by the pad can be calculated. In this formula 'p' is the number of times the pattern is repeated across the surface of the pad, 'i' the ranking number of the cylinder and 'j' the ranking number of the plane.

$$(8) \quad F_{adsorptive} = \sum_{i=1}^{p_1} F_{c,i} + F_{p,j}$$

The maximum force sustained by each of the half-space cylinders can be calculated using a formula provided in the work of Chaudhury and Weaver (1996), which states

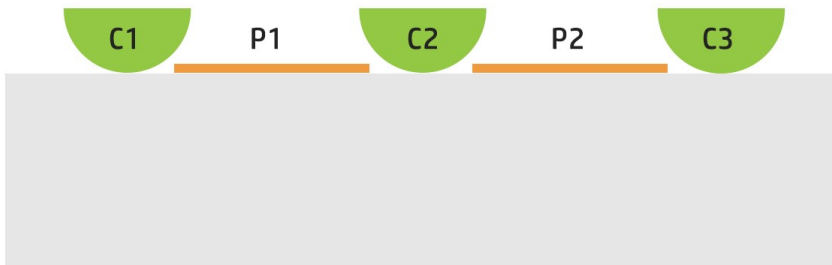


Figure 58 - Decomposed cross-section

that the pull-off force of a soft cylindrical contact from a rigid flat plane can be calculated with equation 9. Any adhesion interaction outside of the contact surface area is ignored in this model, which is an assumption that lies at the roots of the JKR theory.

$$(9) \quad F_{c,i} = 3.16l(KW^2R)^{\frac{1}{3}}$$

In this equation 'K' is the stress intensity factor, 'W' the work of adhesion, 'R' the radius of the cylinder and 'l' is its length. 'W' and 'K' are the two unknowns, which need to be calculated. The stress intensity factor 'W' can be acquired using:

$$(10) \quad K = \frac{4E^*}{\pi a} \quad (11) \quad \frac{1}{E^*} = \frac{1 - \nu_2^2}{E_2} + \frac{1 - \nu_s^2}{E_s}$$

In the left formula 'E*' is the compounded elastic modulus of the two interacting surfaces, which can be calculated by using the formula on the right. In this second formula ' ν_2 ' and ' E_2 ' are the Poisson's ratio and Young's modulus of the adhesion and friction pad. ' ν_s ' and ' E_s ' are respectively the Poisson's ratio and Young's modulus from the substrate.

The work of adhesion, which is the other unknown in the pull off pressure formula, can be determined when the surface free energy of the adhesion and friction pad ' γ_1 ', the substrate ' γ_s ' and their interfacial surface tension ' $\gamma_{1,s}$ ' are known.

$$(12) \quad W = \gamma_1 + \gamma_s - \gamma_{1,s}$$

Although there is no JKR formula for calculating the force needed to separate two flat planes, Kendall (1971) does give a description for removing a rigid cylindrical punch from a soft substrate. Also in this model the adhesion interactions outside of the contact area are ignored. The equation for the pull-off force of such a feature can be calculated using:

$$(13) \quad F_{punch} = \sqrt{\frac{8\pi a^3 W E}{1 - \nu^2}}$$

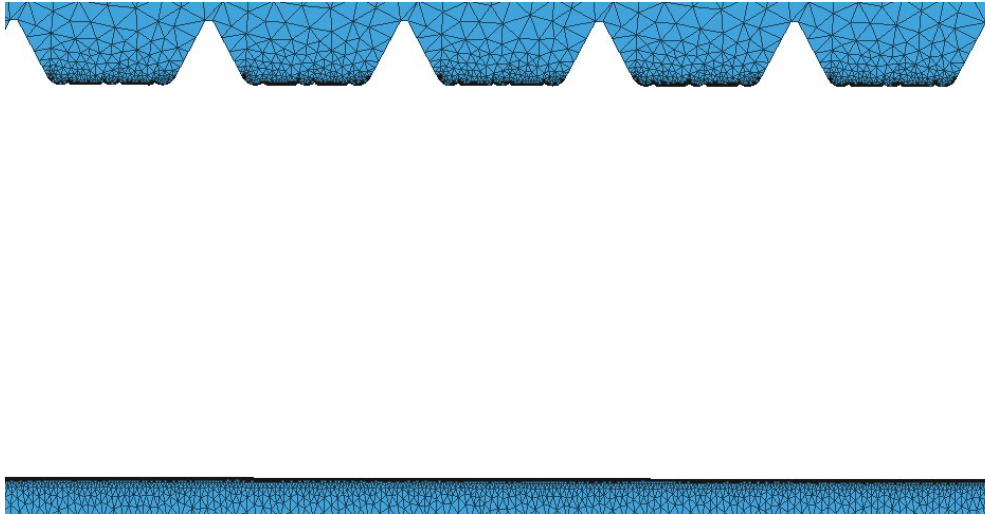
Suction cup design

Since the contact area of the planes is characterized by a donut shape, the pull-off force of this section can be calculated by subtracting the force formed by a punch with the inner boundary of the donut ($r_{p,j,i}$) from the force generated by a punch with the outer diameter of the outer donut. Combining the formulas for the pull-off force of these features leads to the equation below.

$$(14) \quad F_{p,j} = \sqrt{\frac{8\pi^2 r_{p,j,o}^3 W E_2}{1 - \nu_2^2}} - \sqrt{\frac{8\pi^2 r_{p,j,i}^3 W E_2}{1 - \nu_2^2}}$$

Since the dependencies for adhesion have been fully defined only the influences on friction still need to be explored. Normally friction is calculated using the normal force and the friction coefficient. However for this instance it is more convenient to choose an alternative route. Friction for the adhesion and friction pad can be determined when both the true area of contact and the interfacial shear strength of the system are known. If it is assumed that there is no friction due to elastic or plastic deformation taking place the friction equation can be written as:

$$(15) \quad F_{friction} = A_{real} \tau$$



Finite element simulations

With the mental model of the suction cup completed, it needs to be determined whether this structure fits the requirements for the suction adhesion device. Since the suction cup has a complex structure with many layers and intricate details it was chosen to use a finite element model to calculate the behaviour of the system. This model was created and simulated with the finite element software that is embedded in Solidworks 2014.

To be able to achieve the resolution necessary to see the deformation of the microstructure of the adhesion and friction pad, it was decided to make a 2D simplification of the suction cup. This choice was made since almost all features of the suction cup with the exception of the radial grooves are axisymmetric. Since not all features require a very detailed element mesh, the element size was varied across the different components. Figure 59 shows this difference. The smallest elements in the mesh can be found near the edge of the microstructure and have a size of approximately 5 μm . The largest elements used in the model have a size of 0.5 mm and can be found in the support structures of the suction cup (Figure 59). To complete the

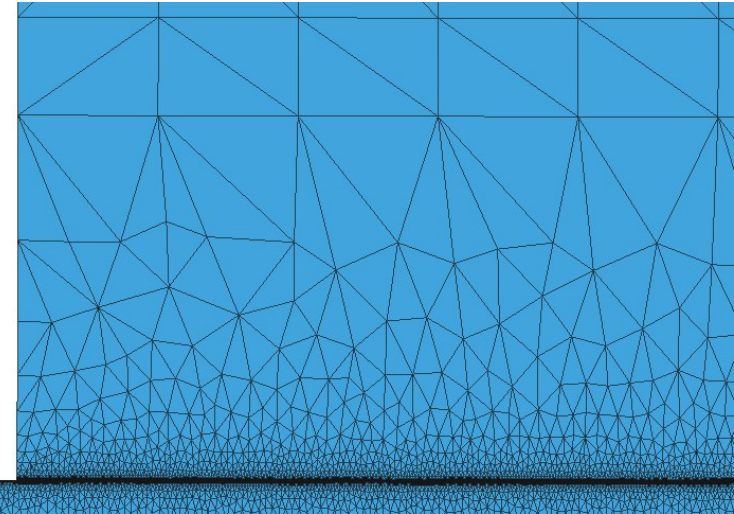


Figure 59 - Element mesh close-up.

Suction cup design

finite element model, each component is assigned material properties. Therefore a suitable material was chosen for all parts of the suction cup.

Soft sealing layer

The soft sealing layer of the suction cup is made from polydimethylsiloxane (PDMS), a silicon based rubber. This material was chosen because of its high wear resistance and its tunability. By varying the curing temperature (Johnston et al., 2014), the amount of hardener (Wang, 2011) and the mixture between different types of PDMS (Palchesko, 2012), the Young's modulus of the material can be varied from a few kilopascal to multiple megapascals. To make an educated guess about the softness required for the soft sealing layer, results from a study by Tramacere et al. (2013) were used. From their work can be concluded that the suction cup surface of an octopus is very soft and has a mean elastic modulus of 7.7 kPa. To put this in perspective, human skin has an elastic modulus of around 150 kPa. In combination with results from the sealing requirements analysis on page 44 it was decided to go for a soft sealing layer with a Young's modulus of 10 kPa. Such a material can be made by mixing two commercially available PDMS types together. Sylgard 184 with 10% hardener has to be mixed with Sylgard 527 at a ratio of 4 to 125 and cured for 12-24 hours at 65°C to obtain the required material properties. Although there is no data available about the Poisson's ratio of this material it can be determined by assuming that the material is non-compressible. This assumption means the behaviour of the material can be simulated by setting the ratio close to 0.5. The material parameters for the soft sealing layer and the rest of the used materials can be found in Appendix E.

Adhesion and friction pad

The material selected for the adhesion and friction pad is also a PDMS based rubber. Arguments for this decision are once again the material's high wear resistance and tunability. However, also the fact that the material can reproduce highly detailed surface geometries without the need for a release agent is an important reason to choose for this type of material. The material parameters for the adhesion and friction pad are based on a study from King et al. (2014). They tested a similar elastomer, textile composite as used in the design of the suction cup and found that an elastomer with a Young's modulus of around 1 MPa yields the best results when it is applied to a

multitude of real world surfaces like aluminium and painted drywall. If the pad is any harder it is unable to conform to rough surfaces, while a very soft elastomer fails to transmit the generated friction forces to the textile. The mechanical properties of the PDMS based rubber have been extracted from the study conducted by Johnston et al. (2014). They measured a Young's modulus of 1.32 MPa on a sample made from 10 parts Sylgard 184 that was mixed with on part curing agent and left to set for 48 hours at a temperature of 25 °C.

Textile backing

The selection of the textile backing is based on a number of criteria. First of all the textile needs to have a high tensile strength to be able to transmit the generated friction forces to the base of the suction cup. Secondly it needs to be flexible to be able to drape over the substrate.

These criteria led to the choice for an aramid fibre textile. This material boasts both an extremely high tensile strength and a high degree of flexibility. The characteristics of the fibres that make up this textile are obtained from work by Quintanilla (1999) and the assumption that the material is non-compressible.

Closed foam ring

As the name suggests the most important properties of the closed foam ring are that it is impermeable to air and compressible. Since the closed foam ring has to mimic the adipose tissue underneath the suction cup's contact surface, it needs to be as soft as possible. One of the softest types of closed foam that is available is closed cell neoprene foam. A material that is made from neoprene rubber riddled with small cells containing nitrogen gas. Unfortunately it is difficult to get reliable information about parameters like the Young's modulus and the Poisson's ratio for this type of material, as it behaves non-linear. However for small deflections the Young's modulus can be derived from the shore hardness of the material. For soft materials this is usually expressed on the shore A or shore-OO scale. For shore-A values higher than twenty the following expression can be used to accurately calculate the Young's modulus (Reuss, 2011).

$$(1) \quad E_4 = e^{0.0235S_a - 0.6403}$$

Suction cup design

The shore-A value of closed-cell neoprene foam is 12.5 ("Celrubberplaat CR") and therefore doesn't comply with the requirements for using the formula above. However since there is no conversion formula for shore-OO scale values it was decided to use the value provided by the shore-A conversion equation as an approximation of the Young's modulus. In the future however this value has to be replaced by a stress/strain curve that describes the behaviour of the foam more accurately. Also the Poisson's ratio for this material is estimated because there is no information available regarding this aspect of the material. In a study by De Vries (2009) which investigates the behaviour of polymeric foams, it is stated that the expansion of closed-cell foam during compression is negligible. The Poisson's ratio can therefore be assumed to be zero.

Supporting foam

The supporting foam of the suction cup is made from the same foam as the closed foam ring. Closed-cell foam was chosen for this component since foam with an open structure is crushed when the air is sucked out from underneath the suction cup. This results in an unfavourable pressure distribution and furthermore increases the time needed for the suction cup to attach and detach.

Velcro

Velcro is a combination of two paired surfaces. One contains numerous hooks and is generally made from polyester or nylon. The other contains an array of woven loops and is made from Nomex. Velcro is normally not used in situations where it is compressed and therefore there is no information available about its behaviour under these circumstances. In order to get at least an approximation of the Young's modulus of this material, some crude measurements were made. A 4 cm² piece of Velcro was put in between two sheets of glass. Upon this sandwiched Velcro weights were laid. By measuring the distance between the two glass plates the deflection of the material was determined. The results of this experiment can be seen in Table 6 and Figure 42. Although it seems that Velcro behaves non-linear it is assumed that the Young's modulus can be determined by drawing a trend line through the data points. This approach was chosen as the quality of the data was considered insufficient to construct a non-linear stress/strain curve. As Velcro does not expand laterally when compressed the Poisson's ratio can be assumed to be zero.

Compressive stress N/m2	Thickness mm	Length difference mm	Strain
0	2.5	0	0
12262,5	2.3	0.2	0.08
24525	2.1	0.4	0.16
36787,5	2	0.5	0.2
49050	2	0.5	0.2
61312,5	2	0.5	0.2
73575	2	0.5	0.2
85837,5	1.9	0.6	0.24
98100	1.8	0.7	0.28

Table 7 - Velcro strain measurements.

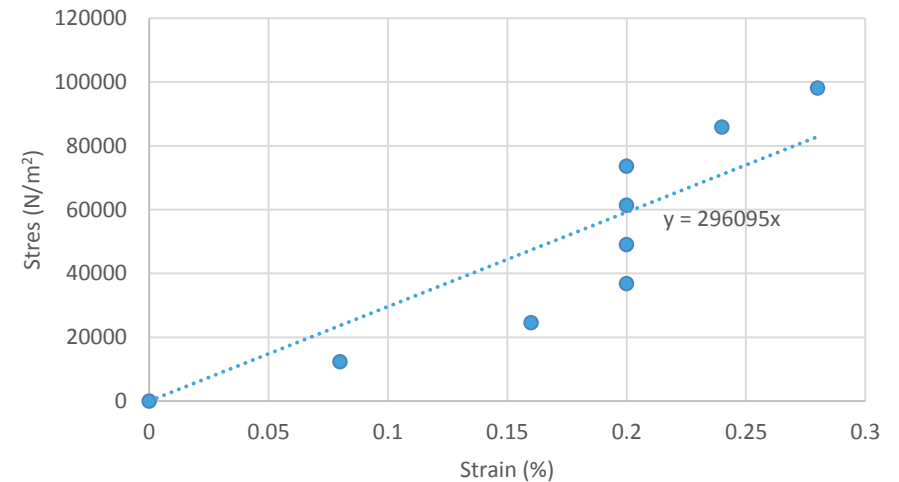


Figure 60 - Stress/strain curve of Velcro.

Suction cup design

Adhesive layer

The adhesive layer in between the suction cup support and the foam ring is made from a thin double sided adhesive. Since this layer is very thin and underneath a foam layer it is assumed that its impact on the behaviour of the suction cup is negligible. The material properties of the adhesive layer are therefore assumed to be the same as the seals.

Suction cup base

The suction cup base needs to be made from a sturdy material that is able to handle the forces that are applied on it by the textile backing. The material furthermore needs to be as light as possible and non-corrosive.

Taking these requirements into account has led to the choice for Polyoxymethylene (POM), a polymer used frequently for making high performance engineering components. The material parameters for POM were acquired from the material database from Solidworks 2014.

Suction cup support

The suction cup's support material has been selected by looking at two criteria. First of all, the material needs to be flexible. Secondly it needs to be strong enough to prevent the sealing rim from moving inward. A material that fits this description is rigid PVC. The material parameters were retrieved from the Solidworks material database.

Seals

The suction cup seals need to conform to the components of the suction cup to form an airtight seal. A material that is used frequently for this task is neoprene rubber. The specifications for this material were fetched from the Matweb online material database ("Armocell Monarch"). The Young's modulus for the material was calculated using a shore-hardness conversion chart ("Durometer* conversion chart") and the shore-A conversion formula. Since the seals are rubber based it is assumed that they are non-compressible and have a Poisson's ratio of 0.5.

Forces and constraints

The next step in simulating the behaviour of the suction cup is to add loads and constraints to the model. In Figure 61 the radial cross-section of the model that is used for the simulations can be seen. In this model the green arrows represent the constraints that make the system behave in the desired way. A fixed flat substrate is added to push the suction cup upon and a component above the top seal simulates the connection with the casing of the suction cup device. The centre of the suction cup is set up in such a way that it keeps itself aligned with the centre of the substrate during the simulation. Additional green arrows can be seen on the side of the suction cup base component 3. These were added to make sure that this part also slides along the suction cup centre. This part of the suction cup base is thus assumed to be rigid and the effect of its deformation on performance is ignored. This measure is necessary as it prevents the simulation solver from running into numerical difficulties.

Constraints are also added to control how the components are connected to each other. Two groups of bonded components can be distinguished. The first group bonds all components together except for component 1 and 2 of the suction cup base (Figure 64). Instead they connect via the textile to the rest of the model (Figure 63). This approach is taken due to initial problems with the pressure distribution of the adhesion

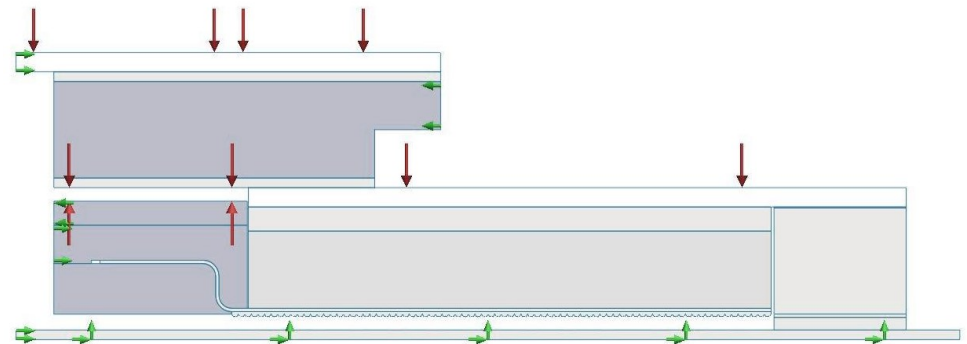


Figure 61 - Radial cross-section of the suction cup

Suction cup design

and friction pad. A persistent high contact pressure spike was present near the centre of the model (Figure 62), which caused the microstructure to collapse. By pre-tensioning the supporting foam (Figure 50) near the middle this spike levels out. The strategy to pre-tension the foam is inspired by the shape of the octopus suction cup, which also retracts inward towards the middle.

Since there is no way to add pre-tension to the model before the simulations, it is calculated together with the rest of the deformations of the model. Two opposing pressures push the suction cup base towards the bottom seal (Figure 62). These pressures are equal and cancel each other out when the two surfaces touch. The cancellation of the pressures was confirmed by changing their magnitude a couple of times. This does not have a noticeable effect on how the suction cup behaves.

The rest of the red arrows illustrate the places where pressures are added to simulate a pressure differential between the surroundings and the underside of the suction cup. Two areas can be distinguished in this distribution. The first contains all the surface area that is not part of the adhesion and friction pad. Since it is fully separated from the substrate this region feels the full force of the pressure differential. In the second area however this is not the case. Since part of the adhesion and friction pad is in contact with the substrate the average pressure for this area can be calculated with the following equation.

$$(16) \quad p_{average} = \Delta p \frac{A_{pad} - A_{contact}}{A_{pad}}$$

Because it is not possible to couple contact area dynamically to the loads applied on the model, the average pressure is used to approximate the pressure felt by the adhesion and friction pad. This is considered justifiable because the suction cup support and supporting foam layer are designed to even out pressure differences.

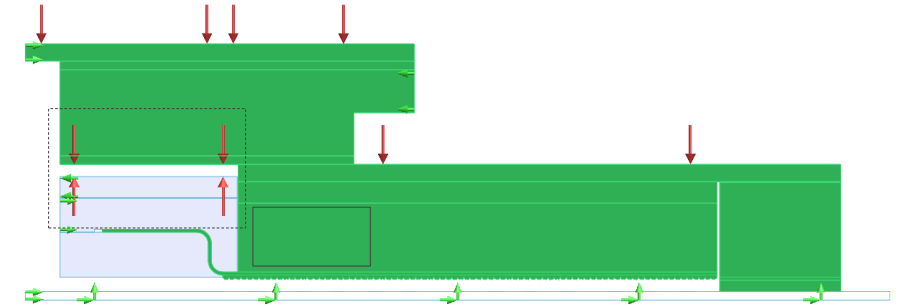


Figure 64 - First group of bonded components. Dotted lines = pre-tension pressures. Solid lines = area of the support foam that is pre-tensioned

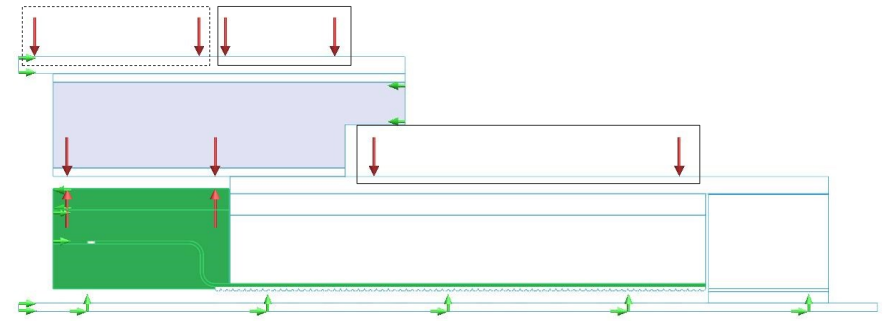


Figure 63 - Second group of bonded components. Dotted lines = pressure differential. Solid lines = average pressure differential.

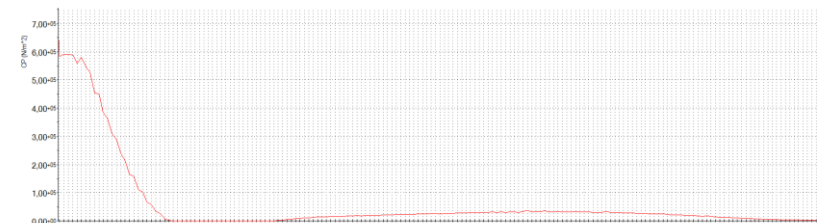


Figure 62 - Initial unwanted contact pressure distribution.

Suction cup design

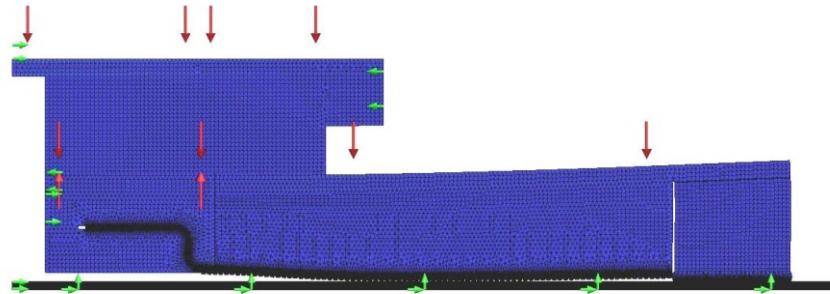


Figure 65 - Suction cup deformation at an 8 kPa pressure differential.

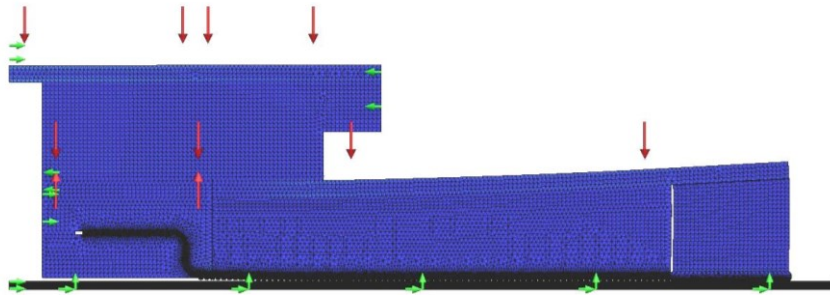


Figure 67 - Suction cup deformation at a 38 kPa pressure differential.

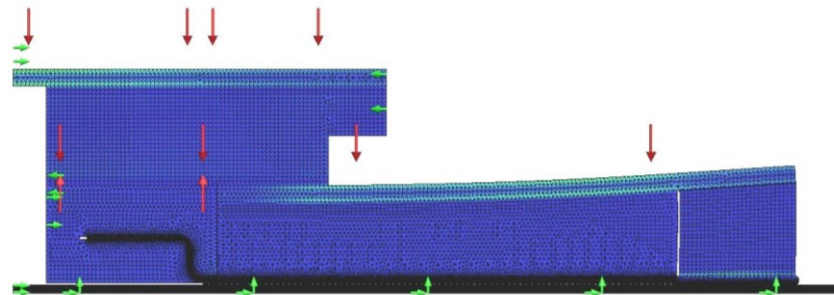


Figure 66 - Suction cup deformation at a 78 kPa pressure differential.

Simulation results

To gain insight in how the suction cup behaves under different circumstances eight simulations were performed. The difference between these simulations are the pressure differential and average pad pressure that is applied onto the model.

To determine what pressure differentials are realistic, market research was done to find a suitable vacuum pump for the suction adhesion device. The requirements for the pump are that it is compact, lightweight and relatively inexpensive. The pump furthermore has to work on 12V and has to consume low amounts of power. After comparing multiple pumps, it was established that a pressure differential of 80 kPa and a pumping speed of 17l/min is viable ("Store:Shenzhen Yanhua"). This coincides with requirement 15, which states that the pump has to deliver the same performance at an atmospheric pressure of 80 kPa and 106 kPa. A pump that can create a higher pressure differential is therefore not useful.

To make sure that the device is able to attach within a reasonable amount of time the maximum pressure differential is set to 78 kPa. The eight simulations therefore represent the behaviour of the suction cup at pressure differentials of 8, 18, 28, 38, 48, 58, 68 and 78 kPa.

The results generated by the finite element simulations are analysed with the help of an Excel spreadsheet that uses a number of equations to calculate the amount of friction and adhesion that is generated by the system. To get a good understanding of how this works each step within the worksheet is explained.

Because of space constraints the entire spreadsheet cannot be included in this rapport. This is due to the high resolution of the simulation which returns around 20,000 data points each time the deformations of the model are calculated. The data points list the contact pressure for points that lie on the surface of the friction and adhesion pad. One data point is comprised of a node number, a contact pressure value and a position value (X). These can be seen in the first three columns of the spreadsheet. The node number is used to sample the right values from the total element mesh. This reduces the amount of manual work involved in the simulation since the contact lines of the

Suction cup design

adhesion and friction pad only have to be selected once. The second and third values combined provide the contact pressure plot that forms the input for the adhesion and friction calculations. When displayed in a graph they give valuable information about the behaviour of the pad.

Figure 68 shows the pressure distribution plot with a simulated pressure differential of 78 kPa. When comparing it with Figure 62 it can be seen that the pre-tensioned suction cup design (Figure 64) results in a much smoother contact pressure distribution. Although the pressure still rises towards the middle, all values are now within the same order of magnitude. Furthermore the pad is in contact with the substrate over its entire length. The different densities of blue are caused by the peaks of the different microstructure sections. This can clearly be seen when looking at the pressure

distribution plot more closely. Figure 69 shows a small detail of the plot that contains the contact pressures of two consecutive microstructure cross-sections. In addition to showing the level of detail of the plot also the different JKR shapes can be distinguished by looking at the width and the shape of the pressure distribution. The double saw tooth shapes are caused by the planar areas of the cross-section (P1, P2), while the round or pointy shapes are caused by the cylinders (C1, C2, C3) pressed onto the substrate.

The pressure distribution plots for the other 7 simulations can be seen in Appendix C and show that the contact surface between the pad and the substrate rises steadily as the pressure differential increases. The first area of contact is near the middle of the pressure plot and expands in size when more pressure is applied to the system.

A. Node	B. Value MPa	C. X mm	D. Pressure length mm	E. Sum Contact length mm	F. Max contact length mm	G. Plane cont. length mm	H. Cyl. cont. length mm	I. Total pressure 1D mm	J. Total contact 1D mm	K. Plane inner boundary mm	L. Cyl. radius mm	M. Groove width mm
238950	0	22.825	0.019	0	0	0	0	34.04	22.871	0	0	0.96
357807	1.318	23.012	0	0.002	0	0	0			0	0	0.96
252318	0.2769	23.033	0	0.023	0.023	0	0.023			0	23.022	0.96
357795	0	23.035	0.002	0	0	0	0			0	0	0.96
357778	0.6617	23.057	0	0.003	0	0	0			0	0	0.96
252345	0.496	23.158	0	0.104	0.104	0.104	0			23.054	0	0.96

Table 9 – Condensed spreadsheet part 1 (78 kPa).

N. Groove inter. mm	O. Plane ads. adhesion N	P. Cyl. ads. adhesion N	Q. Pres. surf. mm2	R. Total pres. surf. mm2	S. Total cont. surf mm2	T. Total friction N	U. Total suction adhesion N	V. Pressure differential kPa	W. Simulated pad pressure kPa	X. Average pad pressure kPa	Y. Adsorption adhesion N
0	0	0	2.726	14247.3	5858.9	1757.7	1111.3	78	53.2	53.3	127.5
	0	0	0.086								
	0	0.187	0.086								
	0	0	0.289								
	0	0	0.13								
	0.031	0	0.13								

Table 8 – Condensed spreadsheet part 2 (78 kPa).

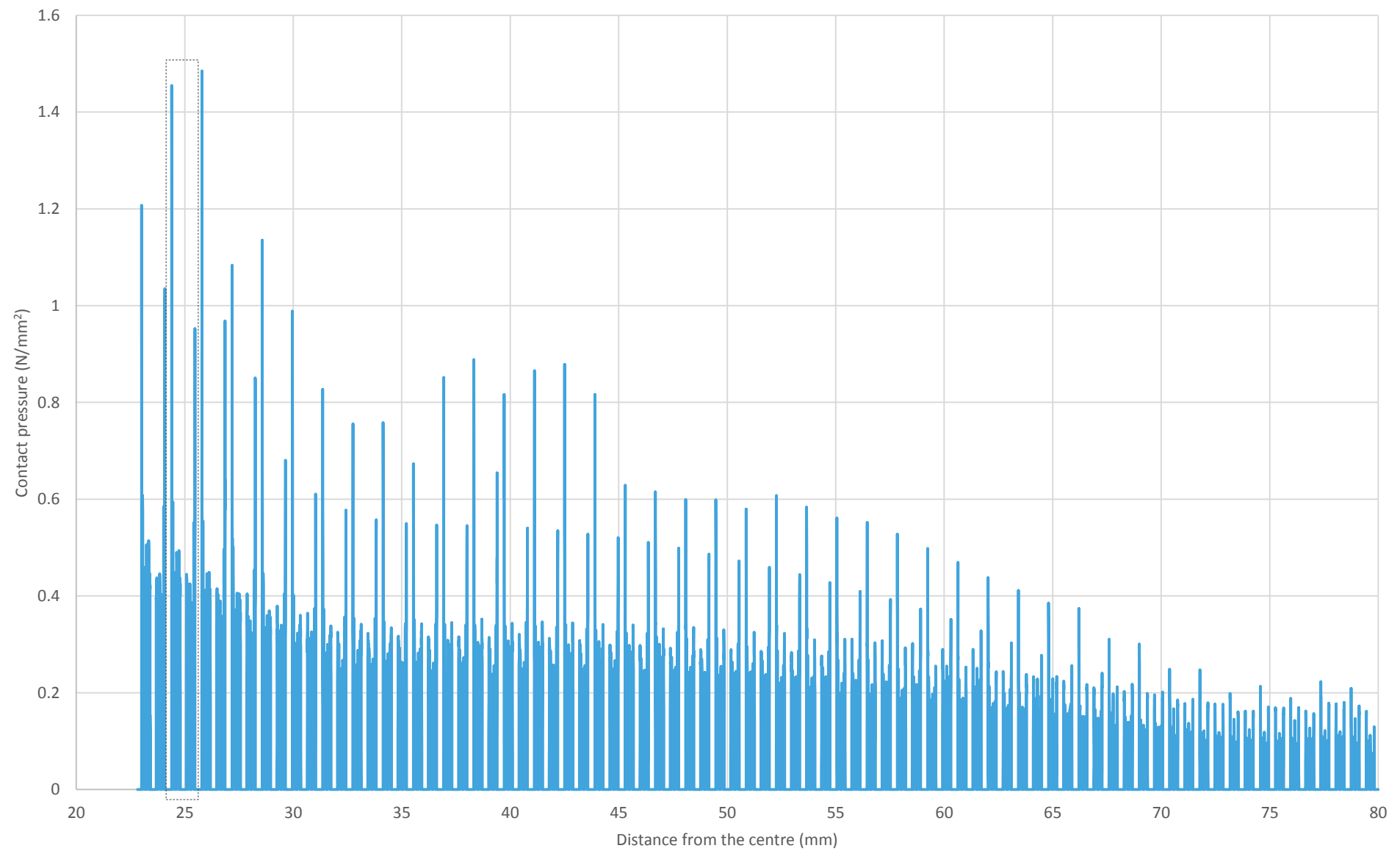


Figure 68 - Pressure distribution of the adhesion and friction pad at a 78 kPa pressure differential (MPa, mm). Dotted lines = close-up Figure 69.

Suction cup design

Because of the high level of detail of the pressure distribution plots they can be used to make a fairly accurate prediction of the forces generated by the suction cup. The first step in making this prediction is to calculate the amount of contact and pressure surface. This was done using column B, C, D, P, I, J, O, P and Q. First column 4 determines whether there is contact at the interval between the nodes by looking at the second column. If this second column is zero the equation returns the length of the interval using the formula below.

$$(17) \quad D_n = IF(B_n = 0; C_n - C_{n+1}; 0)$$

When these lengths are added they form the total 1D pressure length. This operation is performed using the following algorithm.

$$(18) \quad I_2 = SUM(D_2; Dn)$$

To obtain the 1D contact surface length one can just simply deduct the 1D pressure length from the total pad length.

$$(19) \quad J_2 = (C_n - C_2) - I_2$$

This operation was verified by using algorithm 17 and 18 to calculate the total 1D contact length. The results from these two methods match and it can thus be concluded that the equations work correctly. To go from a one dimensional pressure length to a two dimensional pressure surface, column O contains the formula seen below.

$$(20) \quad Q_n = IF(B_{n+1} = 0; \pi C_{n+1}^2 - \pi C_n^2; 0) + IF(B_{n+1} = 0; 0; M_n * (C_{n+1} - C_n))$$

This algorithm returns the area of the circle with $r = C_{n+1}$ minus the circle with $r = C_n$ when $B_{n+1} = 0$ and can be visualized as a thin two dimensional donut shape. On this

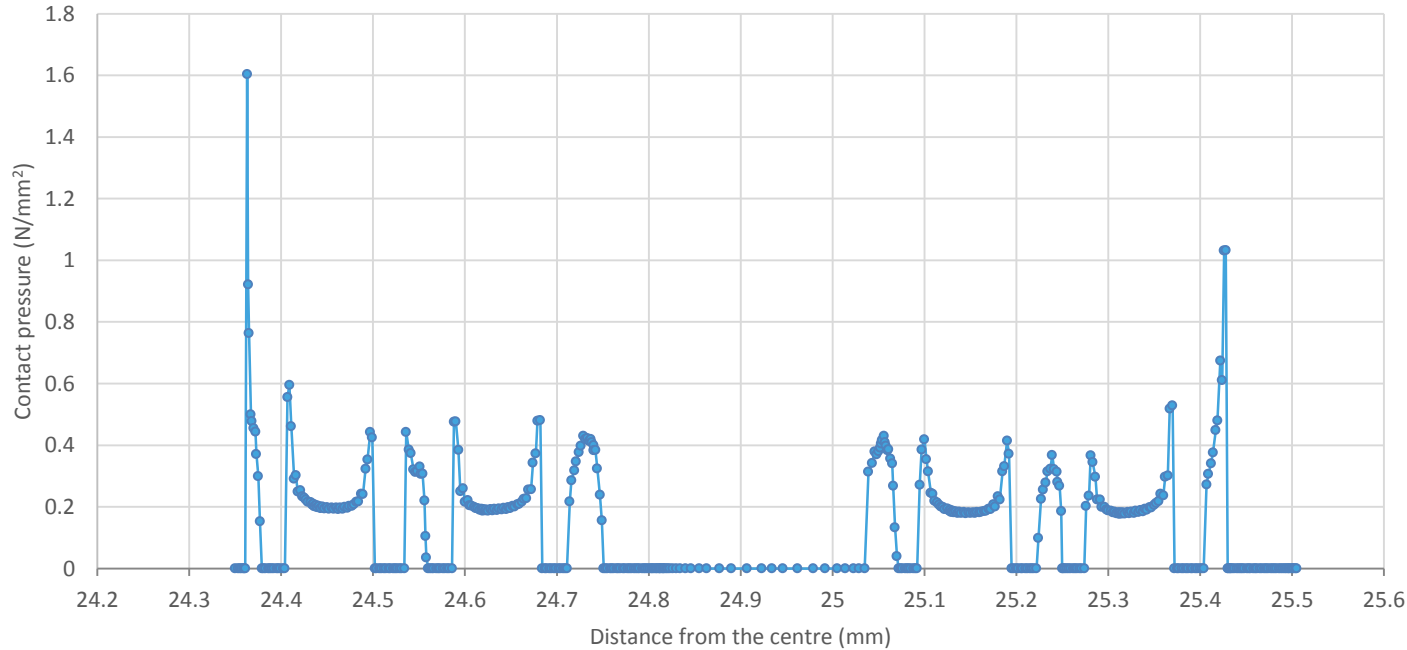


Figure 69- Close-up of the pressure distribution plot. Each dot represents a data-point.

Suction cup design

shape the entire pad surface is separated from the substrate and thus provides suction adhesion. By adding these surface areas together the total pressure surface is determined. To complete the formula the section underneath the suction cup base is added as well as the radial grooves. By doing this the lack of radial grooves in the 2D simplification is compensated. To be able to do this it is assumed that width of the radial grooves stays the same when to pad is pressed onto the substrate.

$$(21) \quad R_2 = SUM(Q_2:Q_n) + \pi r_4^2$$

By subtracting the total pressure surface from the total pad surface the total contact surface can be calculated. The value that comes out of this equation was once again checked by using the same algorithms to calculate the total contact surface.

$$(22) \quad S_2 = \pi r_3^2 - R_2$$

By using equation 7 the total pressure surface can be transformed into the total amount of suction adhesion that is generated by the suction cup. This value can be found in cell U_2 . The amount of friction can then be calculated when the interfacial shear strength of the system is known. A study by Okamoto et al. (2007) determined that this value is 0.3 N/mm^2 for a PDMS surface that is in contact with glass. Since PDMS is able to conform to the substrate and the fact that glass has a very low surface roughness, it can be assumed that the total contact area calculated by the spreadsheet is equal to the area of real contact. The total amount of friction generated by the adhesion and friction pad can thus be calculated using equation 15. The result of this calculation can be found in cell T_2 .

$$(23) \quad T_2 = 0.3S_2$$

$$(24) \quad U_2 = V_2R_2$$

The final columns that are related to the pressure and contact surface distribution are columns W and X. Cell W_2 contains the average pressure that was used as the input for the simulation. Cell X_2 contains an algorithm used to check this value by calculating the average pad pressure based on equation 16. Since there is no direct coupling between the calculated average pressure and the simulated average pressure it is required that

the deformations are simulated multiple times with different simulated pad pressures. Using a trial and error method the simulation is repeated until the simulated average pressure is within 0.5kPa of the calculated average pad pressure. The algorithm for the calculated pressure is:

$$(25) \quad X_2 = \frac{\pi r_3^2 - \pi r_4^2 - S_2}{\pi r_3^2 - \pi r_4^2} V_2$$

To estimate the amount of adsorption adhesion that is generated by the pad another solution path needs to be taken. The lengths of P1 and P3 and the number of cylinders that are in contact with the substrate are obtained with the formulas from columns E, F, G and H. Column E is used to add the lengths of the node sections together. The equation for these cells looks at the value of column B. If it is non-zero it adds the contact length to the sum of the previous contact lengths in that string. When it does encounter a zero the algorithm resets and starts counting again when it reaches the next contact section.

$$(26) \quad E_n = IF(B_n = 0; 0; E_{n-1} + (C_{n+1} - C_n))$$

Column F then picks the maximum value from each section from column E using:

$$(27) \quad F_n = IF(E_{n+1} > E_n; 0; E_n)$$

These values subsequently get sorted according to their length by the algorithms in columns G and H. Any contact longer than 0.07 mm is considered to be a planar contact, while contacts that are smaller indicate a cylindrical contact. This value was obtained by looking at the values of column B and their accompanying pressure distribution shape.

$$(28) \quad G_n = IF(F_n > 0.070; F_n; 0)$$

$$(29) \quad H_n = IF(F_n \leq 0.070; F_n; 0)$$

Now that every contact length is known and has been sorted into the correct category, the adsorption adhesion by the pad can be determined. Equation 13 is used in column O to calculate the adhesion created by the planar contacts.

Suction cup design

The value for the work of adhesion ($W = 7.9 \cdot 10^{-5}$ N/mm) was obtained from an instructional video concerning the JKR theory by Rich (2015) and represents the work of adhesion between glass and PDMS.

$$(30) \quad O_n = IF(G = 0; 0; \left(\sqrt{\frac{8\pi^2 C_n^3 W E_2}{1 - \nu_2^2}} - \sqrt{\frac{8\pi^2 K_n^3 W E_2}{1 - \nu_2^2}} \right) \frac{\pi C_n^2 - \pi K_n^2 - p_1 M_n (C_n - K_n)}{\pi C_n^2 - \pi K_n^2})$$

The equation looks at whether column G has a value and then returns the result from equation 14. From the algorithm can be seen that $r_{j,n,o}$ is substituted by values from column C and the value for $r_{j,n,i}$ is fetched from column K. This second column determines the values of the inner boundary radius by subtracting the planar contact length from the outer boundary (Equation 31). The adsorption adhesion value that is calculated is compensated for the lack of radial grooves in the model by multiplying it with a ratio that signifies the amount of plane contact surface with radial grooves versus the total plane contact surface.

$$(31) \quad K_n = C_n - G_n$$

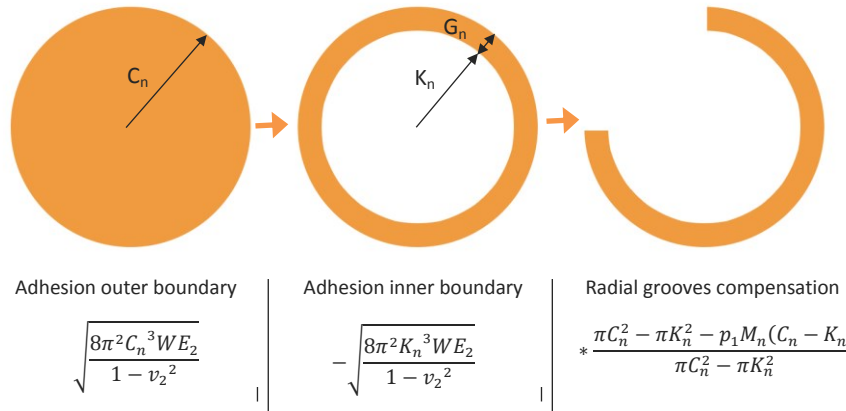


Figure 70 - Planar adsorption adhesion explanation.

The adhesion generated by the cylindrical features is calculated using algorithm 32.

$$(32) \quad N_n = 3.16 p_1 \left(\frac{2\pi L_n}{p_1} - M_n \right) (0.05 K W^2)^{\frac{1}{3}}$$

From the algorithm can be seen that the cylindrical contact length (l) has been substituted for the values from column L. This column determines the radius of the circumferential length of the feature by looking at its position and finding the middle by subtracting half the contact length (Equation 33). In this way the surface area lost towards the centre of the suction cup shape is compensated by the extra area towards the rim. It can also be seen in Figure 71 that the value for cylindrical adhesion is first calculated for a single cylindrical contact and subsequently compensated for the lack of radial grooves by subtracting the width of the radial groove (M_n) from the contact length. It is assumed that this width stays the same in all deformation simulations. The total adhesion created by the cylindrical features lying on the circle can be calculated by multiplying the adhesion value for a single cylindrical feature with the number of grooves at coordinate L_n .

$$(33) \quad L_n = IF(H_n = 0; 0; C_n - 0.5 H_n)$$

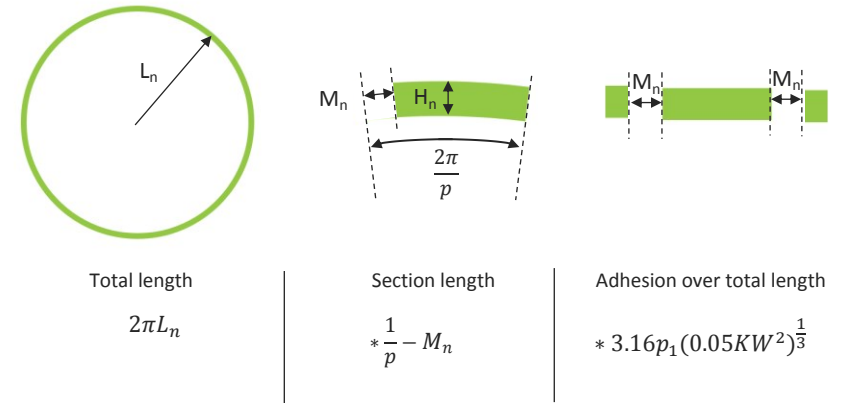


Figure 71 - Cylindrical adsorption adhesion explanation.

Suction cup design

The total amount of adsorption adhesion created by the adhesion and friction pad is displayed in cell W_2 and can be determined by summing up all adsorption adhesion contributions.

$$(34) \quad Y_2 = \sum_2^n O_n + P_n$$

By plotting the amount of suction adhesion, adsorption adhesion and friction in a graph valuable insight can be gained with respect to the performance of the suction cup under different pressure differentials.

The graph on the top left corner on the next page shows the values from the eight simulated scenarios. Because the spreadsheet uses material parameters of glass the graph represents the performance of the suction cup when applied on a glass substrate. When looking at the graph it becomes clear that the suction cup produces a lot of friction, a reasonable amount of suction adhesion and a small amount of adsorption adhesion. The value for suction adhesion seems to increase almost linearly with the pressure differential, while the friction and adsorption adhesion curves have a kink in them in the middle. This kink can be explained when looking at the difference between the pressure distribution curves before and after 38 kPa (Appendix E). The graphs before 38 kPa show that the contact distribution expands to the centre of the suction cup as well as to the rim. This causes a rapid rise in contact surface during the first phase of the pressure differential increase. However as soon as the pressure distribution hits the rim its growth is slowed down as it can now only expand to one side. When the entire pad is in contact with the substrate growth is almost halted and depends on the deformation of the microstructure.

Another conclusion that can be made based on the first adhesion and friction graph is that its performance is not isotropic. Even when suction and adsorption adhesion are added together they fall short on the amount of friction that is created. However since the scenario used in the simulation is the worst case scenario for suction adhesion and the best case scenario for friction it cannot be said that the design does not meet requirement 14. This is because the suction adhesion device has to work on multiple types of materials. The influences of their surface characteristics on performance

therefore have to be taken into account. To achieve this goal, data acquired from the study by King et al. (2014) is used. They tested their friction pad on multiple materials including glass, acetate, painted drywall and aluminium. Although their design differs in a number of ways it is assumed that the performance differences between the different substrates scale in the same way. Because of this assumption the results of this method are only a rough approximation of the performance differences. The performance of the suction design on rough substrates thus needs to be verified experimentally on a later instance.

The ratios that predict the difference in adhesion friction between the materials can be found in Table 10. The amount of friction on painted drywall for example can now easily be calculated by multiplying its friction ratio (R_f) with the value obtained for glass. They show that indeed a glass substrate is the best scenario for generating high amounts of friction. The decrease of friction performance on the other substrate is mostly caused by the higher surface roughness. The asperities on the substrate prevent the pad from coming in full contact with it. In other words the real area of contact is not equal to the nominal contact area.

Another aspect of the materials that influences the pads friction performance is surface energy. When surfaces are more attracted to each other they generate larger friction forces. These differences however are ignored in this model as the normal forces due to adsorption adhesion are insignificant when compared to the normal forces generated by suction adhesion. In chapter 3.3 it was furthermore established that the surface energies of the different types of materials do not differ significantly.

To complete the performance prediction for the other materials the influence of the decrease in real area of contact on suction adhesion and adsorption adhesion needs to be determined. Since adsorption adhesion decreases with a drop in real area of contact it was decided to multiply its value with the friction ratio.

	Acetate	Painted drywall	Aluminium
Friction ratio with glas	233/259	151/259	129/259

Table 10 - Friction ratios.

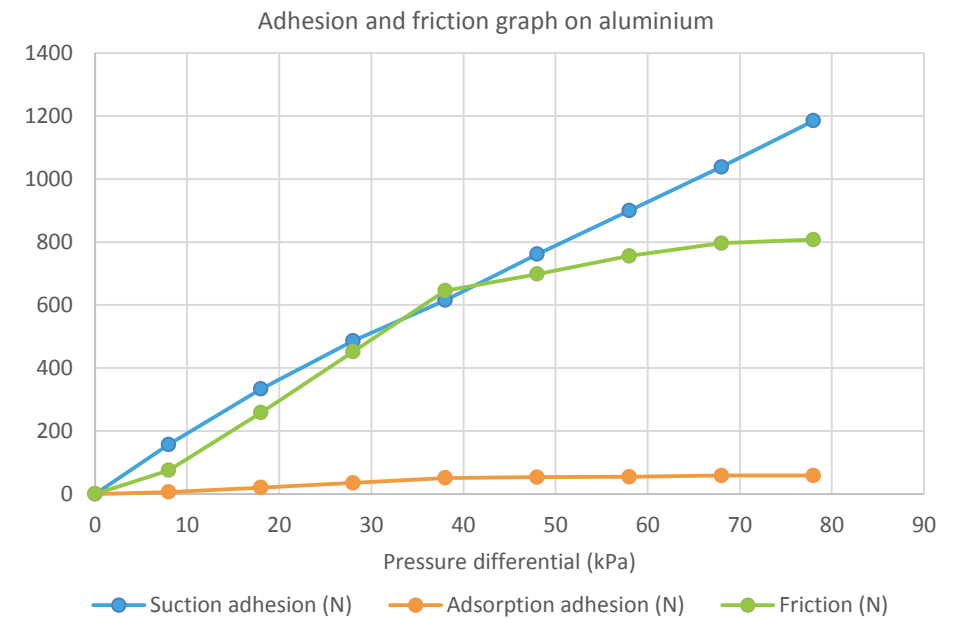
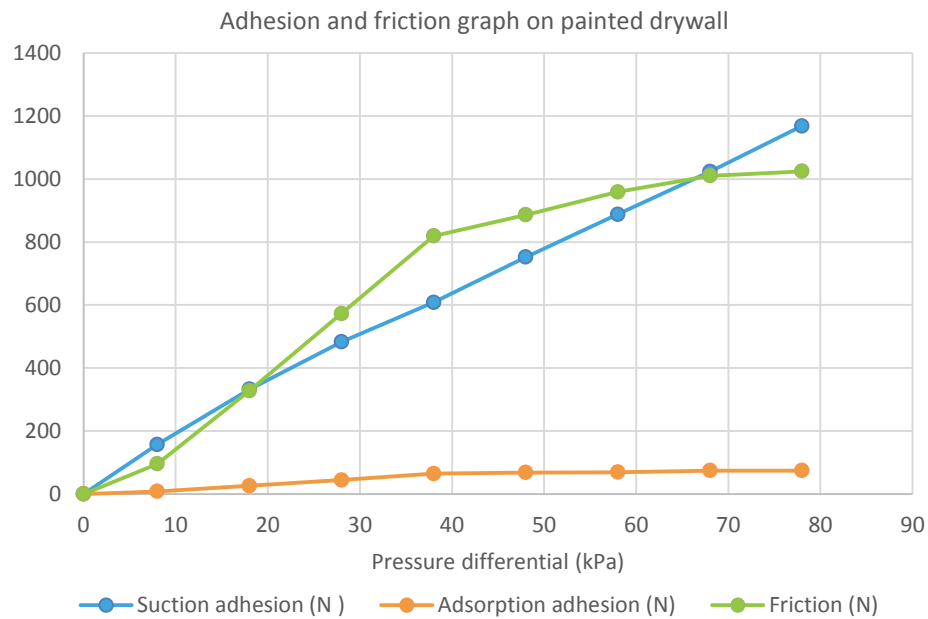
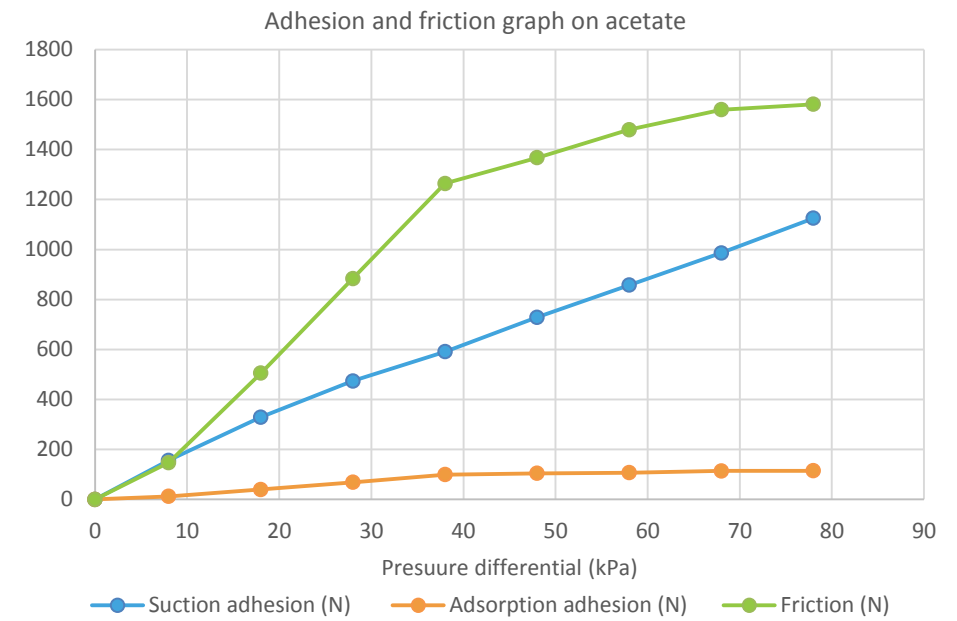
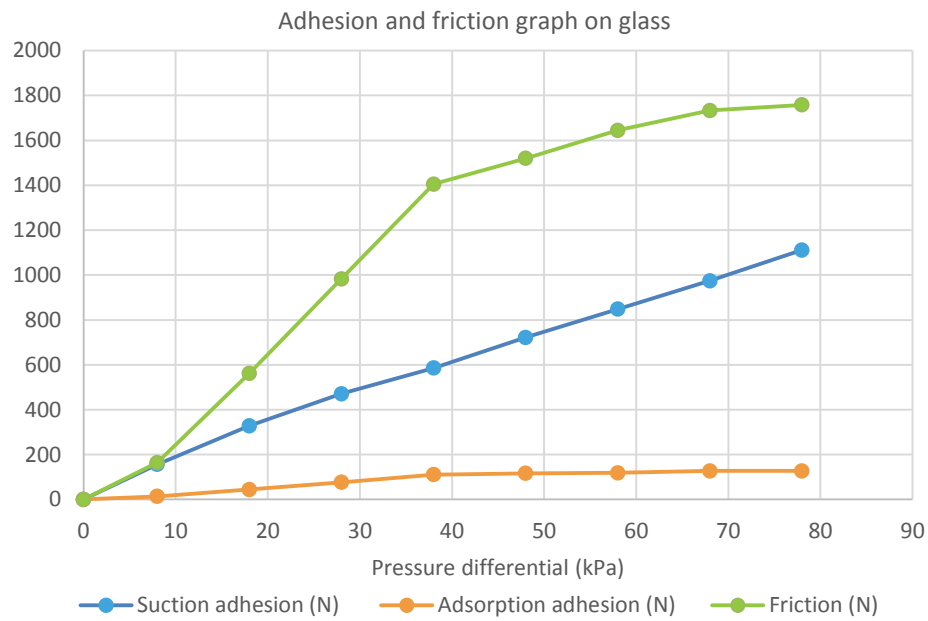


Figure 72 - Predicted performance on of the suction cup on various real world surfaces.

Suction cup design

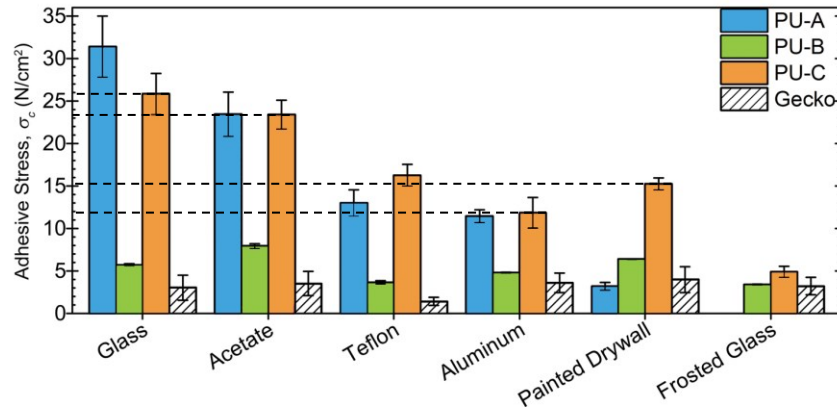


Figure 74 - Performance of a Geckskin adhesive on various substrates (King et al, 2005). Dotted lines = values used for the friction ratios.

Suction adhesion on the other hand increases, as parts of the pad become dislodged from the substrate. The increase of suction adhesion is equal to the amount of detached surface area times the pressure differential. The resulting equation for this relation can be seen below.

$$(35) \quad F_{suction} = ((1 - R_f)R_2 + S_2)V_2$$

In reality the increase in suction adhesion will affect the deformations of the model. However due to time constraints it was decided not to rerun the simulations for the other three materials. The changes in adhesion and friction will thus be less than predicted by the model. The adhesion and friction curves seen in Figure 72 however are still believed to be reasonably accurate, since the total pressure surface only rises by 6.5% in the most extreme scenario. Based on the adhesion and friction curves it can therefore be concluded that on rougher surfaces the pad loses a large chunk of its friction generation abilities. This decrease however is compensated by the initial surplus of friction. It is for this reason that the adhesion and friction pad performs the most isotropic on surfaces with an intermediate roughness.

This observation is backed up by the graphs in Figure 75. In these graphs the isotropic pulling boundary is determined using the force formulas at the beginning of this chapter. By projecting the pulling force onto the x and y axis the pulling resistance for each pulling angle can be calculated. The formula that describes the curve that is formed when the pulling resistance is plotted against the pulling angle can be seen on page 78. Peel forces are ignored in this model as they do not affect the isotropic boundary when $F_{adhesion}$ is not exceeded. This is verified on page 91.

$$(36) \quad F_{resistance} = \sin \alpha * F_{suction} + \sin \alpha * F_{adsorptive} + \cos \alpha * F_{friction}$$

When looking at the shape of the pulling resistance it becomes clear that the isotropic boundary either lies at 0° or 90°. This observation was used to calculate the isotropic boundaries for the rest of the scenarios. The outcomes of these calculations can be seen in Figure 73. The graph shows that the isotropic boundaries on smooth materials like glass and acrylic increase linearly with the pressure differential while rough substrates result in a curve that is bounded by the amount of friction that is created.

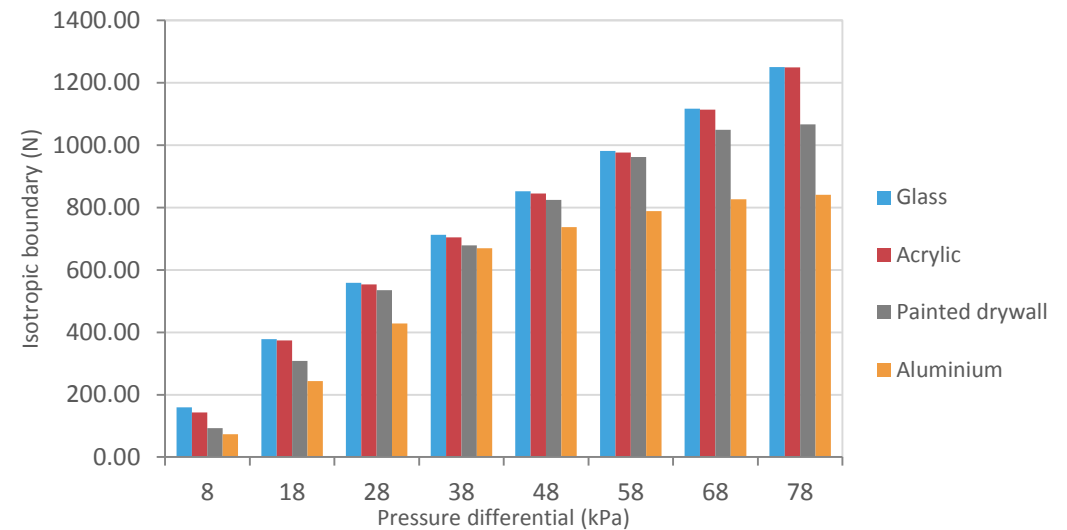


Figure 73 - Isotropic boundaries.

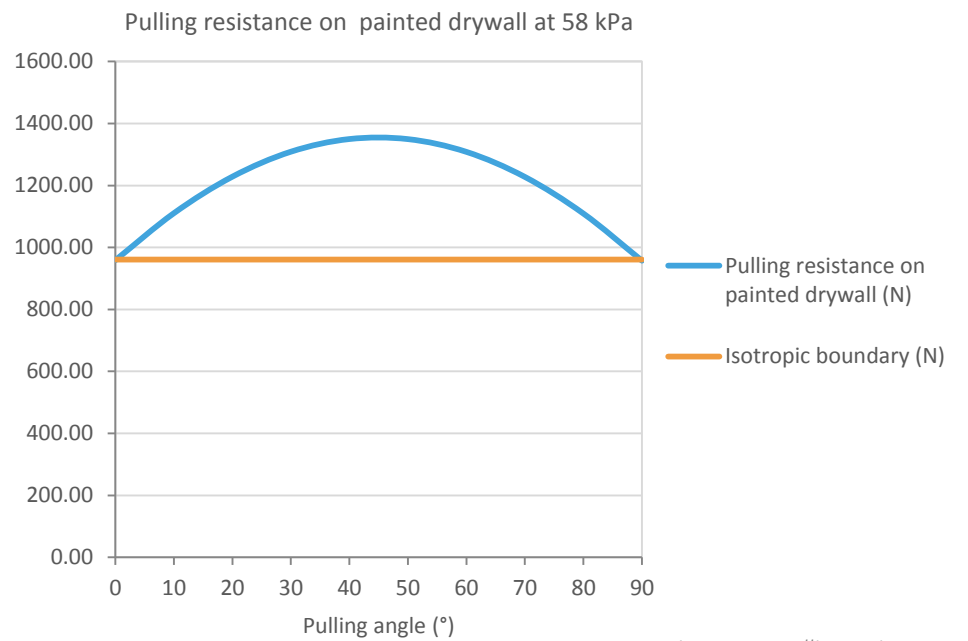
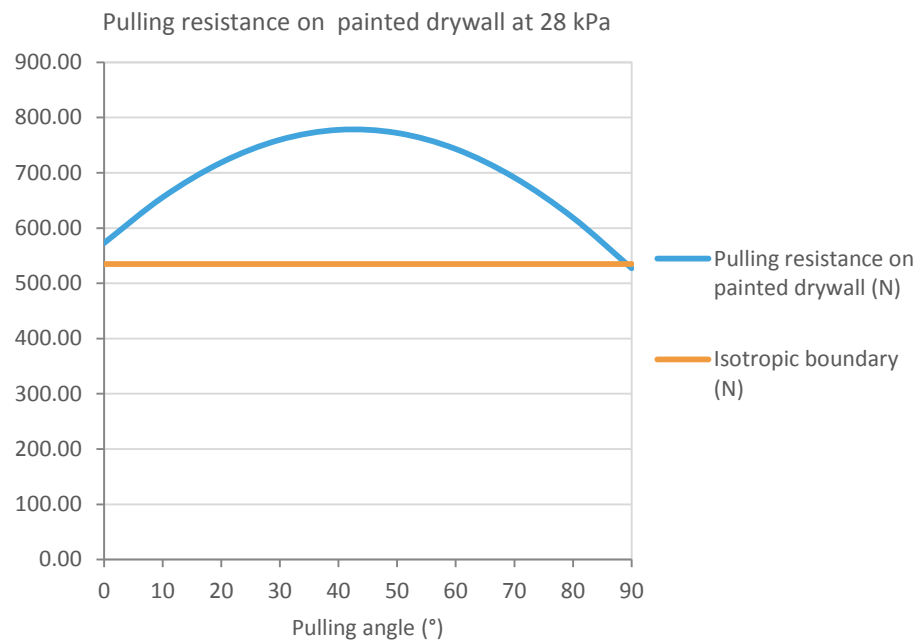
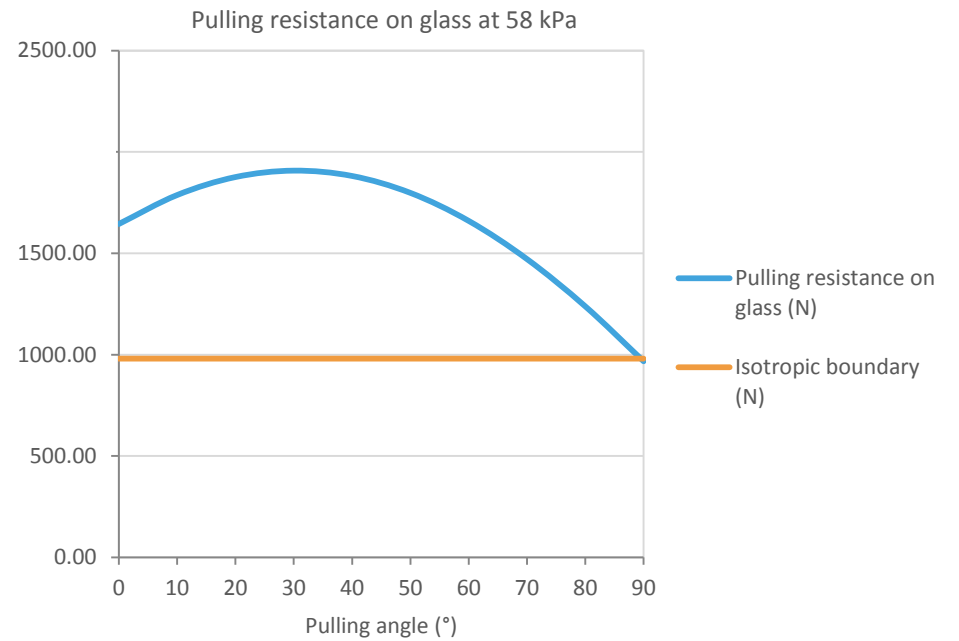
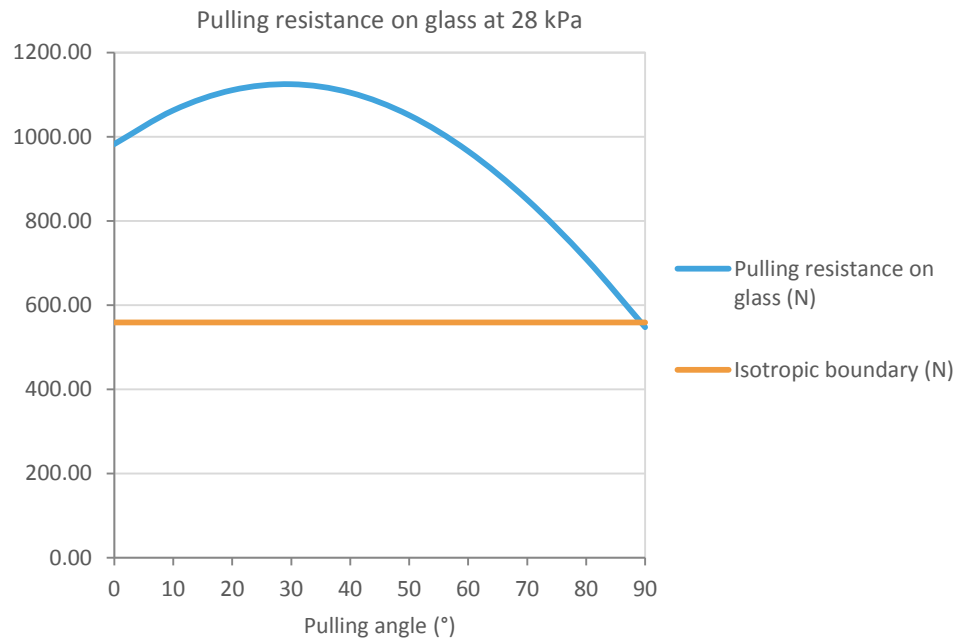


Figure 75 – Pulling resistance under different circumstances.

Suction cup design

Despite the performance dip on rough materials the suction cup still complies with requirement 14 (Figure 77), which states that the device has to be able to withstand a pulling force of 80 kg (784.8N).

The reason why the discrepancy between the performance on smooth and rough substrates is not solved by adding more contact surface is because wear has not yet been factored in. The features created by the laser engraving machine are tiny and even very modest amount of wear can have a large impact on the performance of the adhesion and friction pad.

In order to get a better understanding of the influences of wear the simulation results are modified by increasing the amount of contact surface. The increase in surface area is based on the pattern's cross-section. Each time 2% of the cross-section is shaved off which increases the length of the contact features (Figure 76). This approach assumes that the adhesion and friction pad wears evenly and that the deformations in the model do not change when wear sets in. Because of these assumptions the model tends to exaggerate the impact of wear.

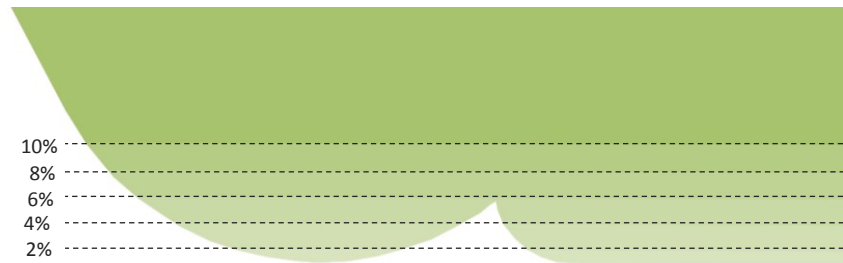


Figure 76 - Wear percentages and their effect on the cross-section shape.

To calculate the new adhesion and friction curves the cross-section contact length is transformed in a ratio that signifies the percentage of the pad's surface that is in contact with the substrate (Table 12). This ratio is multiplied by the area over which the pad interacts with the substrate. The interaction area is determined by looking at the pressure distribution curves and finding the location of the inner and outer pressure peak. By determining the surface area of the circles that coincide with the pressure peaks and subtracting the outer boundary surface from the inner boundary surface the interaction surface is acquired (Table 11).

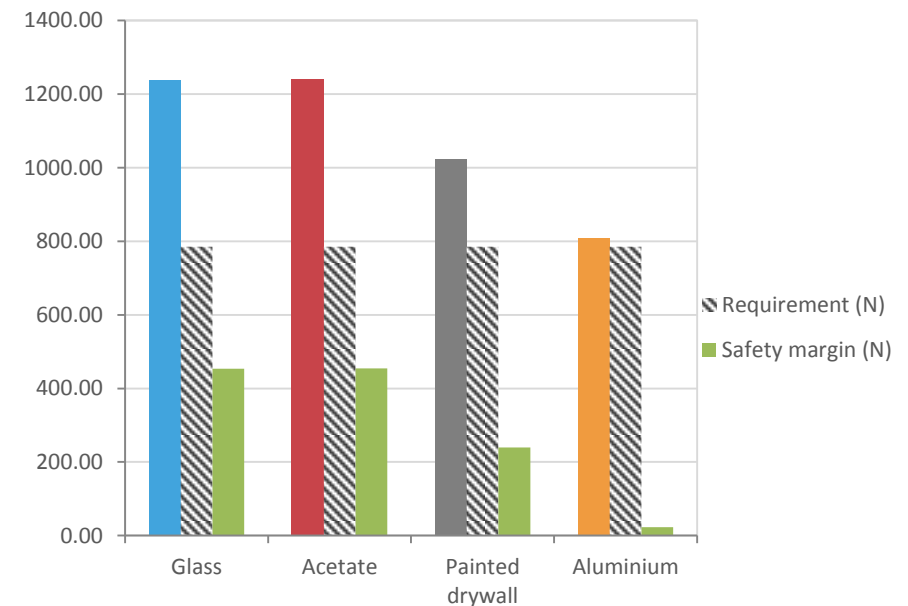


Figure 77 - Isotropic boundaries vs. requirement 14.

Suction cup design

The results from this method to predict the influence of wear on performance can be seen in Figure 78, Figure 79 and Figure 80. From the graphs can be concluded that wear results in a severe reduction of performance on smooth surfaces while it increases the isotropic boundary on rough substrates. This is because wear increases the amount of friction surface at the expense of pressure surface. Another aspect that contributes to the reduction in adhesion is that the cylinders on the microstructure are worn down and start acting as planar features. This decreases adsorption adhesion significantly as planar features have a much lower pull-of force (Table 8). The results of the reduction of adhesion can be seen in Figure 78, which shows that at high wear rates the suction cup starts to perform below par on smooth surfaces. It was decided not to compensate for this as it would impair the performance of new pads on rough surfaces (Figure 77). Instead it is theorized that the lack of adhesion is resolved by the suction cup's detachment force conversion mechanism. When the pulling force exceeds the amount of adhesion that is being generated the pad will lift off the substrate at the centre, which leads to an increase of both the pressure differential and pressure surface. The perpendicular pull-off force of the suction cup therefore lies higher than what is predicted by the wear model.

Wear	Cross-section contact length mm	Ratio contact	Ratio pressure
2%	0.3565	0.513	0.487
4%	0.415	0.598	0.403
6%	0.4357	0.627	0.373
8%	0.4442	0.639	0.361
10%	0.4509	0.649	0.351

Table 12 - Cross-section contact length, contact ratio and pressure ratio.

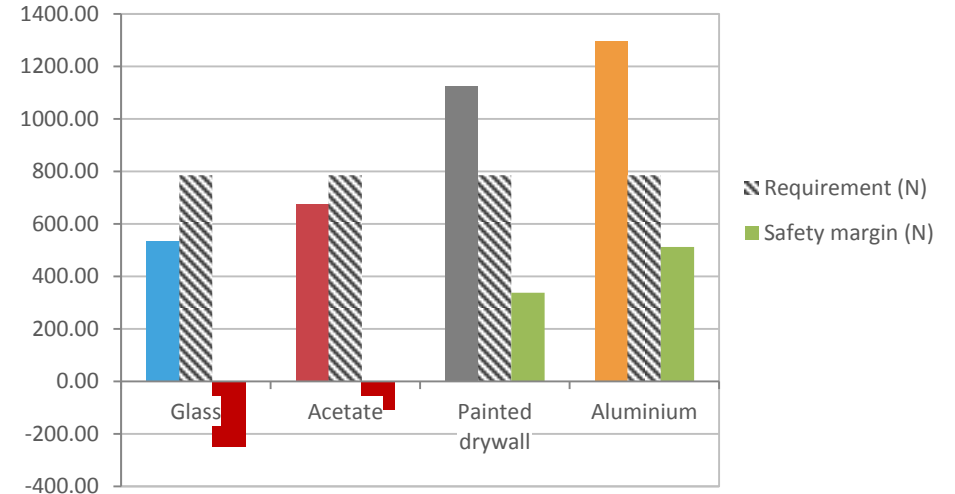


Figure 78 - Isotropic boundaries vs. requirement 14 at 10% wear.

Pressure kPa	Inner interaction boundary mm	Outer interaction boundary mm	Interaction surface mm2
8	47.442	53.105	1788.8
18	42.508	61.697	6281.9
28	39.071	71.328	11187.7
38	36.235	79.819	15890.5
48	32.36	79.824	16728.0
58	27.182	79.824	17696.6
68	23.012	79.824	18354.2
78	23.012	79.824	18354.2

Table 11 - Pressure distribution interaction boundaries and interaction surface.

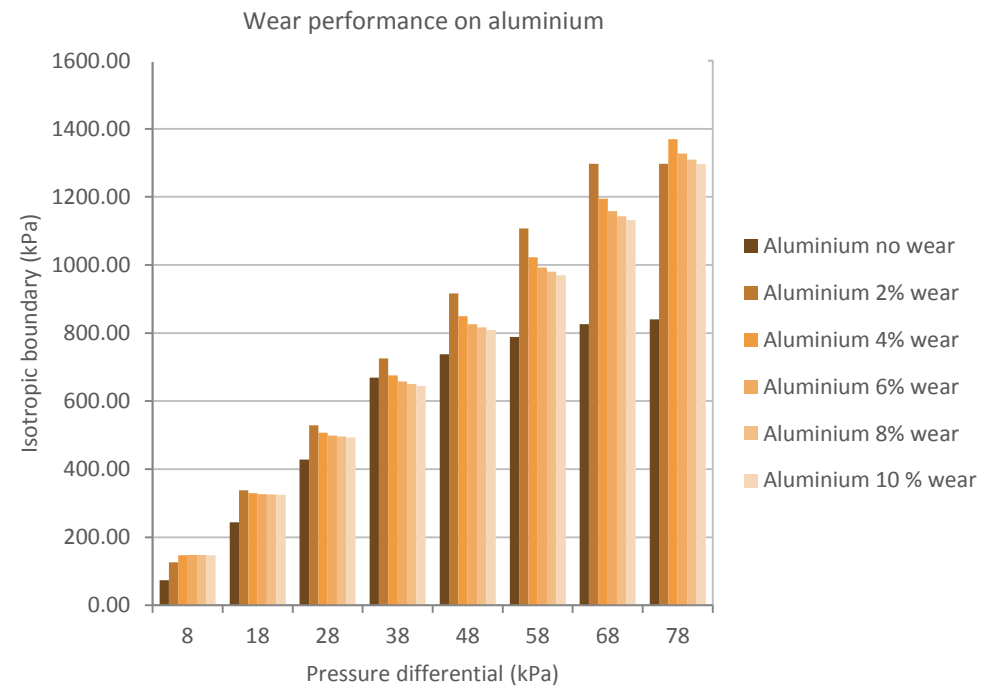
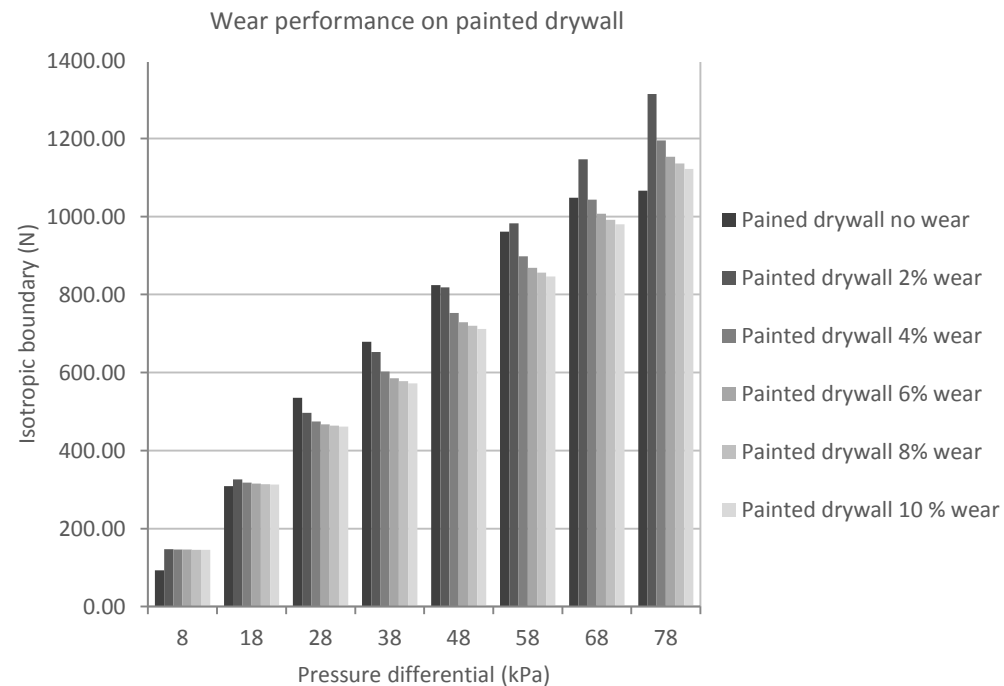
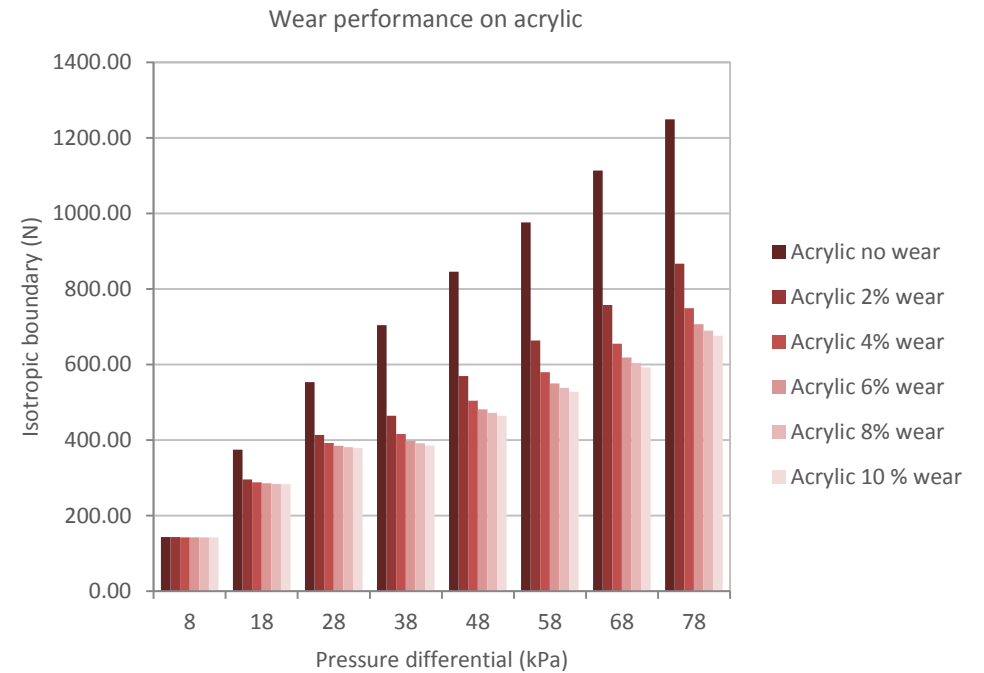
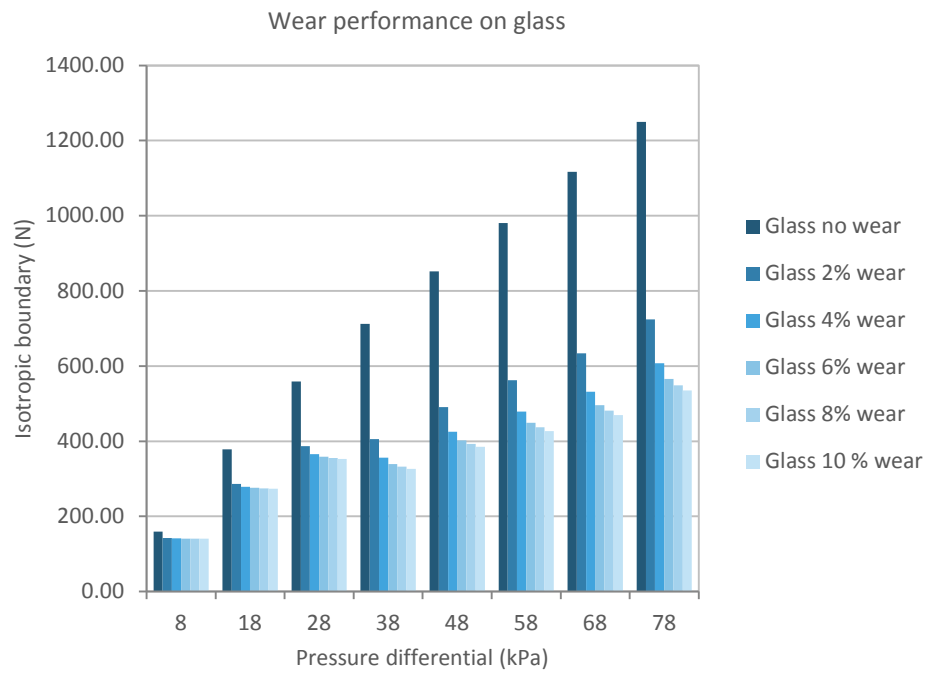


Figure 79 - Impact of wear on performance.

Suction cup design

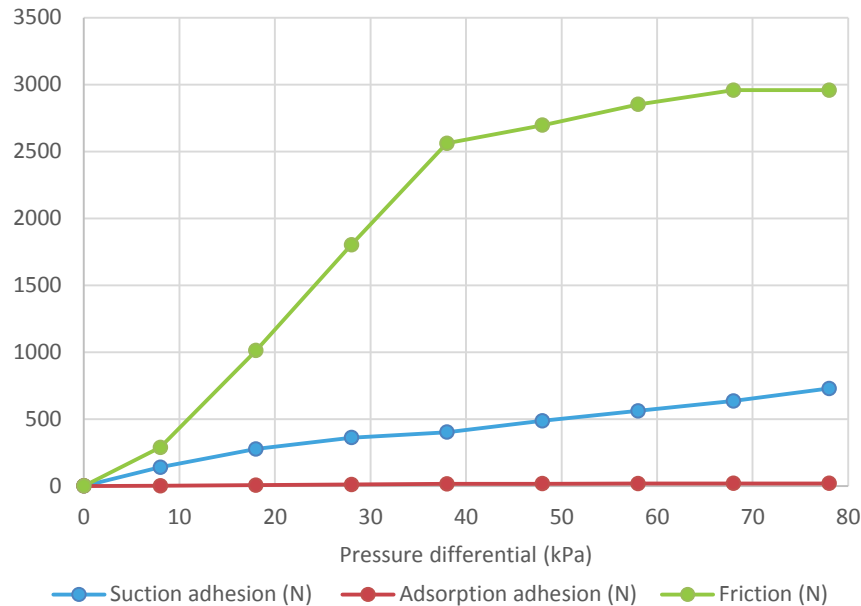


Figure 80 - Performance on acetate at 4% wear.

Pressure differential drop

One aspect of the suction cup that has to be checked before its design can be signed off on is the pressure differential drop in the system. The small size of the pressure distribution grooves can result in drag that has a negative effect on the performance of the suction cup. This reduction in air flow means the suction cup reacts sluggish to pressure changes and the vacuum pump needs to switch on and off multiple times before it reaches the intended pressured differential. Since requirement 2 states that the suction cup has to attach within 5 seconds the pressure drop in the system has to be kept within an acceptable level.

To calculate the extent to which the pressure differential drops underneath the suction, cup an online version of SF Pressure Drop is used. SF Pressure Drop is a software tool

that is normally used to calculate the pressure drop in pneumatic systems, but that can be repurposed to determine the pressure differential drop underneath the suction cup. The tool is based on work by Eck (1988), Wagner (2001) and Poling Prausnitz and O'Connel (2000). A screenshot of the tool can be found in Annex B. The software takes into account a large array of parameters that includes surface roughness, temperature and dynamic viscosity and can therefore give an accurate prediction of the pressure drop in a system. The values used for these constants can be seen in Table 13.

In addition to the fixed constants also a number of variables have to be entered into the pressure drop calculator. The graph seen in Figure 81 is used to determine the inlet pressure and volume flow. These variables are related to each other because the suction cup forms a sealed system. It is therefore assumed that the pumping speed of the vacuum pump decreases linearly with a drop in absolute pressure. This is because the pump has to work harder when the pressure differential with the outside environment increases. To obtain the volume flow for each groove the total flow is divided by the number of grooves.

To determine the length of pipes the interaction boundaries in Table 11 are used. By subtracting the outer boundary from the inner boundary the length of the radial grooves is acquired. In this model any pressure drop outside of the interaction zone is considered negligible since the air can flow unhindered underneath these sections of

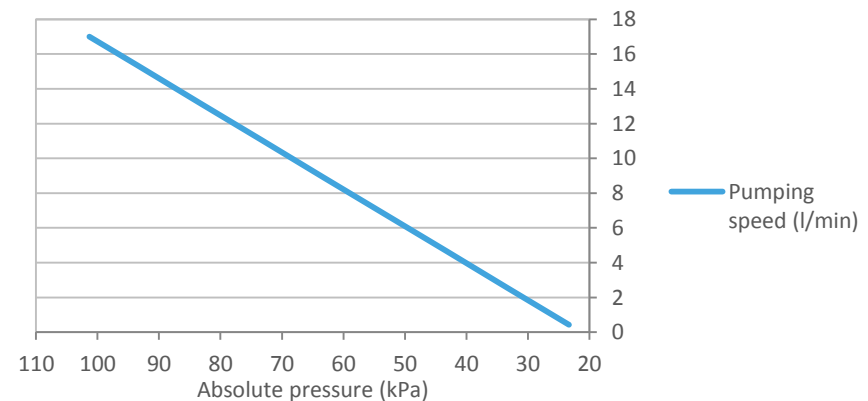
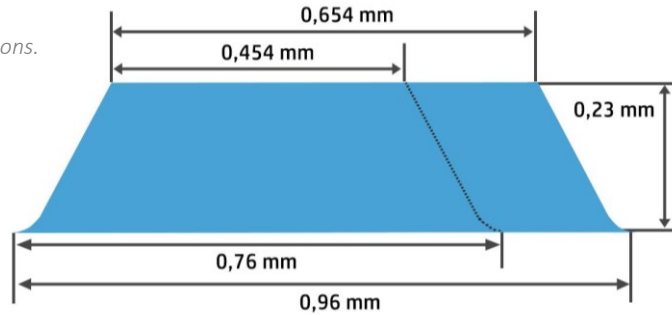


Figure 81 - Relation between volume flow and absolute pressure.

Suction cup design

Figure 82 - Radial groove cross-sections.



the suction cup. Since the radial grooves are not square an equivalent pipe width has to be found. In Figure 82 the dimensions of the radial grooves are listed. Since they split at 40 mm from the centre two cross-sections exist. This means the pressure drop for each section has to be calculated separately (Table 14). The equivalent width of both cross-sections is determined by dividing the surface area of the cross-sections by the depth of the grooves.

By plotting the outcomes of the pressure drop calculations against the pressure differentials, an assessment can be made whether the pressure drop is a hindrance for the functioning of the suction adhesion device. Figure 83 shows that the maximum pressure drop occurs at 38 kPa. Since this pressure drop is 10.83% of the pressure differential its impact on attachment speed is considered acceptable. It is not expected that a pressure drop of this magnitude will result in intermitted pumping behaviour. A slight pressure drop during the first phase of the attachment process is furthermore considered beneficial for the suction cup's ability to form a good seal with the substrate. The pressure differential between the centre of the suction cup and the area towards the rim provides additional suction adhesion that pushes the sealing rim onto the substrate.

Constant	Value
Groove height mm	0.23
Equivalent width before split mm	0.778
Equivalent width after split mm	0.578
Pipe roughness mm	$1.07 \cdot 10^{-2}$
Dynamic viscosity ¹ cP	0.01066161
Density ² kg/m ³	1.1995-0.2725
Inlet temperature °C	20
Outlet temperature °C	20

Table 13 – The pressure drop calculation constants. ¹: “Air density calculator” ²: “Gas viscosity calculation”

Pressure differential kPa	Pressure drop before split kPa	Pressure drop after split kPa	Total pressure drop kPa	Pressure drop %
8	0	0.671	0.671	0
18	0	1.975	1.975	8.39
28	0.109	2.723	2.832	10.97
38	0.359	2.806	3.165	10.11
48	0.556	2.133	2.689	8.33
58	0.643	1.462	2.105	5.60
68	0.465	0.793	1.258	3.63
78	0.077	0.131	0.208	1.85

Table 14 – The results of the pressure drop calculation.

Suction cup design

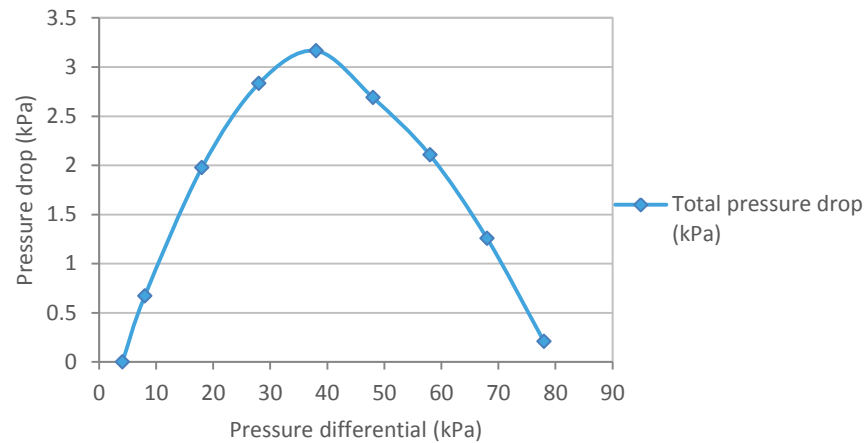


Figure 83 - Pressure drop for each pressure differential.

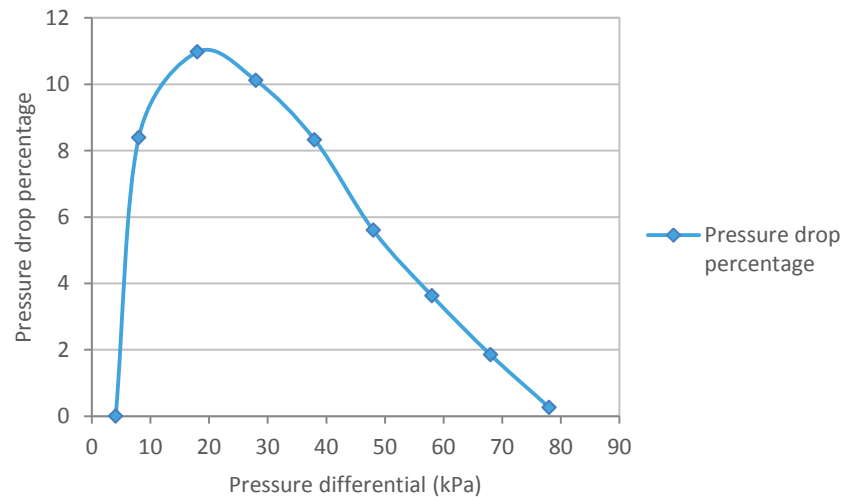


Figure 84 - Pressure drop percentage for each pressure differential.

Sealing

An important prerequisite for the functioning of the suction adhesion device is that it can create a seal on rough surfaces. The highest roughness that the sealing rim has to conform to was determined in chapter 3.3. With an average roughness of 300 μm , plaster is considered the most challenging substrate to which the device needs to be able to adhere.

In order to determine the performance of the sealing rim two finite elements method models are used. The first model is the same model as the isotropic boundaries model and is used to calculate the pressure that is exerted on the rim during different scenarios. The second model determines the effect of this pressure on a small section of the sealing rim. The choice for using two models was made since the effect of roughness on the sealing rim cannot be accurately calculated in a two dimensional simulation.

The first set of simulations is done to mimic the effect of a user that pushes the device onto the substrate. This is done by applying a force to the top of the suction cup. Three simulations were performed that vary in the amount that the user is pushing onto the suction cup (Table 15). The resulting rim pressure plot from one of these simulations can be seen in Figure 85. Based on the shape of the graph can be concluded that the rim is pushed harder onto the substrate near the edges. It can furthermore be seen that the rim pressure scales linearly with an increase in pushing force (Table 15).

Pushing force N	Average pressure (von Mises) N/m^2
30 N	1164.2
50 N	1941.1
70 N	2718.0

Table 15 - Pushing forces and the resulting average rim pressures.

Suction cup design

The intention of the second set of simulations is to see the effect of a pressure differential on the rim. This is important since the device has to take over the job of providing an attachment force from the user once a seal has been established. At this point the force needed to conform the rim to the substrate becomes the responsibility of the device itself. From the results provided in Table 16 and Figure 86 can be concluded that a pushing force of 70 N is equal to a pressure differential of approximately 3.5 kPa. Figure 86 furthermore shows that the steep initial rise of the rim pressure flattens after about 18 kPa.

In order to give an approximation of the deformation of the rim under these circumstances the pressure distribution plot is used as an input for a second finite element model. Since it is impossible to perform a simulation for each value of the pressure distribution the outcomes of multiple simulations are used to generate a trend curve that predicts the deformation for the other rim pressure values. This deformation is subsequently used to determine the pressure drop across the rim with the same

methodology as presented in the last section.

The model that forms the basis of the rim deformation calculations can be seen in Figure 88. It represents a small rectangular section of the rim that is pressed onto a substrate. This substrate is designed to be the worst case scenario for the functioning of the sealing rim. The substrate features relatively sharp asperities (top diameter = 0.08 mm) that are packed closely together (peak to peak = 0.96 mm).

Pressure differential kPa	Average pressure (von Mises) N/m ²
2	1565.0
4	3130.9
8	4403.0
18	5661.1
58	7716.7
68	8201.6
78	8708.2

Table 16 – Pressure differentials and the resulting average rim pressures.

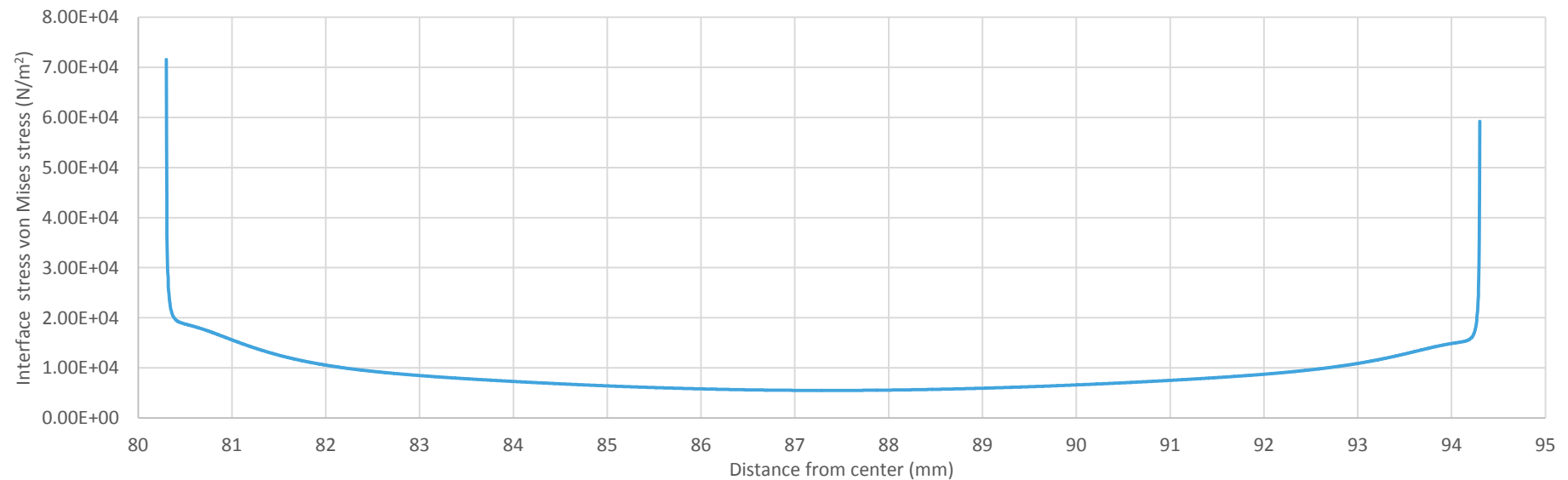


Figure 85 - Pressure distribution of the rim at 8 kPa.

Suction cup design

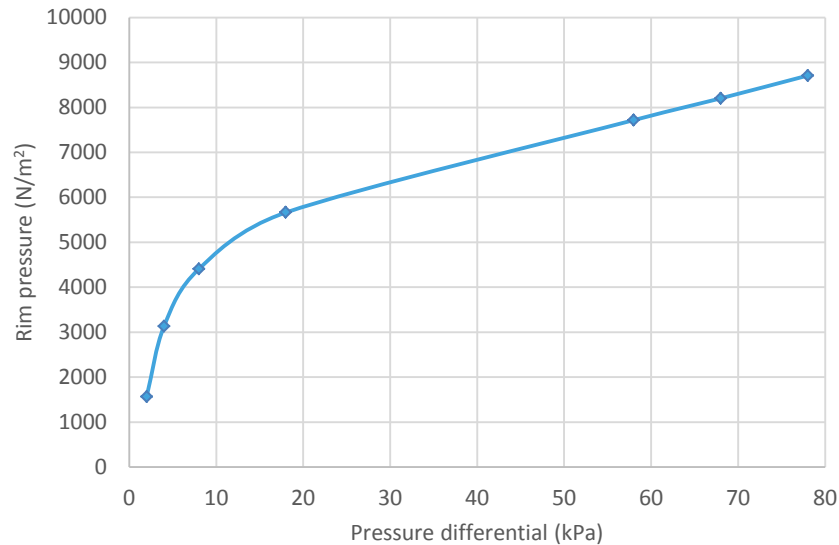


Figure 86 - Average rim pressure for each pressure differential.

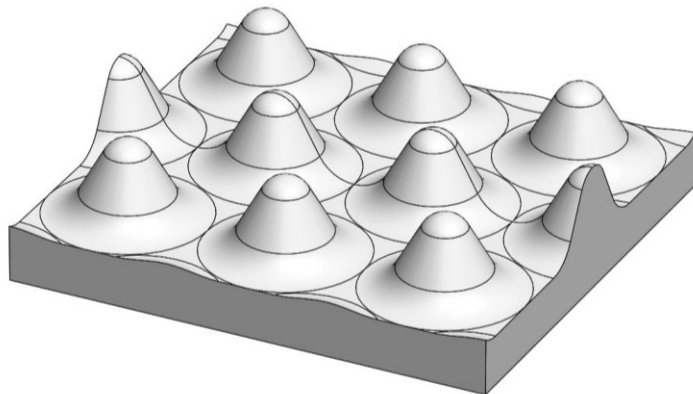


Figure 87 - Substrate 3D model with centre line.

This means that if the rim can seal against this substrate it will be able to handle everything that is thrown at it in real-life.

The other parts that are contained in the model are the same as the rim structure presented in the isotropic boundary calculations. The components are bonded together in the simulation and are constrained in such a way that they cannot protrude the virtual walls of the model. This mimics the presence of neighbouring rim sections. To finish the setup of the simulation a pressure is added to the top of the rim that represents the rim pressures measured in the 2D simulations.

The results from one of the simulations can be seen in Figure 89. It shows the deformation of the rim perpendicular to the substrate. The red dots represent the contact points with the substrate and the blue sections show the areas in between the asperities. To obtain a workable dataset from the simulation the deformations and y-coordinates of the substrate are extracted from a line that runs across the middle of the substrate (Figure 87). In Figure 89 can be seen that this line has a much higher element count, which improves the quality of the data for this section of the model.

Just as with the boundary calculations the dataset is analysed with the help of an Excel spreadsheet. A condensed version of this sheet can be seen in Table 17. Column A, B, C and E contain the raw data that is extracted from the simulation. Column D determines the Y coordinate of the deformed rims shape by adding it to the substrate asperity height.



Figure 88 - 2D view of the rim model.

Suction cup design

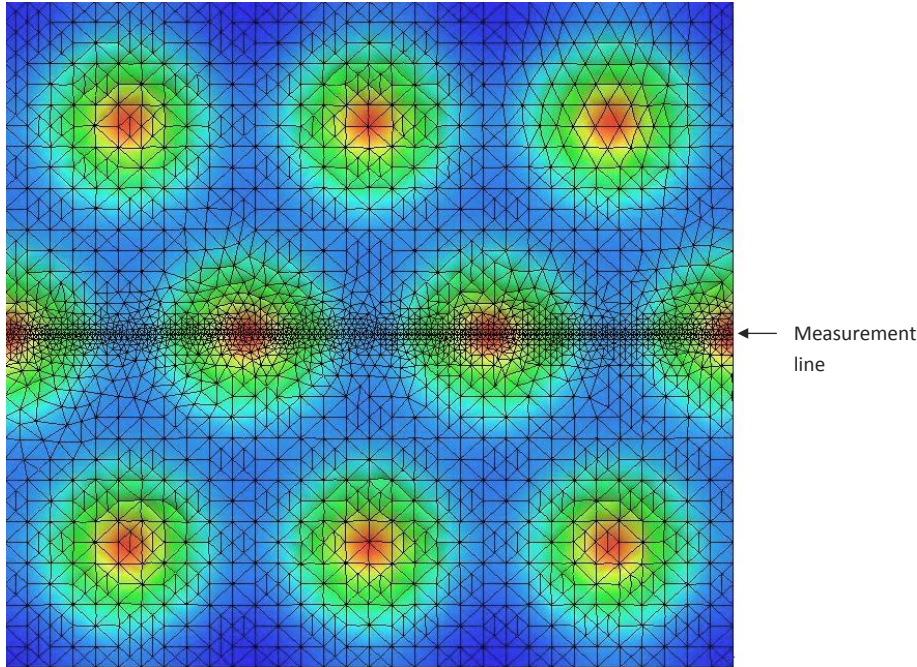


Figure 89 - Deformation of the rim perpendicular to the substrate. Red = asperity peaks. Blue = rim deformation in between the peaks.

The outcomes of column D and E are then compared in column F. Due to the limited resolution of the simulation this value is never exactly zero since the elements tend to crumble (Figure 90). It is assumed however that very small values in column F indicate that the surfaces are in full contact with each other.

To get rid of this noise in the data, column G looks at column F and leaves out values below 0.006 mm or higher than -0.006 mm. Values that pass this test are used as an input for an algorithm that calculates the area of the gap using Reimann sums.

$$(37) \quad G_n = IF \left(OR(F_n > 0.006; F_n < -0.006); \frac{(D_n - E_n) + (D_{n+1} * E_{n+1})}{2} (B_{n+1} - B_n); 0 \right)$$

The output in column G can be seen in Figure 91. Adding all values of this graph together and dividing them by three gives the average gap size, which can be found in Column H. Since the pressure drop across the rim is of interest, the gap size needs to be transformed into a radius that has an equivalent surface area. This radius can then be used as an input for SF Pressure Drop. To obtain the other important variable for the pressure drop calculations the pumping speed of the pump (17/min) is divided by the number of gaps across the circumferential length of the sealing rim. The radius of this circumference is assumed to be equal to the x-coordinate of the inner edge plus half the width of the rim. In this way surface area lost towards the end is compensated by a surplus area towards the middle.

$$(38) \quad K_2 = \frac{17}{0.96 * 2\pi 87.3}$$

A. Node	B. X mm	C. Y deformation mm	D. Y coördinate mm	E. Substrate Y coördinate mm	F. Y difference mm	G. Gap surface mm2	H. Average gap mm2	I. Equavalent diameter mm	J. Gap length mm	K. Air flow per gap l/min	L. Pressure drop kPa
41160	0	-0.000621	0.299	0.3	0.0006	0	0.0773	0.314	42.22	0.01984	3.93
49006	0.071	-0.023420	0.277	0.27	-0.0066	0.000176					
41370	0.323	-0.101100	0.199	0	-0.1989	0.000597					
41353	0.577	-0.016780	0.283	0.276	-0.0072	0.000187					
48866	0.641	-0.000274	0.300	0.3	0.0003	0					

Table 17 - Condensed spreadsheet. Rim pressure = 1930N

Suction cup design

The other constants and variables used in the pressure drop calculations are borrowed from Table 13. The only new constant that needs to be determined is the length of the gaps. In Figure 89 can be seen that the air cannot travel in a straight path underneath the rim but needs to meander around the asperities. This means that the airflow is stretched with a factor pi for each 0.96 mm that it moves towards the centre of the

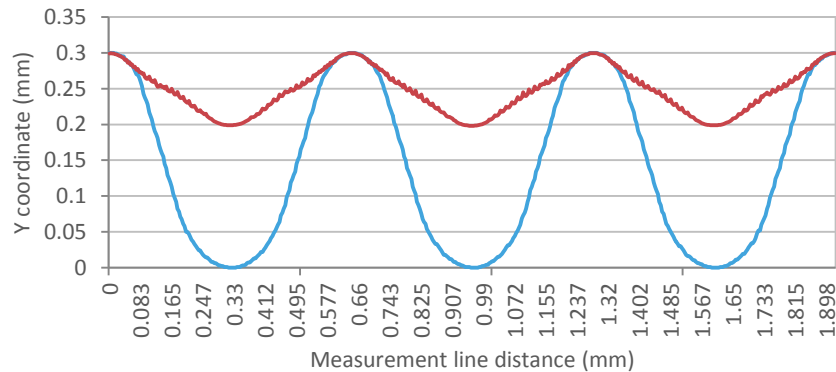


Figure 90 - Y coordinates of the rim (red) and the substrate (blue) along the centre line.

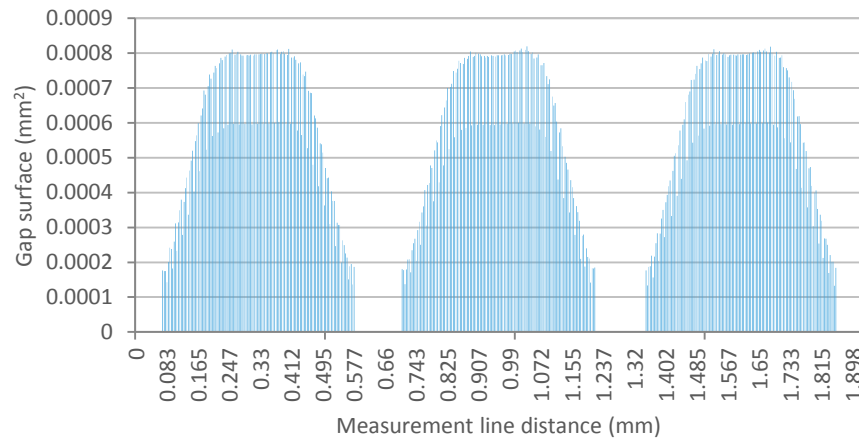


Figure 91 - Outcomes of the Reimann sums algorithm.

suction cup. The total length of the gaps thus becomes:

$$(38) \quad J_2 = (r_1 - r_2)0.96\pi$$

When the values discussed above are entered into SF Pressure Drop the values in Table 18 are returned. It can be concluded that a pressure drop of around

11 kPa is created when the device is pushed on the substrate. This should be enough to give the suction cup a chance to attach to the surface.

After the user has let go, the device needs to provide its own rim pressure. To determine whether the seal created by the rim is sufficient to generate a sustainable pressure drop, the values from Table 18 are connected with a trendline. The formula that describes this trendline is subsequently used to predict the equivalent diameter of the deformed sealing rim for each pressure differential.

Figure 92 shows that the trend line is best described by a logarithmic function ($r=0.994$). When the average rim pressures belonging to the pressure differentials are plugged into this equation the values in Table 19 are obtained.

Rim pressure N/m ²	Pressure drop kPa
820.0	10.505
1158.1	10.836
1930.4	11.416
2702.6	11.723
7273.0	12.886

Table 18 - Pressure drop for the simulated rim pressures.

Average rim pressure N/m ²	Equivalent radius m ²
1565.0	0.31461
3130.9	0.30976
4403.0	0.30737
5661.1	0.30561
7716.7	0.30344
8201.6	0.30302
8708.2	0.3026

Table 19 - Estimated equivalent radius for the rim pressures belonging to the pressure differentials in Table 16.

Suction cup design

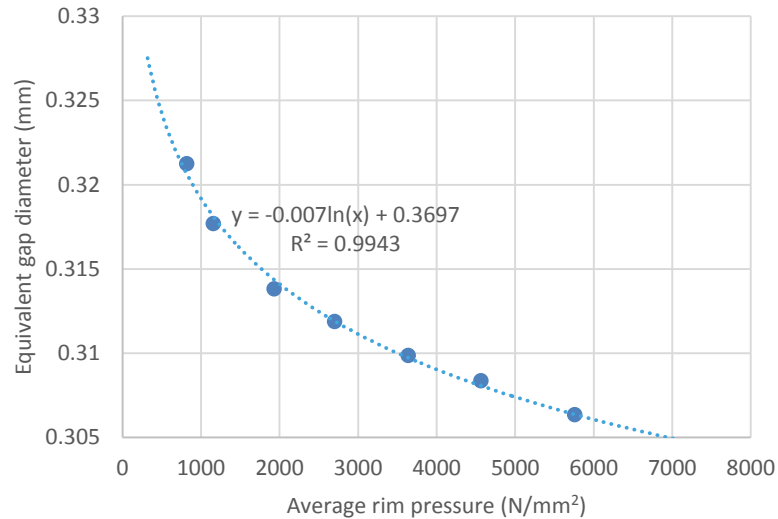


Figure 92 - Trend line equivalent diameter and average rim pressure.

To calculate the pressure drop that belongs to each pressure differential the following scenario is used. Just as in the previous section it is theorized that the air flow drops linearly with a decrease in absolute pressure. Since the rim is not fully sealing off the substrate it is furthermore assumed that the density of the air drops linearly with the distance it has travelled underneath the rim. The average density can thus be calculated by adding the air density inside the suction cup to the atmospheric air density and dividing them by two. Both these variables are compensated for the pressure drop caused by the adhesion and friction pad by subtracting it from the absolute pressure.

When these variables are taken into account SF Pressure Drop returns the values that can be seen in Figure 93. The total pressure drop in the system can be approximated by adding the pad pressure drop to the rim pressure drop. This gives a rough idea where the equilibrium lies between leakage and air flow due to pumping.

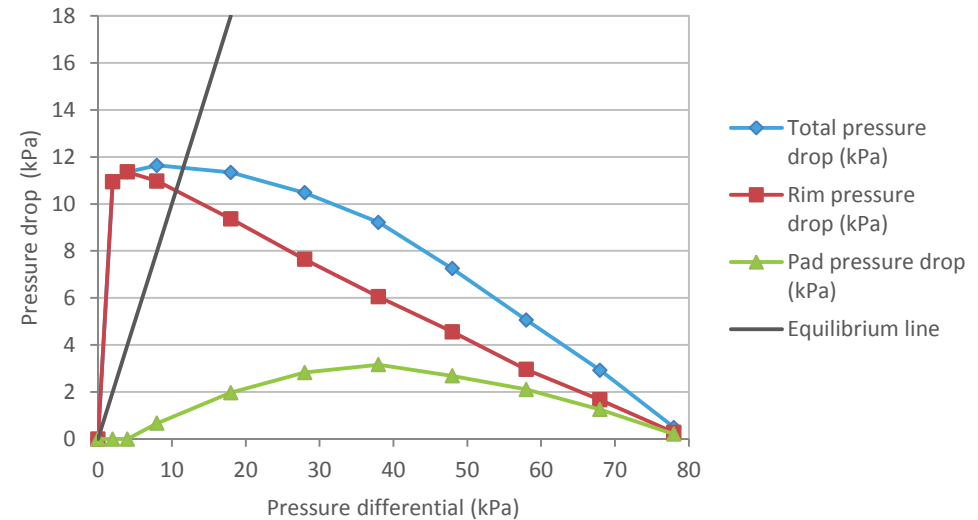


Figure 93 - Pressure drop vs. Pressure differential.

This equilibrium is the result of the drop in air flow due to the limited pumping capacity of the vacuum pump. The location of this equilibrium lies at the intersection of the total pressure drop curve and a line that scales linearly with the pressure differential and the pressure drop. When the total pressure drop curve is underneath this line the vacuum pump can no longer provide a large enough air flow to sustain the pressure differential.

In this worst case scenario the equilibrium lies at around 12 kPa, which translates into an isotropic boundary of 200 N. This is considered acceptable since the substrate used in these simulations is not likely to be encountered in the real world. The suction adhesion device is furthermore able to alert the user of such a low isotropic boundary through the user interface.

Suction cup design

In the cases where the pump has to work continuously to compensate for leaks the pressure differential underneath the suction cup is not equal due to the pad's pressure drop (Figure 94). Additional suction adhesion is furthermore being generated underneath the suction rim of the suction cup. Also the effects of a pulling force on the sealing capabilities of the rim are unknown. The isotropic boundaries that are predicted under these circumstances are therefore not accurate. The effects of the differences mentioned are hard to predict and should be determined experimentally. When this information is available it could be used by the device to give a more accurate isotropic boundary reading. This requires the device to keep track of how much effort it cost to stay attached to the substrate. If it continuously needs to keep pumping then the isotropic boundary on the interface has to be adjusted.

Despite these concerns it can be concluded that the sealing rim works as intended. Even though it does not fully seal off the suction cup, the pressure drop that is created over the width of the rim is large enough to keep the device attached.

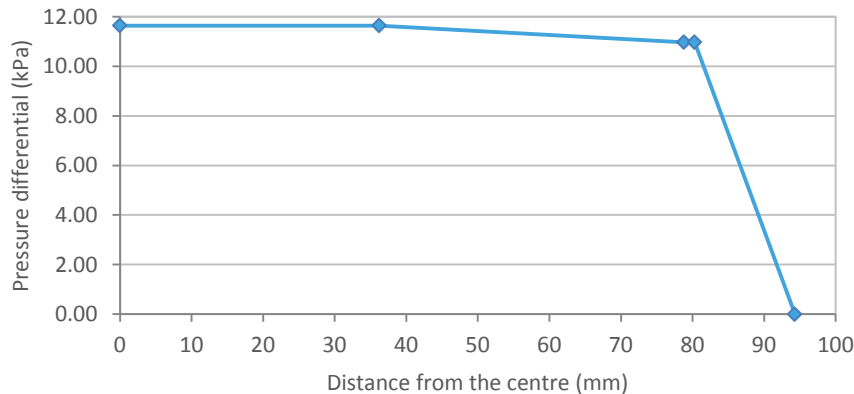


Figure 94 - pressure differential underneath the pad and the rim (mm) at the pumping equilibrium.

Peel forces

On page 20 it was stated that the peel forces that are developed by a pulling force parallel to the substrate can be ignored when the ratio between l_3 , l_4 and l_2 is large enough. Now that more is known about the performance of the suction cup this statement can be verified.

Because the peeling forces problem cannot be simplified into an axi-symmetrical 2D simulation and because the entire suction cup model proved to be too complex to predict its deformations in three dimensions, it is decided to solve the problem using equation 3. This approach does require that the suction cup behaves like a rigid body. The calculations presented here thus underestimate the effect of a peeling moment. This is because point A, around which the suction cup hinges, lies closer to the middle in reality than assumed in Figure 54. On the other hand the flexibility of the support prevents that the full peeling force is transmitted onto the edge of the suction cup. The exact effects of these mechanisms however need to be determined experimentally.

The results from the 78 kPa pressure differential simulations are used as an input for the peeling force calculations. The amount of friction generated in this scenario is 1758 N. This is equal to the maximum pulling force that the suction cup needs to be able to resist. The force of gravity is assumed to be 22.6 N, which is derived from requirement 7. l_3 and l_4 are furthermore assumed to be equal.

The amount of adhesion generated by the pad as a function of the distance from A can be described by the following equation.

$$(39) F_{adhesion,A} = IF \left(l_5 < x < l_2; \left(\frac{\cos\left(\frac{r_3 - (x - l_5)}{r_3}\right)}{\pi} \pi r_3^2 - 0.5(r_3 - (x - l_5)) \sqrt{r_3^2 - (r_3 - (x - l_5))^2} \right) F_{adhesion}; 0 \right)$$

The same equation but then for the perpendicular force generated by the peeling moment can be described using:

Suction cup design

$$(39) F_{peeling, A} = \frac{2l_3(F_{gravity} + F_{pull})x}{l_2^2}$$

By plotting both equations in the same graph it can be established whether the suction cup generates enough adhesion to overcome the peel force (Figure 95). It can be seen that for a suction adhesion device where l_3 is 45 mm, sufficient adhesion is created to counter the forces due to peeling.

Furthermore if the peeling force becomes higher than the adhesion force the conversion mechanism comes into play. The mechanism causes a reduction in the maximum peeling force and increases adhesion by trading in contact surface for pressure surface. This means that the system has a higher resistance against peeling than is calculated with the peeling force model. The suction cup is more likely to slide downward from the substrate than to peel off.

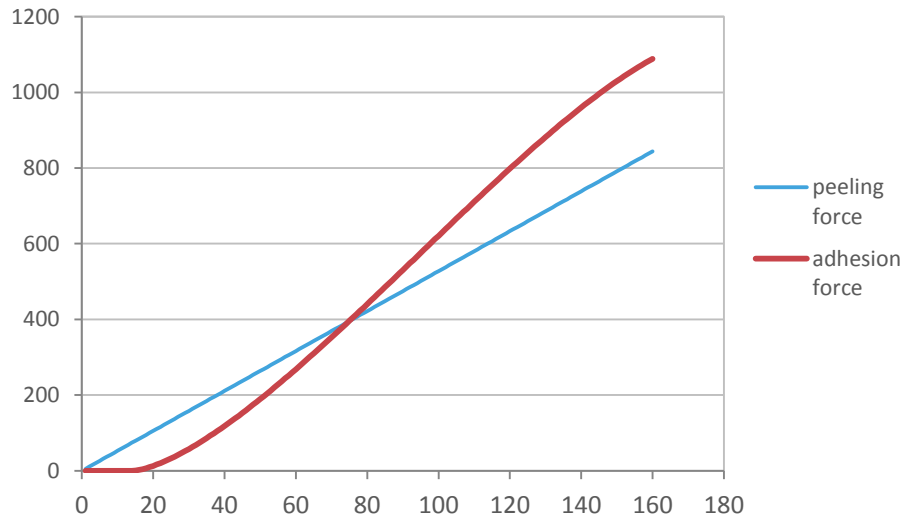


Figure 95 - Peeling force (N) and adhesion force (N) when measured from point A (mm).

Detachment mechanism

Up till now the suction adhesion value predicted by the theoretical model signifies the amount of adhesion that the cup is creating in rest. However as stated a number of times before this value might actually be higher since it is likely that a conversion mechanism is at play during this detachment phase. To get a better understanding of this mechanism its effects on performance is analyzed.

The conversion mechanism can be divided into two effects. The first effect is that the partial detachment of the adhesion and friction pad increases the amount of pressure surface. When it is assumed that the entire adhesion and friction pad is allowed to come loose from the substrate without breaking the seal, the increase in suction adhesion can be described by the following formula.

$$(39) F_{conversion} = A_{contact}(P_{ambient} - P_{detachment})$$

In this equation ' $A_{contact}$ ' is the contact area of the adhesion and the friction pad during rest ' $P_{ambient}$ ' the absolute pressure outside the suction cup and ' $P_{detachment}$ ' the absolute pressure during detachment. When the assumptions made here are valid the total amount of suction adhesion at detachment can be described as a function of the total surface of the adhesion and friction layer (A_{pad}) and the pressure differential.

$$(40) F_{suction} = A_{pad}(P_{ambient} - P_{detachment})$$

Although this effect seems straightforward it is influenced by a second effect that can occur during detachment. The second effect increases the pressure differential due to the increase in volume underneath the suction cup. The increase in volume subsequently results in a temporary pressure spike that leaks away depending on the leak rate of the suction cup. This means that the second conversion mechanism effect depends on the speed at which the suction cup is pulled from the substrate and the surface topography. When the suction cup is pulled rapidly from a smooth substrate, this results in a large pressure spike that lasts for a long period of time. A slow pull on a rough surface on the other hand results in a small spike that quickly fades away.

In situation where no leakage occurs the increase in the pressure differential can be

Suction cup design

calculated with Boyle's law (equation 39). This however requires detailed information about the enclosed volume in the suction cup and the amount of death space in the system. Since the theoretical model does not contain this information it is advised to use test data from a vacuum sensor to calculate the exact extent of the conversion mechanism.

$$(41) P_{detachment} = \frac{V_{rest} P_{rest}}{V_{detachment}}$$

Strength

The final aspect of the suction cup design that needs to be verified is whether the components can handle the large shear forces that the isotropic boundary calculations predict. The highest amount of friction that was encountered in these results occurs with a fully worn pad on a glass substrate. A massive 3572.33 N is generated in this case. Even though this is way above the isotropic boundary that the device will indicate, it is important to check whether the device can handle such forces. If it is overloaded for example the device should come off without any structural damage.

To determine if this is likely, the 2D finite element model is subjected to a force that is applied to the top of the suction cup. This force is equal to the amount mentioned above. By fixing the microstructure a realistic scenario is created, in which the force applied on the device needs to travel through the suction cup base, the textile backing and the adhesion/friction layer.

Scanning the simulation plots for stress hotspots, results in two areas that might be vulnerable. The first hotspot is located in the textile backing where it meets with the suction cup base (Figure 96). The second hotspot is located in the plate that simulates the housing of the suction cup device (Figure 97). Neither of these hotspots however is particularly worrying. The first hotspot has a maximum stress value of 124.1 MPa, whilst the Kevlar has a tensile strength of 3.62 Gpa. The second hotspot has a maximum value of 43.69 Mpa. If the housing of the device is made out of Nylon 6/10 then it more than strong enough since this polymer has a yield-strength of 139 MPa (Solidworks material library).

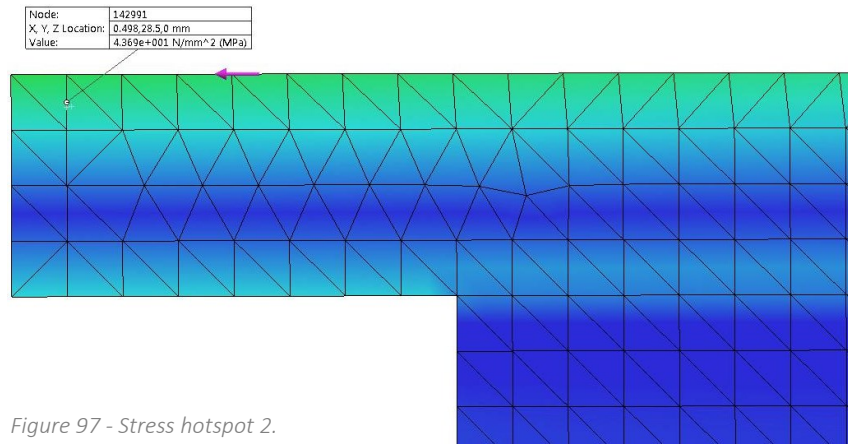


Figure 97 - Stress hotspot 2.

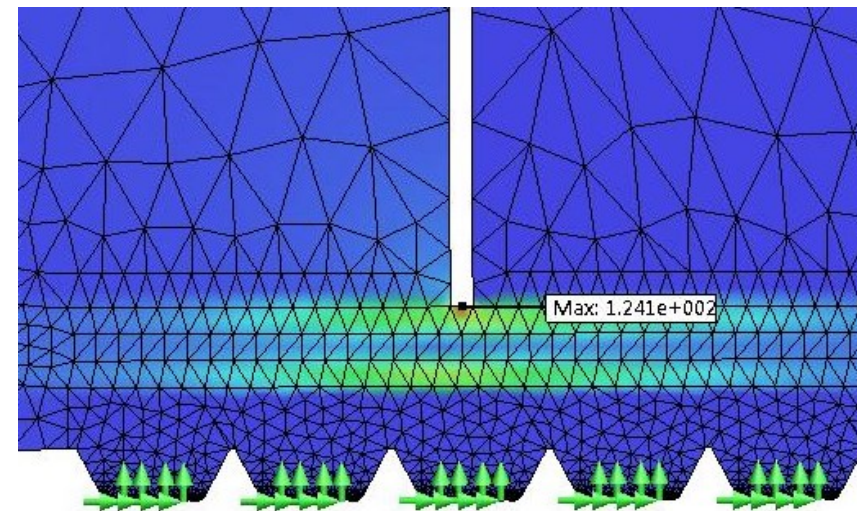


Figure 96 - Stress-hotspot 1.

Suction cup design

Overview

In this chapter the design of the suction cup was discussed and analysed. However no comprehensive visualization of the design was given. Figure 98 therefore shows an overview of the suction cup. The suction cup is presented as an exploded view to be able to show the hidden components of the design. In addition to this the materials used for each component can be seen in Table 20.

Component	Material
1. Suction cup base component 1	POM / Delrin
2. Adhesion/friction layer	PDMS rubber
3. Textile backing (adhesion and friction layer)	Kevlar
4. Supporting foam	Closed cell neoprene foam
5. Soft sealing layer	PDMS rubber
6. Suction cup base component 2	POM / Delrin
7. Velcro	Nylon / Nomex
8. Textile backing (soft sealing layer)	Kevlar
9. Closed foam ring	Closed cell neoprene foam
10. Adhesive layer	Polymer film
11. Suction cup base	Rigid PVC
12. Seal	Neoprene rubber
13. Suction cup base component 3	Pom / Delrin
14. Seal	Neoprene rubber

Table 20 - Suction cup component overview.

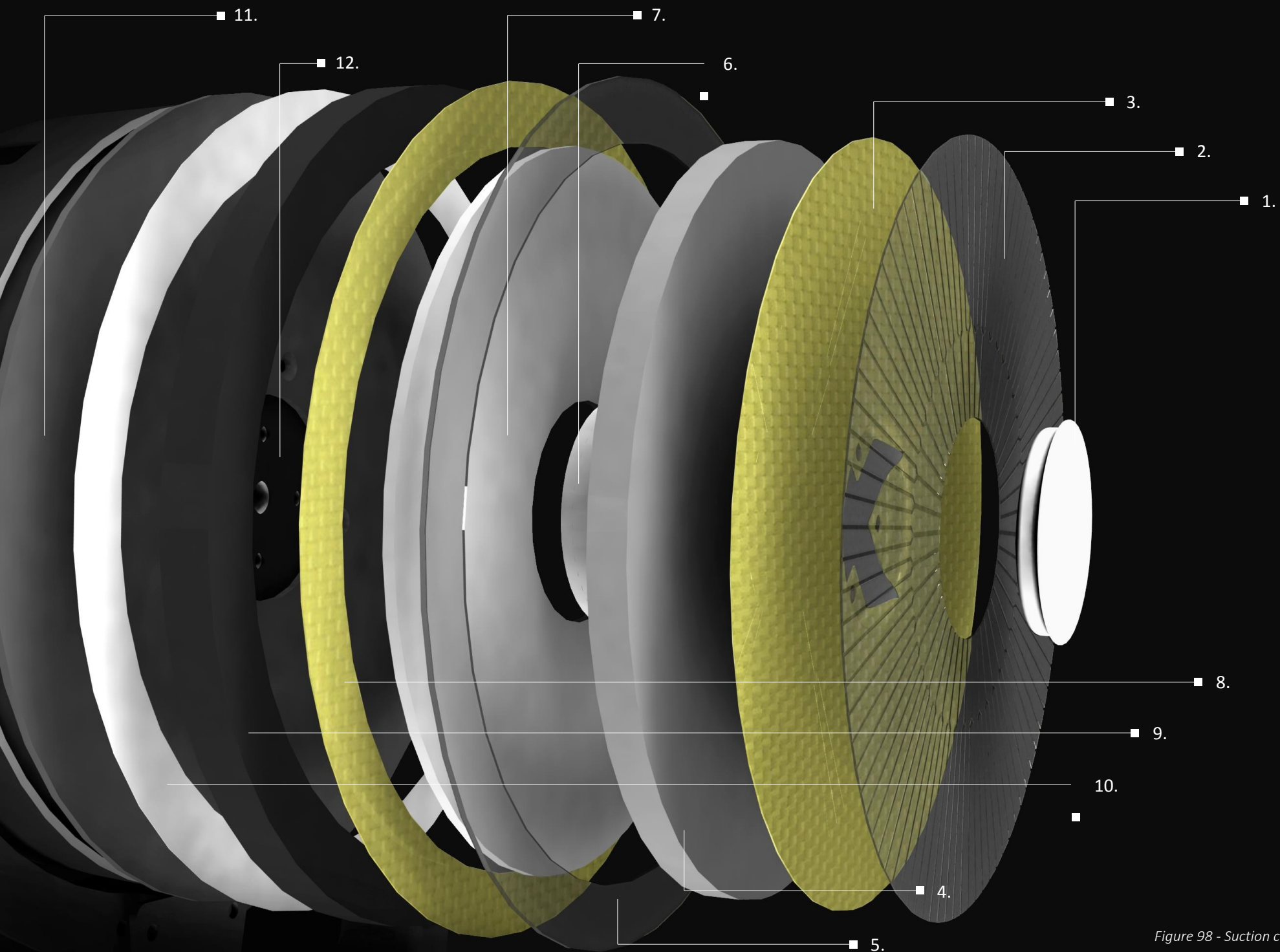


Figure 98 - Suction cup components.

System architecture

Now that the design of the suction cup has been completed, the system behind it needs to be defined. The first step of this process is to sketch out the layout of the system and to determine which components are necessary for the device to function according to the list of requirements.

Figure 99 shows an overview of the system that is intended to power the suction adhesion device. The diagram is largely based on Figure 45 but contains more specific component descriptions. The system is divided in three groups of components that fulfil a distinct part of the device's functionality. The electrical system components play a supporting role by providing the correct amount of electrical power to the rest of the device. An internal lithium iron phosphate (LiFePO₄) battery can be charged by connecting it to the grid via a battery charger. The battery in turn powers the other components. To be able to provide the control system and interface system with a stable supply of 5 volt the electrical system contains a dc/dc converter and a voltage regulator. This prevents the electronics from being affected by the voltage drop that arises when the battery is drained. In contrast to the rest of the system the vacuum pump is powered directly from the battery. To give the control circuitry the ability to turn the vacuum pump on and off a solid state relay is placed in between the pump and the battery. A solid state relay is chosen since it has no moving parts, which increases reliability. It is also able to switch the pump on and of much faster than a conventional relays.

The brains of the device are formed by an 8-bit microprocessor. This component receives all the inputs from the sensors and various interface components, analyses them, and generates the required output. The pressure underneath the suction cup is measured by a gage vacuum sensor. This sensor can determine the pressure differential by comparing the pressure inside the device with the atmospheric pressure. With the help from the theoretical model and future experimental results the pressure differential can be used to give a prediction of the isotropic boundary. To keep the software that is used to calculate the isotropic boundary up to date, the device is equipped with a Bluetooth 4.0 module. This allows updates to be send to the device and also enables it to communicate with other suction cups and smart devices. It

furthermore allows the producer to develop new types of suction cups and make them compatible with existing devices.

To let the device know which type of suction cup is connected the interface contains a menu button that is incorporated in a sliding ring that is similar to the one shown in Figure 46. When this menu is opened the user can select the correct suction cup by rotating the ring. The movement of this ring is sensed by a rotary encoder. Each time when the ring is turned a few degrees an electric pulse is send to the microprocessor. The combination of a menu button and the sliding ring opens up the possibility to make the sliding ring multifunctional. This option is leveraged for the pulling resistance setting. A short push on the sliding ring unlocks the pulling resistance setting, which also can be changed by rotating the sliding ring. Pressing the menu button again makes the changes made by the user definitive. The third and final button on the interface can be used by the user to connect the suction cup with other devices using Bluetooth. A connect button is necessary since it costs energy for the module to look for devices. Not including a button would therefore result in a waste of energy.

The output that is generated by the microprocessor is communicated to the user by two components. A segmented E-ink display module is used to show the settings and the status of the device. This type of screen was chosen since it lowers the burden on the microprocessor as it does not have to calculate the state of each pixel. Electronic ink screen are furthermore known for their extremely low power consumption. In contrast to normal displays they only require energy to change the state of a segment or a pixel. This means that when the suction adhesion device is sealed properly on a substrate it can stay attached for long periods of time. The ability to medium-long term reversible adhesion opens up new uses for the device. The suction cup could for example serve as a winching point that is useful for lifting heavy items to the next floor. The second means for the device to communicate with the user is via a speaker. This component needs to be included to fulfil requirement 6. Using the speaker the device can warn the user when the suction cup is at risk of letting go and can also be used to clarify certain interface interactions.

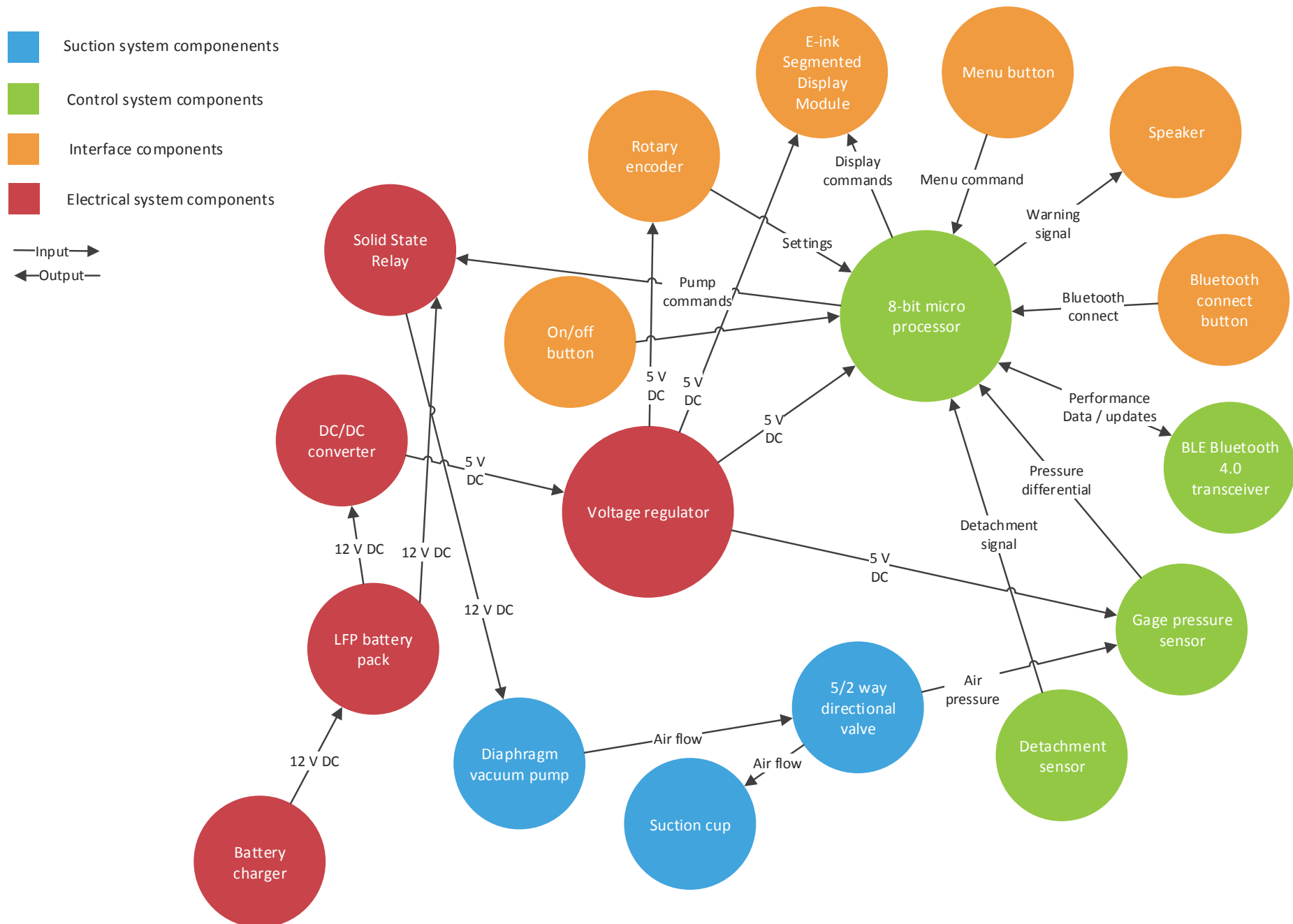


Figure 99 - Final concept functional component diagram.

Design embodiment

To make the proposed system architecture less abstract, an impression is created that shows what the suction adhesion device looks like in its final form. This impression is based on the functional component diagram in Figure 99 and the drawings made for the harness concept. To make the design embodiment of the suction cup as realistic as possible an attempt is made to include as many production related aspects as possible. Also effort is put into making sure that the design fits the new circular design paradigm by selecting healthy materials and making components easy to disassemble. This is done because of the personal beliefs by the author that considerations regarding sustainability have to be included into the design at an early stage.

Styling

As indicated by requirement 12 it is important that the styling of the device fits the preferences of the user. To achieve this, market research was performed to look at similar products that are used by the target group. Especially the design features found on power-tools are considered a good representation of the desired design language. This design language is comprised of many angular shapes and pronounced edges to give the power tool a rugged and masculine appearance. Other key features that can be identified are the exposed vents and bolts that give a sense of power and strength. This



Figure 102 – An example of power tool design that contains all of the characteristic design features.

is enhanced by incorporating highly contrasting materials in the design, which is done by combining a brightly coloured casing with either black or grey over-moulded sections (Figure 102).

To set the design of the suction adhesion device apart from other power-tools, hints of the biological inspiration sources are included in the design. This is done to make the suction adhesion device look more bionic and to signal to the potential customers that the device contains advanced technology that makes it a good investment.

The centre of the design is formed by a spherical e-ink display. The inspiration source for the placement and the shape of the display comes from the eye of a squid. These species have a large round eye in the middle of their body (Figure 100). Around the screen the interface buttons and sliding ring are placed, which due to their contrasting colour with the e-ink display are made to look like the iris of the squid's eye. Further outward the casing changes into a grey coloured shield that protects the internals of the device. The grooved shape of this part of the housing is inspired by the shape of a limpet shell (Figure 101) and gives it additional strength. Towards sides the grooves end in a



Figure 100 - Squid eye.



Figure 101 - Limpet shell.



Figure 103 - Lamprey gill openings.



Figure 104 - Final concept design overview

Design embodiment

mounting point for the bolts that connects the shield with the rest of the casing. The exposed bolts are an important accent in the design of the casing and are copied from the harness concept. On the sides of the device two sections of the casing form the detachment paddles. Pressing both of them reverses the flow in the pneumatic system and detaches the suction cup. To make them stand out a bit more the detachment paddles have a dimple pattern on them. This pattern signals to the users that the detachment paddles of the casing can be pressed down and are inspired by the gill openings of the sea lamprey (Figure 103).

By directing the flow of air or water towards the outside of the device and making the casing water tight, the suction cup is able to pick up submerged objects and should even be able to function underwater. This is made possible by the indifference of the diaphragm pump to pumping air water. Although this feature is not strictly speaking a styling feature, it is a clear reference to the aquatic habitat of the creatures that the device is based upon. It also opens up new application areas, such as marine exploration and underwater maintenance.

Production, material selection and costs

Although having the right styling is an important aspect of the design, it is useless when the components cannot be produced or cost way too much to be economically viable. Therefore it is decided how the components are made, or whether they are bought in from a supplier. An attempt is made to source as many existing parts as possible in order to be able to produce a high quality device for a low cost price. Attention is furthermore paid to make sure that the components that form the unique selling point of the device are not outsourced to other parties. In the case of the suction adhesion device these components can be found in and around the suction cup. To be able to make an estimation of the costs to make the device it is assumed that it is mass produced at a production size of around 5,000 units. This number is chosen based on the fact that in the Netherlands there are almost 500 professional furniture moving companies (K.v.K, 2016). When keeping in mind the other application fields for the device and the possibility to sell the products abroad it is believed that this is a viable production size.

Casing and handle

The casing and the handle of the suction cup is made from nylon 6 which is reinforced with 30% glass fibre to give it additional stiffness. This blend is a commonly used in high quality power-tool casings. The casing is created using an injection moulding process, which is considered an efficient way to produce these parts in a mass production setting. The major contributions of the costs for producing these parts can be divided into two categories. The fixed costs are predominantly determined by the costs to make the injection moulds. The variable costs on the other hand contain expenses such as labour and material costs. To be able to give a prediction of these costs a cost calculator is used from custompart.net, a leading online resource for estimating manufacturing costs. In addition to the injection moulded parts the casing and handle consists out of two ergonomic handles and some cork gaskets to keep it watertight. These parts are all bought in from a supplier.

Electronics

The electronics contained within the device are bought in from a supplier to guarantee their quality. These components, like the Bluetooth transceiver and the 8 bit microprocessor, are mounted on three custom designed circuit board that are connected to the battery, the sensors and the interface components using standardized JST connectors. In this way the circuit boards or one of the other components can be

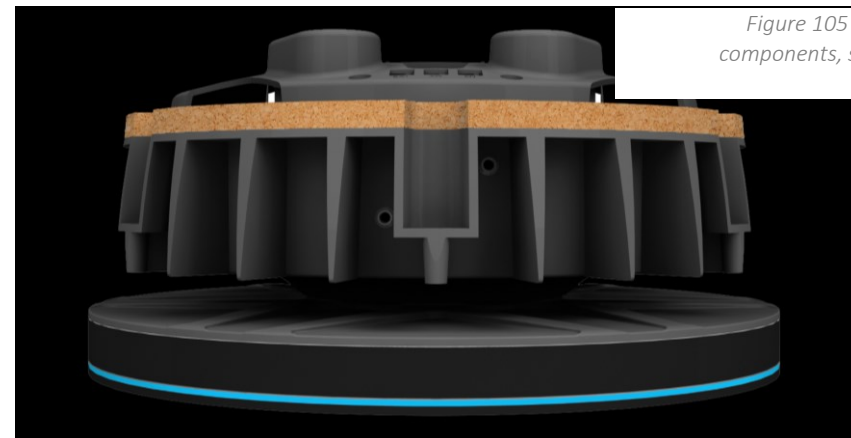


Figure 105 - Internal components, side view.

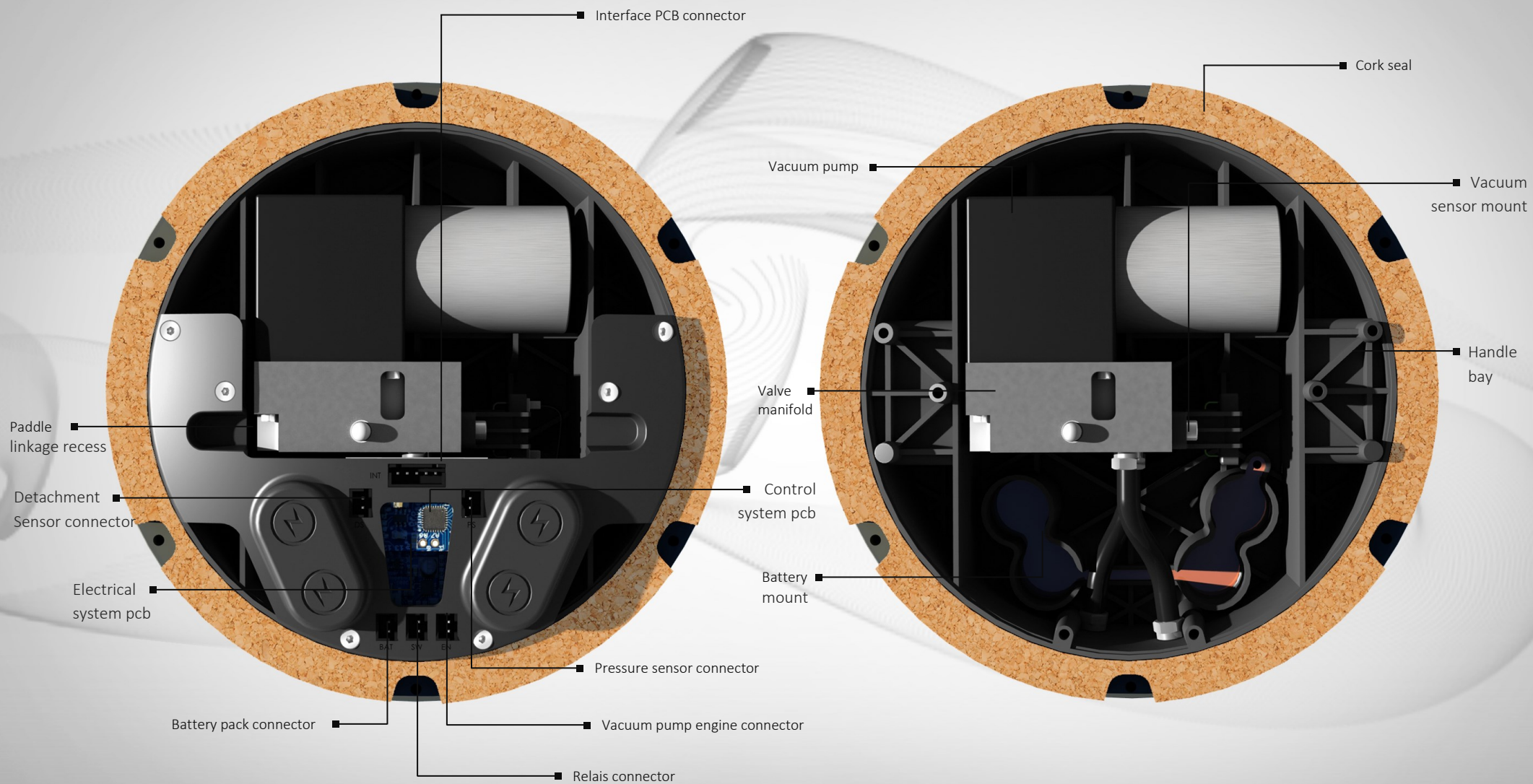


Figure 106 - Internal components overview.

Design embodiment

easily upgraded or replaced. The circuit board itself is made from epoxidized linseed oil and flax fibre with copper and tin traces. This is a more environmental friendly alternative for conventional PCB substrates (Deng et al., 2011). The total costs for the circuit board are estimated using a cost calculator from pcbcart.com and prices of the most important components.

Battery and charger

The battery pack for the suction adhesion device is made out of four rechargeable lithium iron phosphate batteries (LFP). Each of these cells produces 3.2 V and is wired in series with the other batteries to produce 12.8 V. Lithium iron phosphate batteries are chosen because they are made from non-toxic materials that are abundant and cheap. They are also safer and suffer less from performance degradation than conventional Li-ion batteries. These advantages of LFP batteries is offset by their lower energy density which means that more room in the suction adhesion device has to be reserved by the battery pack. To charge the LFP battery a management board has to be incorporated into the battery pack. This is because LFP batteries do not self-balance. The power management system and the battery charger can however be much simpler than for a Li-ion battery. This is because LFP batteries have a much larger overcharge tolerance, which gives them comparable safety performance as lead acid batteries ("How to charge", 2016). The costs for the LFP battery pack is based on the price for a single cell. It is assumed that when buying in bulk this price drops so that the management board is included into the price. The price of the charger is estimated based on the prices of similar LFP battery chargers that are already on the market.

Pump and pneumatic valve

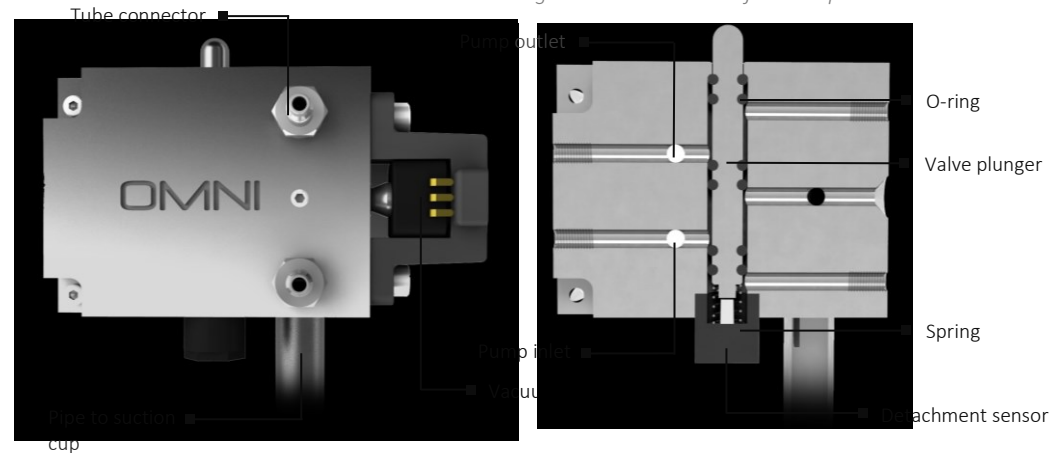
The diaphragm vacuum pump for the suction adhesion device is sourced from a supplier and its characteristics are based on existing offerings. The pump is powered by an 11 Watt brushless DC engine and has the same performance characteristics as the pump selected for the suction cup design. To control the flow of air exiting the pump a custom manifold replaces the casing lid of the pump. This manifold is machined from a billet of aluminium and contains various air channels. The air flow is governed by a spring loaded plunger that slides up and down in the manifold to open or close exhaust

ports. When the plunger is pushed in the manifold the flow in the system is reversed and the suction cup detaches. Letting go of the release paddles restores the normal flow in the manifold. This working principle is similar to a 5-2 directional control valve. The advantage of producing a custom manifold is that the pressure sensor can be incorporated into its design. This eliminates the need for expensive pneumatic couplings. Another advantage of this approach is that the amount of dead space in the pneumatic system can be minimized as the manifold is designed to fit perfectly within the dimensions of the suction cup device. The costs for buying the pump and making the manifold are based on the price given by the manufacturer for the vacuum pump, the material costs and labour costs for making the manifold.

Suction cup

The design of the suction cup of the final concept is largely the same as presented in the previous chapter. However a number of adjustments have been made to make the suction cup more user-friendly, cheaper and more sustainable. Since the adhesion and friction pad is subjected to wear it needs to be replaced at a regular interval. For this reason the pad is made significantly cheaper by using linen fibres instead of Kevlar for

Figure 107 - Valve manifold components.



Design embodiment

the textile backing. This is considered possible since the strength analysis in chapter 4.5 showed that the textile backing is a factor 100 stronger than needed. To reduce the total costs of ownership further the Velcro layer is moved beneath the supporting foam, which means that the foam does not need to be replaced together with the adhesion and friction pad. Also the bottom two suction cup base components do not have to be thrown away together with the pad. Instead the fabric is stiffened up near the centre using a PLA based epoxy. The textile backing is therefore just held in place by the clamping force of the suction cup base parts and the cup shape of both the backing and the base. To make the bottom part of the suction cup base easy to remove a stainless steel locking ring is added. This part rotates in the bottom suction cup base part and has an internal thread that locks it to a tube sticking out of the suction cup casing. The steel ring is fitted with a number of dimples that allows it to be rotated by a fork shaped tool. This system can also be seen on a lot of angular grinders, and allows the user to quickly replace the pad.

Component overview, total production costs and weight

In order to get a better perspective on the total production costs of the suction adhesion device all parts and their associated costs are listed in Appendix F. It was chosen to calculate the costs and weight of two variants of the suction adhesion device: a basic device that does not have any sensors or interface components and the smart device discussed in the previous sections. The goal is to determine if the added costs and weight are justified by the functionality that they add to the device. When looking at the results in Appendix F it can be concluded that both the weight and price are at the upper limit of what is allowed according to the list of requirements. The basic device costs €171,96 to produce while the cost for the smart device accumulate to €225,36. From own experience this translates into a retail price of about €700,- and €900,-. The total weight amounts to 2194,9 for the basic device and 2323,3 for the smart version.

Material cycles

To illustrate that the final concept has been designed with the circular economy in mind the system behind the material cycles is explored. Although all chosen materials are

healthy and can be re-used or composted, a method needs to be in place in order to get them back. Therefore a take-back system makes sure that the materials are returned after they have been used. To stimulate the user to return the pads and the device to the producer, a deposit system is in place that offers cashback or discount on future purchases. After the materials have been recollected the device is dis-assembled and the technical nutrients contained in the parts are returned to a material bank. Such banks lend out technical nutrients, like high quality plastics and metals, and keep them in a closed loop.

Materials that belong in the biological cycle like the adhesion and friction pad are composted under the right circumstances and subsequently returned to the environment once they have been broken down into biological nutrients.

Some of the parts contained in the suction adhesion device will at first not comply with the circular economy's requirements. These parts, like the vacuum pump and some electronic components, are sent back to the original manufacturer. It is their task to develop their own material cycles. To guarantee that the materials are handled in the right way a contractual agreement needs to be in place with the supplier. This stimulates them to develop more sustainable products and think about their place in the circular economy. A graphical representation of the system explained here can be seen in Figure 109. This proposed business model can be seen as a substitute for the inability of technological systems to repair themselves. For a truly bio-inspired product the business model is thus an integral part of the design.

Suction cup locking ring



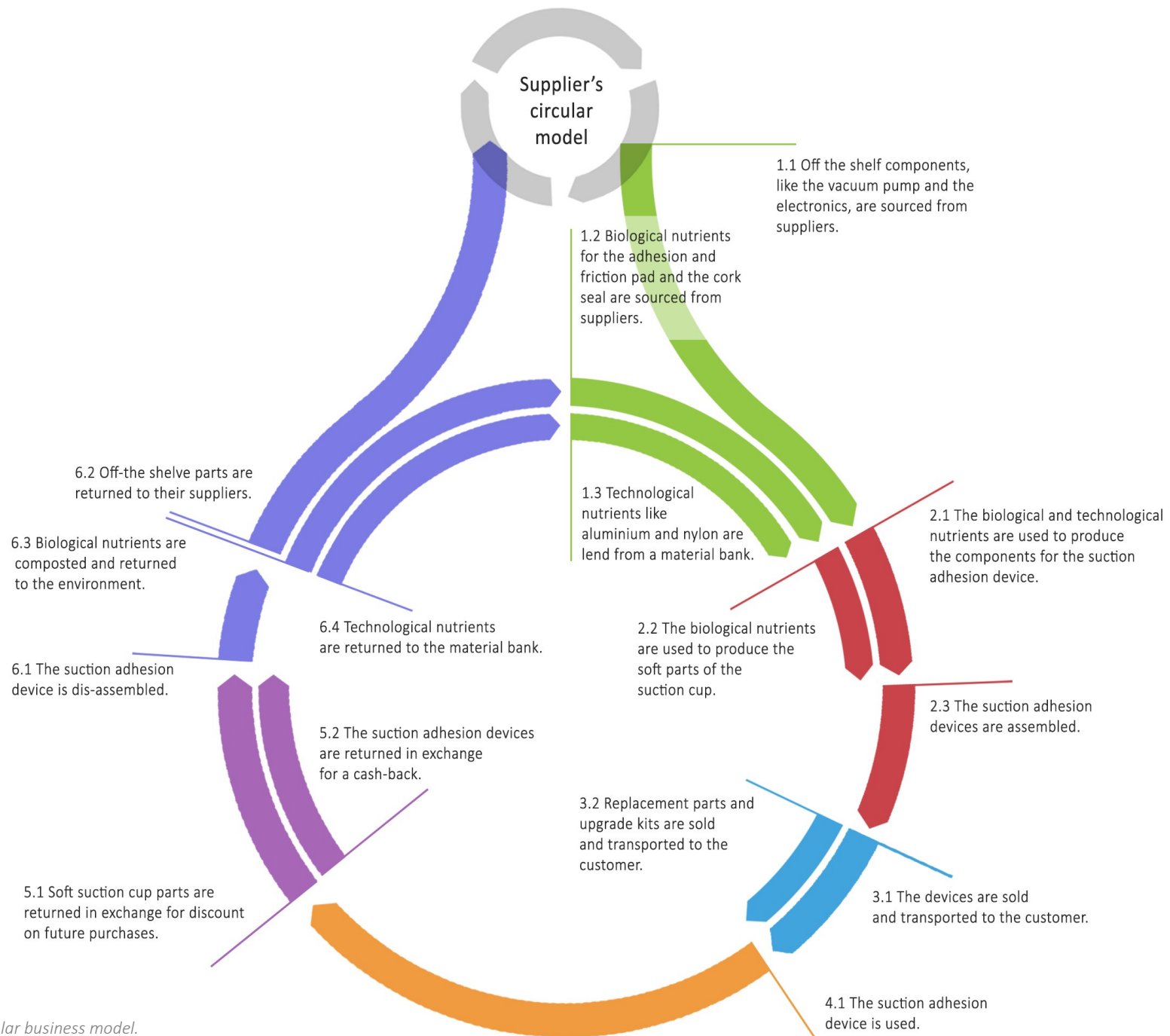


Figure 109 - Proposed circular business model.

Use and interface design

Now that a detailed impression of the final product has been created, a start can be made to explore the interactions between the user and the device. These interactions are made possible by a user interface that is incorporated into the device itself, but the interface also entails an application that can run on a variety of smart devices.

A passive interface feature that does not fit these two categories, is the method to display the amount of wear of the adhesion and friction pad. This is communicated passively to the user by a colour change of the pad. This colour change sets in when the pad is worn to such an extent that the isotropic boundary displayed by the device can no longer be guaranteed. To be able to change its colour the pad is made out of two parts (Figure 108). On the bottom a grey colour indicates that wear is not yet affecting the isotropic boundary. When the coloured part on top however starts to shine through, the user should consider changing the pad.

To get a better understanding of how the interface works a State Transition Diagram is created. This diagram can be seen in Figure 110 and visualizes the structure of the interface. It shows what the response of system is to actions of the user or disturbances from the outside. The central part of the diagram is formed by two states that show in what phase of use the system is. These states are the situations where the suction cup is attached and when it is detached. Certain triggers are used to let the system switch between those states. To get from the detached to the attached state, the system scans for small pressure spikes. These are the result of the user pushing the suction cup onto a substrate. An advantage of this method is that the system automatically selects which substrates it can adhere to and on which substrates a seal is not possible. The threshold for activation is coupled to the type of suction cup that is attached to the device. A smaller suction cup for example generates a smaller pressure spike than a larger suction cup. To give the user feedback about his efforts to create a seal, a ring of lines is present at the edge of the display (Figure 111). To activate the suction cup all lines need to be visible. Once this has been achieved the device will beep once and the lines disappear one by one. However as the pressure-differential starts to climb again, the lines reappear. This time each line represents a percentage of the pulling resistance that is set by the user. It was chosen to use lines to visualise this since the system

cannot give a very accurate prediction of the isotropic boundary. This exact value depends on variables that cannot be measured by the device, like the ambient temperature. When the target pulling resistance is reached by the device all lines are visible and two beeps can be heard.

During the attachment phase the device is set to monitor the pressure differential underneath the suction cup. As stated before the system can compensate for leakage by switching on the vacuum pump. When this is not enough to keep the pressure differential within a certain range of the set value, a loud beep is sounded. This safety feature gives the user a bit of time to put the object back on the ground. To prevent confusion the alarm is disabled when the user presses the detachment paddles. This is made possible by a push button mounted beneath the valve plunger that acts as a detachment sensor.

To detach the suction cup the user has to keep pressing the release paddles until the suction cup pops off the substrate. Releasing them sooner will cause the system to restore the pressure differential because the system is still in attachment mode. Only when the suction cup is fully detached and the pressure sensor value drops to zero is the system switched back into the detached state.

Outside of the normal use sequence the device's interface also allows the user to change the settings of the system. As stated in chapter 4.7 there are two setting menus. One menu allows the user to set the required pulling resistance and the other menu is used to let the system know which suction cup is connected. When the user presses the sliding ring shortly, the menu name appears on the interface. This is to show the user which setting is being edited. When the user rotates the sliding ring the value is adjusted. The interface shows the minimum and maximum weight that can be lifted using the ring of lines. Once the user has selected the desired pulling resistance the choice is validated by pressing the pulling weight button again. The menu name disappears and the system calculates the new required pressure differential. This calculation is made using performance data stored on the internal memory of the 8 bit

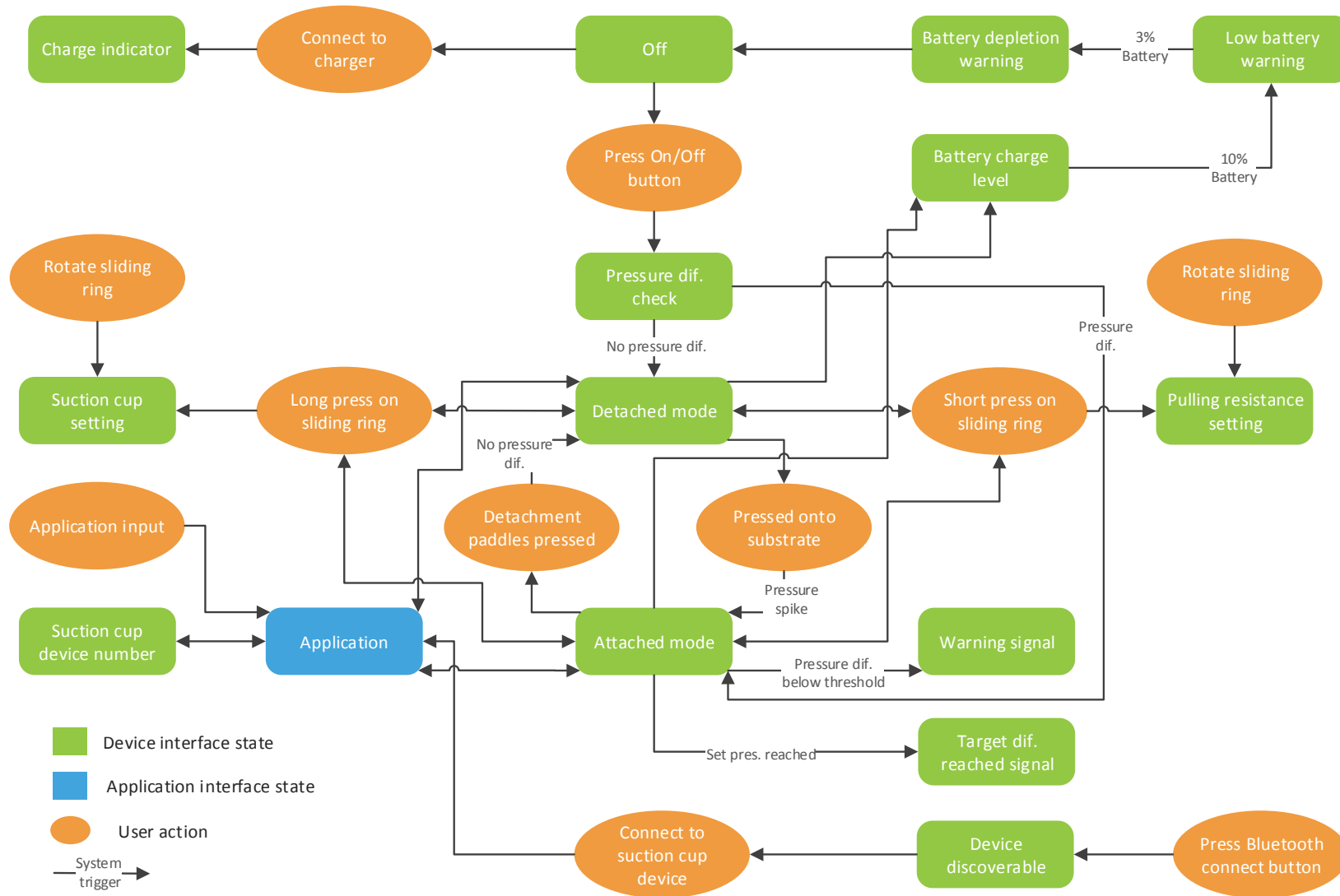


Figure 110 - State transition diagram.

Use and interface design

processor. To couple the pressure differential to the right pulling resistance the user needs to select the correct suction cup setting. The steps that need to be taken are explained on the packaging of each replacement pad. First the user has to open the suction cup setting menu by a long press on the sliding ring. The digits in the middle of the display disappear and a two-digit code appears (Figure 111). This code corresponds with an ID code on the replacement packaging. When a different code is shown the user needs to rotate the sliding ring until the correct code is shown on the screen. To accept the selection the user presses on the suction cup selection button and the code is replaced again by the pulling resistance setting.

To connect the suction cup to other devices the interface contains a Bluetooth connect button. When this button is pressed a Bluetooth icon on the interface starts to flash. This means that the suction cup is discoverable for other Bluetooth devices during a period of thirty seconds. A successful connection with a device is indicated when the Bluetooth icon stops flashing and stays visible. When no connection is made the icon disappears and the Bluetooth module goes back into sleep mode. This mode of operation is similar to many wireless Bluetooth speakers, which should make it more intuitive to use for the user.

Once the suction cup is connected to a smart device the user can access additional interface features and set up a network of suction cups that work together during lifting. The interface of the application that is used for this is formed by an oversight of all connected suction cups. These suction cups are given a number that corresponds with a number shown on the device's interface after the Bluetooth icon. This allows the user to quickly pin-point problem areas during lifting. The app also serves as a lift coordinator by automatically adjusting the pressure differential underneath the suction cup when needed. This can come in very handy when for example one of the suction cups starts to leak during lifting. In this case the application will send a command to the neighbouring suction cups to increase their grip on the object.

In addition to the networking feature the application interface can also be used to control the settings of each suction cup. Since the interface is not limited to the capabilities of the segmented e-ink screen much more information can be given to the

user. When selecting a suction cup for example, information about its capabilities is displayed in the app. In this way the user can make a more informed decision about choosing the right suction cup. To make the most out of the device the application also contains tutorial videos which show the best way to lift items. This increases the total benefits of ownership by educating the user about its capabilities. The benefits of ownership are maintained or even increased over time by sending updates the suction cup when it is connected to the application. In this way the manufacturer can keep developing new and improved suction cups without having to bring out new versions of the device each time.

After a period of use the battery of the suction cup will become drained. The charge contained in the battery can be estimated by looking at a battery bar on the suction cup's e-ink screen. This bar contains four sections that represent how full the battery is. When the battery voltage dips beneath a certain threshold this icon starts blinking. In addition to this a low battery warning can be heard from the speaker. Also a notification is sent to the user using the application when the suction cup is connected to Bluetooth. When the suction cup is not connected to a wall outlet it will shut down completely. This is preceded by another low battery warning.



Figure 111 - Device interface.

Conclusion

The work done in this chapter has shown that analysing natural systems can be helpful to create new and innovative product ideas. The information gathered in chapter 1 has proven to be a great source of inspiration in the conceptual design phase as well as during the development of the final concept. In some instances the data obtained from literature is very close to what can be concluded from the results from the theoretical model. The Young's modulus of the sealing rim from the octopus for example, which was determined by a study from Tramacere et al. (2013), is a good estimation of the value for the suction adhesion device to be able to adhere. If this value had to be determined without a guideline to point into the right direction, it would have taken a lot more time.

Also the other analysis work performed in chapter 2 and 3 have helped to generate three concepts that solve a relevant problem and fit the user's requirements. By using the same function structure but by varying the complexity of the system, the concepts appeal to different market segments. However since they share a lot of their functionality, a system developed for one concept can be used by the other concepts. This approach thus facilitates the creation of a product portfolio around the same technology.

Since it is not possible to create designs for all concepts, the decision was made to choose the harness concept for further elaboration. When comparing this concept with the Keydrivers for the device it can be concluded that its level of complexity has the right balance between costs of ownership and performance. It is furthermore believed that the market size and demand for this type of product is the largest of all three concepts.

For the design of the suction cup it was chosen to follow a parametric approach. In this way the theoretical model can be used for different types of suction cups. Although only one design is presented in this chapter it is believed that an optimal suction cup design can be created for any use situation by applying the insights from the theoretical model. With more work the model could even be used the other way around. By mapping the influence of changes for each parameter on the performance of the suction cup, it becomes possible to let the model generate the ideal suction cup for the

task at hand. If for example a large isotropic pulling resistance is required and the device is going to be used on rough surfaces, the model will generate a large diameter suction cup with a thick and soft sealing rim.

The other part of the suction adhesion device is formed by the mechanical and electric components that control the suction cup. From section 4.5, 4.6 and 4.7 can be concluded that the envisioned system is a realistic proposal that can be made at a competitive price. The system uses cutting edge technologies like an e-ink screen and Bluetooth 4.0 to communicate with the user and other devices. This injection of smart technologies is believed to be a promising direction for the design of future powertools. Not only does the added connectivity open up new ways for the user to interact with the device, it also allows it to become part of a network of suction cups. This modular system greatly expands the capabilities of the device and makes it in theory possible to lift any object.

The choice to give the suction cup device the ability to connect with other devices is furthermore motivated by the intent to make it a sustainable product. Instead of throwing out of date equipment away the suction cup device can be continuously updated with new software. This allows for the introduction of suction cups independent from the device. Also the hardware of the device is designed in such a way that it can be easily serviced. Broken components can be switched out for new or better parts by using a system of detachable interfaces. By making the components out of pure and high quality materials these broken parts become an integral part of the device's business model. This is because the materials contained in the components can be kept in a closed loop. Such a method significantly reduces waste and material costs.

Prototype design and performance testing

In this chapter a prototype of the suction cup device is created and its performance is tested. The prototype is based on the suction cup design from chapter 4 and contains the components needed to test the basic functionality of the device. A frame is designed that can handle the forces that are unleashed on the prototype during testing. This frame is subsequently filled with 3D models from the prototype's components to make sure that they all fit within the restricted space that is available. Once all the components are in place, a schematic drawing of the electrical system is used to create a wiring diagram.

A short section is dedicated to the fabrication of the prototype. This is done to make sure that the results obtained with the device are reproducible. Any changes or imperfections in the prototype are discussed and the influences on performance are determined.

With the help from the prototype the suction cup design is tested. The experiments are based on the subjects that are contained within the theoretical model. In the first experiment the sealing capabilities shows whether the suction cup can adhere to the same challenging substrates as its biological counterparts. Next the isotropic boundaries predicted by the model are tested by pulling the suction cup from a variety of substrates. Finally the wear sensitivity of the suction cup is checked to verify that it is durable enough for the application it is designed for.

Any discrepancies between the experiments and the theoretical model are discussed and possible causes as well as methods to correct them in the future are provided.

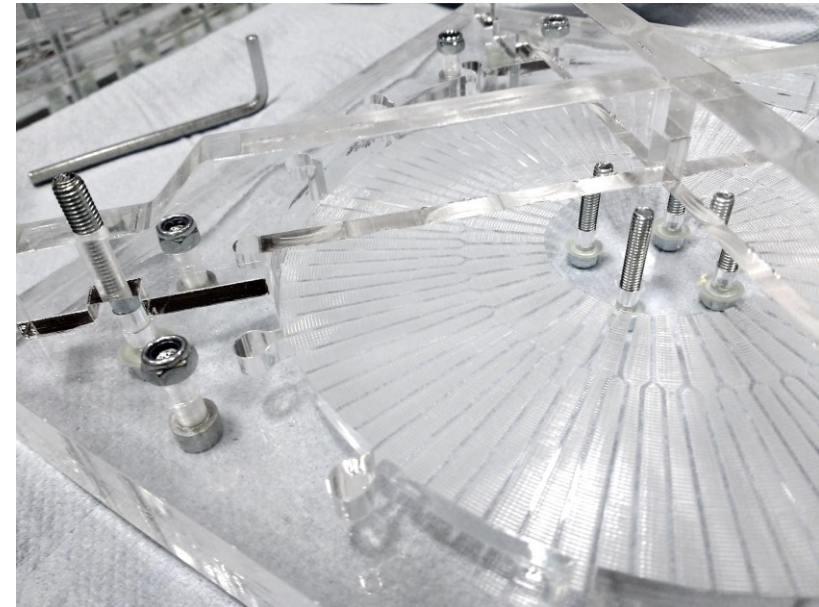


Figure 112 - Adhesion and friction pad mould detail view.

Prototype design

To be able to put the developed concept and its accompanying theoretical model to the test a prototype of the design is required. The design of the prototype is intended for testing some of the most fundamental aspects of the suction adhesion device and is therefore a simplified version of the final concept design shown in the last chapter.

In order to be able to build the prototype within the available timespan many standardized components from established manufacturers are used. These include all the electronic and pneumatic components. An overview of the functional parts that are included in the design can be found in Appendix G.

To create the design of the prototype the suction cup from chapter 4 is combined with a sturdy frame. This frame holds all the components of the prototype together and transmits the forces generated during testing towards the suction cup. The structure used for the frame can be seen in Figure 113, Figure 114 and Figure 115 and consists out of lasercut steel plates. The entire frame is held together with bolted connections. This type of connection is chosen since the frame has to fit closely onto the suction cup to create an airtight seal. Any heat inducing method of connecting the frame pieces, like welding, is expected to result in distortion and is therefore avoided.

To test the pulling resistance of the prototype a tensile strength tester is connected to the handle by a bolt. To give the handle the structural rigidity to cope with the forces during testing, it is made out of steel plates that are spaced apart to increase their stiffness. In addition to a mounting point for the tensile strength tester, the handle also features a handlebar. This is not strictly needed for testing but makes it easier to demonstrate the device outside of an experimental setting. To test the device at multiple pulling angles the handle can hinge freely around the centreline of the frame. This hinging motion is facilitated by two sliding bearings that are fitted in between the frame and the handle. The mounting point for the bearing is formed by a steel tube that is fitted through two steel ribs and is secured using a bolt. This structure locks the tube in place and provides a strong anchor for the handle. To prevent the ribs from buckling when the device is pulled perpendicular from the substrate they are locked in place by two horizontal ribs.

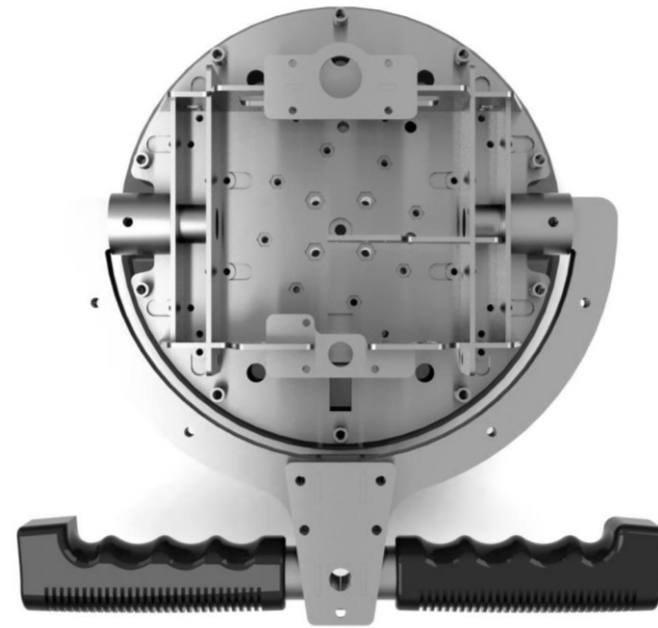


Figure 114 - Frame top view.

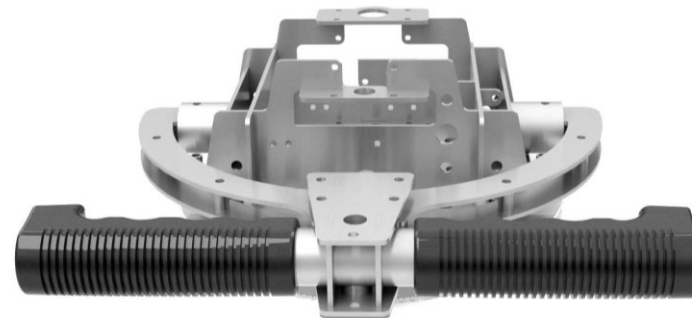


Figure 113 - Frame front view

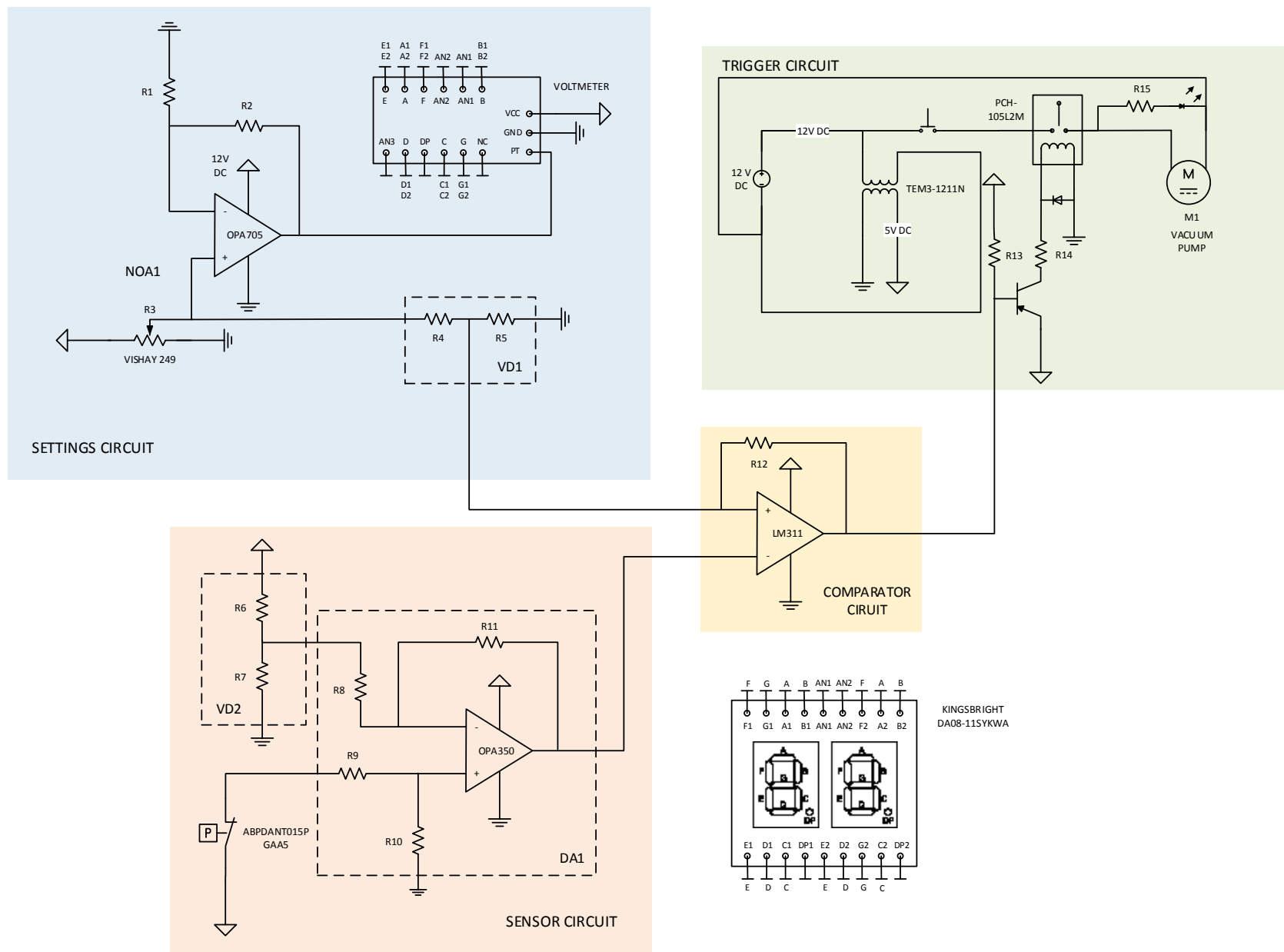


Figure 115 - Schematic drawing of the suction cup electronics.

Prototype design

The rib structure is subsequently fixed to a base plate by inserting locking keys into the ribs and bolting them to the steel base plate. This plate consists out of two layers to increase its strength, but also to allow the bolts to be fixed into position by making hexagonal cut-outs. This makes it possible to replace the suction cup without having to disassemble the entire prototype to get to the bolts.

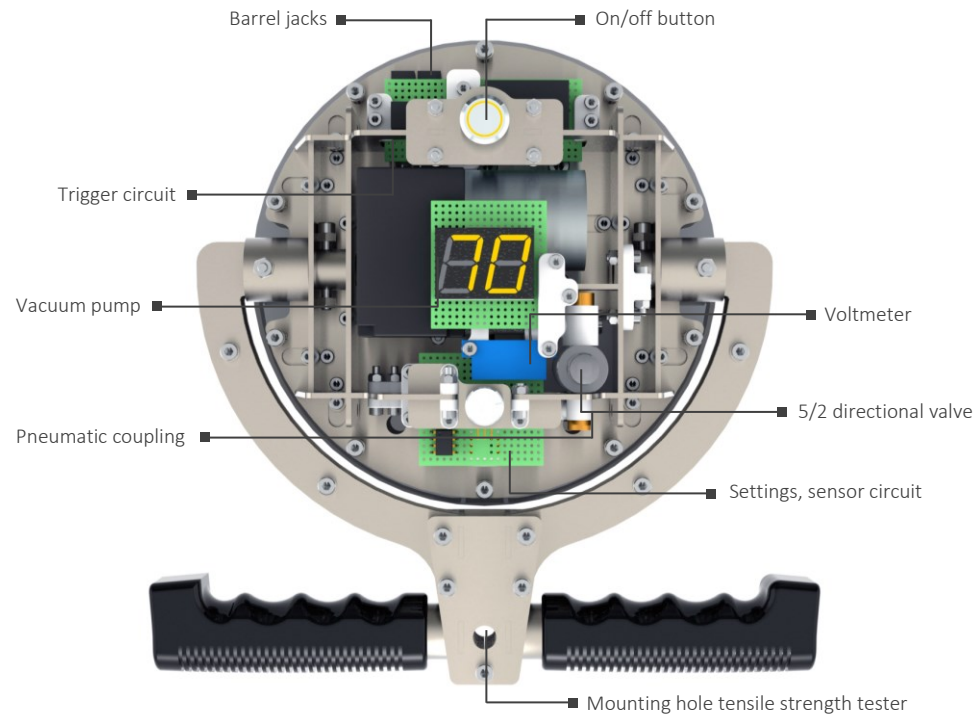


Figure 116 - Prototype component placement.

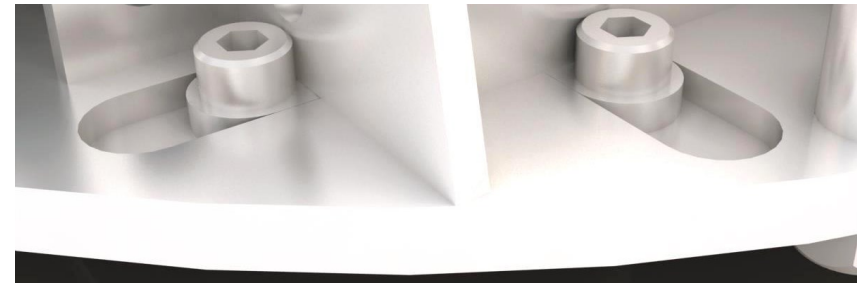


Figure 117 - Keys that lock the ribs to the base plate.

To make sure that the components chosen for the prototype fit inside the frame their 3D models are added into the assembly. These models were acquired from the manufacturer or recreated using dimensional drawings. After a satisfying layout was found their location was fixed and brackets and mounting holes were added. The result from this exercise can be seen in Figure 116. Most of the room within the device is taken up by the vacuum pump, which is placed in a central location. The placement of the vacuum pump subsequently dictates the layout of the rest of the components. The 5-2 directional valve for example, which is used to detach the suction cup, is placed in a corner of the frame opposite to the outlets of the pump. The valve used in this prototype is chosen for its small size and is connected to the vacuum pump by two universal elbow pneumatic couplings and some polyurethane rubber hosing. To connect the valve to the suction cup a pneumatic line runs down to a double universal elbow coupling. At this intersection the pneumatic line splits into two outlets. One of the outlets is plugged with a gauge pressure sensor and the other connects to the suction cup using another universal elbow coupling.

The electronics that govern the behaviour of the suction cup are placed on four solderable breadboards that are mounted onto the frame using 3D printed mounting brackets. It was chosen to keep the electronics as simple as possible and use analogue components to switch the suction cup on and off. A schematic drawing of the components used in the suction cup can be found in Figure 115. From this overview can

Prototype design

be seen that the electronics are divided into four circuitries. The settings, sensor and comparator circuit operate on either 5 V DC or 9 V DC while the trigger circuit functions on 12 V DC. The input voltage, provided by a 12 V wall adapter, is converted into stable 9 V and 5 V outputs using two regulated DC-DC converters. This type of converter was chosen to make sure that the measured data provided by the pressure sensor is as accurate as possible.

The heart of the 5 V/ 9 V circuits is formed by an LM311 comparator. As its name suggests this component compares the voltages provided by the sensor circuit and the settings circuit. If the sensor circuit provides a lower voltage than the settings circuit the output of the comparator will open, while a higher voltage provided by the sensor will shut down the current through the comparator. A resistor (R12) is used to add some hysteresis to the system. This prevents the vacuum pump from turning on and off all the time around the set pressure value. The switch by which the comparator can turn the vacuum pump on and off is formed by a transistor and a non-latching relay. The transistor is used to beef up the current through the relay and provides the separation between the 5V and 12 V circuits. A flyback diode between the input and the output of the relay prevents that the voltage spike due to the change in magnetic flux in the coil damages the electronics. To prevent that the vacuum pump starts pumping as soon as the device is plugged in a latching on/off switch is fitted between the relay and the vacuum pump. Another flyback diode is added over the vacuum pump to keep the electronics as stable as possible.

The components added to the sensor and settings circuit are there to make sure that the voltage output can be compared with each other. This is because the voltage provided by the sensor is not the same as the output of the settings turning knob. The sensor puts out a voltage of 0.5 V at 0 psi and 4.5 at 15 psi, while the settings knob which is formed by a high precision potentiometer generates an output between 0 V and 5 V. To make the voltages compatible the sensor voltage is decreased by 0.5 V using a TI OPA350 operational amplifier that is wired to act as a differential amplifier. When $R_8=R_9=R_{10}=R_{11}$ the amplifier outputs the voltage on its plus port pin minus the voltage on the minus pin. To achieve a voltage of 0.5 V on the minus pin a voltage

divider is used. This combination of the two divider resistors (R6, R7) is formed by a potentiometer to allow the circuit to be fine-tuned afterwards.

A voltage dividing potentiometer is also used to divide the settings knob voltage by a factor 1.389. In this way the maximum voltage from the settings knob corresponds with an 80 kPa pressure differential. To communicate the set pressure differential voltage from the pressure differential is amplified by a factor 1.6 so that 5 V becomes 8 V. This is achieved using a TI OPA705 operational amplifier, which is set to the correct value by R1 and R2. This resistor pair is once again formed by a potentiometer. To get the correct amplification the resistor values need to be chosen such that:

$$(40) \quad \frac{V_{output}}{V_{input}} = 1 + \frac{R_2}{R_1}$$

The output voltage from the amplifier is read by a voltage meter and is displayed on a two digit 7-segment LED display. By leaving the pin to the point in between the digits unconnected 8.0 is displayed as 80, which corresponds with the set pressure differential in kilopascal.

Using the schematic drawing a wiring diagram is created by placing the components on virtual representations of the breadboards and connecting the right pins with each other. This wiring diagram can be seen in Appendix J. In addition to components seen in the schematic drawing, two barrel power connectors are added to the electronics. The right barrel connector facilitates the connection between the wall adapter and the 12V circuitry, while the left connector provides a place from where the pressure sensor value can be read out. This is an important prerequisite to be able to test the prototype.

To give the prototype some curve appeal and to protect its internal components a plastic casing covers the frame. This casing is designed so that it can be easily vacuum formed and contains styling features from both the harness concept, as well as the final concept. A decorative stainless steel plate is furthermore added to the handle which shows the name of the prototype. This is done to give people an idea of the purpose for which the prototype is designed for.

Prototype fabrication

To illustrate the process of building the prototype and to highlight any changes with regard to the prototype design, a photographic timeline can be found on the next page. From the building process can be concluded that the design for the prototype is viable but challenging. This is in part due to inexperience of the author in some fields. The electronics for example proved to be a real struggle because of the cramped space available on the breadboards. In hindsight more space should have been reserved to mount the electronics.

The first step in creating the prototype was to lasercut the frame. Each part was subsequently sanded down to give it a brushed stainless steel look. To maintain this look and to prevent the frame from rusting it was coated with a double layer of clear varnish. Although the bolted connection on the frame proved to take more time than anticipated this part of the prototype was completed without any major problems. To complete the structural part of the device the suction cup base components were turned out of several pieces of POM using a lathe. The results from this combined effort can be seen in the first photograph on the next page.

The next step in the building process was to add the pneumatic components to the frame. This was quite a challenge because of the tight spaces available around the suction pump. After resolving some fitment issues, all components fit nicely within the frame. Finally some leaks were fixed by adding longer pneumatic tubes and a few dots of epoxy glue to complete the pneumatic system.

Before committing to the wiring diagram from 5.1 the electronics were first tested on a solderless breadboard. This allowed troubleshooting the electronics without the hassle of re-soldering and proved to be very useful in order to get the system working. After the circuits worked as intended to components were transferred to the solderable breadboards.

During this stage of the build most problems were experienced. An error in the wiring in front of the base of the transistor caused a short circuit that blew out both the transistor and the comparator. In addition to the copious amount of time spend

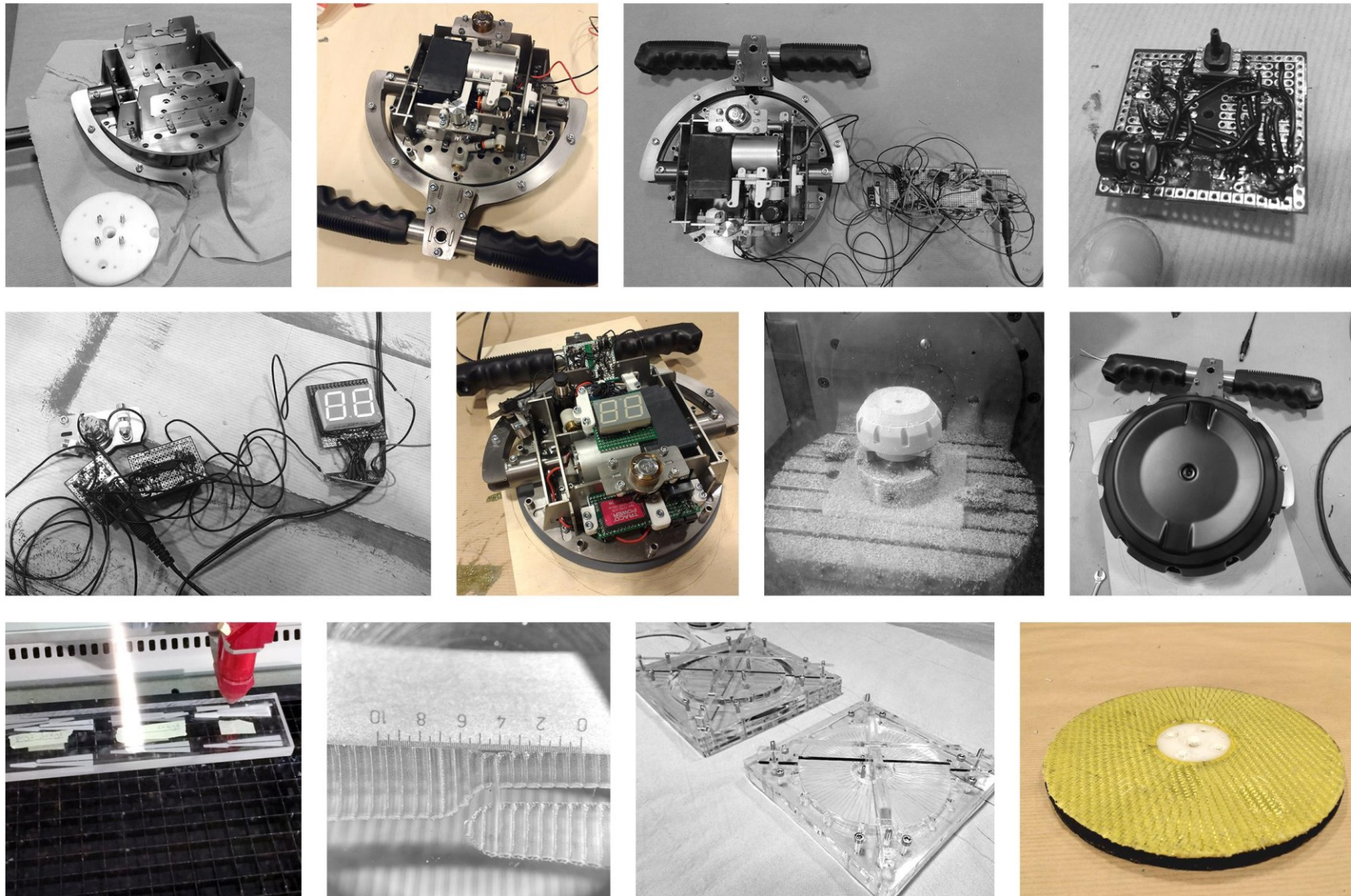
troubleshooting also fixing the problem proved challenging since the components had to be de-soldered from a very crowded breadboard.

To make the housing of the prototype a large chunk of polyurethane was turned into the basic shape of the casing using a lathe. The other details of the housing were subsequently added using a CNC milling machine. The resulting plug was used in combination with a vacuum forming machine to force a sheet of 2 mm thick polystyrene into the right shape. By trimming off the excess material and drilling holes for the buttons and handle the final housing was obtained. To finish of the device and to hide the edge between the display and the housing a front cover was lasercut from stainless steel. This cover was texturized to give the prototype a more sophisticated look.

The suction cup of the prototype was made as close as possible to the specification of the design from chapter 4. The neoprene foam parts of the suction cup and the Velcro layer were cut using a template and the Kevlar textile using a CO2 laser cutting machine. To glue the layers of the suction cup together a neoprene based adhesive was used. This glue is chosen because its stays flexible after drying. The suction cup rim was spaced 3 mm from the suction cup base with a neoprene rubber rings. This was done since there is no 11 mm thick neoprene foam available with the right specifications. It is not expected that this modification influences the behaviour since the rubber ring is on top of the foam. After gluing the kevlar backing to the foam the backing was fixed in the suction cup base using epoxy. The resulting assembly was subsequently heated at 60 °C for an hour to help the epoxy to harden.

To add the silicone rubber layer to the Kevlar backing a mould was created from acrylic. The bottom part of this mould was textured by a laser engraving machine. Although an attempt was done to apply the information provided by Snakenborg and Kutter (2003), it was quickly realized that this is not possible. The machine used by Snakenborg and Kutter varies is too many areas to be able to use their settings. An example is that their machine steers the laser beam using mirrors while the Trotec machines used to

Figure 118 - Prototype build overview.



Prototype fabrication

engrave the mould moves the laser on the x and y axis using stepper motors. Another challenge of using the Trotec Speedy 400 is that no physical values for the speed and the power of the laser can be set in its software. All power and speed settings are relative to the maximum of the machine. This is probably because the laserhead needs to accelerate and decelerate for each segment and therefore cannot maintain a constant speed. This difference in speed also translates into a slight difference in width along the length of each segment. This effect can be seen in Figure 119 and leads to pointy shapes at the end of each debossed segment. It is expected that this effect leads to a slight decrease in contact area with the substrate.

After a number of trial and error tests a setting was found that more or less satisfies the specifications of the grooves from Snakenborg and Kutter. This was verified by making a photograph of the pattern and measuring the distances in the photo. By chiselling out some of the grooves also a rough measurement of the depth of the grooves was obtained using a digital sliding gage. When these values corresponded with the intended pattern six more tests were done in which the power settings were varied slightly. These six patterns were studied using a confocal microscope to accurately determine their cross-section. From the data obtained by this study the best setting was chosen (Table 21).

Unfortunately the final mould had to be made on a slightly different machine as the person responsible for the Speedy 400 was unwilling to engrave without air-assist as it damaged the lens. Therefore a slightly different machine had to be used. In order to get

Machine	Trotec Speedy 400 (130 Watt)
Lens	II-VI Infrared, plano convex, ZnSe, 63.5 mm diameter
Bias	+1 mm
Power setting	9
Speed setting	0.96
Frequency	30000
Air-assist	Off

Table 21 - Settings and characteristic of the speedy 400 laser engraver.

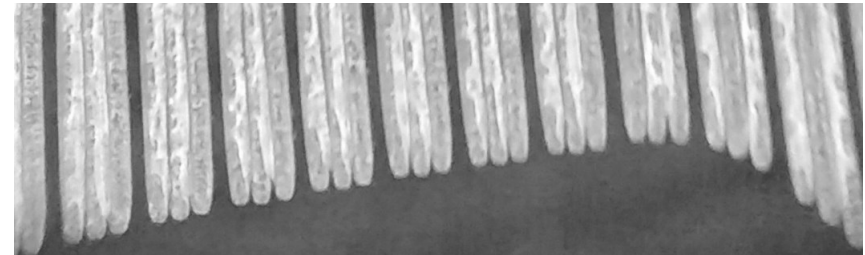


Figure 119 - Width variation near the end of the segments.

the same groove depth the power setting was converted since this machine has a different power output. The used settings can be seen in Table 22. To verify that the grooves match the grooves made earlier the mould was analysed using the confocal microscope. The resulting cross-section of both analyses can be seen on the next page. Despite using similar settings for both machines a number of differences can be seen.

Whereas the test sample grooves made with the Speedy 400 are in almost perfect accordance with the theoretical model, this is not the case for the mould. Although the grooves have the right width and depth, the overlap between the laserbeams could be better. The misalignment results in spikes at either the sides of the cross-section or near the middle. It is therefore believed that the adhesion and friction pad needs some time to wear in before it produces the right amount of friction. It was decided not to

Machine	Trotec Speedy 400 (200 Watt)
Lens	II-VI Infrared, plano convex, ZnSe, 63.5 mm diameter
Bias	+1 mm
Power setting	6.5
Speed setting	0.96
Frequency	30000
Suction	On

Table 22 - Settings and characteristics of the Speedy 500 laser engraver.

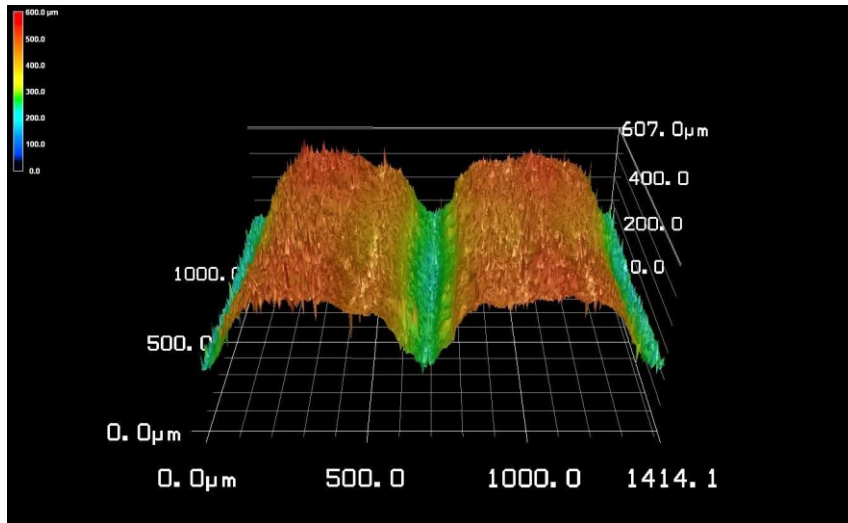


Figure 121 - Confocal microscope images of the geometry of the sample grooves.

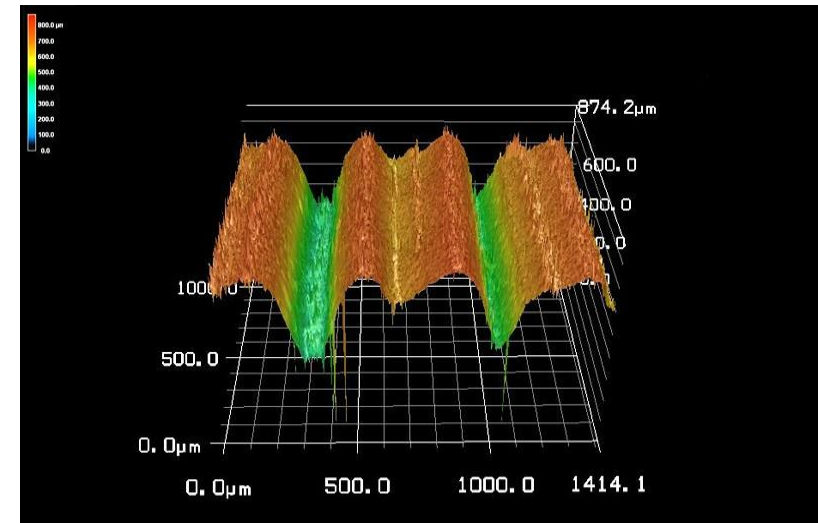


Figure 120 - Confocal microscopy images of the geometry of the mould grooves.

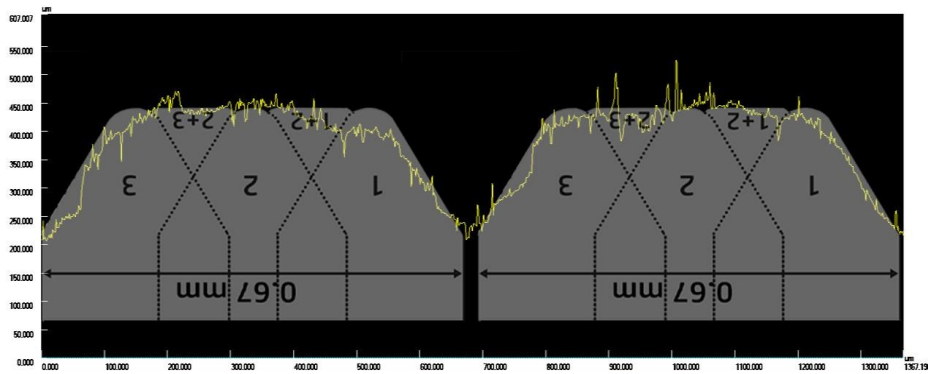


Figure 123 - Cross-section of the sample grooves in comparison with the suction cup design.

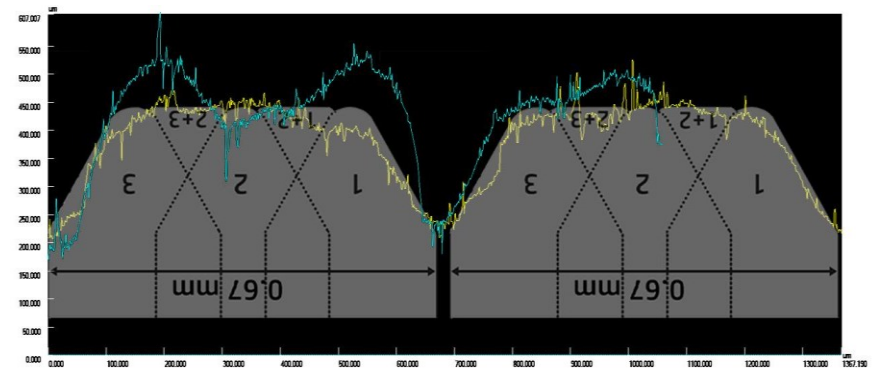


Figure 122 - Cross-section of the cross-section of the mould grooves (blue) the sample grooves (yellow) and the suction cup design.

Prototype fabrication

fabricate this complicated part for a second time due to time constraints and the fact that the deviation from the theoretical model is considered acceptable.

After the base plate was engraved, the same laser cutting machine was used to cut out parts of the moulds for the adhesion and friction layer and the soft sealing layer. This ensures that the cutting lines match with the location of the engraving. The moulds that were constructed with the cut out parts can be seen in Figure 125 and Figure 124. The design of the mould is such that they create the exact thickness needed for the adhesion and friction layer and the soft sealing layer. A lid that is placed on top of the foam presses the textile into the silicone rubber and is locked using laser cut clamps. To make sure that the pattern is fully filled with PDMS and that no bald spots emerge, the design of the mould contains channels along the edge of the suction cup. When the lid is pressed on, any excess PDMS is pushed towards these channels and can be removed after the PDMS has cured.

The PDMS mixture for the adhesion and friction pad was prepared according to the prescriptions given in chapter 4. The mixture for the soft sealing layer however was altered, because of concerns that the rubber would not be durable enough. A study from Palchesko et al. (2012) reports that a silicon rubber with an elastic modulus of 10 kPa feels more like a gel than an elastomer. The ratio of Sylgard 184 to Sylgard 527 was therefore increased to 1:10. According to Pelchesko et al. this results in an elastomer with an elastic modulus of 50 kPa. Both mixtures were degassed for 30 minutes before they were casted to ensure that no air bubbles were trapped in the PDMS. The moulds were subsequently put into a temperature controlled environment and allowed to harden.

To remove the casting from the mould the sides of the mould were removed and the rim was slowly peeled off from the acrylic. The resulting castings can be seen in Appendix I. In the photograph of the adhesion and friction pad three areas are highlighted. In these areas air was trapped during the casting process and the grooves have not been imprinted in the silicone. This surface area amounts to about 10% of the total surface area. These defects will most likely reduce friction as the flat spots remain very soft and can therefore not transmit any force to the textile backing.

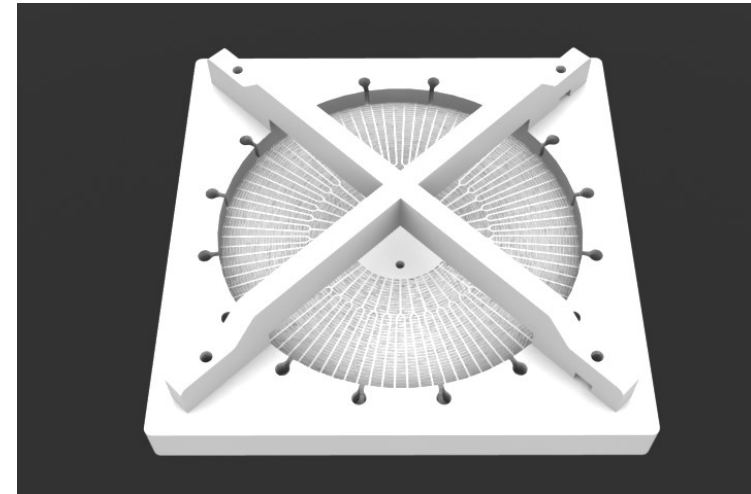


Figure 124 - Adhesion and friction pad mould design (without lid).

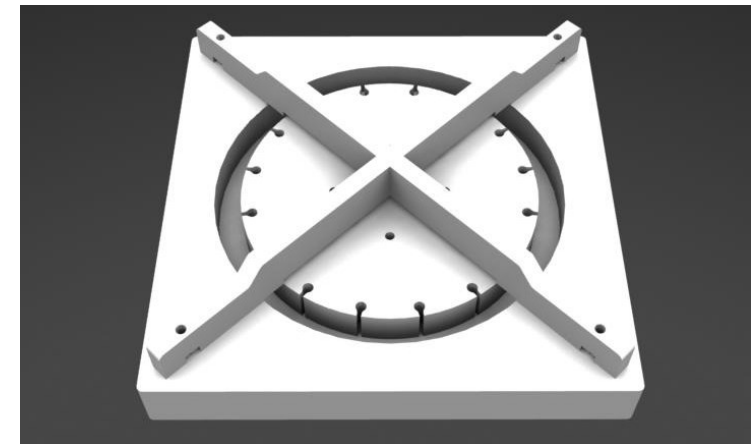


Figure 125 - Soft sealing rim mould design (without lid).



Figure 126 - The finished prototype.

Performance testing

To determine whether the designed suction adhesion device works as predicted four experiments are performed with the prototype. The design of the experiments is such that the results can be compared with the theoretical model from chapter 4. However the main goal of the experiments is to prove that the biomimicry strategies that are incorporated into the design work as anticipated. The most important of these is whether the rim can create a seal on rough substrates and the resistance of the suction cup against shear forces.

Preparation

To be able to perform the experiments some preparations need to be made. These include arranging all the requirements that can be found in the experiment diagrams (Appendix L) and measuring the characteristics of the substrates that are going to be used in the experiments. These substrates were chosen to give a good idea of the performance of the prototype on the materials that the suction adhesion device is likely to encounter during daily use. They include 5 wood substrates with different finishes: a brushed aluminium substrate, a textured paint substrate and a glass substrate. The roughness for each substrate is measured with the help from a roughness tester. The device used for measuring the surface roughness of the substrates is a Mitutoyo SJ-201P, which works by pulling a sharp diamond tip over the surface topography of the substrate. The average roughness is calculated by making four passes on each substrate with a length of 2.5 mm. Table 23 shows the results from the roughness measurements. It can be seen that two substrates could not be measured since their roughness exceeds the maximum measurement value of 360 μm . The measurements on the wood surfaces furthermore show some inconsistencies. Although the sample sanded with 1200 sandpaper is clearly smoother than the sample sanded with a 100 grid sanding pad, the measurements show otherwise. This gives reason to doubt the accuracy of the tests. Most likely the inaccuracy is due to the type of tester, which is normally used to determine the roughness of metal parts. The wood is probably too soft and the needle ploughs straight through it. It is thus recommended that the roughness of the wooden substrates is measured a second time using a more appropriate measurement technique.

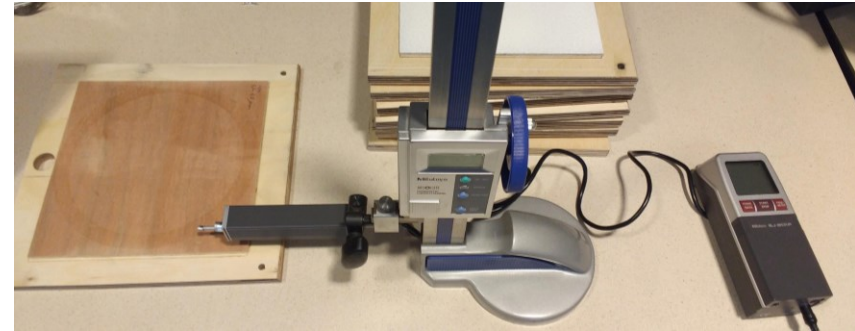


Figure 127 - Surface roughness measurements test set-up.

Sample	Pass 1 (Ra, μm)	Pass 2 (Ra, μm)	Pass 3 (Ra, μm)	Pass 4 (Ra, μm)	Mean (Ra, μm)
Textured paint					>360 μm
Sandblasted wood					>360 μm
40 grid	12,87	9,88	6,1	9,14	9,4975
100 grid	4,25	4,07	3,88	4,37	4,1425
400 grid	3,71	5,71	2,59	4,91	4,23
1200 grid	4	5,94	5,4	5,62	5,24
Brushed aluminium	1,69	1,5	1,4	1,48	1,5175
Glass	0,02	0,01	0,01	0,01	0,0125

Table 23 - Surface roughness measurements.

Performance testing



Figure 128 - Substrateholder with and without substrate.

To be able to switch the substrates during testing and connect them to the tensile strength tester a substrateholder was designed and fabricated. The holder which is made from sheet metal and multiplex can be seen in Figure 2. Two metal ridges allow the substrate to slide in the holder. The holder is locked by bolting a c-shaped metal plate to the metal ridges. By making connecting holes in both the side and the bottom of the holder, the substrate can be mounted at 0° and 90° with respect to the pulling direction.

The data that is gathered during the experiments is provided by the vacuum sensor. In order to be able to read the sensor data, a datalogger was built using an Adafruit Huzzah board and a USB serial converter. The first component collects the analogue data, while the second piece of electronics makes it readable for any computer with a USB port. Since the Huzzah's analogue port can only read values up to 1V the sensor voltage is reduced using a voltage divider. To obtain the original sensor value the serial readout is therefore multiplied by 11.0. This value was determined by measuring the sensor voltage using a multimeter and coupling it to the serial output.

Experiment 1: Sealing capabilities

To determine whether the suction can attach to the types of surfaces described in requirement 14, the sealing rim of the prototype is put to the test. The substrates described before are used to determine the correlation between surface roughness and the maximum achievable pressure differential.

Method

The suction cup prototype is attached to the substrates from Table 23 and is set to the maximum pressure differential so that the vacuum pump is pumping continuously. The maximum achievable pressure differential is determined by looking at the data that is provided by the pressure sensor. Once the pressure differential curve has stabilized the vacuum pump is turned off. The suction cup is then left untouched until the differential has decayed on its own. This procedure is performed two times for each substrate, which amounts to 16 tests in total. The set-up used during the experiment can be seen in Figure 129.

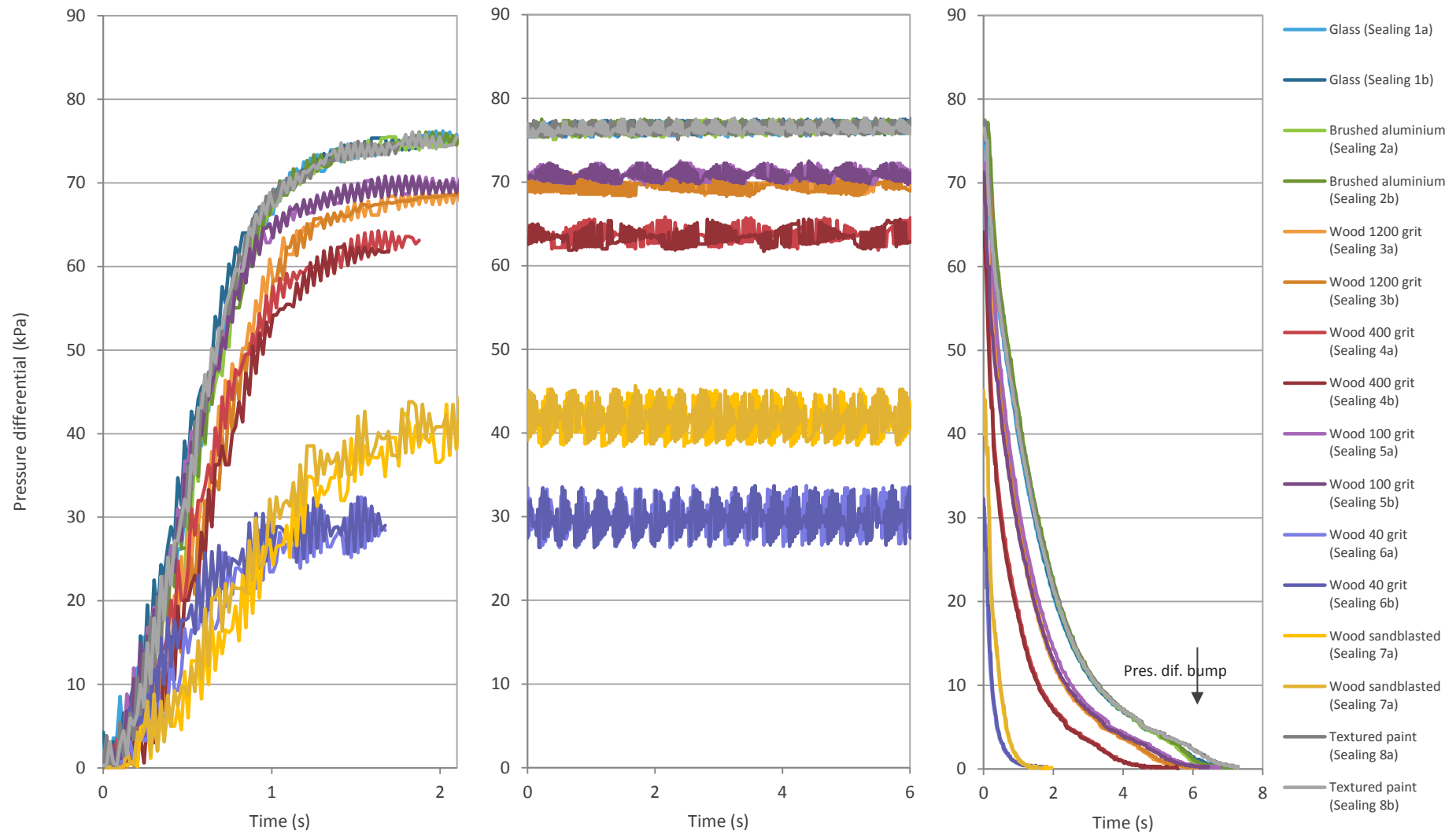
Results and discussion

The resulting pressure differential graphs obtained during this experiment can be seen in Appendix J. Only one graph of each experiment is included since they are almost identical, which means that the prototype is able to deliver reliable and repeatable experimental data. When looking at the graphs generated from the data it becomes clear that three phases can be distinguished. As soon as the vacuum pump is switched on the pressure differential increases steeply and reaches its maximum value in about 1.5 – 2.5 seconds. The length of this period varies for each surface and is most likely dependent



Figure 129 - Test set-up of experiment 1.

Performance testing



Performance testing

on the amount of air that leaks underneath the sealing rim. The end of the pressure differential rise transitions smoothly in what is dubbed the steady state phase. During this time span the pressure differential oscillates around a slowly increasing value (Figure 131).

To investigate whether there is a relation between surface roughness and the maximum achievable pressure differential, they have been plotted in Figure 132. The graphs show that there is a clear non-linear correlation between the two variables. The graph however does not tell the whole story. When looking at Figure 130, it can be seen that the sealing performance of the prototype is almost identical for three substrates. These substrates are the glass, aluminium and textured paint substrates. Since they have very different surface geometries it seems odd that their sealing performance is the same. The reason for this can be sought in the lack of surface features in the intermediate roughness scale ($2\mu\text{m} > \text{Ra} > 10\mu\text{m}$). The glass and aluminium substrates are simply too smooth to possess them, while on the textured paint substrates they

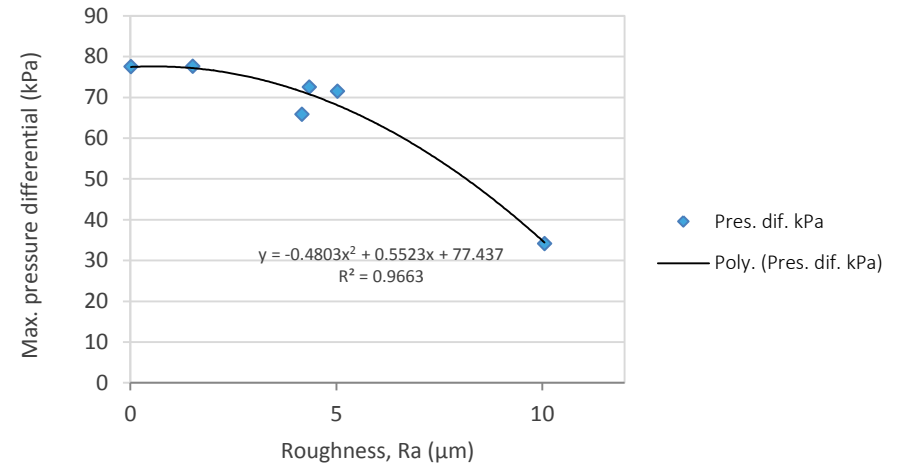


Figure 132 - Relation between surface roughness and maximum pressure differential.

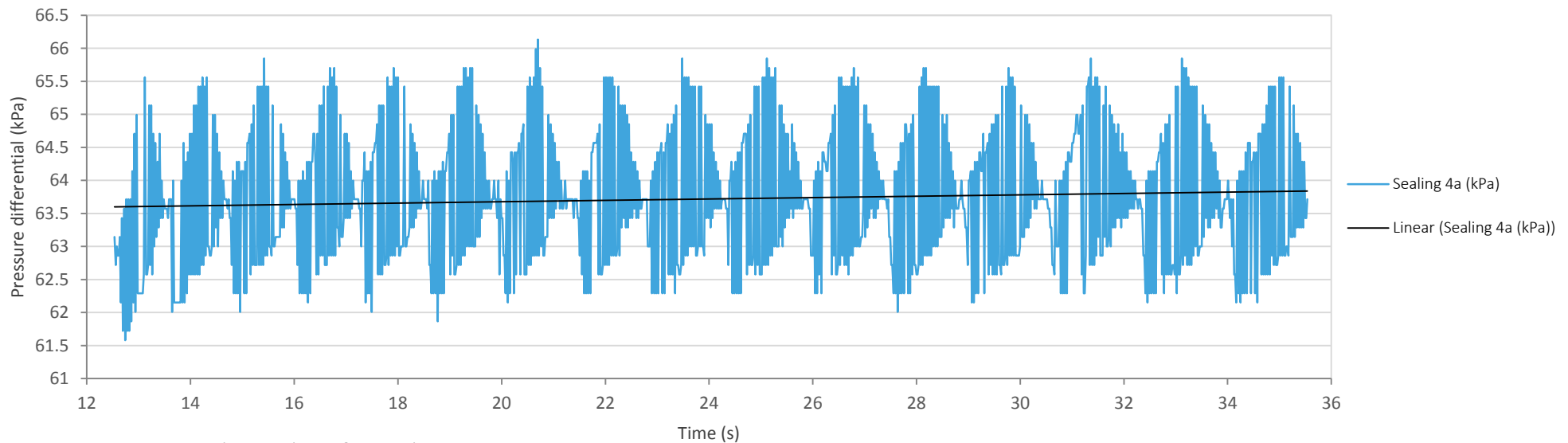


Figure 131 - Steady state phase of test Sealing 4a.

Performance testing

have been smoothed out by the surface tension of the paint. It can thus be concluded that the sealing rim can achieve a good seal on surfaces with a surface roughness of less than 2 μm , or on a surface that contains large blunt asperities. In between these two boundaries lies an area where the rim cannot achieve a full seal, but is still able to generate a respectable pressure differential. The Achilles heel of the rim seems to be surfaces with a surface roughness between 10 μm and 50 μm . More research however is needed to pinpoint its exact value.

In addition to the relation between the maximum achievable pressure differential and the surface roughness also other correlations were analysed. The steady state graph shows for example an interesting pattern that repeats itself over time (Figure 131). These fluctuations are presumably the result of turbulence caused by the pumping action of the vacuum pump. However their amplitude and frequency seem to vary for each substrate. These correlations have therefore been investigated by determining the mean frequency and amplitude for each pressure differential curve. By plotting them against both the pressured differential and surface roughness more insight has been gained whether they are dependable on each other. The amplitude of the fluctuations appears to have a strong relation with the pressure differential (Figure 133) while no clear connections could be found for their frequency.

One final correlation that has been analysed for this experiment is whether the time it takes for the pressure differential to decay has anything to do with the surface roughness of the substrate. Although it proved hard to determine the exact moment when the decay period ends, it can be concluded there is most likely a non-linear relation between these two parameters (Figure 134). The best usage for the pressure decay curve seems to be however to use it to distinguish between low scale roughness and high scale roughness. Since the pressure on the rim drops during this period and there is no disturbance due to pumping, tiny differences in the shape of the curve can hint at variances in the substrate geometry. The only difference between the glass substrate pressure differential curve and the curve belonging to the painted texture substrate for example is a small bump near the end of the decay curve (Figure 130).

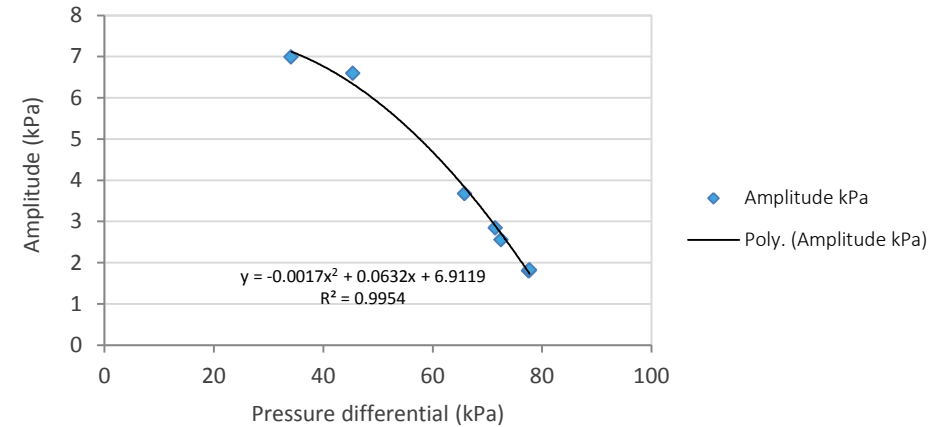


Figure 133 - Relation between steady state fluctuation amplitude and pressure differential.

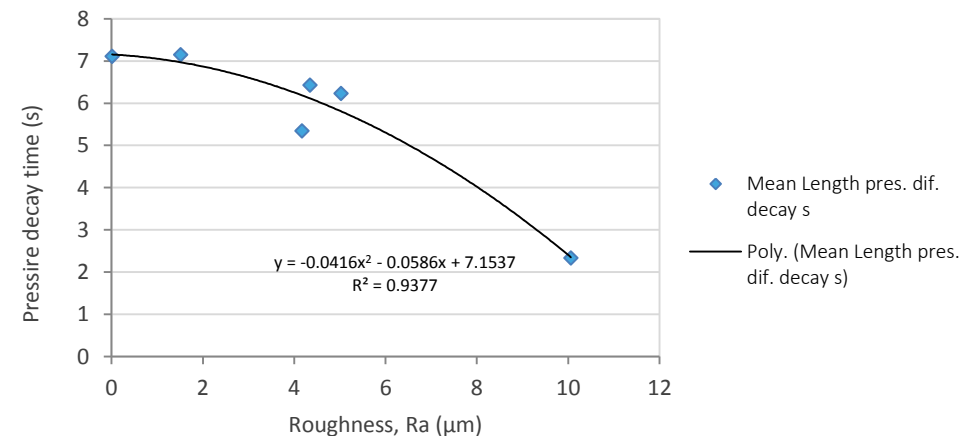


Figure 134 - Relation between the pres. dif. decay time and surface roughness.

Performance testing

Experiment 2: Pulling resistance

The vertical and parallel pulling resistance of the prototype are tested on various substrates. Deviations from the simulation predictions indicate a flaw in the theoretical model, or the prototype and an attempt is made to explain them.

Method

The tenacity of the prototype is tested by allowing it to attach to the each sample and pulling it perpendicularly from the substrate. Next the substrateholder is rotated and the tests are repeated. Each test is performed twice to determine if the results are repeatable. In total the suction cup is thus pulled 32 times from a substrate. Two data streams are gathered during testing. One is generated by the tensile strength tester, while the other information is provided by the vacuum sensor's datalogger. The test set-up used in this experiment can be seen in Figure 135.

Results and discussion

The pull-off forces for each test can be seen in Figure 137 and Figure 136. From the shape of the graphs can be seen that the prototypes detach in a different manner depending on whether it is pulled in the perpendicular or parallel direction. Pulling perpendicularly from the substrate detaches the suction cup with a sudden plop, while pulling the other way does not detach the suction cup but causes it to slide. This sliding motion is in correspondence with the peeling force analysis in chapter 4 and means that the adhesion forces are stronger than the peel forces generated by pulling.



Figure 135 - Test set-up for experiment 2.

When comparing the outcomes from the pull-off tests with the theoretical model it can be concluded that the amount of adhesion generated is slightly higher than expected. The pull-off force on glass is around 1340 N while the theoretical model predicts 1110 N. This discrepancy can be caused by the conversion mechanism but when comparing the friction performance of the prototype with the theoretical model it is more likely that the increase is caused by a lack of contact surface. The parallel pulling resistance on glass (530 N) is well below the predicted 1630 N.

A lack of friction generated by the adhesion and friction pad can be caused by a number of reasons. The PDMS rubber used for the suction cup for example had some trouble setting since the harder used was a few weeks after its expiration date. This has caused the areas which contained air bubbles to remain soft. The bad overlap on the adhesion and friction pad has worsened this effect since the protruding ridges reduce the contact area with the substrate. Finally it is felt that the estimate of the amount of friction generated per mm^2 contact surface between glass and PDMS rubber by Okamoto et al. (2007) is on the high side. The arguments for this are further elaborated in experiment 3.

Fortunately the news around the parallel pulling resistance is not all bad. From the pull-off graphs can be seen that the amount of friction on the other substrates is higher than expected. The prototype seems to have a better grasp on surfaces with a bit of roughness. This is a contradiction with the theoretical model, which predicts that the decrease in real contact area reduces the amount of adhesion friction. The increase seen in the test results can however be explained without throwing this theory out of the window. In the theoretical model the assumption is made that no deformation friction takes place. A simplification that was made since this component can only be determined experimentally. It is thus likely that the additional friction is the result of this left out component. The increase in friction is highest on surfaces with a roughness between 3 and 6 μm and results in a 50% to 60% increase with respect to a fully smooth surface. It is theorized that this increase is caused by the interdigitation of the adhesion and friction pad's ridges with asperities on the substrate.

Performance testing

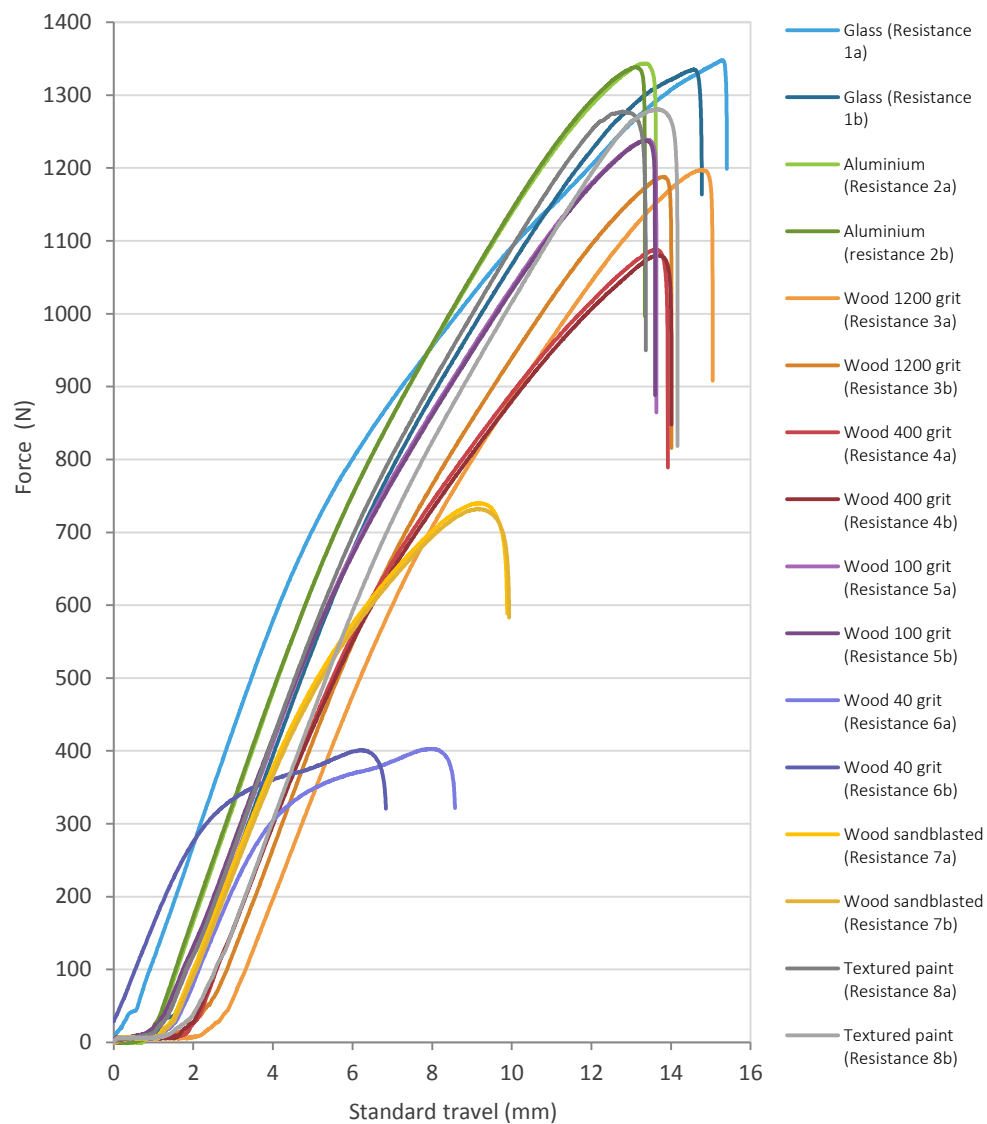


Figure 136 - Pull-off force in perpendicular direction.

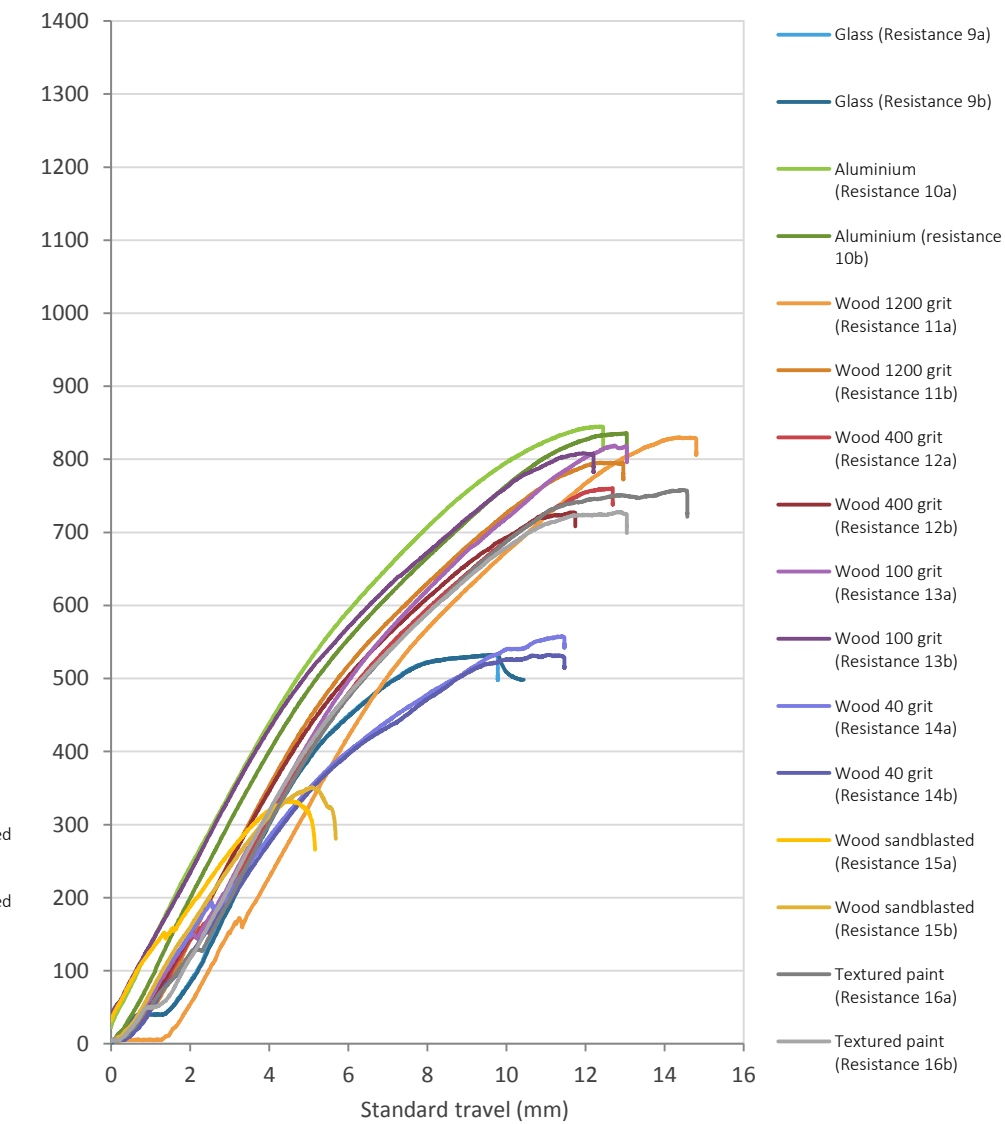


Figure 137 - Pull-off force in parallel direction.

Performance testing

The other datastream generated in this experiment contains the pressure differential curves during the pull-off tests. These curves hold information that can be used by the device to fulfil important functions like predicting the isotropic boundary and warning the user when the suction cup is about to detach.

Figure 140 to Figure 143 show the pressure differential gathered during the pull-off tests. Figure 142 and Figure 145 represent the typical curves that can be seen on most of the substrates while the other graphs are the exceptions encountered during testing. It can be seen that, when pulling in the perpendicular direction, detachment is preceded by a period in which the pressure exponentially decreases. This is presumably caused by a reduction in the pressure on the rim that affects the seal with the substrate. This period lasts about 12 seconds, which should be more than enough to issue a warning signal and having the user react to it. The pressure differential drop of 5 kPa is also more than enough to be detected by the system and it can thus be concluded that the warning function is a realistic proposal. It has to be kept in mind though that the tensile tester pulls very gently. In reality the pre-detachment period will thus last shorter.

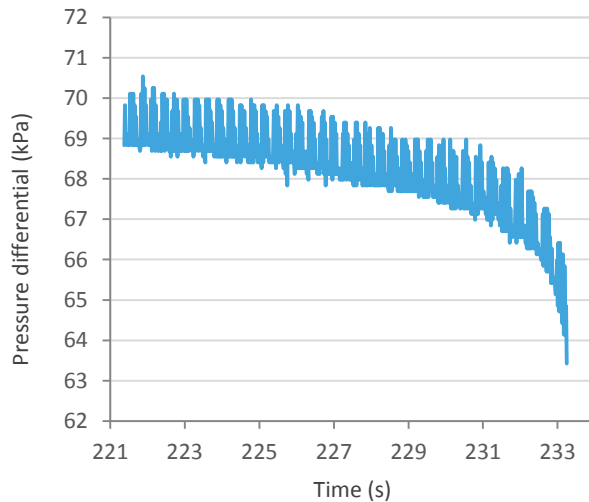


Figure 138 - Detail view of Figure 204 just before detachment.

In contrast to the perpendicular pulling tests the pressure differential curves belonging to the parallel pulling tests do not show a pre-detachment signal. This is because the prototype was shut down manually to prevent it from sliding from the substrate. Since the suction cup does not detach in these situations it is not necessary to issue a warning to the user.

In addition to pre-detachment signals the curves also vary somewhat depending on how much load is applied on the suction cup. In both the perpendicular and parallel pulling tests the fluctuation amplitude becomes smaller and the mean steady state value shifts either up or down. In the case of the perpendicular pulling tests this value usually decreases as a higher load is applied, while it increases when the suction cup is pulled parallel to the substrate. An exception on this rule of thumbs is the

perpendicular pulling test on the sandblasted wood, in this case the steady state value increases when a load is applied. In the future these effects might be used to determine the force that is exerted on the device. However the exact correlation between the pulling force and these pressure differential effects has not been explored any further.

Correlations that have been explored and that are more critical for the functioning of the suction adhesion device, are the relations between pressure differential and pulling resistance. Figure 139 shows that there is a strong linear relation between the maximum perpendicular pulling resistance and the maximum pressure differential. The correlation between pressure differential and the parallel pulling resistance is much weaker. As stated before the performance of the prototype is best on substrates with an intermediate roughness while it drops of at both ends of the spectrum (Figure 147). This correlation results in the non-linear relation between the pressure differential and the parallel pulling resistance visualized in Figure 146.

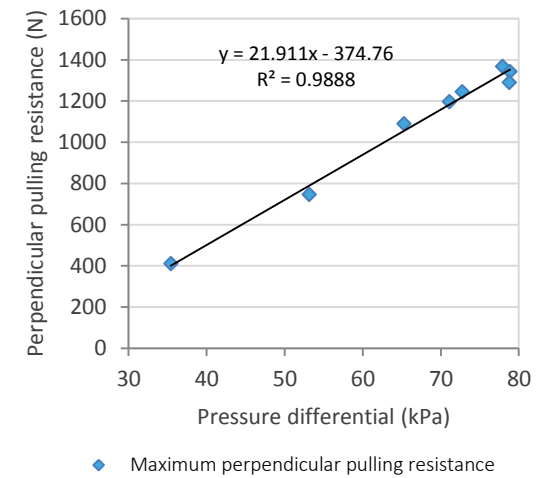


Figure 139 - Relation between pres. dif. and perpendicular pull-off force.

Performance testing

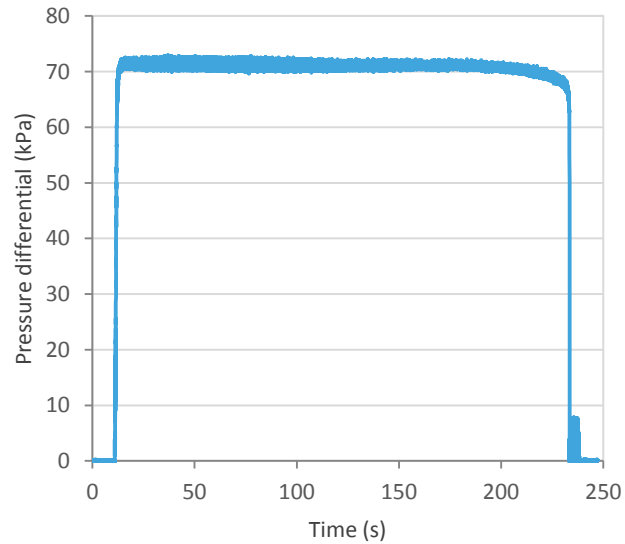


Figure 142 - Pres. dif. during perpendicular test on wood (100 grit).

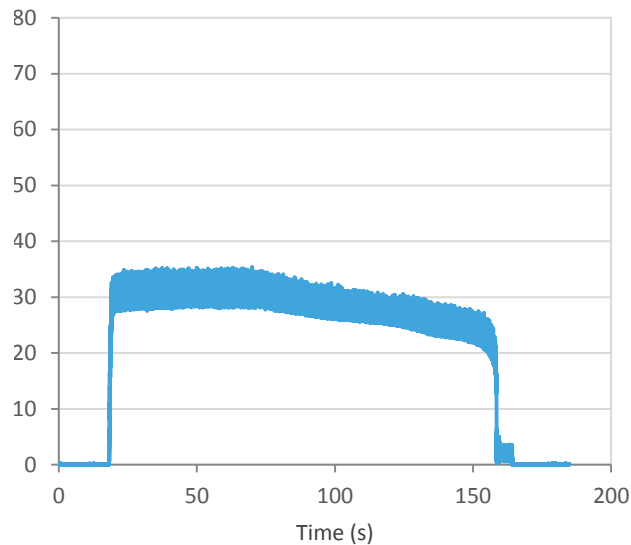


Figure 141 - Pres. dif. during perpendicular test on wood (40 grit).

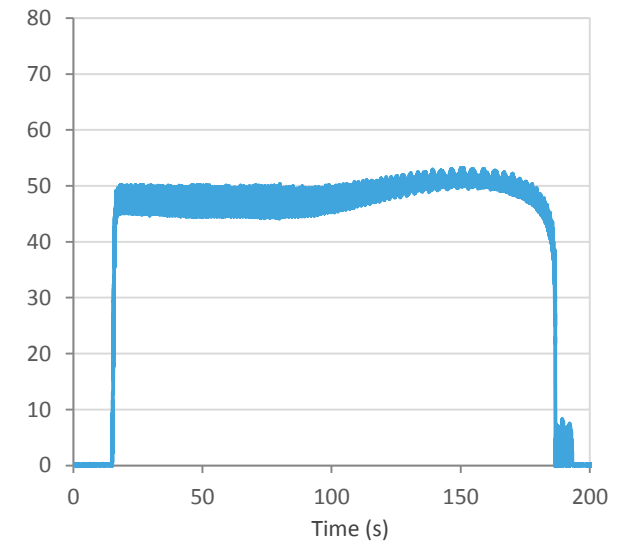


Figure 140 - Pres. dif. during perpendicular test on wood (sandblasted).

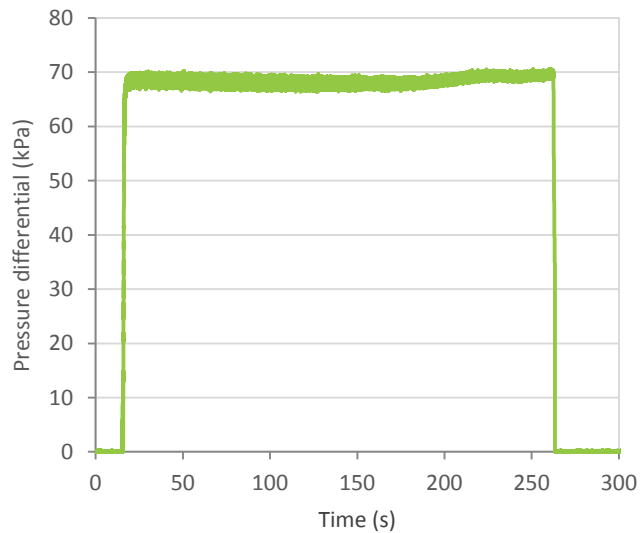


Figure 145 - Pres. dif. during parallel test on wood (100 grit).

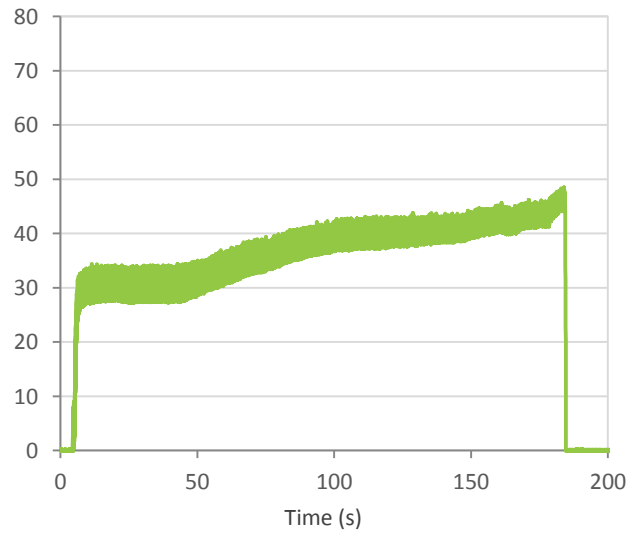


Figure 144 - Pres. dif. during parallel test on wood (400 grit).

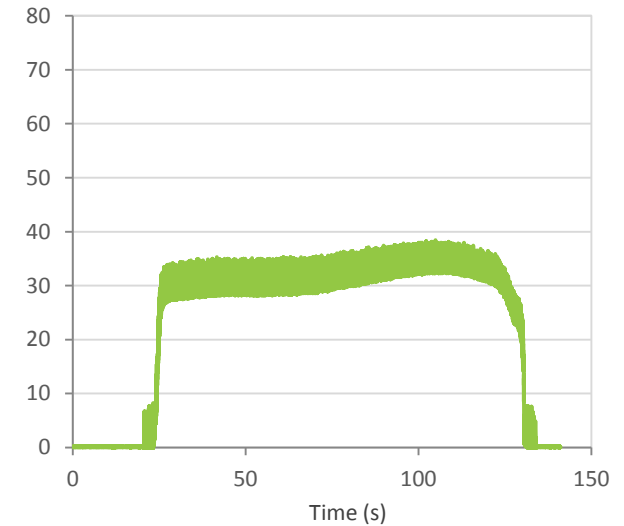


Figure 143 - Pres. dif. during parallel test on wood (sandblasted).

Performance testing

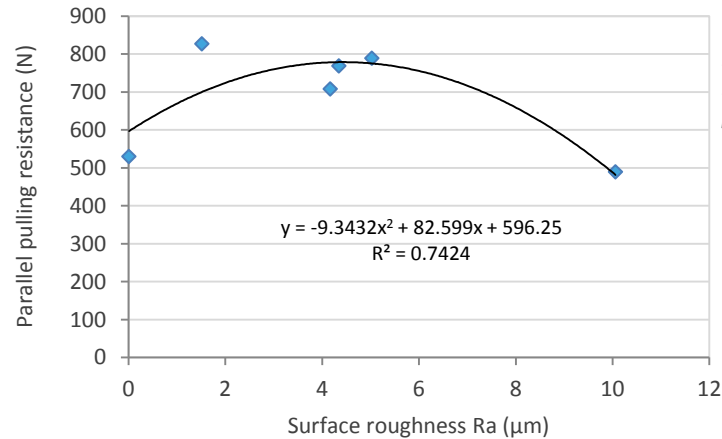


Figure 147 - Relation between substrate roughness and parallel pulling resistance.

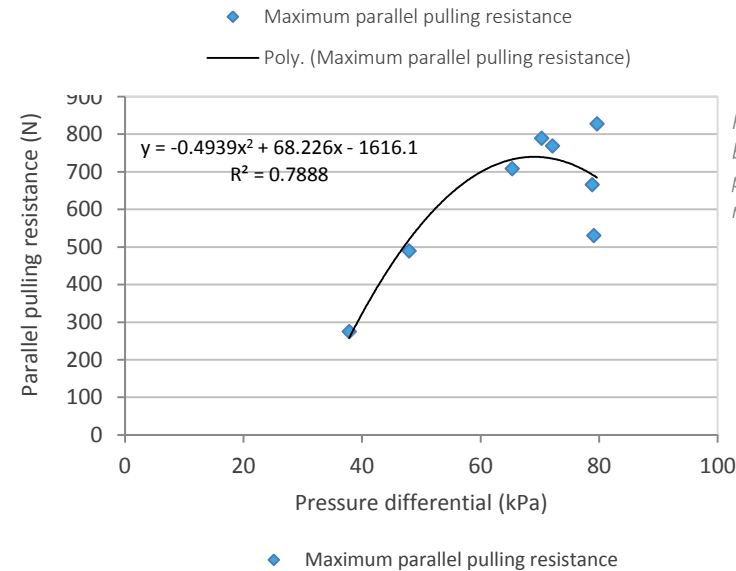


Figure 146 - Relation between pres. dif. and parallel pulling resistance.

Experiment 3: Wear

To check if any wear has occurred during the previous experiments, a number of tests have been done. These are supplemented by visual inspections of the suction cup.

Method

The prototype is attached to glass substrate and pulled off in the vertical and horizontal direction and the results are compared with earlier results. An increase in friction and a decrease in adhesion can give an indication about of the amount of wear that has occurred. By doing a wear test after test Resistance 8 and after Resistance 16 it can be established how much perpendicular pulling and parallel pulling contribute to wear. To make sure that the results from experiment 2 can be compared with each other they have been compensated for wear by assuming that effects of wear have a linear relation with the amount of tests performed.

Results and discussion

In Figure 148 a comparison is made between the tensile strength curves obtained before and after the pull-off tests. The graphs show that the tests have made a significant impact on the performance of the suction cup. Over the first 8 tests not much wear can be noticed. This is backed up by wear curve 1a which shows an almost identical pull-off strength. The difference in shape is probably result of the deformation of the mounting bracket and does not signify any changes with regards to the suction cup itself.

During the parallel pulling tests however the effects of wear have become clearly visible. The tensile strength curves of wear test 1b and 2a show that the amount of adhesion has dropped with 57.4N compared to the first perpendicular pull test on glass. Friction on the other hand increased with 84.5N with respect to the first parallel pull of test. Since the pressure differential did not change significantly it is a clear sign that pressure surface has been traded in for contact surface. In the case of the prototype, which produces too little friction, it can thus be stated that the adhesion pad has been worn in. When interpolating the wear-effects an optimum can be calculated. For glass this optimum lies at 1018.1N, which is equal to the highest isotropic boundary achievable with this prototype.

Performance testing

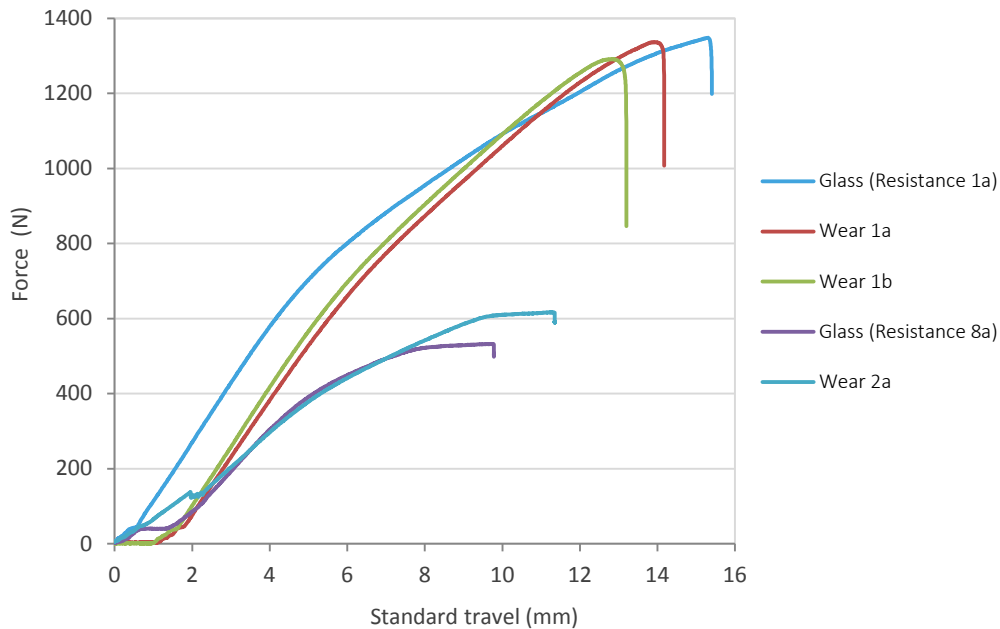


Figure 148 - Wear curves compared to the initial curves.

The increase in friction and accompanying decrease in adhesion give the opportunity to check some of the assumptions made in the theoretical model. Based on information provided by Okamoto et al. (2007) it was estimated that each mm^2 of real contact surface between PDSM rubber and glass would create 0.3N of friction. However when the amount of adhesion that has been lost is compared to the friction increase, a much lower value is obtained. At a pressure differential of 78 kPa a 57.4N decrease in suction adhesion translates in a loss of 735.9 mm^2 pressure surface. When it is assumed that this entire surface area is used to generate friction, an 84.5N increase amounts to a rather low value of 0.115 N/mm^2 . Although these calculations are not very accurate they do show that 0.3 N/mm^2 is not a realistic figure to work with. The reason for the high discrepancy is unknown. However one contributing factor might be that dirt

particles become embedded in the silicon rubber. This reduces the amount of area that is in contact with the substrate and thus leads to a decrease in performance.

During the tests visual inspections of the suction cup furthermore revealed that the silicon rubber used for the prototype is not durable enough to be used in a practical application. Although its softness makes it great for creating a seal on rough substrates it also means that it wears off quite easily. This can be seen in Figure 149. Dozens of rubber flakes hang loose from the suction cups rim, which signals that the friction tests cause severe damage. To complete the tests the flakes were removed after each time a new substrate was mounted in the substrateholder. It is estimated that about halve of the material was scraped off from the rim during testing. Interestingly enough this did not create a lot of performance problems. On smooth surfaces the pressure differentials remained the same and on one wood substrate (40 grit) the pressure differential actually increased. This might be because the loose flakes fill up the grooves in the wood. The only decrease in performance was noticed on the sandblasted wood substrate. It appears that there was simply not enough rubber left to conform to this type of surface roughness. The adhesion and friction pad also sustained some damage. After a number of tests a tear was spotted in the rubber. It appears as if there was some slack in the Kevlar textile that was pulled towards the middle and resulted in the rubber deforming.



Figure 149 - Visual wear effects on the suction cup.

Conclusion

In this chapter a suction adhesion device prototype was designed, fabricated and tested. From the process can be concluded that the basic functionality of the system works as intended. The vacuum pump is able to generate a pressure differential that is large enough to power the suction cup and the prototype is able to attach itself to various substrates without any problem. Some of the prototype's functions however, such as the function to manage the pressure differential, do not work as planned. Because the pressure differential decays quite quickly, the electronics constantly need to switch the vacuum pump on and off. This results in an unstable pressure differential and increases the wear on the electronic components. It was therefore decided not to use this functionality during testing and it is recommended that the function is also scrapped from the final concept. The small efficiency gain that this approach delivers simply does not warrant the added complexity and wear.

Another function that proved to be obsolete is the smart detachment function. The elastic forces stored in the suction cup support were in all cases enough to pop the prototype from the substrate once the pressure differential had decayed. This means that the 5-2 directional valve can be scrapped from the final concept, and replaced by a simple pressure release valve. This will drive the production costs of the device down further.

The suction cup created in this chapter also proved to have its strong and weak points. The sealing capabilities of the rim for example are above expectation. The suction cup is able to generate much larger pressure differentials than anticipated on rough substrates, but this excellent sealing performance is offset by its low durability. The reason behind this is that the design of the suction cup has been mainly focussed on mimicking natural suction adhesion systems. The final product proposal however will need to feature a more durable rim. In the design of this part a balance needs to be found between durability and performance (Figure 150).

This same balance also needs to be found for the adhesion and friction pad. Although the pad remained relatively unscathed during testing, it is expected that it's still too vulnerable for the applications it is designed for. Especially the depth of the grooves is too small to provide reliable performance over an extended amount of time.

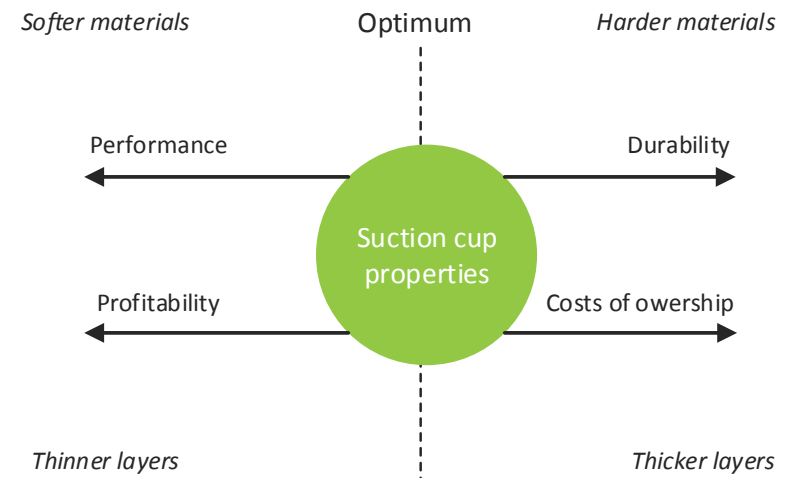


Figure 150 - Tension field of the suction cups material properties.

Requirement check and final conclusion

To assess whether the designed suction adhesion device is viable it is compared with the list of requirements. For each requirement it is determined if the device complies, falls short or if more research is needed.

1. The device mimics natural suction adhesion systems

The first requirement was added to make sure that the information gathered in the first chapter is incorporated into the design. This information was packaged in 12 biomimicry strategies. To determine if the design complies with the requirement it is thus necessary to analyse whether technological translation of the strategies are present in the design. An oversight of the results from this analysis can be found in Table 24.

Passive suction

Passive suction is regarded one of the most important suction adhesion strategies since it dramatically improves efficiency. In this aspect the device shares the most similarities with the oral suckers found on many hill stream fish species. The device uses valves to shut of the air flow once the set pressure differential has been achieved. Another design feature that can be seen as a technological translation for passive suction is the use of a flexible material for the suction cup support. The elastic restorative forces inside this layer maintain the pressure differential. This method is similar as used by the clingfish, which stores elastic forces in its skeletal structure.

Detachment force conversion

Detachment force conversion is a powerful tool to increase the performance and efficiency of the suction cup. This tool has been incorporated into the suction adhesion device by making the suction cup flexible. This allows some regions of the suction cup to come loose from the substrate while the rim stays attached. This increases suction adhesion when necessary and reduces the impact of wear on the functioning of the suction cup. The exact extent to which this effect occurs however still needs to be tested. This can be done for example by replacing the flexible PVC support for a steel plate.

Pressure distribution texture

A pressure distribution texture is present on the adhesion and friction pad and most closely resembles the structures found on the octopus suction cup. Although the size and depth of the groove has been increased with regards to the octopus, it is believed that the structure functions in the same way as its biological counterpart. It was decided not to use the intricate nanostructures found on many biological suckers as it requires frequent replacement of the adhesion and friction layer. Also the performance of the device would fluctuate too much due to the wear of the nanostructure. It is furthermore believed that using a nanostructure in these applications will never be a viable option as technological systems do not have the ability to renew these intricate textures.

Smart detachment

To make the suction adhesion device faster in detaching from a substrate a smart detachment method was chosen. This method looks most like the hyper expiration method used by tadpoles. By reversing the flow in the pumping system it is able to separate its sucker in a heartbeat. The directional control valve, which is operated by the user, mimics this functionality and turns the vacuum pump in a compressor. However from the results in chapter 5 can be concluded that a pressure relieve valve will probably work just as good. In this case the smart detachment method looks more like the retractable flap found on clingfish.

Conforming rim shape

Achieving a good seal is one of the most critical things to make the suction adhesion device function. It was therefore opted to choose the hierarchical structure present on the abalone sucker as an inspiration source. Three hierarchical levels are present on the sealing rim to make the sure that the rim can conform to the waviness, macro roughness and micro roughness of a surface. This is done by increasing the softness of the layers towards the substrate. A good balance between durability and performance still needs to be found though.

Requirement check and final conclusion

	1.1 Passive	1.2 Conversion	1.3 Distribution	1.4 Detachment	2.1 Conforming	2.2 Segmented	2.3 Strengthen	2.4 Secretion	2.5 Compensate	3.1 Resistance	3.2 Adjustment	3.3 Decentralize
Incorporated into the device	x	x	x	x	x		x		x	x		x

Table 24 - The strategies incorporated into the suction adhesion device.

Segmented rim

Segmented rims help biological suckers to attach to uneven objects. However, since the objects that need to be lifted with the suction adhesion device are more or less flat it was decided not to incorporate a segmented rim structure. It is furthermore believed that heavily segmented rims only work well in aquatic environments as water will not flow through the tiny grooves due to its surface tension and coherency. In terrestrial applications however they will increase the rate at which air leaks into the suction cup.

Rim strengthening

In the suction adhesion device the role of the skeletal structure is performed by the suction cup support layer. This sturdy but flexible material prevents the rim from shifting inward when a shear force is applied on the device.

Secretion sealing

One of the more controversial suction adhesion strategies, secretion sealing, has not been included in the design of the device. This is because it is hard to find a technical translation for this strategy. It is also in conflict with some of the other requirements. Requirement 9 for example states that the device may not contain sealants that need to be refreshed. Requirement 10 moreover dictates that the suction cup is not allowed to contaminate the substrate with any type of residue.

Leak compensation

Leak compensation is critical in order to use a suction adhesion system in terrestrial application. Since the suction cup can never be fully sealed off, some kind of system needs to be in place to remove the excess air. The solution incorporated in the suction

adhesion device shares the most similarities with the buccal pumps found in suckermouth fish.

Shear force resistance

The presence of strong collagen fibres just underneath the sucker lining of the garra species has led to the incorporation of a strong textile layer in the suction cup. This layer has proven to be very effective in transmitting shear forces to the frame of the suction cup without comprising the capability of the suction cup to form itself according to the substrate.

Active adjustment

No dedicated active adjustment function has been added to the design of the suction cup. In the future however it might be possible to boost the power supply for the vacuum pump for short amounts of time to brace the suction adhesion device against high pulling forces.

Decentralized suction cup control

While the suction cup design enables the possibility of the suction cups working together, it is still a stand-alone system. All components needed for it to function on its own are incorporated into the design. This makes the system more reliable and also allows it to react faster on incoming disturbances. It can therefore be concluded that the system is a good representation of the decentralized nerve system of the octopus.

C Requirement check and final conclusion

2. The device significantly lowers the effort needed to lift difficult to handle objects.

With the prototype and the proposed methods for lifting one can imagine that the suction adhesion device makes a large difference in the amount of time and effort that is needed to move difficult to lift items. Since the suction cup system does not require securing straps and can attach and detach in a short amount of time, it is expected that the system significantly improve the efficiency at which furniture items can be moved. Also the strain on the body is reduced since the forces during lifting are transmitted to the body in a better way. It is however recommended that this improvement is quantified in the future by conducting use tests. This helps companies to decide how much they can benefit from purchasing the system.

3. The device is easy and intuitive to operate.

In order to be accessible for the target group the device is designed in such a way that it is easy to control and operate. All that needs to be done to attach the device is pressing it on a surface, just like a normal suction cup. Also detaching is considered to be intuitive, as the paddles signal their function to the user due to their shape and placement. Although requirement 3 states that there should be no double functions for buttons, the sliding ring does perform two tasks. However it is not expected that this will result in confusion, as sliding the ring is preceded by pushing on a button for the corresponding menu. The sliding action is furthermore a well-known interface feature that in other products, like the Apple iPod, is also used for multiple functions. Whether the device is actually easy to use should be confirmed with use tests together with members from the target group.

4. The device communicates the remaining adhesion time

To communicate the remaining adhesion time to the user the device shows its battery charge level. It was chosen to do this instead of showing a time since the remaining adhesion time depends on variables that cannot always be measured correctly or anticipated by the device. It is furthermore believed that showing a battery level allows the user to plan his tasks better since a remaining adhesion time can only be shown when the device is attached. Users have furthermore become used to managing their

tasks based on a battery charge level since most own smart device like phones, tablets or laptops.

5. The device communicates the adhesion strength

An important selling point of the suction adhesion device is that it can give the user feedback on the amount of weight that can be suspended on the suction cup when it is attached. This amount is set by the user and the device gives feedback by showing a ring of bars around this value. It was chosen not to give a prediction in kilograms since this is not considered relevant for the user. All the user needs to know is that the device has reached the set value. During lifting the user is generally not looking towards the device and is only interested in the adhesion strength when it dips below the set level. The low adhesion strength warning is therefore communicated with the user using audible signals in which no mention is made of the present adhesion strength in kilograms.

6. The device warns the user when it is about to let go

Before the device detaches a small pressure drop occurs that can be recognized by the system as a signal of imminent detachment. Based on the results from chapter 5.3 it should be possible to give a warning in time for the user to put the object back on the ground. In almost all of these situations the object will not be damaged as overloading occurs during the first stage of lifting. After the device has successfully lifted the item only fast accelerations or a change in the substrate can cause an unwanted detachment. It can therefore be concluded that the suction adhesion device is a safe way to lift valuable items.

7. The suction adhesion device is mobile and easy to handle.

Based on the inventory of the weight of the components in chapter 4 it can be concluded that the total weight of the suction adhesion device is most likely below the set threshold of 2.3 kg. The device is furthermore compact and can be carried in a standard toolbox. Also when the device is used it can easily be moved around by its handle. The incorporation of a battery means that the user is not restricted in its movement by the power cables. When taking all these aspects into account it can thus be established that the designed solution meets this requirement.

C Requirement check and final conclusion

8. The suction adhesion device is rugged and reliable

Although much care has been put into creating a casing that can resist the use conditions it is subjected to, no definitive conclusions can be made whether it is rugged and reliable enough. Finite element simulations and pre-production prototypes should be made to determine whether the device is as rugged and reliable as other powertools. Also the claim that the design of the device allows it to be used in water requires further research. From the test results in chapter 5 however it does become clear that the suction cup is not nearly as rugged as required. More effort has to be put into finding a good balance between performance and durability.

9. The suction adhesion device does not require a lot of maintenance.

During the design process attention has been paid to make sure that the device is as maintenance friendly as possible. All parts that are subjected to wear are designed in such a way that they can easily be replaced. The adhesion and friction pad for example is no more difficult to replace than a disc on an angle grinder. Also the use of a modular system means that replacing parts is easier and can potentially be done by the user itself.

10. The suction adhesion device does not damage or contaminate the handled objects

The large contact area of the suction cup and the microstructure present underneath the adhesion and friction pad means that the adhesion and friction forces are well distributed over the substrate. Because of this reason it is believed that the device will be able to lift most furniture pieces without damaging them. Also no contamination should occur as long as the adhesion and friction pad are kept clean.

11. The suction adhesion device has a modular platform with fixed interfaces and uses standardized components when possible

The advantages of using a modular platform and standardized components have been mentioned multiple times in this report. These strategies help to keep costs down while improving quality and serviceability. The embodiment of these strategies can be seen when looking at the incorporation of standardized connectors within the electronics and the use of an off the shelf vacuum pump.

12. The suction adhesion device has an attractive appearance that fits the preferences of the target group

Although requirement 12 states that the appearance should fit with the preferences of the user, it cannot yet be concluded whether this is the case. As of now the design is mainly the result of personal preferences and the restrictions caused by the choice for a circular business model. This prohibits for example the use of overmoulding since materials have to be separated. To determine if the looks of the device are to the likings of the target group a questionnaire could be handed out during the use test.

13. The suction adhesion device should be affordable for the target group.

The cost estimates in chapter 4 show that asking price for the device can be just within the set limit of €800,-. This relatively high asking price is due to the low number of produced devices, which means that tooling costs are a large contributor to the production costs. A solution would be to reduce the profit made on the device and compensate this by increasing the selling price of the replacement pads. These parts can be made cheaply but have a high inherent value. Also the suggestions made in the conclusion of chapter 5 could help to reduce the costs of the device.

14. The suction adhesion device has to deliver a competitive level of performance

When looking at the performance of the prototype created in chapter 5 it can be concluded that it delivers a competitive level of performance. Even though a lot of optimisation still needs to be done it is believed that an isotropic boundary of 80 kg is within reach.

15. The suction adhesion device is able to adhere under all use circumstances.

Although testing has shown that the prototype is already able to attach itself to some challenging substrates it is not yet known if this is possible under all use circumstances. More testing is required to verify that device can deliver the sealing capabilities that are required to fulfil this requirement.

Requirement check and final conclusion

Requirement	Fulfilled	Recommendation
1. The suction adhesion device mimics natural suction adhesion systems	Yes	
2. The suction adhesion device significantly lowers the effort needed to lift difficult to handle objects.	Yes	Use test
3. The suction adhesion device is easy and intuitive to operate.	Yes	Use test
4. The suction adhesion device communicates the remaining adhesion time.	No	
5. The suction adhesion device communicates the adhesion strength.	Yes	
6. The suction adhesion device warns the user when it is about to let go.	Yes	
7. The suction adhesion device is mobile and easy to handle.	Yes	Use test
8. The suction adhesion device is rugged and reliable.	Unknown	Drop / water test
9. The suction adhesion device does not require a lot of maintenance.	Yes	
10. The suction adhesion device does not damage or contaminate the handled objects.	Yes	Use test
11. The suction adhesion device has a modular platform with fixed interfaces and uses standardized components when possible.	Yes	
12. The suction adhesion device has an attractive appearance that fits the preferences of the target group.	Unknown	Questionnaire
13. The suction adhesion device should be affordable for the target group.	Yes	Simplification
14. The suction adhesion device has to deliver a competitive level of performance.	Yes	Optimisation
15. The suction adhesion device is able to adhere under all use circumstances.	Yes	Additional tests

Table 25 - Requirement check.

Conclusion

When looking at this report as a whole it can be concluded that the initial goal of taking an idea that is present in nature and developing it into an innovative biomimetic product has been met. The device presented in this work can achieve things that no other available product is able to do and can therefore be considered innovative. What makes the suction cup unique is its mobility in combination with the capability to produce reliable reversible adhesion. The reliable performance is in part due to the large shear force resistance created by the adhesion and friction pad, but is also a result from the ability of the device to give the user an estimate of the attachment strength. It is believed that the system the device that can give a prediction of the adhesion force that is being generated.

The proposed design furthermore expands the number of materials on which suction adhesion can be used. The combination of a soft sealing rim and a small vacuum pump allows the suction cup to attach itself to real world surfaces made from wood, metal or ceramics. Although this can also be done with some existing suction lifters, the suction adhesion device uses much less energy and can be used outside of industrial settings.

Table 25 shows that although the device meets most criteria, a lot of work still needs to be done. Especially the interaction of the device with the user is a big unknown. In the future also more effort has to be dedicated to the design of the final concept. It has to be made sure that the device is optimised for mass production and is rugged enough to resist the forces encountered during daily use.

When reflecting upon the work done in this report a structured pattern of steps emerges that has led to the design of the suction adhesion device. This framework does not only apply for this product category, but can in the future also function as a design method for other biomimetic products. To illustrate this, the chapters in the report have been reduced to general descriptions and linked to each other. The resulting flow chart can be seen in Figure 151 and Figure 152. It is believed that following this flow chart can help designers to translate the capabilities of natural systems into useable biomimetic products more successfully. However more work is still needed to optimize the method and add additional case studies need to be done to verify that it works.

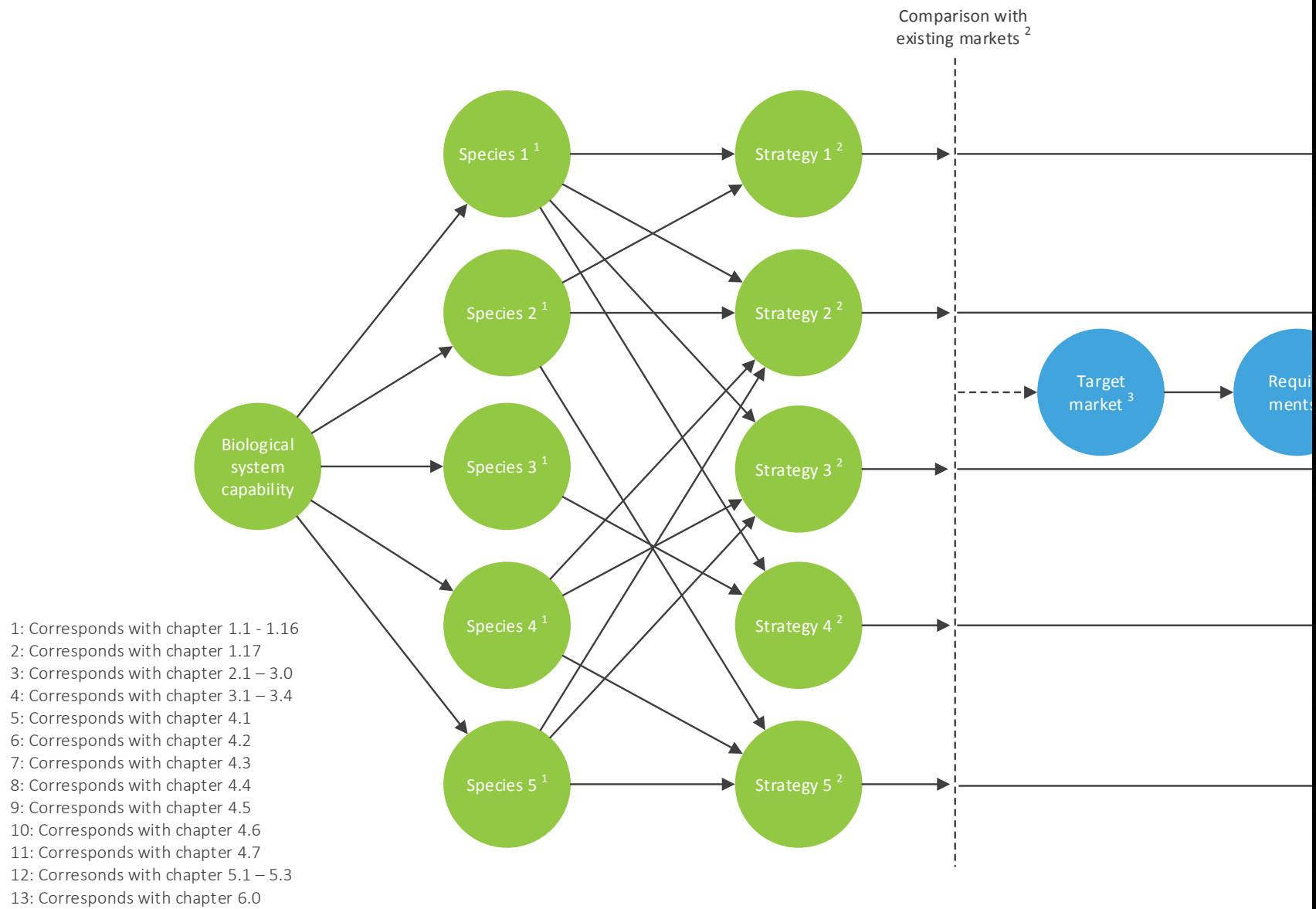


Figure 151 - Biomimetic design approach 1/2.

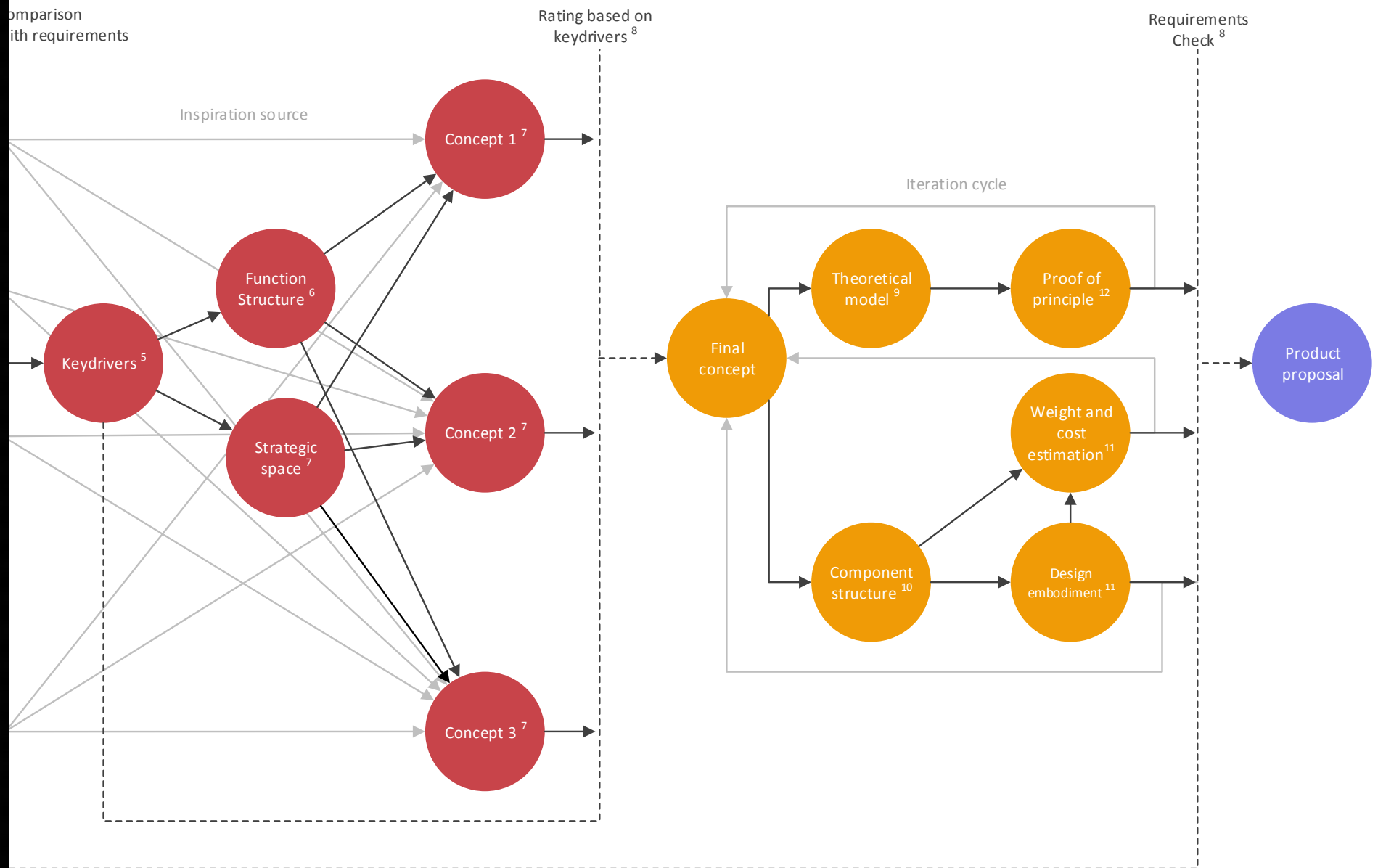


Figure 152 - Biomimetic design approach 2/2.

Appendix A: Industrial suction solutions

Suction adhesion systems in the industry can be divided into three groups of components. One group supplies the vacuum while the other converts the vacuum into adhesion. The third group is used to control the interaction between the two groups. To get a good understanding of all the relevant suction adhesion solutions that are used in the industry a review of them has been made.

Vacuum pumps

Vacuum pumps can be divided into three categories. These categories are called positive displacement pumps, momentum transfer pumps and entrapment pumps. Of the listed categories only displacement pumps can be used independently. Momentum transfer and entrapment pumps need to be assisted by positive displacement pumps, and are used to create high vacuums. Because a high vacuum is not required to generate significant suction adhesion, these categories will not be analysed. The small increase in suction adhesion does not justify the increase in complexity and costs that is the result of adding them to the system.

Reciprocating positive displacement vacuum pump

Piston vacuum pump

The piston vacuum pump is the cheapest type of vacuum pump available and shares a lot of traits with fossil fuel piston engines. However instead of converting fuel into mechanical energy, the piston vacuum pump requires an energy input and turns it into a pressure differential. This is achieved by a reciprocating piston that sucks in the pumping medium from the inlet during the expansion stroke and then pushes it towards the outlet. The flow from the inlet towards the outlet is controlled by valves that seal the outlet during expansion and the inlet when compression occurs. Although this type of vacuum pump is very cheap it is not used in high tech application as it generates a fluctuating vacuum and produces a lot of vibrations.

Diaphragm vacuum pump

Diaphragm vacuum pumps have become popular recently because they can produce a vacuum that is free of contaminations and do not produce any waste water. This is important for environmental reasons but is also a prerequisite for some applications

like laboratory work. The pump creates a vacuum using an oscillating diaphragm. By rotating an eccentric disc that is linked via a connecting rod to the diaphragm, the floor of the suction chamber is pushed up and down (Figure 153). The flow into the chamber is controlled by valves that are arranged in the same way as with the piston vacuum pump. Of all the types of vacuum pumps that are available the diaphragm vacuum pump most closely resembles the buccal pumps used by many suckerfish species. Its disadvantages compared to other vacuum pumps are its low pumping speed due to the limited flexibility of the diaphragm and a limited maximum compression ratio that is the result of dead space present near the intake and exhaust port.

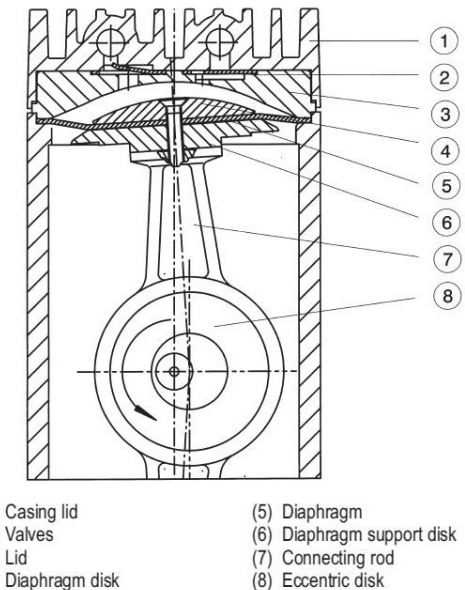


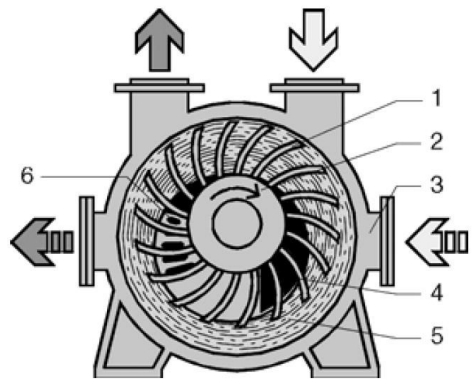
Figure 153 - Schematic overview of a diaphragm vacuum pump (Umrath, 2007).

Rotary vacuum pump

Liquid ring vacuum pump

In applications where the pumping medium is contaminated with a lot of vapours a liquid ring vacuum pump is usually the best option. This is because its working mechanism gives it the ability to cope with all kinds of entrapped droplets. The basis of the pump is provided by a housing that contains an eccentrically placed fan. When the pump is at rest, approximately half of the pump is filled with liquid, which is usually

Appendix A: Industrial suction solutions



- | | |
|---------------|---------------------------|
| 1 Rotor | 4 Intake channel |
| 2 Rotor shaft | 5 Liquid ring |
| 3 Casing | 6 Flex. discharge channel |

Figure 154 - Schematic overview of a liquid ring vacuum pump (Umrath, 2007).

Rotary vane vacuum pump

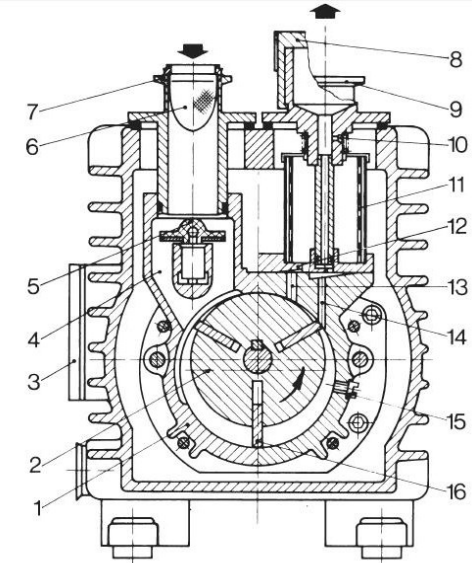
Rotary vane vacuum pumps are the most used type of vacuum pumps and have applications in wide variety of fields. The basis of this pump is once again an eccentrically placed rotor in a round housing. The rotor consists of a round disc that usually has two or three slots in it. These slots allow the vanes of the pump to slide in and out to keep them in close contact with the wall of the housing (Figure 155). This can be achieved by centrifugal force alone or is assisted by springs that push the vanes outward. A downside of the rotary vane vacuum pump is that it needs to be lubricated with oil in order to achieve a good seal. The pumped out gas can therefore become

water. Activation of the pump flings the liquid against the walls of the chamber and forms a concentric ring around the fan. Due to the mismatch of the centre points of the fan and the liquid ring the space present in between the blades varies (Figure 154). Any gas in between thus gets compressed when it travels in between the fan blades. The compression rate of the pump is determined by opening discharge channels close to the intake or further down the line. Liquid ring vacuum pumps are rugged and reliable but are limited by the vapour pressure of the liquid the use. A liquid ring vacuum pump with water that operates at 15 °C cannot operate below 33mbar (Umrath, 2009).

contaminated with oil vapour. This is why rotary vane vacuum pumps usually have an oil filter to prevent the oil particles from entering the environment.

Rotary plunger vacuum pump

Rotary plunger pumps combine an eccentrically placed rotor with a sliding valve (the plunger). The rotor rotates around the centre of the housing and is always in contact with the wall. For a complete suction cycle the rotor has to turn 720°. During the first turn the rotor sucks air past the open sliding valve into the suction chamber. This volume of air is compressed in the second half of the cycle and leaves the pump via an oil sealed pressure valve.



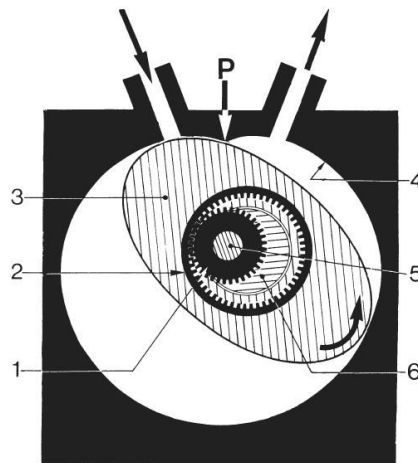
- | | |
|-------------------------|-----------------------|
| 1 Pump housing | 9 Exhaust port |
| 2 Rotor | 10 Air inlet silencer |
| 3 Oil-level sight glass | 11 Oil filter |
| 4 Suction duct | 12 Exhaust valve |
| 5 Anti-suckback valve | 13 Exhaust duct |
| 6 Dirt trap | 14 Gas ballast duct |

Figure 155 - Schematic overview of a rotary vane vacuum pump (Umrath, 2007).

Trochoid vacuum pump

Trochoid vacuum pumps belong to the rotary piston pump class. These work by rotating the centre of gravity of a piston around a circular path. In contrast to rotary plunger types, the rotary piston can be dynamically balanced. This means that it can spin at higher speeds and that it produces much less vibrations. Because of its higher rotational speed and specific volume, trochoid pumps can be four times smaller than a comparable plunger pump. A

Appendix A: Industrial suction solutions



- 1 Toothed wheel fixed to the driving shaft
- 2 Toothed wheel fixed to the piston
- 3 Elliptic piston
- 4 Inner surface of the pump
- 5 Driving shaft
- 6 Eccentric

Figure 156 - Schematic cross-section of a trochoid pump (Umrath, 2007).

performance characteristics scroll pumps are only used for more expensive applications as the pumps scrolls need to be precision machined in order to work.

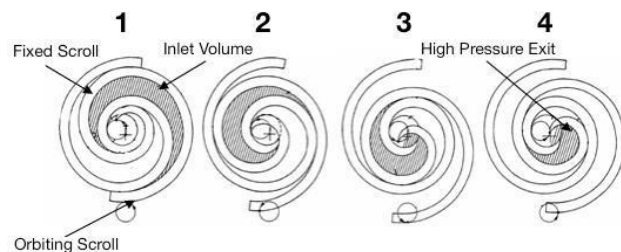


Figure 158 - Working principle of a scroll pump (Umrath, 2007).

downside to trochoid pumps however is that they use oddly shaped pump housings and pistons, which make them more difficult to manufacture.

Scroll pump

A scroll pump is a dry compressing vacuum pump, which means that it does not require any oil to achieve a good seal. In contrast to other dry compressing pumps the lack of an oil seal does not result in a lot of leakage and low compression ratios. This is because of the scroll shape of the internal compressor wheel. As can be seen from Figure 158 the compressor wheel rotates inside a stationary scroll and generates pressure due to the decreasing size of the windings. Scrolls with a large amount of windings have a lot of contact surface with the other scroll and prevent air from escaping once it has been trapped in between the scrolls. Despite its good

Vacuum ejectors

Vacuum ejectors are a special type of vacuum pumps that utilize the Venturi effect. They rely on the fact that a gas or liquid that is flowing through a constricted section will create a low pressure area. This draws in air from the vacuum chamber and thus generates suction. The ability of the vacuum injector to create a vacuum using steam or compressed air and its small size makes it very useful for industrial suction grabbers. It allows the compressor to be decoupled from the sucker and results in faster attachment and detachment. A downside of using vacuum ejectors is that they require a constant flow of gas to maintain suction. This means that passive suction is not possible using this type of pump.

Self-powered vacuum lifters

Self-powered lifters do not require an external vacuum source or pump in order to function. These devices use a small portion of the potential energy created during lifting to create the required suction. In most cases this is achieved by suspending the weight of the lifter and the object on a piston that slides out of a cylinder mounted to the lifter's frame Figure 159. The expansion of the enclosed

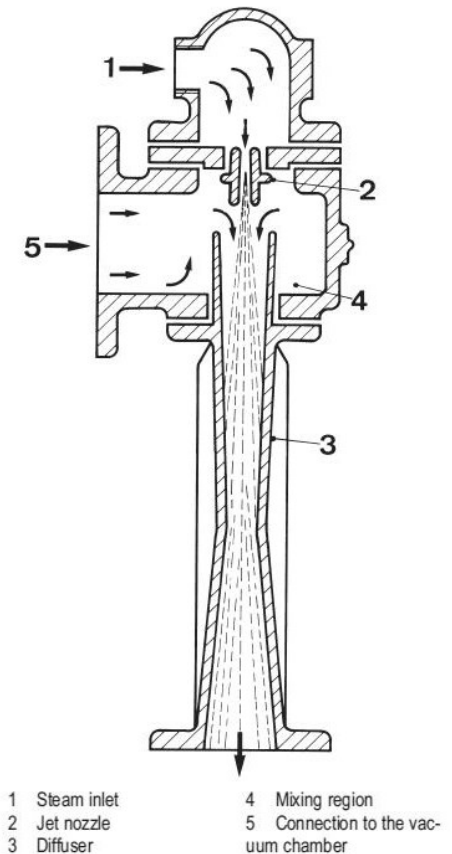


Figure 157 - Schematic overview of a vacuum ejector (Umrath 2007).

Appendix A: Industrial suction solutions

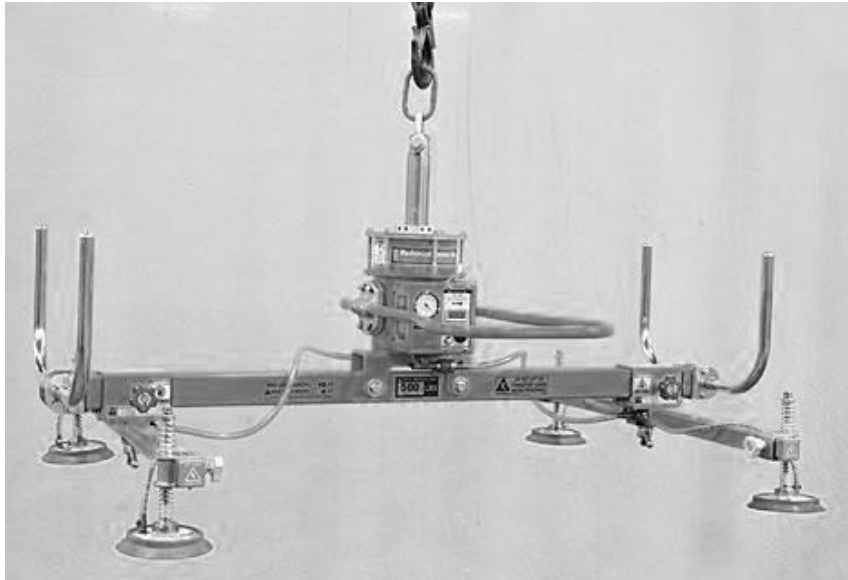


Figure 159 - Self-powered suction lifter ("Mechanical Vacuum Lifters").

volume inside the cylinder results in suction and is subsequently transmitted to one or more suction cups ("Mechanical Vacuum Lifters").

Suction cups

Suction cups in the industry are most of the times specialized for grabbing a surface with a distinct set of characteristics. This increases the reliability and strength of the generated suction adhesion and has led to a number of types of cups. All suction cups listed below are made by the industry leader Piab. Their product range was chosen as the company has a wide variety of suction cups that it has conveniently sorted according to their application ("Suction cups").

Oily surfaces

Sheet metal parts that come from a press line are often covered in oil. For a normal cup this is a very challenging surface to adhere to as the rim struggles to get any grip. Therefore Piab's line up contains suction cups that have been specifically designed to handle this kind of surfaces. Their FCF suction cups for example have rubber friction pads in that are placed around the centre and are separated by radial and circumferential grooves. The edges of each friction pad penetrate the oily boundary layer and make direct contact with the steel. In this way shear force performance is increased 2-4 times compared to normal suction cups.



Figure 160 - Suction cup for oily surfaces ("FCF100P").

Dry surfaces

When a high resistance against shear forces is required during the handling of dry surfaces, it is best to choose for a suction cup that generates a high level of friction. This allows objects to be lifted parallel to the substrate and offers good stability. The friction cups from Piab are covered by small ridges that are separated by pressure distribution grooves. The flat surfaces of the ridges are pressed against the surface due to the pressure differential with the outside of the cup and therefore generate a high amount of friction. This is because they are made from a soft material that conforms to the substrate. The large contact area promotes adhesion mechanisms like adsorption adhesion and interlocking.



Figure 161 - Suction cup for dry surfaces("F150").

Appendix A: Industrial suction solutions

Thin sheets

Thin sheets that need to be grabbed without deforming them require a special type of suction cup that supports the material during suction. This suction cup type can be seen in Figure 162 and has a structure that bears an uncanny resemblance to the protrusions on the whip lash squid's suction cup (page ...). The supporting ridges prevent the material to collapse inward while distributing the pressure through the channels in between them.



Figure 162 - Suction cup for opening bags ("F33 FCM").

Porous surfaces

In a lot of applications in the industry slightly porous materials like cardboard need to be lifted. For a suction adhesion system this means that the suction chamber can never be fully sealed as air travel through the substrate into the cup. However as long as these leaks can be compensated by the vacuum pump picking up porous surfaces with suction adhesion remains possible. To reduce energy consumption and to minimize leakage, suction cups designed for this application have a broad flexible rim that conforms to the substrate. This adjustment is aimed at increasing the energy needed for air to travel from the outside to the inside of the cup. As the air needs to travel a longer distance through the substrate, the resistance that it encounters increases.



Figure 163 - Suction cup designed for porous surfaces ("B110XP").

Heavy objects

Heavy objects like glass windows and thick sheets of steel require heavy duty suction cups. Piab therefore offers a range of sturdy suction cups that can deal with the extra weight. The material used for the cups is stiffer and is covered with friction pads. To increase the reliability of the suction cup further it has a double suction rim. If the outer rim where to fail an inner rim quickly seals of the remaining suction area and therefore prevents the heavy sheet from falling.



Figure 164 - Suction cup for heavy plates ("XLF").

Rough surfaces

Surfaces with a high roughness cannot be grabbed using conventional suction cups. This is because the coherency of the rim prevents the leaks in between the asperities of the substrate to be filled up. Piab therefore offers closed foam rims that due to their low material coherency can fill up the space in between the surface grains. The foam mimics a segmented rim as the thin walled cells in the foam can move more or less independently. This means that only a small part of the strain felt by one cell is not transmitted to its surrounding cells. A downside to using a foam ring is that it renders part of the suction area useless as the internal pressure differential cannot be distributed underneath it.



Figure 165 - Suction with foam rim ("NEW Piab").

Appendix A: Industrial suction solutions

Flexible/uneven surfaces

When handling very flexible substrates like bags or surfaces with an intricate surface topography, you need a very flexible suction cup that can form itself according to the surface. To achieve this Piab offers suction cups made from a material called Duraflex. The material is said to have the elasticity of rubber and the wear resistance of polyurethane. Flexible suction cups tend to have one or more bellows that allow the rim to adjust its angle when it's not perpendicularly orientated towards the opposing surface. This feature is reminiscent of the pivoting mechanism of the diving beetles suction cup (page ...).



Figure 167 - Suction cup made from Duraflex ("BF110P").

Varying surfaces

In some instances like robotics or variable production lines where multiple types of materials need to be lifted, it is useful to have a suction cup that can be adjusted without having to disassemble to entire system. Piab therefore sells a modular system called piGRIP that allows the user to switch between different suction cup configurations by clicking on different rims or bellows. Such a system is inherently more sustainable and cost efficient, because the producer only has to replace the part of the suction cup that it is worn. The rims for example tend to wear out faster than the rest of the suction cup.



Figure 166 - Modular piGRIP suction cup ("piGRIP®").

Complex surfaces

The best way to grab complex parts with an unknown surface geometry is to resort to a suction adhesion system with multiple self-selecting suction cups as demonstrated by Kessens. Piab's version of such a system is called piSAVE sense and is a part of their energy saving line-up ("piSAVE sense"). The mechanism can be integrated with existing suction cups and looks like a sturdier version of the pressure sensitive valve proposed by Kessens and Dessai. The exact working mechanism however is a closely kept secret.



Figure 168 - piSAVE sense mechanism ("piSAVE™ sense").

Submerged surfaces

The conclusion of chapter 1 suction has shown that adhesion in aquatic and terrestrial applications differs in a number of ways. Some companies therefore offer suction cups that are specialized for underwater use. Forum a company that supplies equipment for subsea operations for example sells a suction cup intended for ROVs. This behemoth of a sucker can be seen in Figure 169 and delivers a suction adhesion force of 1950 kg. The



Figure 169 - Suction cup for ROVs ("ROV suction foot").

Appendix A: Industrial suction solutions

flexible polyurethane material in combination with the shape of the cup allows it to attach to round objects covered in marine growth like ship hulls and oil pipes. The ball joint that supports the cup furthermore gives it the ability to swivel to the correct angle. Once the cup is in engaged, multiple edges present on the rim prevent water from re-entering the suction chamber ("ROV suction foot").

Control systems

To ensure that the vacuum is delivered to the suction cup in a timely manner and with the required amount of strength, suction adhesion systems can contain numerous control components that govern the flow and strength of the applied vacuum. In this review only sensors and valves relevant to suction adhesion systems are discussed.

Vacuum sensors

Vacuum sensors measure the amount of pressure inside the system compared to the absolute vacuum or the environment. This information can be used in a feedback loop to adjust the pressure according to the circumstances. In a situation where for example more leakage occurs than normal, information from a vacuum sensor can be used to compensate by increasing the pumping speed of the vacuum pump.

Three types of integrated sensors are typically used to measure vacuum pressure. They all rely on the pressure acting on a diaphragm that deforms in a predictable way. Electrical components are placed around the element to transform the displacement into a measurable change in output voltage.

- Piezo resistive strain gauge

These sensors work by detecting the difference in resistance that is caused by the elongation of an electric circuit (Figure 170).

- Capacitive

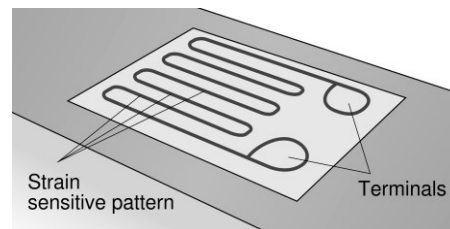


Figure 170 - Piezo resistive strain gauge (Umrath, 2007).

The pressure diaphragm of the sensor is used as a variable capacitor (Figure 171). By measuring the change in the value of the capacitor the pressure acting on the diaphragm can be calculated.

- Electromagnetic

The diaphragm moves a core through a magnetic field. The changes in flux caused by this movement can be used to retrace the change in pressure.

Vacuum valves

Vacuum valves are used to activate suction adhesion components or to change the flow direction inside the system. The valves are characterized by their flow paths, intake and exhaust ports and the way the valve is controlled.

- Directional control valves

Directional control valves govern the flow that the air takes by opening and closing ports by moving a spool into a different position.

- Logic valves

Logic valves provide the pneumatic circuit with the logical AND / OR operations. This means that the circuit is activated when both valves (AND) are activated or only one of the two (OR).

- Manually, mechanically, electrically or pneumatically actuated

Valves can be activated in a number of ways. Some valves can be manually activated using a pushbutton or a lever, while electrically operated valves allow a control system to operate them. In some cases the valves are operated by the pneumatic circuit itself by actuating the spool with compressed air.

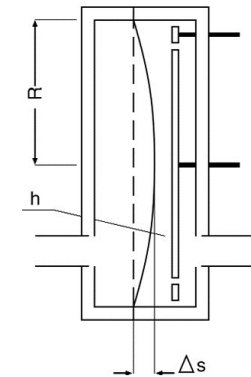


Figure 171 - Capacitive vacuum sensor (Umrath, 2007).

Appendix B: Consumer market suction solutions

To be able to pinpoint possible market opportunities and to see whether some of the strategies from chapter 1 are already present in consumer products, a review is made of all product categories that use suction adhesion. For each category products with the most interesting and innovative features have been selected.

Suction cup hooks

Suction cup hooks are probably the best known and most used suction adhesion product on the market today, as everyone at some point has seen or owned a set of them. The suction hooks allow the consumer to attach a hook to the bathroom wall without having to damage the tilework. However in almost all cases they eventually get replaced by a more permanent solution. This is because even on very smooth surfaces air tends to get in overtime and causes the cups to fall from the wall.

One of the more reliable suction hook products is made by the company ProSuction Hooks. They produce a heavy duty cup that differs in a number of ways from standard suction hooks. In contrast to the normal hooks the pro suction hooks seen in Figure 173 have a tightening mechanism that results in additional suction. By rotating the top wheel the flexible inner-lining is pulled upward and the enclosed volume of air is expanded. The use of an active pulling force and a locking mechanism that holds the lining is similar to how limpets generate suction. Just like the limpet the adhesion force of the pro suction hook is significant, as one hook is able to carry 11 kg. However despite its improved design the suction hook still has the same flaw as its competitors. The company recommends that the suction hook is detached and attached each 30



Figure 173 - Pro suction hooks ("HEAVY DUTY").

days for optimal performance, which is a lot of hassle just to be able to hang up your towel ("Instructions").

Suction cup grab bars

For elderly people and people with disabilities it can be difficult to get in and out of the bath tub or to stand up after having gone to the toilet. Therefore they usually mount grab bars in their bathroom to have extra support. However when they are on holiday or visiting someone these handles are in most cases not installed. Numerous companies therefore offer reversible attachable grab bars that use suction cups to cling onto the wall.



Figure 174 - Suction cup grab bar ("Mommy's helper").

The reason that they are marketed as temporary handles has to do with the fact that they suffer from the same disadvantage as suction cup hooks. After a number of weeks or months they lose suction and become dangerously loose. This feature, which has probably caused many broken hips, led some manufacturers to include a safety indicator in the handle ("Suction Cup Grab Bar").

This rudimentary indicator measures the distance between the cup and the handle and turns red when the cup is about to come loose from the wall (Figure 175).



Figure 175 - Grab bar safety indicator ("Drive Suction").

Appendix B: Consumer market suction solutions

Suction cup mounts

Suction cup mounts are used to fix smart devices, camera gear or navigation equipment to smooth surfaces usually in or around the car. More sturdy mounts have levers, screw wheels or push buttons that can be used to increase their tenacity (Figure 172). To make the mounts more stable and to increase their reliability some manufacturers equip their products with two or more cups (Figure 177). More professional mount also have an indicator that shows if the pressure level inside the cup is still sufficient. This indicator is formed by a tube that contains a spring. When a vacuum is present inside the cup the tube is pulled in towards the suction chamber and shows a green indication strip. When suction is lost the spring pushes the tube back out and a red section of the cylinder is revealed.



Figure 177 - Smartphone suction mount with multiple cups ("Tri-base suction").



Figure 176 - Two types of suction cup dent removers ("55mm MINI") ("Klutch Heavy").

Suction cup dent pullers

In some cases dents can be repaired by pulling the sheet metal carefully outward. The ability of suction cups to attach reversibly to smooth surfaces makes them perfect for this job. The devices that are available on the market are quite simple and consist of a suction cup with a handle attached to them. To create the necessary adhesion, their tenacity is boosted with a handle that pulls on the sucker lining. This handle is placed in such a way that the energy generated during pulling is converted into extra suction. A clever mechanism that is also used by remora fish and squid species.

Suction cup reacher grabbers

People that are bound to their chair or that cannot bend down can have difficulty with grasping items that are just outside their reach. Therefore special reacher grabber tools are available to extend a person's reach. These grabbers usually are bad at handling smooth and slippery items, which has led some manufacturers to equip them with a set of suction cups. The suction cup reacher grabber in Figure 176 for example has two suction cups that are pressed onto the item that needs to be grabbed. These are actuated by pulling onto the lever situated at the handle. The suction cups themselves are fairly standard and provide suction using releasing elastic restorative forces in the material after being flattened.



Figure 178 - Suction cup reacher grabber ("Reacher Grabber").

Appendix B: Consumer market suction solutions

Suction cup toilet plungers

Suction cup plungers have made one of the least attractive tasks around the house a bit more bearable. Clogged toilets and sinks can be unplugged by blasting the congestion through the drain by creating an area of high pressure before the clot. The standard plunger, which is just a suction cup on a stick, has been improved over the years and more advanced designs have come onto the market that aim to get rid of even the most persistent obstructions. Figure 179 for example shows a toilet plunger with a built-in piston pump that allows the user to put more pressure on the clogged drain. The other plunger uses a similar solution but has opted for compressible bellows. This design has the advantage that it is more flexible and can therefore get to hard to reach drain openings.



*Figure 179 - Suction cup toilet plungers
(Journey's Edge) ("Monument MP1600")*

Appendix C: Market research

Chapter 2 has already provided insight in the technical solutions that are available with regard to suction adhesion. However now that an application has been chosen it is important to have an idea about the existing products which aim to solve the same problem.

Grippey

The Grippey is a set of handles that can be mounted on any square piece of household appliance or furniture to make it easier to grasp. The handles are secured with a strap that has to be tucked underneath the object ("GRIPPEY snel en").

Maximum lifting weight	46 kg
Price	?



EZ moves

EZ moves is a system that supposedly makes moving objects a lot easier. The kit consists of a crowbar device that multiplies the force of the user to lift heavy furniture pieces. Sliding pieces are then inserted underneath the object, which reduce friction with the surface ("About us").

Maximum lifting weight	1600 kg
Price	€39,20



Tiller

The Tiller is an electric lifting trolley to move objects up to 120 kg. The device is basically a miniature forklift with an on-board battery that contains enough energy for 300 lifts. When an item is lifted the user needs to slide a spade like plate underneath the object and secure it with a strap to the lifter. This prevents items from falling off. The same procedure in reverse is needed for unloading ("LM75 Hefmobiel").

Maximum lifting weight	120 kg
Price	€4416,50



Liftmate

The Liftmate is a set of dollies that can transform any square item into a four wheeled cart. To lift an object the dollies need to be slid underneath the item and secured to it with a strap. Manual hydraulic pumps have been added to make lifting objects up to 600 kg possible ("Furniture and Appliance").

Maximum lifting weight	600 kg
Price	€759,-



Appendix C: Market research

UpCart

Upcart is a trolley that can be used to transport goods weighing up to 75 kg. It has a clever wheel design that allows it to climb stair more easily. To make it convenient to take the UpCart with you the trolley can be folded flat which allows it to fit in a car booth ("The UpCart is").

Maximum lifting weight	75 kg
Price	€78,30



Liftkar SAL

The liftkar SAL is a lightweight trolley that can carry up to 170 kg. It has been equipped with an electrically powered mechanism that can crank itself up the stairs. In this way it greatly reduces the amount of energy needed for moving heavy loads from one floor to the other. Loading and unloading the objects is similar to the tiller. A fork is slit underneath and the object is secured using straps ("The extremely fast").

Maximum lifting weight	170 kg
Price	€3295,-



Stairmobil

The stairmobil is a hybrid between the Liftkar and the Tiller as it can both climb stairs and lift objects up to the desired height. It is therefore ideal for moving heavy household appliances around. These benefits however don't come cheap as the device has a hefty price tag of almost €8000,- ("De stairmobil, de").

Maximum lifting weight	170 kg
Price	€7850,-



KS Glass Robot 180

The KS Glass Robot 180 is a lifting aid that helps with removing and placing heavy windows. The robot uses 4 suction cups that are powered by a vacuum pump. A second vacuum pump is used to move the pneumatic actuators. These actuators have enough power to lift windows weighing up to 180 kg ("KS Rob 180").

Maximum lifting weight	180 kg
Price	?



Appendix D: Use environment analysis

To determine under which circumstances the suction adhesion device has to fulfil its application, an analysis of the use environment is made. The analysis includes a review of the characteristics of the substrates that the device is likely to encounter, a short listing of the contaminants that may hinder its functioning and a review of the influence of the atmospheric conditions is provided.

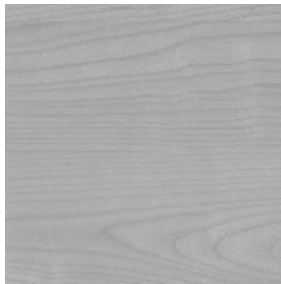
Surfaces

To characterize a surface a number of variables need to be known. These are related to the surface topography of the substrate and the material. The typography of a surface is determined by three hierarchical characteristics. These are macro-deviations, surface waviness and roughness. In this analysis only roughness values are listed as macro-deviations and waviness differ for each substrate and are not dependent on the type of material. The influence of the type of material on adhesion is determined by looking at its surface energy. This is because high surface energies can generate large van der Waals forces. Consequently materials with a lower surface energy produce less adsorption adhesion.

Wood

Wood is a heterogeneous material that is mainly composed out of cellulose and lignin. This heterogeneity in both composition and structure makes it hard to determine the surface energy of wooden surfaces. Mijer et al. (2000) however gave it their best shot and examined wood surfaces from a multitude of tree species. According to them the surface energy density is typically between 30 and 50 mJm⁻². The surface roughness of wood is also highly variable and depends on grain direction and the method used to finish the surface. According to Kilic et al. (2005) the roughest wood surfaces are created using sawing and the smoothest result was achieved using sanding. The R_a values were measured for aspen and beech wood samples and came out at between 4.50 and 13.26 μm .

Typical roughness (R_a) μm	4.5-13.3
Surface free energy (γ) mJm ⁻²	30-50



Ceramic

Ceramics in the home environment are usually made from fired clay, which contains aluminium phyllosilicates and traces of other minerals. This type of material can be found in tiles, bricks and roof tiles. The roughness of the fired clay differs based on the finishing method used. Gazulla et al. (2011) made measurements on fired clay roof tiles and found that a standard roofing tile has about a roughness of 3.5 μm . A credible measurement of the surface energy for fired clay could not be found as the material tends to absorb moisture. Measurements from Matziaris et al. (2011) however show that a drop of distilled water has a contact angle on low fired clay of 43°. This indicates that the material hydrophilic and has a high surface energy.

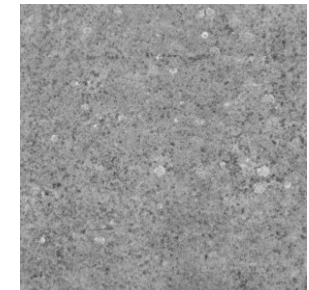
Typical roughness (R_a) μm	3.5
Surface free energy (γ) J/m ²	?



Concrete

Concrete is a mixture of coarse rocks such as limestone and granite mixed with fine materials like sand. The mixture is held together with cement which consists out of hydraulic lime. Concrete forms the basis of many homes and in modern buildings is usually left in its bare form. Due to the incorporation of granular materials concrete has a high surface roughness. Work done by Leising (2010) shows that the mean surface roughness of concrete is 125.9 μm . The surface energy of concrete has been determined by Courard et al. (2011). They found that cement paste has a surface energy of 44.3 mJ/m².

Typical roughness (R_a) μm	125.9
Surface free energy (γ) mJ/m ²	44.3



Appendix D: Use environment analysis

Plaster

Plaster has been used for centuries to give walls a smooth appearance. Most indoor plasters consist out of gypsum, lime or cement. The finish depends on the method used to apply the plaster and the coarseness of the grains incorporated in the mixture. Measurements made by Sandberg et al. (2013) show that the mean roughness of plaster is between 200 μm and 400 μm , depending on whether the plaster is wood float finished, steel float finished or brushed finished. Although no surface energy measurements could be found it is assumed that at least cement plaster has a very similar surface energy as concrete since it contains the same ingredients.



Typical roughness (R_a) μm	200-400
Surface free energy (γ) mJm^{-2}	44.3

Metal

Metals are a broad category of materials with a large variety in roughness and surface energy. However due to tendency to oxidize most metals are covered by a protective layer. The only bear metals that can be found frequently in the home environment are stainless steel and aluminium. Aluminium which is mostly covered in a protective anodized oxide layer has a typical roughness of about 2.4 μm (LeBlanc, 2009) and a surface energy of 169 mJm^{-2} (Kinloch, 1987). Stainless steel on the other hand was found to have a typical surface roughness of only 0.2 μm and a surface energy of around 41 mJm^{-2} (Bernardes et al., 2010).



Typical roughness (R_a) μm	0.2-2.4
Surface free energy (γ) mJm^{-2}	41-169

Glass

Glass is an amorphous non-crystalline solid usually made from a mixture of silica, sodium oxide, sodium carbonate, calcium oxide and lime. Glass is used as a transparent heat barrier in most buildings and can be found increasingly more in modern buildings. Because the material needs to be as transparent as possible, in most cases it has a very smooth surface finish. The roughness of untreated glass was determined by Silva et al. (2012), who found that it has a R_a value of 0.0006 μm . The surface energy of glass was found in a study by Courard et al. (2011) who states that it has a surface energy of 43.4 mJm^{-2} .



Typical roughness (R_a) μm	0.0006
Surface free energy (γ) mJm^{-2}	43.4

Painted

Many surfaces in the home environment are painted to give them a more attractive colour or to prevent the underlying material from degrading. A typical indoor paint consists out of 20% acrylic resin and 80% vinyl resin (Sickler). Because the paint is applied in thin layers on a substrate, its roughness depends on the underlying material. Because of the surface tension inside the paint however it tends to smooth out some of the topographical features. Surface energy values for normal house paints are difficult to obtain but Raghavan (2014) states that acrylic polymers have a surface energy of between 30-50 mJm^{-2} .



Typical roughness (R_a) μm	?
Surface free energy (γ) mJm^{-2}	30-50

Appendix D: Use environment analysis

Plastics

Since they were introduced in the 50s plastic surfaces can be found on an increasing amount of items in the house. Especially cheap wood board furniture tends to be covered by a wood mimicking plastic layer. The surface roughness of plastics depends on the texture of the mould and the ingredients used. ABS for example can have a very low surface roughness of $0.025\text{ }\mu\text{m}$. Fibre reinforced plastics on the other hand can have an R_a up to $25\text{ }\mu\text{m}$. The surface energy of most plastics is between $30\text{--}50\text{ mJm}^{-2}$ (Raghavan, 2014).

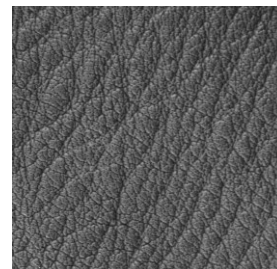
Typical roughness (R_a) μm	0.025-25
Surface free energy (γ) mJm^{-2}	30-50



Leather

Leather is a product created by tanning animal hides. It is frequently used to upholster sofas and chairs. The surface texture of top-grain or full grain leather is due to the grooves present on the skin of the animal. According to measurements made by Leising this top layer has a mean roughness of about $14\text{ }\mu\text{m}$. Its surface energy was measured by Kayaoglu (2013). He found that an untreated piece of leather has a surface free energy of 38.5 mJm^{-2} . In contrast to the surfaces analysed up till now leather is flexible and slightly permeable. This means that special attention needs to be paid to make sure that the material is not sucked into the suction cup, and that the system can compensate for the air that is leaking through the material.

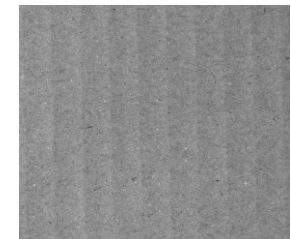
Typical roughness (R_a) μm	14
Surface free energy (γ) mJm^{-2}	38.6



Cardboard

Cardboard is used to transport heavy parcels and also forms the basis of moving boxes. Almost all of these boxes are made from kraft paper that is glued together to form corrugated cardboard. A typical roughness for this type of paper is provided by the Cham Paper Group. They state that their craft paper has a roughness of $2.5\text{ }\mu\text{m}$. The surface free energy of kraft paper is given in a study by Moutinho et al. (2009), who determined that kraft paper has a surface free energy of 39.5 mJm^{-2} . In addition to the roughness and surface free energy of cardboard the suction adhesions device also has to take into account the permeability and flexibility of cardboard. It is furthermore important that the suction cup does not have sharp protruding features as this would puncture the paper. A measure of the permeance of cardboard can be derived from information provided by the Scandinavian pulp, paper and board testing committee, who state that a sheet of 70 gm^{-2} kraft paper has a permeance of $10\text{ }\mu\text{mPa}^{-1}\text{s}^{-1}$. Kraft liners used in cardboardboxes are typically twice as heavy ("Containerboard") and when glued together consists out of three layers. When it is assumed that the permeance decreases linearly with an increase in thickness the air permeance of corrugated cardboard can be calculated.

Typical roughness (R_a) μm	2.5
Surface free energy (γ) mJm^{-2}	39.5
Air permeance $\mu\text{mPa}^{-1}\text{s}^{-1}$	1.67



Contaminants

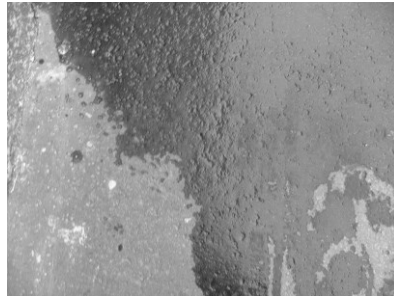
Contamination of the substrate or the suction cup rim can lead to a difference in performance of the suction adhesion device. Adsorption adhesion generated between the suction cup and the substrate could be hindered for example as the real area of contact decreases due to the presence of contaminants at the interface. Also the amount of friction between the substrate and the suction cup can be affected. Liquid contaminants can for example act as a lubricant. In addition to these tribological

Appendix D: Use environment analysis

aspects also the functioning of the device itself can be affected by contamination. Pressure distribution grooves can get clogged up or pneumatic valves become jammed open or closed.

Water

Water is the most common contaminant that will affect the functioning of the adhesion device. The presence of water in between the interface can affect the amount of adhesion between two hydrophobic surfaces. In contrast to homogeneous hydrophobic surfaces where the water is pushed out between the interface, heterogeneous hydrophobic surfaces are known to trap small bodies of water (Defante et al., 2014). This is because the water moves to spots where the surface is slightly more hydrophilic. As a result of the trapped water the adhesion energy can decrease with 50% when compared to a perfectly dry contact. This same drop in real area of contact due to the presence of water can also negatively influence the amount of friction. The coefficient of friction between rubber and asphalt for example decreases 23% when water is added (Beardmore, 2013). Just as with a tire it is therefore important that the suction cup is textured in such a way that it can drain away water efficiently. Attention should also be paid to prevent water from entering the device. The non-compressible nature of water can damage the vacuum pump and its conductivity can short-circuit vulnerable electronics.



Grease

Grease is an assortment of fats and oils that over time covers kitchen appliances. In contrast to water it cannot easily be pressed out from between the contact area and therefore has a large effect on the amount of adsorption adhesion that is generated. Also static friction will drop significantly due to this contaminant, as the oil and fat mixture acts as lubricant. The static coefficient of friction between leather and metal for example drops from 0.6 to 0.2 (Beardmore, 2013). A final hazard of grease is that it can clog up pressure distribution grooves and seize moving parts. This is because the layer of grease catches dirt particles, which speeds up the creation of obstructions.



Dust

Dust is a combination of micro particles that contains skin flakes, fabric strands, pollen, dirt, dust mite fecals and insect fragments ("Composition of building dust"). Little is known about the influence of dust on reversible adhesion. A study from Krofova and Müller (2015) on the effect of dust on adhesive bond strength concludes that small particles up to 250 μm decreased the bond strength of the adhesive with 18%, while larger particles improved the bonding strength with 5%. It is uncertain however whether this is also valid for glue-less adhesion. As stated before the functioning of the suction adhesion device can be hindered by dust in combination with grease as it deposits itself on crucial components.



Appendix D: Use environment analysis

Atmospheric conditions

Atmospheric conditions can affect some of the properties of the materials involved in the attachment process. These conditions are temperature, humidity and atmospheric pressure.

Temperature

The temperature of the surroundings in which the suction adhesion device is used, affect it in a number of ways. The surface energy of many materials is for example temperature dependent and polymers can conform better to surfaces when their temperature is increased. The temperature in which the suction adhesion device has to perform its function will be at room temperature. However when the device is used outdoor it can encounter temperatures from -6 till about 40 °C (“Kou”).

Humidity

When humidity is high, water can spontaneously condensate between the substrate and the suction cup surface. This can have an influence on adhesion as discussed in the previous section. The maximum amount of water that the air can contain is determined by its temperature. At 40 °C, the highest temperature under which the device has to function, 1 kg of air can contain up to 49.8 g of water (“Moisture holding capacity of air”).

Atmospheric pressure

Atmospheric pressure limits the amount of suction adhesion that can be generated. If for example the suction adhesion device is used on top of a mountain its performance will be reduced. On top of a 2000 meter high mountain the atmospheric pressure drops from 100 kPa to 80 kPa. A realistic range of atmospheric pressures under which the device has to function is from 80 to 106 kPa (“Altitude above Sea”).

Appendix E: Pressure distribution curves

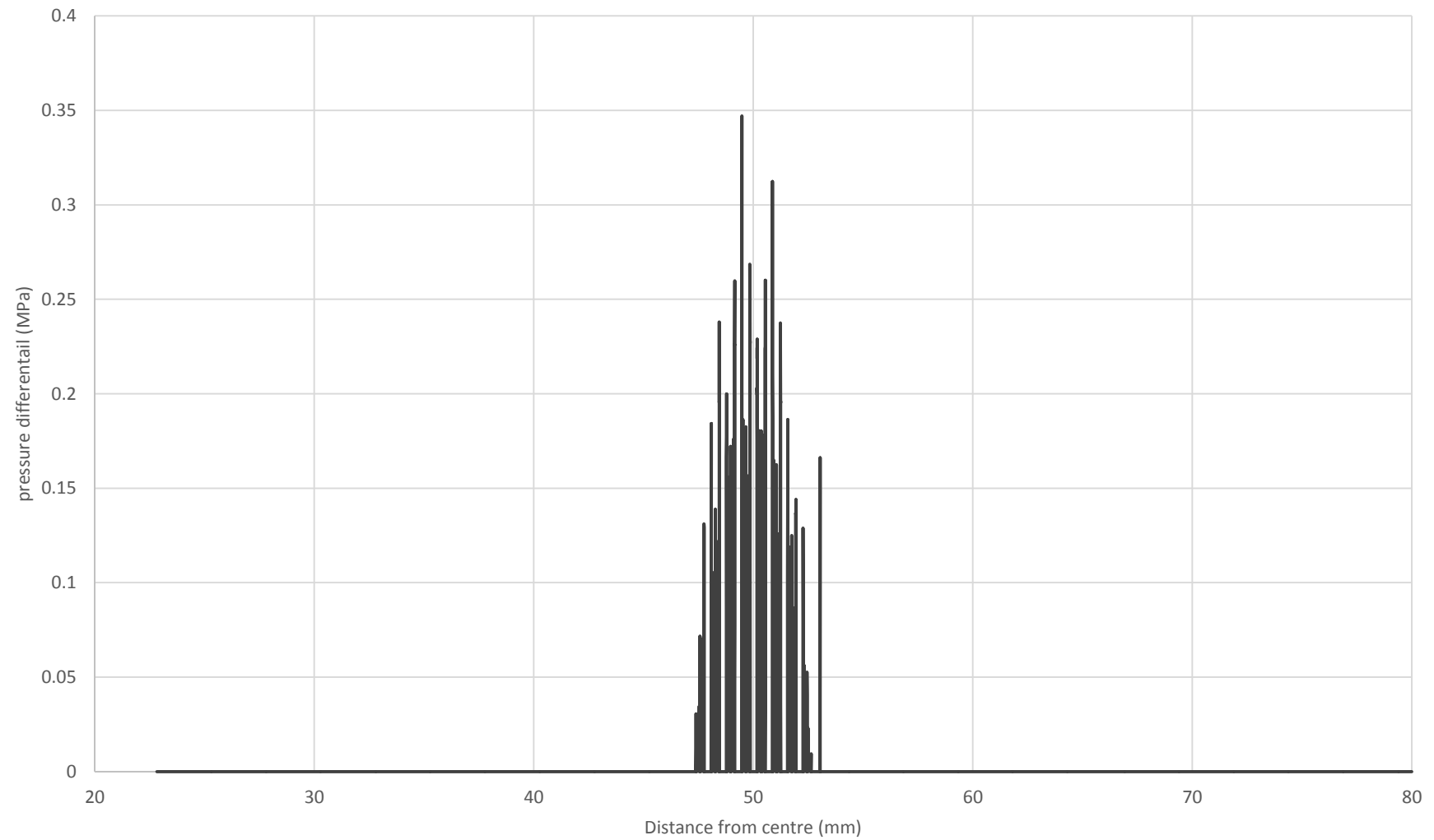


Figure 180 - Pressure distribution at 8 kPa.

Appendix E: Pressure distribution curves

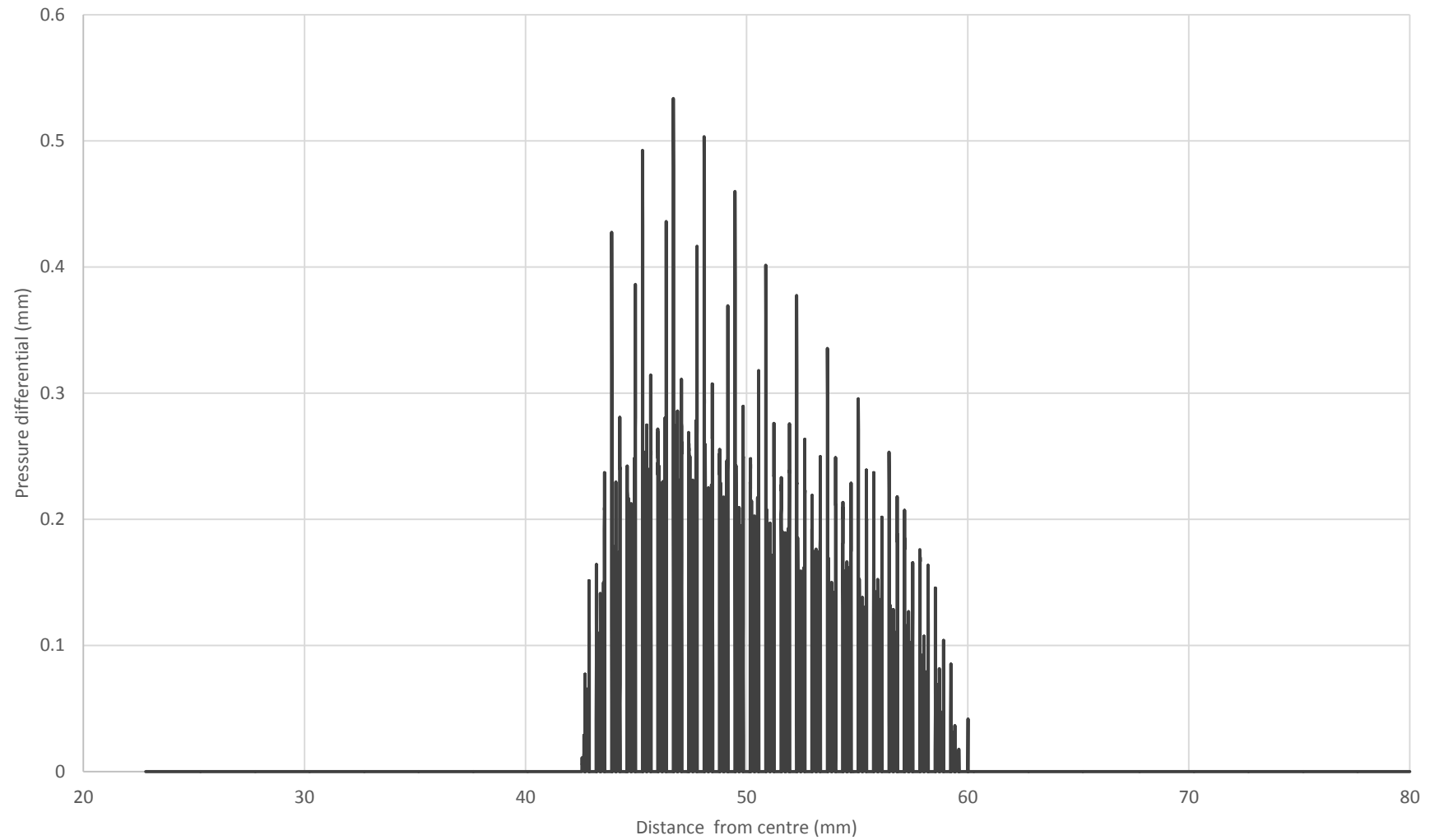


Figure 181 - Pressure distribution at 18 kPa.

Appendix E: Pressure distribution curves

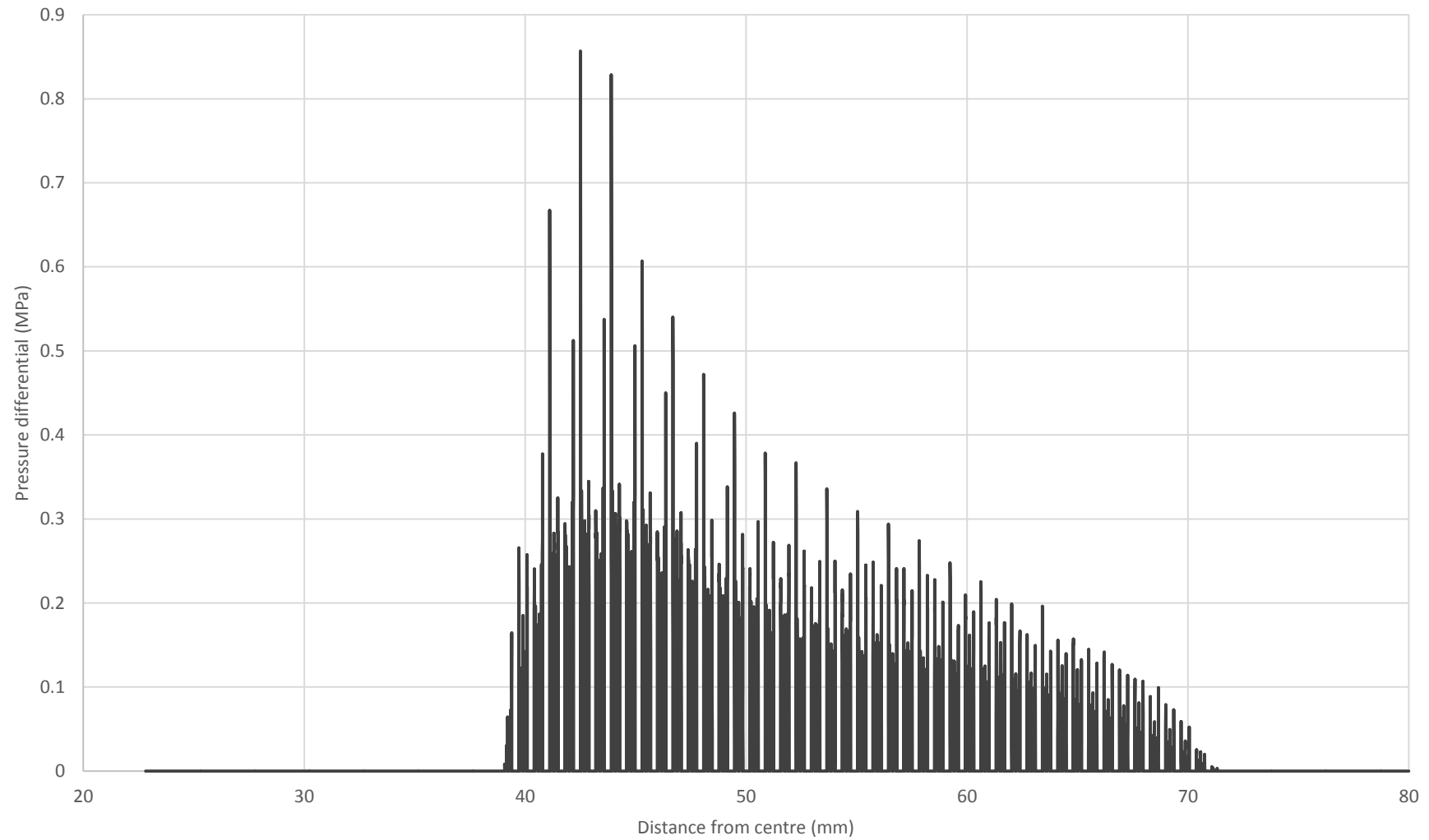


Figure 182 - Pressure distribution 28 kPa.

Appendix E: Pressure distribution curves

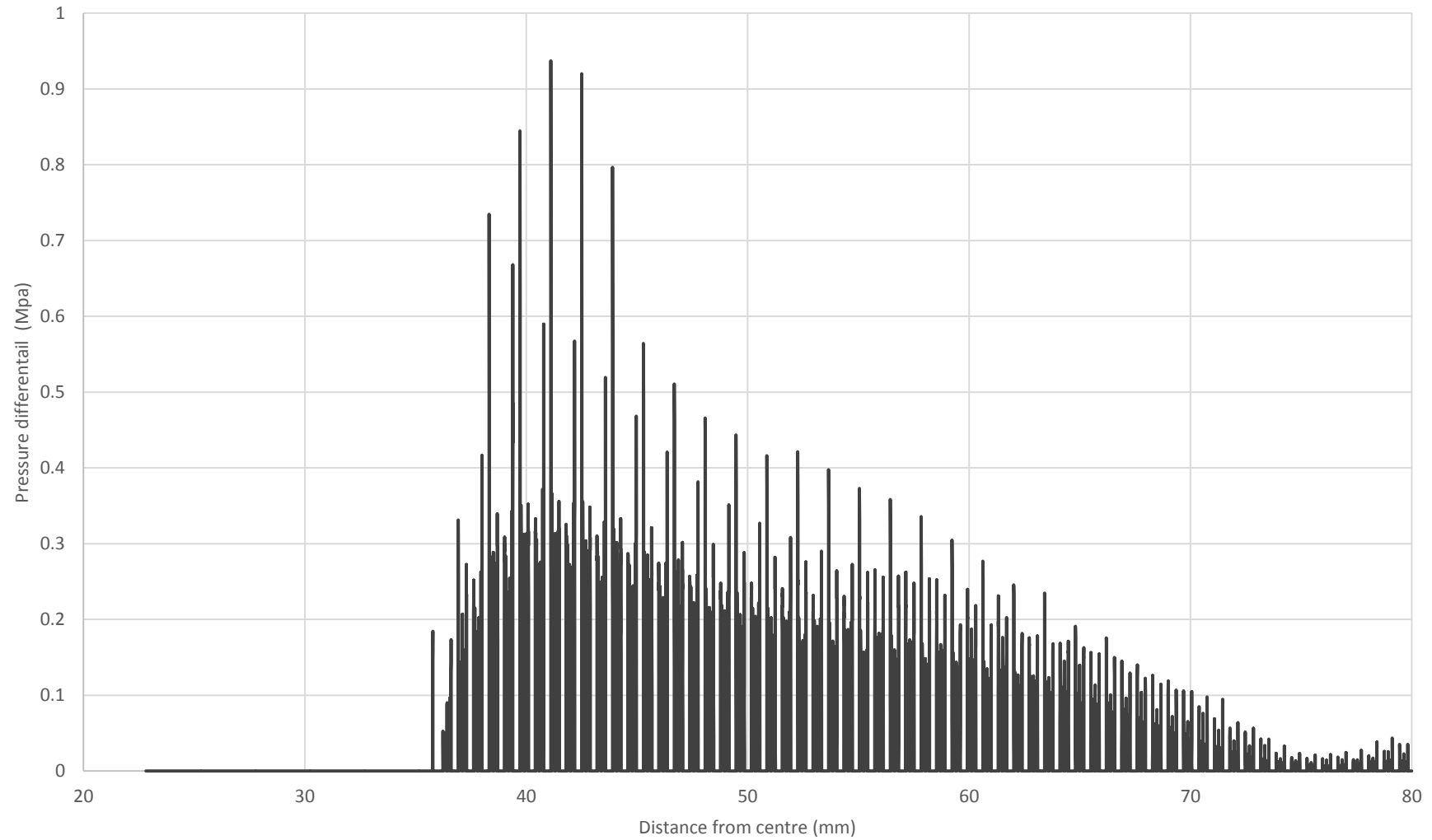


Figure 183 - Pressure distribution at 38 kPa.

Appendix E: Pressure distribution curves

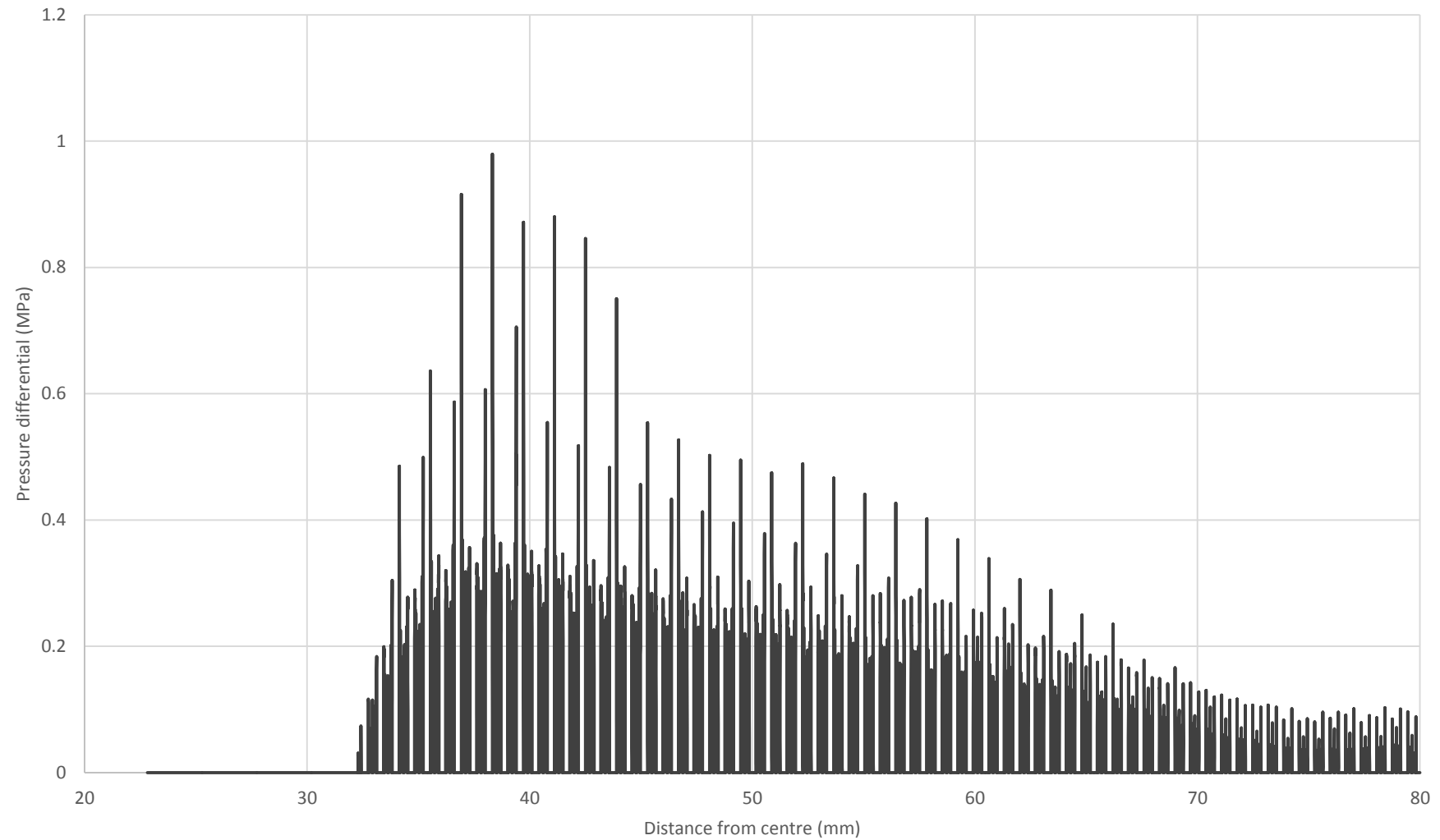


Figure 184 - Pressure distribution at 48 kPa.

Appendix E: Pressure distribution curves

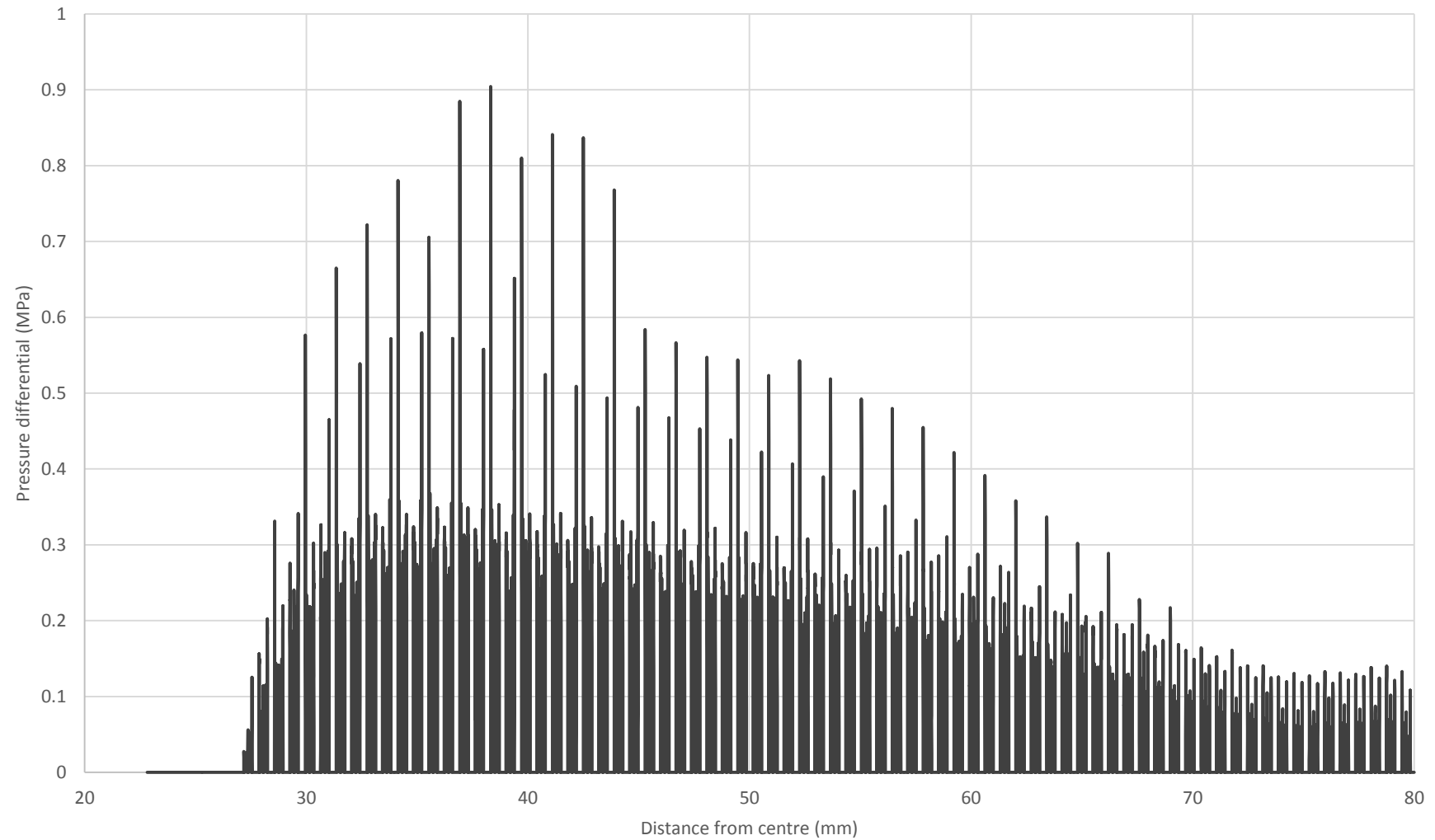


Figure 185 - Pressure distribution at 58 kPa.

Appendix E: Pressure distribution curves

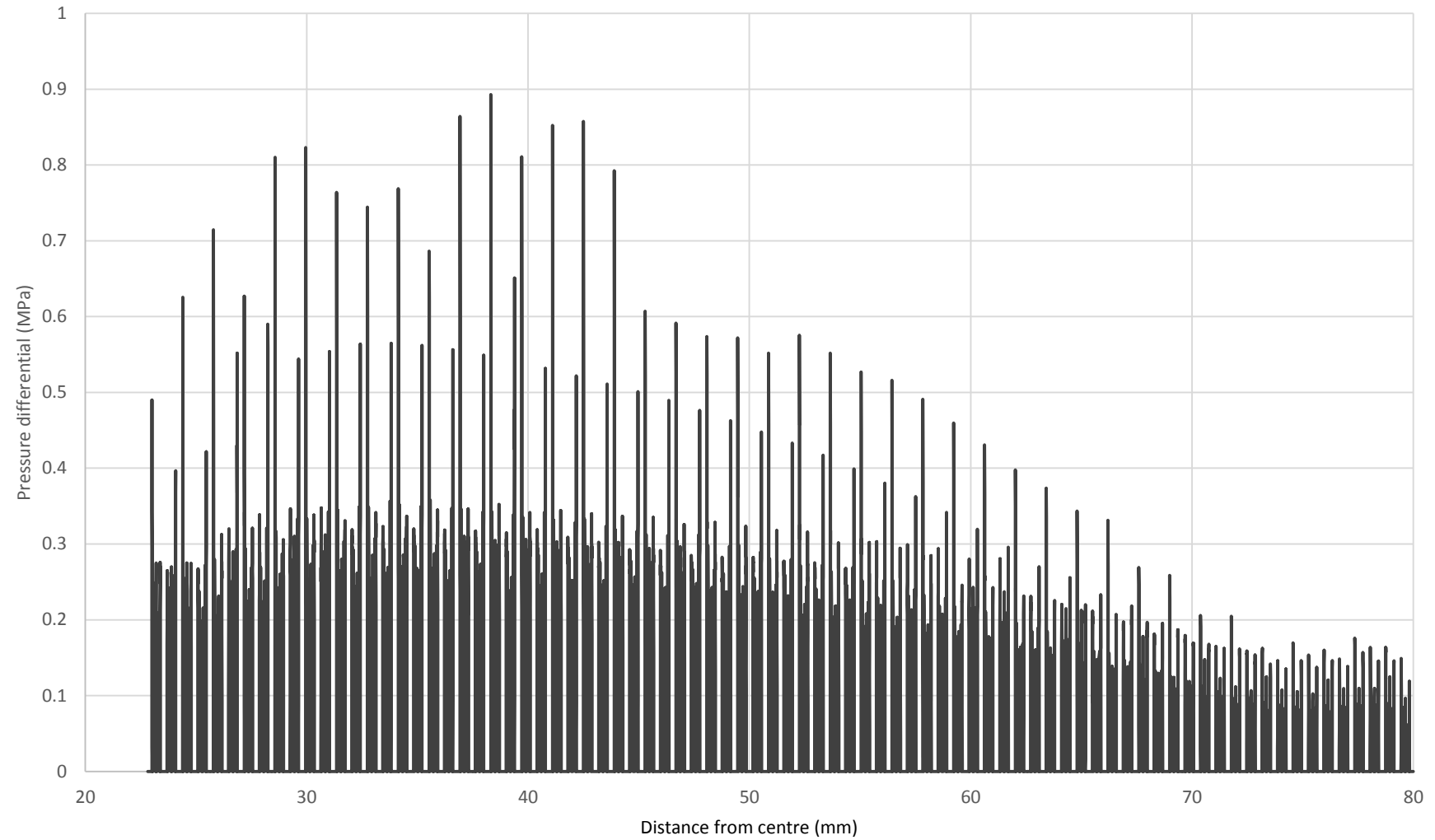


Figure 186 - Pressure distribution at 68 kPa.

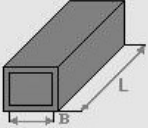
Appendix F: Pressure drop calculator

Pressure Drop Online-Calculator

Note: Calculations are possible only, if Javascript is activated in your browser.
[Pressure Drop Online-Calculator for Mobile and PDA](#). This version is usable for browsers without Javascript also.

Element of pipe

Group: **Straight pipes** Subgroup: **rectangular**



Width of pipe B: mm

Height of pipe H: mm

Length of pipe L: m

Pipe roughness: mm

Flow medium

Flow medium:

Condition: ☐ liquid ☒ gaseous

Volume flow: l/min

Weight density: kg/m³

Dynamic Viscosity: 10-6 kg/ms

Additional data for gases:

Pressure (inlet, abs.): MPa

Temperature (inlet): °C

Temperature (outlet): °C

Output of values: ☒ metrical ☐ US

Pressure Drop Online-Calculator

Calculation output

Flow medium: Air 20 °C / gaseous
Volume flow:: 0.146388889 l/min
Weight density: 1.225 kg/m³
Dynamic Viscosity: 19.83 10-6 kg/ms
Element of pipe: rectangular
Dimensions of element: Width of pipe B: 0.63695915 mm
Height of pipe H: 0.23 mm
Length of pipe L: 0.019189 m

Velocity of flow: 16.65 m/s
Reynolds number: 348
Velocity of flow 2: -
Reynolds number 2: -
Flow: laminar
Absolute roughness: 0.01066161 mm
Pipe friction number: 0.19
Resistance coefficient: 10.99
Resist.coeff.branching pipe: -
Press.drop branch.pipe: -
Pressure drop: 18.88 mbar
0.02 bar

Figure 187 - Pressure drop calculator.

Appendix G: Suction cup design parameters

Parameter	Symbol	Value
Soft sealing layer		
Outer radius of the soft sealing layer.	r_1	90.3 mm
Inner radius of the soft sealing layer.	r_2	90 mm
Thickness of the soft sealing layer.	t_1	1.3 mm
Young's modulus of the soft sealing layer.	E_1	10 kPa
Poisson's ratio of the soft sealing layer.	ν_1	0.49
Adhesion and friction layer		
Outer radius of the adhesion and friction layer.	r_3	80 mm
Inner radius of the adhesion and friction layer.	r_4	22.825 mm
Thickness of the adhesion and friction layer.	t_2	0.5 mm
Young's modulus of the adhesion and friction layer.	E_2	1.32 MPa
Poisson's ratio of the adhesion and friction layer.	ν_2	0.49
Width of the radial grooves.	w_1	0.76;0.96 mm
Number of radial grooves.	p_1	45; 90
Width of the circumferential grooves.	w_2	0.04;0.382 mm
Number of circumferential grooves.	p_2	83;249
Surface free energy of the adhesion and friction layer.	γ_1	20.8 mJ/m ²
Textile backing		
Outer radius of the soft sealing layer backing.	r_1	90.3 mm
Inner radius of the soft sealing layer backing.	r_2	80.3 mm
Outer radius of the adhesion and friction pad backing.	r_3	80 mm

Thickness of the textile backing.	t_3	0.35 mm
Young's modulus of the textile backing.	E_3	2.9 GPa
Poisson's ratio of the textile backing.	ν_3	0.49
Yield strength of the textile backing.	σ_{y1}	3.62 GPa
Closed foam ring		
Outer radius of the closed foam ring.	r_1	90.3 mm
Inner radius of the closed foam ring.	r_2	80.3 mm
Thickness of the closed foam ring.	t_4	11 mm
Young's modulus of closed foam ring.	E_4	0.707 MPa
Poisson's ratio of the closed foam ring.	ν_4	0
Supporting foam		
Outer radius of the supporting foam.	r_3	80 mm
Inner radius of the supporting foam.	r_5	22.825 mm
Thickness of the supporting foam.	t_5	8 mm
Young's modulus of the supporting foam.	E_4	0.707 MPa
Poisson's ratio of the supporting foam.	ν_4	0
Velcro		
Outer radius of the Velcro.	r_3	80 mm
Inner radius of the Velcro.	r_5	22.825 mm
Thickness of the Velcro.	t_6	2.5 mm
Young's modulus of the Velcro.	E_5	0.296 MPa
Poisson's ratio the Velcro.	ν_5	0

Appendix G: Suction cup design parameters

Adhesive layer		
Outer radius of the adhesive layer.	r_1	94.3 mm
Inner radius of the adhesive layer.	r_2	80.3 mm
Thickness of the adhesive layer.	t_7	0.1 mm
Young's modulus of the adhesive layer.	E_6	3.61 MPa
Poisson's ratio of the adhesive layer.	ν_6	0.49
Suction cup base		
Outer radius of suction cup base component 1.	r_4	22.825 mm
Inner radius of suction cup base component 1.	r_6	4 mm
Thickness of suction cup base component 1.	t_8	5.35 mm
Outer radius of suction cup base component 2.	r_7	24.5 mm
Inner radius of suction cup base component 2.	r_6	4 mm
Thickness of suction cup base component 2.	t_9	11.3 mm
Outer radius of suction cup base component 3.	r_8	38 mm
Inner radius of suction cup base component 3.	r_6	4 mm
Thickness of suction cup base component 3.	t_{10}	10 mm
Young's modulus of the suction cup base.	E_7	2.9 GPa
Poisson's ratio of the suction cup base.	ν_7	0.3
Yield strength of the of the suction cup base.	σ_{y2}	63 MPa
Suction cup support		
Outer radius of the suction cup support.	r_1	94.3 mm
Inner radius of the suction cup support.	r_5	22.825 mm

Thickness of the suction cup support.	t_{11}	2 mm
Young's modulus of the suction cup support.	E_8	2.41 GPa
Poisson's ratio of the suction cup support.	ν_8	0.3825
Yield strength of the suction cup support.	σ_{y3}	41 MPa
Outer radius of the seals.	r_7, r_9	38;45 mm
Inner radius of the seals.	d_6	4 mm
Thickness of the seals.	t_{12}	1 mm
Young's modulus of the seals.	E_6	3.61 MPa
Poisson's ratio of the seals.	ν_6	0.49

Table 26 - Design parameter values.

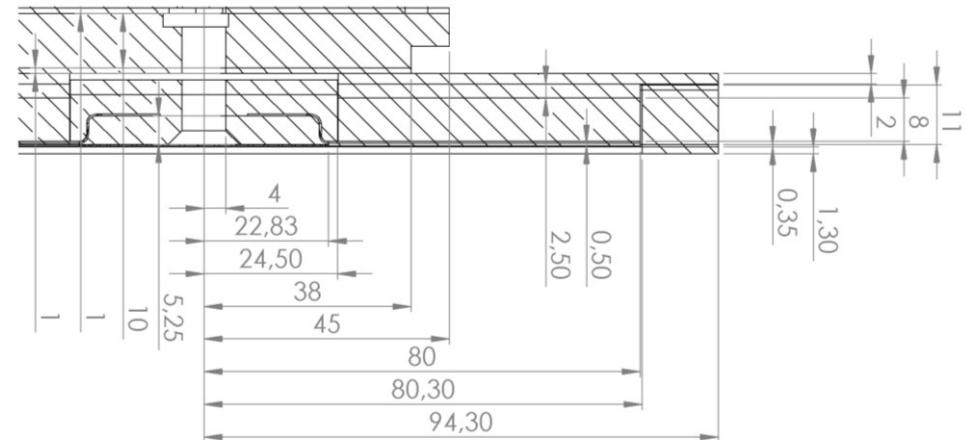


Figure 188 - Suction cup design drawing.

Appendix H: Cost and weight estimation

Component	Material	Production	Weight (g)	Costs (€)	Basic device	Smart device
Casing bottom ¹	Nylon 6 30% glass-fibre	Injection moulding	257,5	9,24	1	1
Casing shield ¹	Nylon 6 30% glass-fibre	Injection moulding	152,1	8,98	1	1
Casing display ¹	Nylon 6 30% glass-fibre	Injection moulding	13,5	2,81		1
Vacuum sensor mount ¹	Nylon 6 30% glass-fibre	Injection moulding	2,6	2,03		1
Release paddles ¹	Nylon 6 30% glass-fibre	Injection moulding	5,8	3,17	1	1
Release paddles linkage ¹	Nylon 6 30% glass-fibre	Injection moulding	18,4	2,23	1	1
Battery cover ¹	Nylon 6 30% glass-fibre	Injection moulding	18,4	3,44	1	1
Sliding ring ¹	Nylon 6 30% glass-fibre	Injection moulding	32,3	3,87		1
On/off button ¹	Nylon 6 30% glass-fibre	Injection moulding	13,5	1,76		1
Bluetooth button ¹	Nylon 6 30% glass-fibre	Injection moulding	13,5	1,76		1
Interface cover ¹	Injection moulding	Injection moulding	13,5	2,81	1	
Pump button ¹	Injection moulding	Injection moulding	13,5	1,76	1	
Handle mounts ¹	Nylon 6 30% glass-fibre	Injection moulding	15,2	2,40	4	4
Handle ¹	Nylon 6 30% glass-fibre	Injection moulding	108,1	4,99	2	2
Handle reinforcement ^{2,3}	Aluminium 6061	laser-cutting	88,2	1,80	1	1
Suction cup support ¹	Nylon 6	Injection moulding	74,0	5,64	1	1
Suction cup base ¹	Nylon 6 30% glass-fibre	Injection moulding	3,8	2,61	1	1
Gasket ^{4,5}	Cork	Die-cutting	7,3	0,35	1	1
Circuit board ⁷	Flax fibre, copper, tin	Routing, etching	4,7	0,33	1	3
8-bit processor ^{8,9}	-	Bought in	1,1	1,16		1
Bluetooth module ^{10,11}	-	Bought in	9,6	0,40		1

Appendix H: Cost and weight estimation

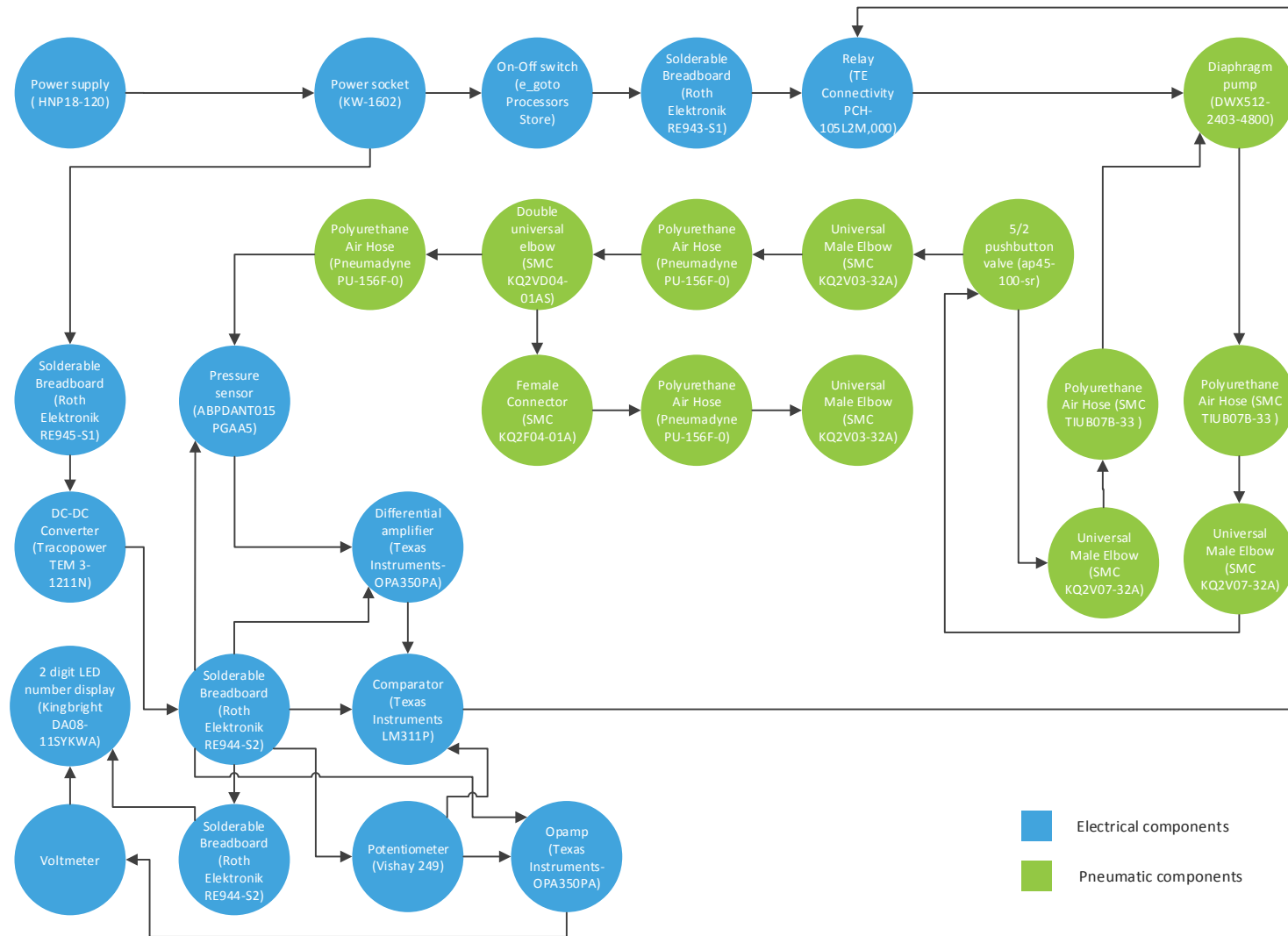
Pressure sensor ^{12, 13}	-	Bought in	4,5	29,58		1
Detachment sensor ^{1, 14}	Nylon 6	Injection moulding, bought in	1,1	1,82		1
E-ink screen ¹⁵	-	Bought in		9,40		1
Potentiometer ¹⁶	-	Bought in	24,3	0,92		1
Speaker ¹⁷	-	Bought in		0,36		1
Button switches ^{18, 19}	-	Bought in	15	0,14	1	3
Solid state relay ²⁰	-	Bought in		1,03		1
Voltage regulator ²¹	-	Bought in		0,13		1
Batteries ²²	-	Bought in	135	9,60	4	4
Battery charger ²³	-	Bought in		3,75	1	1
Battery connectors ^{24, 25}	Copper	Die-cut	1,3	1,40	2	2
Cables and connectors ²⁶	-	Bought in	50	0,48	1	1
Vacuum pump ²⁷	-	Bought in	300	18,8	1	1
Valve manifold ²⁸	Aluminum: 6061-T4	CNC machining	131.2	2,83	1	1
Valve plunger ²⁸	Aluminum: 6061-T4	CNC turning	1,9	3,06	1	1
Tube connectors ^{29, 30}	-	Bought in	2,6	0,66	4	4
O-rings ³¹	-	Bought in		0,03	8	8
Pneumatic hose ³²	-	Bought in	1,1	0,70	2	2
Adhesion and friction pad ³³	Natural rubber, linen fibers	Compression moulding	37,6	0,46	1	1
Foam ring ³⁴	Silicon rubber foam	Die-cut	21,1	2,43	1	1
Supporting foam ³⁴	Silicon rubber foam	Die-cut	36,3	5,04	1	1
Velcro	-	Bought in		0,16	1	1

Appendix H: Cost and weight estimation

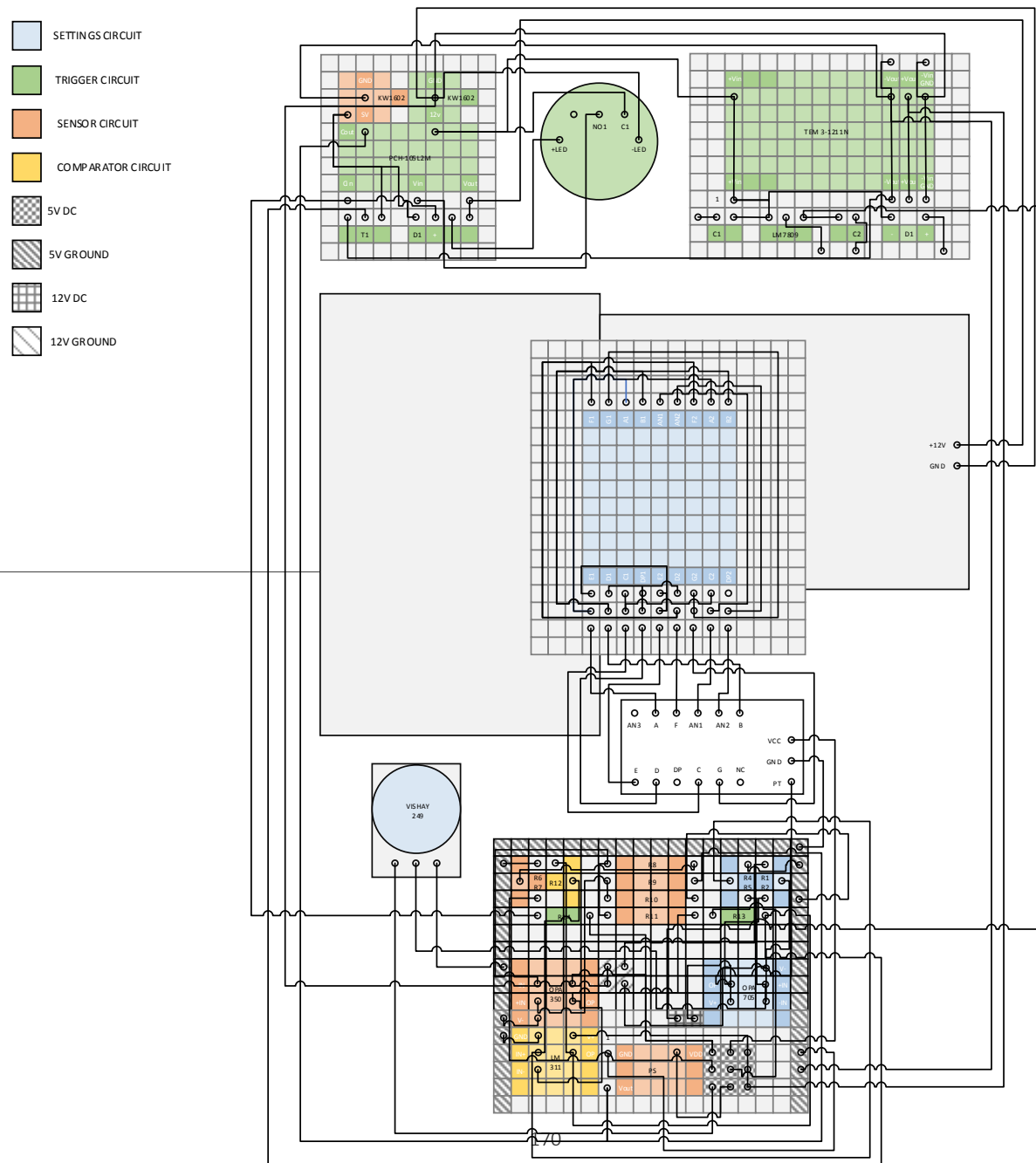
Locking ring ³⁵	Stainless steel	CNC turned	112,4	2,09	1	1
Nuts and bolts ³⁶	-	Bought in		0,11	30	30
Assembly				20	1	1
Packaging				2	1	1
Total production costs basic device	€171,96					
Total production costs smart device	€225,36					
Total weight basic device	2194,9 g					
Total weight smart device	2323,3 g					

Table 27 - 1."Cost estimator", 2."Costimator - Cost", 3."Aluminium sales", 4."Aluminum 6061" 5."1m x 10m" 6."Cork, solid", 7." Standard PCB" 8."Free-Shipping-10PCS", 9."Product description", 10." Free-Shipping-Interface", 11." HC-05 Bluetooth" 12." 40PC015V2A" 13." HONEYWELL 40PC015V2A", 14." 10PCS-6-6-5MM-SMD", 15."custom e-paper design", 16."3590 precision", 17."2PCS-LOT-Phone-speaker", 18."10pcs-250V-5A", 19."KW11-3Z 5A", 20."5v 12v", 21." 1PCS-LM2596T" 22." LiFePO-IFR-18500", 23." 14.6v1a charger", 24."99.9% Pure Copper", 25."Densities of materials", 26." 10PCS-150mm-JST", 27." 2400mbar Pressure", 28."Cost Estimator 2", 29."M5 Threads", 30." Metals and Alloys", 31."O-Ring", 32."1000' real", 33." NATURAL LINEN", 34." siliconen schuim", 35." Klittenband 160 mm", 36." M4-x-16mm", calculated with exchange rate 1 EUR=1,06 USD=0,87 GBP

Appendix I: Prototype components



Wiring diagram



Appendix K: Prototype suction cup



Appendix L: Experiment diagrams

1: The effect of surface roughness on leakage						
Hypothesis: If the surface roughness increases leakage will increase						
IV: Substrate roughness						
Experiment name	Pressure differential (kPa)	Substrate	Trials	Files	Remarks	
Sealing 1	0-max	glass	2	Sealing1a.txt, Sealing1b.txt	Suction cup leaves a mark on the substrate	
Sealing 2	0-max	aluminium	2	Sealing2a.txt, Sealing2b.txt	Suction cup leaves a mark on the substrate	
Sealing 3	0-max	1200 grid	2	Sealing3a.txt, Sealing3b.txt	Suction cup leaves a mark on the substrate	
Sealing 4	0-max	400 grid	2	Sealing4a.txt, Sealing4b.txt	Suction cup leaves a mark on the substrate	
Sealing 5	0-max	100 grid	2	Sealing5a.txt, Sealing5b.txt	Suction cup leaves a mark on the substrate	
Sealing 6	0-max	40 grid	2	Sealing6a.txt, Sealing6b.txt	none	
Sealing 7	0-max	sandblasted wood	2	Sealing7a.txt, Sealing7b.txt	none	
Sealing 8	0-max	textured paint	2	Sealing8a.txt, Sealing8b.txt	Surprisingly high pressure differential	
DV: Pressure differential						
Constants: Ambient temperature						
Requirements: Substrates, voltage datalogger						

2: The effect of a change in the maximum achievable pressure differential on the perpendicular and parallel pulling resistance						
Hypothesis: If the pressure differential increases the perpendicular and parallel pulling resistance increase as predicted by the theoretical model						
IV: Substrate roughness, pulling direction						
Experiment name	Pres. diff. (kPa)	Substrate	Pulling angle (°)	Trials	Files	Remarks
Resistance 1	max	glass	90	2	Resistance1a.txt, Resistance1b.txt	Suction cup leaves a mark on the substrate
Resistance 2	max	aluminium	90	2	Resistance2a.txt, Resistance2b.txt	Suction cup leaves a mark on the substrate

Appendix L: Experiment diagrams

Resistance 3	max	1200 grid	90	2	Resistance3a.txt, Resistance3b.txt	Suction cup leaves a mark on the substrate
Resistance 4	max	400 grid	90	2	Resistance4a.txt, Resistance4b.txt	Suction cup leaves a mark on the substrate
Resistance 5	max	100 grid	90	2	Resistance5a.txt, Resistance5b.txt	Suction cup leaves a mark on the substrate
Resistance 6	max	40 grid	90	2	Resistance6a.txt, Resistance6b.txt	none
Resistance 7	max	sandblasted wood	90	2	Resistance7a.txt, Resistance7b.txt	none
Resistance 8	max	textured paint	90	2	Resistance8a.txt, Resistance8b.txt	none
Resistance 9	max	glass	0	2	Resistance9a.txt, Resistance9b.txt	Silicon rubber on the rim wears off
Resistance 10	max	aluminium	0	2	Resistance10a.txt, Resistance10b.txt	Silicon rubber on the rim wears off
Resistance 11	max	1200 grid	0	2	Resistance11a.txt, Resistance11b.txt	Silicon rubber on the rim wears off, tear in the adhesion and friction pad
Resistance 12	max	400 grid	0	2	Resistance12a.txt, Resistance12b.txt	Silicon rubber on the rim wears off
Resistance 13	max	100 grid	0	2	Resistance13a.txt, Resistance13b.txt	Silicon rubber on the rim wears off
Resistance 14	max	40 grid	0	2	Resistance14a.txt, Resistance14b.txt	Silicon rubber on the rim wears off, device needs to be pushed on lightly to attach
Resistance 15	max	sandblasted wood	0	2	Resistance15a.txt, Resistance15b.txt	Silicon rubber on the rim wears off, device needs to be pushed on lightly to attach
Resistance 16	max	textured paint	0	2	Resistance16a.txt, Resistance16b.txt	Still surprisingly high pressure differential
DV: Pulling resistance, pressure differential						
Constants: Ambient conditions (temperature, humidity)						
Requirements: Substrates, voltage datalogger, tensile strength tester						

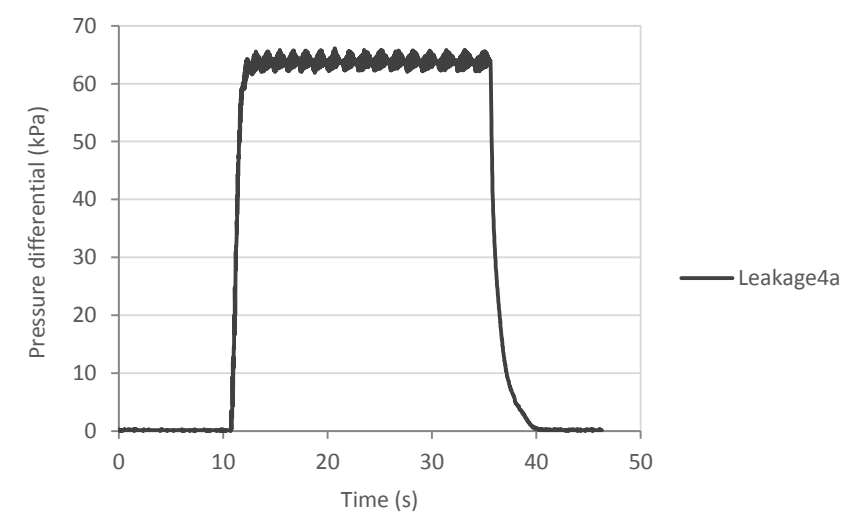
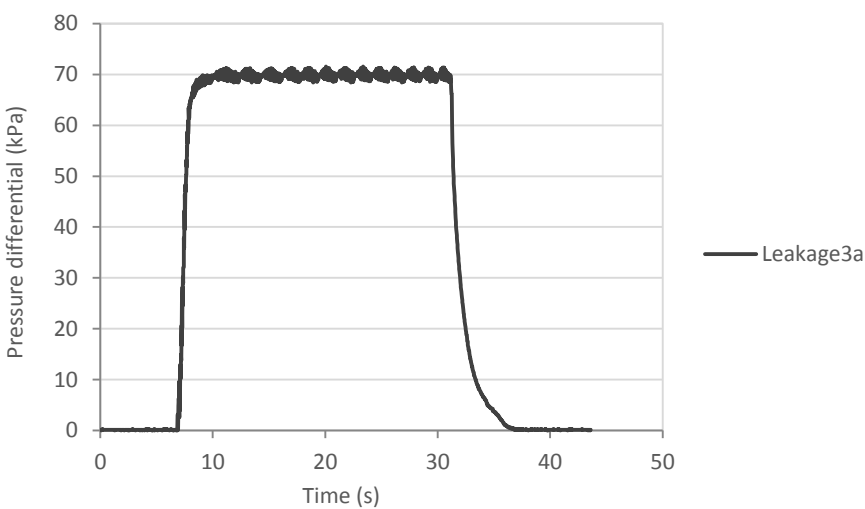
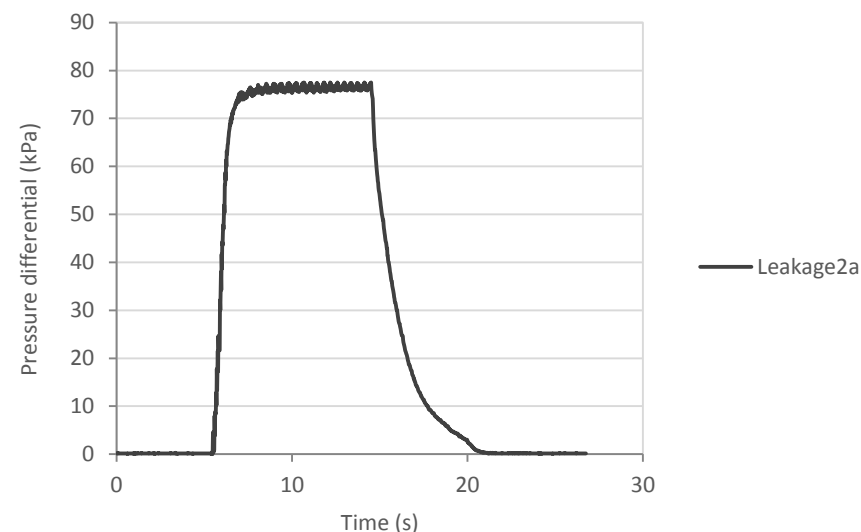
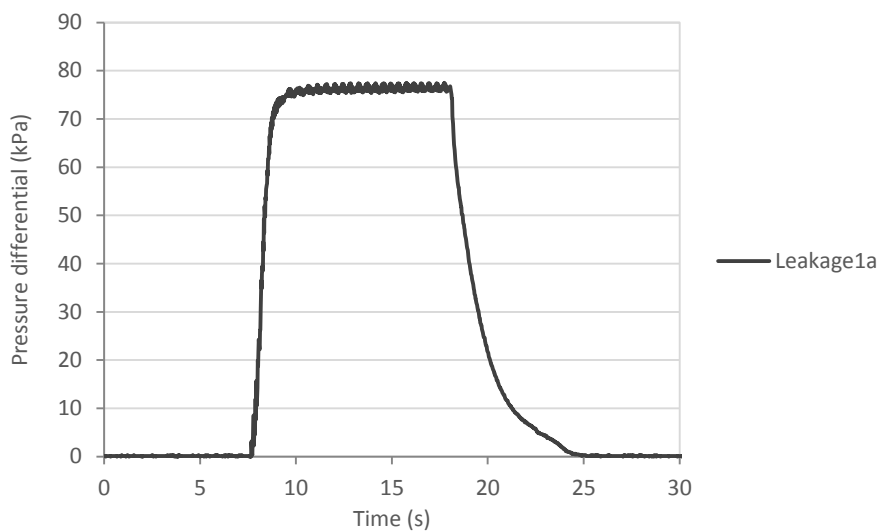
3: The effect of wear on the perpendicular and parallel pulling resistance

Hypothesis: When wear increases the perpendicular pulling resistance decreases and the parallel pulling resistance increases

Appendix L: Experiment diagrams

IV: Substrate roughness, pulling direction					
Experiment name	Pressure differential (kPa)	Substrate	Trials	Files	Remarks
Wear 1a	max	glass	1	Wear1a.txt	Performed after Resistance 8b
Wear 1b	max	glass	1	Wear1b.txt	Performed after Resistance 16b
Wear 2	max	glas	1	Wear2a.txt	Performed after Resistance 16b
DV: Pressure differential, pulling resistance					
Constants: Ambient conditions (temperature, humidity)					
Requirements: Substrates, voltage datalogger, tensile strength tester					

Appendix M: Pressure differential curves



Appendix M: Pressure differential curves

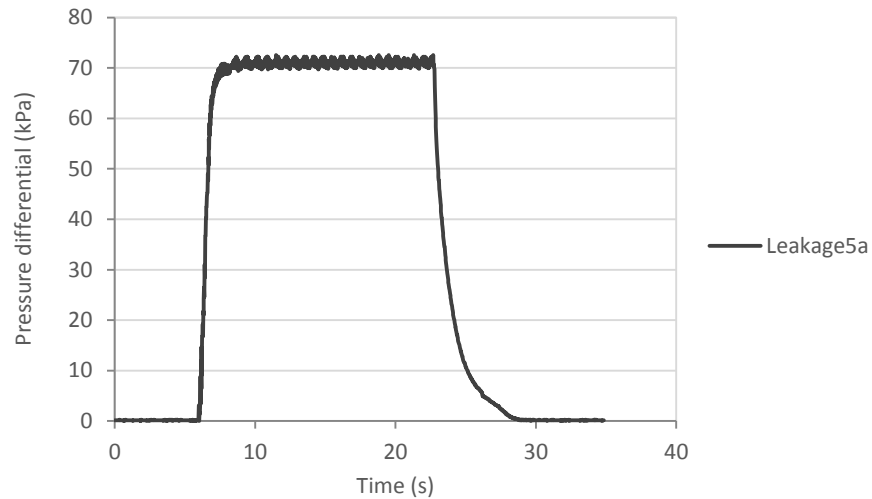


Figure 196 - Pressure differential curve on wood (100 grit).

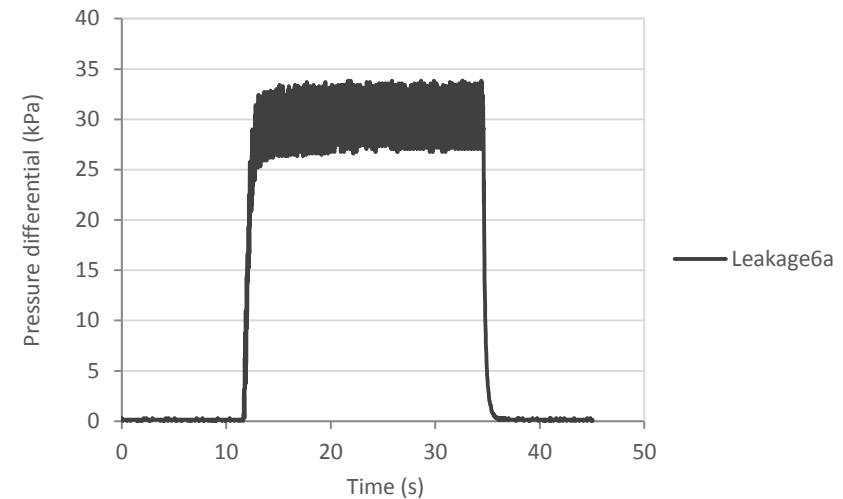


Figure 195 - Pressure differential curve on wood (40 grit).

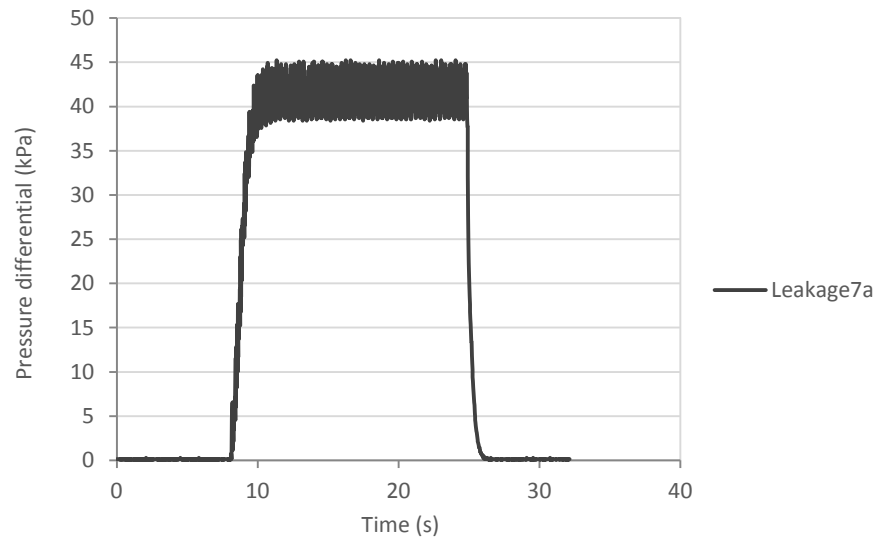


Figure 193 - Pressure differential curve on wood (sandblasted).

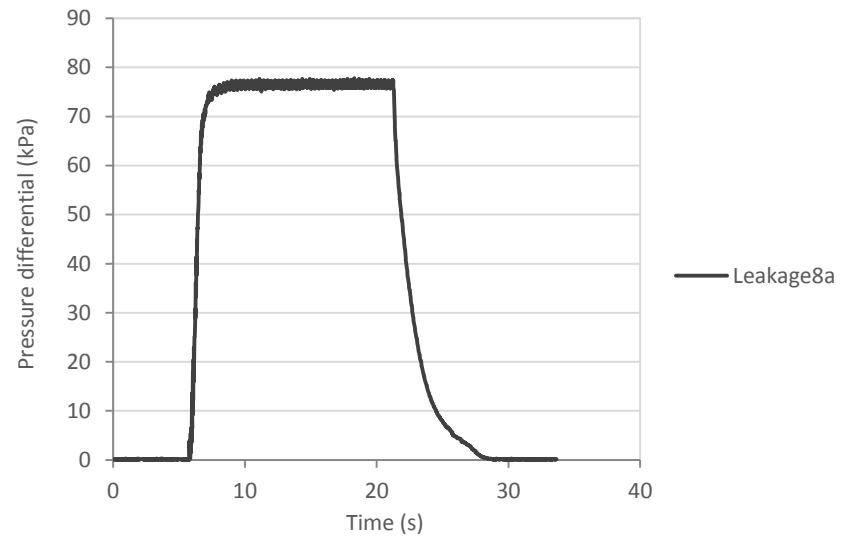


Figure 194 - Pressure differential curve on textured paint.

References

1. *10 stks 150mm jst mannelijke stekker voor rc lipo batterij deel nieuwe hv5n 2 p aansluiting voor.* (sd). Retrieved from [www.aliexpress.com](https://nl.aliexpress.com/item/10PCS-150mm-JST-Male-Connector-Plug-for-RC-Lipo-Battery-Part-New-hv5n-2P-connector/32474071169.html?spm=2114.010208.3.10.wdT6Lx&ws_ab_test=searchweb0_0,searchweb201602_3_10065_10068_10000009_10084_10083_10080_10082_10081_101): https://nl.aliexpress.com/item/10PCS-150mm-JST-Male-Connector-Plug-for-RC-Lipo-Battery-Part-New-hv5n-2P-connector/32474071169.html?spm=2114.010208.3.10.wdT6Lx&ws_ab_test=searchweb0_0,searchweb201602_3_10065_10068_10000009_10084_10083_10080_10082_10081_101
2. *1000' Reel (1/4 OD x 1/8 ID Polyurethane Tubing).* (sd). Retrieved from www.pneumadyne.com: <http://www.pneumadyne.com/1000-reel-polyurethane-tubing-p-3199.html#1-YToxOntzOjQ6ImdyYWQiO2k6MDt9>
3. *10PCS-150mm-JST-Male-Connector-Plug-for-RC-Lipo-Battery-Part-New-hv5n-2P-connector.* (sd). Retrieved from [www.aliexpress.com](https://nl.aliexpress.com/item/1PCS-LM2596T-5-0-5V-LM2596-TO-220-5-New-and-original/32560606270.html?spm=2114.010208.3.25.XT6YHz&ws_ab_test=searchweb0_0,searchweb201602_3_10065_10068_10000009_10084_10083_10080_10082_10081_10110_10111_10112_10060_10113_101): https://nl.aliexpress.com/item/1PCS-LM2596T-5-0-5V-LM2596-TO-220-5-New-and-original/32560606270.html?spm=2114.010208.3.25.XT6YHz&ws_ab_test=searchweb0_0,searchweb201602_3_10065_10068_10000009_10084_10083_10080_10082_10081_10110_10111_10112_10060_10113_101
4. *10pcs-250V-5A-3-Pin-Tact-Switch-Sensitive-Microswitch-Micro-Switches-Handle-KW11-3Z-Best-Price.* (sd). Retrieved from [www.aliexpress.com](https://nl.aliexpress.com/item/10pcs-250V-5A-3-Pin-Tact-Switch-Sensitive-Microswitch-Micro-Switches-Handle-KW11-3Z-Best-Price/32765174655.html?spm=2114.010208.3.163.G7SfnW&ws_ab_test=searchweb0_0,searchweb201602_3_10065_10068_10000009_10084_10083_10080_10): https://nl.aliexpress.com/item/10pcs-250V-5A-3-Pin-Tact-Switch-Sensitive-Microswitch-Micro-Switches-Handle-KW11-3Z-Best-Price/32765174655.html?spm=2114.010208.3.163.G7SfnW&ws_ab_test=searchweb0_0,searchweb201602_3_10065_10068_10000009_10084_10083_10080_10
5. *10PCS-6-6-5MM-SMD-Silent-push-button-switch-microswitch-Tact-Switch-Free-shipping.* (sd). Retrieved from [www.aliexpress.com](https://nl.aliexpress.com/item/10PCS-6-6-5MM-SMD-Silent-push-button-switch-microswitch-Tact-Switch-Free-shipping/32751670518.html?spm=2114.010208.3.261.apquZH&ws_ab_test=searchweb0_0,searchweb201602_3_10065_10068_10000009_10084_10083_10080_10082_10081_101): https://nl.aliexpress.com/item/10PCS-6-6-5MM-SMD-Silent-push-button-switch-microswitch-Tact-Switch-Free-shipping/32751670518.html?spm=2114.010208.3.261.apquZH&ws_ab_test=searchweb0_0,searchweb201602_3_10065_10068_10000009_10084_10083_10080_10082_10081_101
6. *14-6V1A-Charger-4S-14-6V-Smart-Lifepo4-Charger-12V-12-8V-Lifepo4-battery-Charger-Free.* (sd). Retrieved from [www.aliexpress.com](https://nl.aliexpress.com/item/14-6V1A-Charger-4S-14-6V-Smart-Lifepo4-Charger-12V-12-8V-Lifepo4-battery-Charger-Free/32764691612.html?spm=2114.010208.3.27.cdhw4y&ws_ab_test=searchweb0_0,searchweb201602_3_10065_10068_10000009_10084_10083_10080_10082_10081_): https://nl.aliexpress.com/item/14-6V1A-Charger-4S-14-6V-Smart-Lifepo4-Charger-12V-12-8V-Lifepo4-battery-Charger-Free/32764691612.html?spm=2114.010208.3.27.cdhw4y&ws_ab_test=searchweb0_0,searchweb201602_3_10065_10068_10000009_10084_10083_10080_10082_10081_
7. *1m x 10m x 6mm CORK ROLL UNDERLAY SHEET - THICKNESS 6 mm - 10 m2.* (sd). Retrieved from www.amazon.co.uk: www.amazon.co.uk/10m-CORK-ROLL-UNDERLAY-SHEET/dp/B00QN3M380
8. *2400mbar Pressure 17 L/M DC Electric Diaphragm Brushless Small Air Pump.* (sd). Retrieved from www.yanhuafaitn.en.made-in-china.com/: <http://www.yanhuafaitn.en.made-in-china.com/product/uBaJoTZYgSVU/China-2400mbar-Pressure-17-L-M-DC-Electric-Diaphragm-Brushless-Small-Air-Pump.html>
9. *2PCS-LOT-Phone-speaker-Tablet-PC-micro-speaker-1W8R-1015-10-15MM-thick-4mm.* (sd). Retrieved from [www.aliexpress.com](https://nl.aliexpress.com/item/2PCS-LOT-Phone-speaker-Tablet-PC-micro-speaker-1W8R-1015-10-15MM-thick-4mm/32776396222.html?spm=2114.010208.3.1.pfSe1l&ws_ab_test=searchweb0_0,searchweb201602_3_10065_10068_10000009_10084_10083_10080_10082_10081_10110_10111_): https://nl.aliexpress.com/item/2PCS-LOT-Phone-speaker-Tablet-PC-micro-speaker-1W8R-1015-10-15MM-thick-4mm/32776396222.html?spm=2114.010208.3.1.pfSe1l&ws_ab_test=searchweb0_0,searchweb201602_3_10065_10068_10000009_10084_10083_10080_10082_10081_10110_10111_
10. *3590 precision multi-turns wire wound rotary 50k 20k potentiometer.* (sd). Retrieved from [www.alibaba.com](https://www.alibaba.com/product-detail/3590-precision-multi-turns-wire-wound_266571109.html?spm=a2700.7724838.0.0.kdVIEE&s=p): https://www.alibaba.com/product-detail/3590-precision-multi-turns-wire-wound_266571109.html?spm=a2700.7724838.0.0.kdVIEE&s=p
11. *40PC015V2A.* (sd). Retrieved from [www.arrow.com](https://www.arrow.com/en/products/40pc015v2a/honeywell?gclid=CMvhskW8vdECFclp0wodKqEMBA): <https://www.arrow.com/en/products/40pc015v2a/honeywell?gclid=CMvhskW8vdECFclp0wodKqEMBA>
12. *55mm MINI SUCTION CUP PULLER.* (sd). Retrieved from [www.autopoweronline.co.uk](http://www.autopoweronline.co.uk/Product/rolson%202x%2042441-11/2-x-Mini-Suction-Cup-Dent-Puller-Imac-Apple-Screen-Remover-Tool-Glass): <http://www.autopoweronline.co.uk/Product/rolson%202x%2042441-11/2-x-Mini-Suction-Cup-Dent-Puller-Imac-Apple-Screen-Remover-Tool-Glass>
13. *5v 12v 24v dc to ac no output solid state relay.* (sd). Retrieved from [www.alibaba.com](https://www.alibaba.com/product-detail/5v-12v-24v-dc-to-ac_60421374729.html?spm=a2700.7724838.0.0.qo6JoL&s=p): https://www.alibaba.com/product-detail/5v-12v-24v-dc-to-ac_60421374729.html?spm=a2700.7724838.0.0.qo6JoL&s=p
14. *99.9% Pure Copper Cu Metal Sheet Plate 0.5mm*200mm*100mm.* (sd). Retrieved from [www.banggood.com](http://www.banggood.com/99_9-Pure-Copper-Cu-Metal-Sheet-Plate-0_5mm200mm100mm-p-999286.html): http://www.banggood.com/99_9-Pure-Copper-Cu-Metal-Sheet-Plate-0_5mm200mm100mm-p-999286.html
15. *Air Moisture Holding Capacity - SI Units.* (sd). Retrieved from [www.engineeringtoolbox.com](http://www.engineeringtoolbox.com/moisture-holding-capacity-air-d_281.html): http://www.engineeringtoolbox.com/moisture-holding-capacity-air-d_281.html
16. *Altitude above Sea Level and Air Pressure.* (sd). Retrieved from [www.engineeringtoolbox.com](http://www.engineeringtoolbox.com/air-altitude-pressure-d_462.html): http://www.engineeringtoolbox.com/air-altitude-pressure-d_462.html
17. *Aluminium 6061-t6.* (sd). Retrieved from [www.matweb.com](http://www.matweb.com/search/datasheet_print.aspx?matguid=1b8c06d0ca7c456694c7777d9e10be5b): http://www.matweb.com/search/datasheet_print.aspx?matguid=1b8c06d0ca7c456694c7777d9e10be5b
18. *Aluminium sales.* (sd). Retrieved from [www.ukaluminium.co.uk](http://www.ukaluminium.co.uk/http://www.ukaluminium.co.uk/aluminium-sheet-metal/uk-aluminium-sheet-metal-2000x1000x2-1050_H14.htm): http://www.ukaluminium.co.uk/http://www.ukaluminium.co.uk/aluminium-sheet-metal/uk-aluminium-sheet-metal-2000x1000x2-1050_H14.htm
19. *Ancistrus.* (2014, November 18). Retrieved from [www.aquariospeixescuidadoseespecies.blogspot.nl](http://aquariospeixescuidadoseespecies.blogspot.nl/http://aquariospeixescuidadoseespecies.blogspot.nl/2014/11/ancistrus.html): <http://aquariospeixescuidadoseespecies.blogspot.nl/http://aquariospeixescuidadoseespecies.blogspot.nl/2014/11/ancistrus.html>
20. Anver corporation. (sd). *Mechanical Vacuum Lifters – Save Energy while Increasing Productivity.* Retrieved from [www.anver.com](http://anver.com/vacuum-lifters/standard-mechanical-lifters/): <http://anver.com/vacuum-lifters/standard-mechanical-lifters/>
21. Arita, G. (1967). *A comparative study of the structure and function of the adhesive apparatus of the Cyclopteridae and Gobiesocidae.* Vancouver: The University of British Columbia .
22. *Armaceil Monarch® F-03991 (Gray) EPDM.* (sd). Retrieved from [www.matweb.com](http://www.matweb.com/search/datasheet.aspx?matguid=9648c09749774eb7ba01f810fa2d3571): <http://www.matweb.com/search/datasheet.aspx?matguid=9648c09749774eb7ba01f810fa2d3571>
23. *B110XP.* (sd). Retrieved from [www.piab.com](https://www.piab.com/en-US/products/suction-cups/shape/bellows/b---bellows-duraflex-10-110-mm0.4-4.5/b110xp/): <https://www.piab.com/en-US/products/suction-cups/shape/bellows/b---bellows-duraflex-10-110-mm0.4-4.5/b110xp/>
24. *Backyard Gardening Tools that work hard, keep gardening fun .* (sd). Retrieved from [www.indoorgardeningclub.com](http://indoorgardeningclub.com/product/backyard-gardening-tools-that-work-hard-keep-gardening-fun-ergonomic-soft-grip-handle-gardening-gifts-for-mom-best-3-piece-garden-tool-set-square-foot-garden-raised-bed-gardening-supplies-great/): <http://indoorgardeningclub.com/product/backyard-gardening-tools-that-work-hard-keep-gardening-fun-ergonomic-soft-grip-handle-gardening-gifts-for-mom-best-3-piece-garden-tool-set-square-foot-garden-raised-bed-gardening-supplies-great/>
25. Beardmore, R. (2013, January 17). *Coefficient of Friction .* Retrieved from [www.roymech.co.uk](http://www.roymech.co.uk/Useful_Tables/Tribology/co_of_frict.htm#method): http://www.roymech.co.uk/Useful_Tables/Tribology/co_of_frict.htm#method
26. *Beaufortia leveretti.* (sd). Retrieved from [www.nanofish.com.ua](http://www.nanofish.com.ua/http://www.nanofish.com.ua/bephortija-beaufortia-leveretti.html): <http://www.nanofish.com.ua/http://www.nanofish.com.ua/bephortija-beaufortia-leveretti.html>

References

27. Bernardes, P., de Andrade, N., Ferreira, S., Nataline de Sá, J., Araújo, E., Delatorre, D., & Luiz, L. (2010). Assessment of hydrophobicity and roughness of stainless steel adhered by an isolate of *Bacillus cereus* from a dairy plant. *Brazilian Journal of Microbiology*, 984-992.
28. *BF110P*. (sd). Retrieved from [www.piab.com: https://www.piab.com/en-US/products/suction-cups/shape/bellows/bf---bellows-flat-duraflex-80-110-mm3.3-4.5/bf110p/](https://www.piab.com/en-US/products/suction-cups/shape/bellows/bf---bellows-flat-duraflex-80-110-mm3.3-4.5/bf110p/)
29. Bing-shan, H., Li-wen, W., Zhuang, F., & Yan-zheng, Z. (2009). Bio-inspired Miniature Suction Cups Actuated by Shape Memory Alloy. *International Journal of Advanced Robotic Systems* 6 (3), 151-160.
30. ChamcPaper Group. (2013). *Technical Data Sheet: Brown cake s*.
31. Chaudhury, M. W. (1996). Adhesive contact of cylindrical lens and a flat sheet. *Journal of Applied Physics* 80 (1), 30-37.
32. *Cork, solid*. (sd). Retrieved from [www.aqua-calc.com: http://www.aqua-calc.com/page/density-table/substance/cork-coma-and-blank-solid](http://www.aqua-calc.com/page/density-table/substance/cork-coma-and-blank-solid)
33. *Cost Estimator*. (sd). Retrieved from [www.custompartnet.com: http://www.custompartnet.com/estimate/injection-molding/?low=1](http://www.custompartnet.com/estimate/injection-molding/?low=1)
34. *Cost Estimator 2*. (sd). Retrieved from [www.custompartnet.com: http://www.custompartnet.com/estimate/machining/](http://www.custompartnet.com/estimate/machining/)
35. *Costimator - Cost Modeler Online Demo*. (sd). Retrieved from [www.mtissystems.com: https://www.mtissystems.com/costmodels/Lasercut.php](https://www.mtissystems.com/costmodels/Lasercut.php)
36. Courard, L., Michel, F., & Martin, M. (2011). The evaluation of the surface free energy of liquids and solids in concrete technology. *Construction and Building Materials* 25, 260-266.
37. *custom e-paper design segment type,DKE-E-paper display Manufacturer,custom e-paper supply*. (sd). Retrieved from [www.alibaba.com: https://www.alibaba.com/product-detail/custom-e-paper-design-segment-type_60335424620.html](https://www.alibaba.com/product-detail/custom-e-paper-design-segment-type_60335424620.html)
38. De Vries, D. (2009). *Characterization of polymeric foams*. Eindhoven: Eindhoven University of Technology.
39. Defante, A., Burai, T., Becker, M., & Dhinojwala, A. (2015). Consequences of Water between Two Hydrophobic Surfaces on Adhesion and Wetting. *Langmuir* 15, 2398-2406.
40. Deng, Y., Van Acker, K., Dewulf, W., & Dufloy, J. (2011). Environmental Assessment of Printed Circuit Boards from Biobased Materials. *Proceedings of the 18th CIRP International Conference on Life Cycle Engineering* (pp. 605-610). Braunschweig: Technische Universität Braunschweig.
41. *Densities of materials*. (sd). Retrieved from [www.coolmagnetman.com: http://www.coolmagnetman.com/magconda.htm](http://www.coolmagnetman.com/magconda.htm)
42. Diederichsen, K., & Olsen, F. (2012). Qualification of a DP-Based FPSO Offloading Vessel. *Offshore Technology Conference* (pp. 1-34). Houston: Offshore Technology Conference.
43. Ditsche, P. (2015, March 19). *Clingy fish (or how to hold tight when it gets rough)*. Retrieved from www.depts.washington.edu: http://depts.washington.edu/fhl/tidebites/Vol19/
44. Ditsche, P., & Summers, A. (2014). Aquatic versus terrestrial attachment: Water makes a difference. *Beilstein Journal of Nanotechnology*, 2424-2439.
45. Ditsche, P., Wainwright, D., & Summers, A. (2014). Attachment to challenging substrates – fouling, roughness and limits of adhesion in the northern clingfish (*Gobiesox maeandricus*). *The Journal of Experimental Biology* 217, 2548-2554.
46. Donovan, D., & Taylor, H. (2008). Metabolic consequences of living in a wave-swept environment: Effects of simulated wave forces on oxygen consumption, heart rate, and activity of the shell adductor muscle of the abalone *Haliotis iris*. *Journal of Experimental Marine Biology and Ecology* 354, 231-240.
47. drive medical . (sd). *Suction Cup Grab Bar*. Retrieved from www.drivemedical.com: http://www.drivemedical.com/index.php/suction-cup-grab-bar-291.html
48. *Drive Suction Cup Grab Bar*. (sd). Retrieved from www.activeforever.com: https://www.activeforever.com/drive-suction-cup-grab-bar
49. *Durometer* Conversion Chart*. (sd). Retrieved from <http://mechanicalrubber.com: http://mechanicalrubber.com/elastomericolutions/wp-content/uploads/2013/08/Durometer-Conversion-Table.pdf>
50. Eck, B. (1988). *Technische Strömungslehre*. Springer.
51. ezmoves. (sd). *About us*. Retrieved from [www.ezmoves.com: https://ezmoves.com/about-us/](https://ezmoves.com: https://ezmoves.com/about-us/)
52. *F150*. (sd). Retrieved from [www.piab.com: https://www.piab.com/en-US/products/suction-cups/application/dry-sheet-metal/f---flat-15-300-mm0.6-11.8/f150/](https://www.piab.com/en-US/products/suction-cups/application/dry-sheet-metal/f---flat-15-300-mm0.6-11.8/f150/)
53. *F33 FCM*. (sd). Retrieved from [www.piab.com: https://www.piab.com/en-US/products/suction-cups/application/bag-openingthin-paper---slip-sheetsfilm/f33-fcm/](https://www.piab.com/en-US/products/suction-cups/application/bag-openingthin-paper---slip-sheetsfilm/f33-fcm/)
54. *FC100P*. (sd). Retrieved from [www.piab.com: https://www.piab.com/en-US/products/suction-cups/application/oily-sheet-metal/fcf---flat-concave-friction-25-125-mm1.0-4.9/fcf100p/](https://www.piab.com/en-US/products/suction-cups/application/oily-sheet-metal/fcf---flat-concave-friction-25-125-mm1.0-4.9/fcf100p/)
55. Feng, H., Dong, W., & Chai, N. (2014). A bionic micro sucker actuated by IPMC. *IEEE International Conference on Orange Technologies*. Xian.
56. Feng, H., Dong, W., & Chai, N. (2014). A bionic microsucker actuated by IPMC. *IEEE International Conference on Orange Technologies*, (pp. 223-226). Xian.
57. Follador, M., & Tramacere, F. (2014). Dielectric elastomer actuators for octopus inspired suction cups. *Bioinspiration & Biomimetics* 9, 046002.
58. Follador, M., Tramacere, F., & Mazzolai, B. (2014). Dielectric elastomer actuators for octopus inspired suction cups. *Bioinspiration & Biomimetics* 9, 046002.
59. Forearm Forklift Lifting Straps. (sd). *Product Description*. Retrieved from www.forearmforklift.com: http://www.forearmforklift.com/ForearmForkliftLiftingStraps.html
60. Forum Subsea Technologies. (sd). *ROV Suction Foot*.
61. *Free-Shipping-10PCS-LOT-atmega328p-au-atmega328p-atmega328-QFP32-In-stock-Best-price-High-quality-Hot*. (sd). Retrieved from [www.nl.aliexpress.com: https://nl.aliexpress.com/item/Free-Shipping-10PCS-LOT-atmega328p-au-atmega328p-atmega328-QFP32-In-stock-Best-price-High-quality-Hot/1560784229.html?isOrig=true#extend](https://nl.aliexpress.com: https://nl.aliexpress.com/item/Free-Shipping-10PCS-LOT-atmega328p-au-atmega328p-atmega328-QFP32-In-stock-Best-price-High-quality-Hot/1560784229.html?isOrig=true#extend)
62. *Free-Shipping-Interface-Base-Board-Serial-Transceiver-Bluetooth-Module-HC-05-06-For-Arduino-For-Sale*. (sd). Retrieved from [www.nl.aliexpress.com: https://nl.aliexpress.com/item/Free-Shipping-Interface-Base-Board-Serial-Transceiver-Bluetooth-Module-HC-05-06-For-Arduino-For-Sale/32322461982.html?spm=2114.010208.3.44.5ZuF1K&ws_a_b_test=searchweb0_0_searchweb201602_3_10065_10068_1000009_10084_10083_100](https://nl.aliexpress.com: https://nl.aliexpress.com/item/Free-Shipping-Interface-Base-Board-Serial-Transceiver-Bluetooth-Module-HC-05-06-For-Arduino-For-Sale/32322461982.html?spm=2114.010208.3.44.5ZuF1K&ws_a_b_test=searchweb0_0_searchweb201602_3_10065_10068_1000009_10084_10083_100)
63. (2009). *FRN Average Weights*. furniture re-use network.

References

64. Gazula, M., Sanchez, E., Gonzalez, J., Portillo, M., & Orduna, M. (2011). Relationship between certain ceramic roofing tile characteristics and biodeterioration. *Journal of the European Ceramic Society*, 2753-2761.
65. Grassberger, M., & Hoch, W. (2006). Ichthyotherapy as Alternative Treatment for Patients with Psoriasis: A Pilot Study. *Evidence-Based Complementary and Alternative Medicine* 3 (4), 483-488.
66. *Grip System Ergonomics & Product Information*. (sd). Retrieved from [www.gripsystem.com](http://www.gripsystem.com/ergonomics.htm): <http://www.gripsystem.com/ergonomics.htm>
67. *GRIPPEY snel en veilig tillen*. (2010, June 21). Retrieved from [www.youtube.com](https://www.youtube.com/watch?v=QROwysAyw8): <https://www.youtube.com/watch?v=QROwysAyw8>
68. Hamid, J. (2007, November 13). *Malaysia "fish" spa targets discreet Mideast women*. Retrieved from www.reuters.com: Malaysia "fish" spa targets discreet Mideast women/article/us-malaysia-spa-idUSKLR22007720071114
69. Harmon, K. (2011, April 12). *Octopuses and squids are damaged by noise pollution*. Retrieved from [blogs.scientificamerican.com](http://blogs.scientificamerican.com/observations/octopuses-and-squids-are-damaged-by-noise-pollution/): <https://blogs.scientificamerican.com/observations/octopuses-and-squids-are-damaged-by-noise-pollution/>
70. *HC-05 Bluetooth to UART converter COM serial communication master and slave mode*. (sd). Retrieved from www.amazon.com: <https://www.amazon.com/Bluetooth-converter-serial-communication-master/dp/B008AVPE6Q>
71. *HEAVY DUTY SUCTION CUP HOOK - bag of 3 or 6 (MULTI-COLORS)*. (sd). Retrieved from www.amazon.ca: https://www.amazon.ca/HEAVY-DUTY-SUCTION-CUP-HOOK/dp/B00H38RRHQ/ref=pd_sim_201_5?_encoding=UTF8&psc=1&refRID=GKBPED6B1QYJ6G524PA
72. *HONEYWELL 40PC015V2A*. (sd). Retrieved from [www.tme.eu](http://www.tme.eu/en/details/40pc015v2a/pressure-sensors/honeywell/): <http://www.tme.eu/en/details/40pc015v2a/pressure-sensors/honeywell/>
73. Hou, H., Wright, E., Bonser, R., & Jeronimidis, G. (2012). Development of Biomimetic Squid-Inspired Suckers. *Journal of Bionic Engineering* 9, 484-493.
74. *How to charge Lithium Iron Phosphate Rechargeable Lithium Ion Batteries*. (2016, December 12). Retrieved from www.powerstream.com: <http://www.powerstream.com/LLLF.htm>
75. Irschick, D., Austin, C., Petren, K., Fisher, R., Loson, J., & Ellers, O. c.-b. (1996). A comparative analysis of clinging ability among pad-bearing lizards. *Biological Journal of the Linnean Society* 59, 21-35.
76. Johnston, I., McCluskey, D., Tan, C., & Tracey, M. (2014). Mechanical characterization of bulk Sylgard 184 for microfluidics and microengineering. *Journal of Micromechanics and Microengineering* 24, 1-7.
77. Jones, W., & Demetropoulos, A. (1968). Exposure to wave action: measurements of an important ecological parameter on rocky shores on Anglesey. *Journal of Experimental Biology and Ecology*, 46-63.
78. *Journey's Edge Powerful Manual Multi Drain Plunger*. (sd). Retrieved from www.amazon.com: <https://www.amazon.com/Journeys-Edge-Powerful-Manual-Plunger/dp/B00008KJTM>
79. K.v.K. (sd). *Adressen downloaden*. Retrieved from www.kvk.nl: <https://www.kvk.nl/handelsregister/adressenbestand/>
80. Kayaoglu, B., & Öztürk, E. (2013). Imparting Hydrophobicity to Natural Leather through Plasma Polymerization for Easy Care Effect. *Fibers and Polymers* 14 (10), 1706-1713.
81. Kelly, K. (2009, November 20). *Kevin Kelly: Technology's epic story*. Retrieved from www.ted.com: https://www.ted.com/talks/kevin_kelly_tells_technology_s_epic_story#t-416520
82. Kendall, K. (1971). The adhesion and surface energy of elastic solids. *Journal of Applied Physics* 4 (8), 1186-1195.
83. Kessens, C., & Desai, J. (2010). Design, Fabrication, and Implementation of Self-sealing Suction Cup Arrays for Grasping. *International Conference on Robotics and Automation*, (pp. 765-770). Anchorage.
84. Kier, W., & Smith, A. (2002). The Structure and Adhesive Mechanism of Octopus Suckers. *Integrative and Comparative Biology* 42, 1146-1153.
85. Kilic, M., Hiziroglu, S., & Burdurlu, E. (2006). Effect of machining on surface roughness of wood. *Building and Environment* 41, 1074-1078.
86. King, D., Bartlett, M., Gilman, C., Irschick, D., & Crosby, A. (2014). Creating Gecko-Like Adhesives for "Real World" Surfaces. *Advanced materials* 26, 4345-4351.
87. Kinloch, A. (1987). *Adhesion and Adhesives*. Springer Science & Business Media.
88. Klappenbach, L. (2015, June 6). *11 Facts About Octopuses*. Opgeroepen op March 16, 2016, van <http://animals.about.com/od/molluscs/a/octopus-facts.htm>
89. *Klittenband 160 mm, HAAK - 25 m*. (sd). Retrieved from www.meubelstoffenvoordeel.nl: <https://www.meubelstoffenvoordeel.nl/benodigdheden-fournituren/klittenband-klitteband-velcro/klittenband-10-160mm-naaibaar/klittenband-160-mm-haak-25-meter.html>
90. *Klutch Heavy-Duty Dent Puller*. (sd). Retrieved from www.northerntool.com: <http://www.northerntool.com/shop/tools/NTEsearch?Ntx=mode%20matchallpartial&Ntk=All&storeId=6970&N=0&Ntt=dent%20puller%20tool>
91. Krofová, A., & M., M. (2015). Influence of dusty micro-particles contamination on adhesive bond strength. *Agronomy Research* 13(3), 654-661.
92. KS Machinebau. (sd). *KS Rob 180*. Retrieved from www.ksschulten.com: <http://www.ksschulten.com/en/products/lifting-technology-ks-robot/ks-rob-180.html>
93. *KW11-3Z 5A 250V touch switch*. (sd). Retrieved from www.meedstudio.com: <http://www.meedstudio.com/goods-510.html>
94. LeBlanc, R. (2009). *The Effect of Anodizing to Minimize Friction and Wear of Aluminum Surfaces*.
95. Leising, C. (2010, November 3). *Surface Roughness of Concrete*. Retrieved from www.concreteconstruction.net: <http://www.concreteconstruction.net/mergers-and-acquisitions/surface-roughness-of-concrete.aspx>
96. Leising, C. (sd). *Processed Leather Surface Finish Using 3D Profilometry*.
97. *LiFePO-IFR-18500-Rechargeable-Lithium-ion-3-2V-1000mAh-Battery-Cell-Flashlights-Batteries-Free-DHL*. (sd). Retrieved from www.nl.aliexpress.com: https://nl.aliexpress.com/item/LiFePO-IFR-18500-Rechargeable-Lithium-ion-3-2V-1000mAh-Battery-Cell-Flashlights-Batteries-Free-DHL/32270092814.html?spm=2114.010208.3.17.hKqXrG&ws_a_b_test=searchweb0_0_searchweb201602_3_10065_10068_1000009_10084_10083_10080

References

98. Liftmate. (sd). *Furniture and Appliance Mover Set*. Retrieved from www.liftmate.co.uk: <https://www.liftmate.co.uk/fml60-furniture-and-appliance-mover-set>
99. Lin, A., Brunner, R., Chen, P., Talke, F., & Meyers, M. (2009). Underwater adhesion of abalone: The role of van der Waals and capillary forces. *Acta Materialia* 59, 4178-4185.
100. *M4-x-16mm-Self-Tapping-Screws-Allen-Hex-Socket-Head-Cap-Stainless-Steel-50-pcs*. (sd). Retrieved from www.nl.aliexpress.com: <https://nl.aliexpress.com/item/M4-x-16mm-Self-Tapping-Screws-Allen-Hex-Socket-Head-Cap-Stainless-Steel-50-pcs/32409924079.html>
101. *M5 Threads (Straight Connector Fittings)*. (sd). Retrieved from www.pneumadyne.com: <http://www.pneumadyne.com/threads-straight-connector-fittings-p-2419.html#1-YToxOntzOjQ6ImdyYWQ6MDt9>
102. Ma, M. (2015, May 4). *Puget Sound's clingfish could inspire better medical devices, whale tags*. Retrieved from www.washington.edu: <http://www.washington.edu/news/2015/05/04/puget-sounds-clingfish-could-inspire-better-medical-devices-whale-tags/>
103. Massar, B. (2015). Scanning Electron Microscopy of Adhesive Apparatus of Garra lissorhynchus (McClelland) of Meghalaya, India. *International Research Journal of Biological Sciences*, 48-53.
104. Matziaris, K., M., S., & Karagiannis, G. (2011). Impregnation and superhydrophobicity of coated porous low-fired clay building materials. *Progress in Organic Coatings* 72, 181-192.
105. Meijer, M., Haemers, S., Cobben, W., & Holger, M. (2000). Surface Energy Determinations of Wood: Comparison of Methods and Wood Species. *Langmuir* 16, 9352-9359.
106. *Metals and Alloys - Densities*. (sd). Retrieved from www.engineeringtoolbox.com: http://www.engineeringtoolbox.com/metal-alloys-densities-d_50.html
107. Middlesworth, M. (sd). *A Step-by-Step Guide to Using the NIOSH Lifting Equation for Single Tasks*. Retrieved from ergo-plus.com: <http://ergo-plus.com/niosh-lifting-equation-single-task/>
108. Ministerie van Sociale Zeken en Werkgelegenheid. (sd). *Kou*. Retrieved from www.arboportaal.nl: <http://www.arboportaal.nl/onderwerpen/kou>
109. *Mommy's Helper 24-inch Safe-er-Grip*. (sd). Retrieved from www.overstock.com: <https://www.overstock.com/Baby/Mommys-Helper-24-inch-Safe-er-Grip/6162296/product.html>
110. Mondi. (2013). *Containerboard*. Vienna: Mondi Paper Sales GmbH.
111. *Monument MP1600 Toilet Plunger*. (sd). Retrieved from www.dibranto.co.uk: <https://www.dibranto.co.uk/Monument-MP1600-Toilet-Plunger-pid-191970-pType-Product>
112. Moutinho, I., Kleen, A., Figueiredo, M., & Ferreira, P. (2009). Effect of surface sizing on the surface chemistry of paper containing eucalyptus pulp. *Holzforschung* 63, 282-289.
113. *Não há nada mais português do que o Desenrascanço*. (sd). Retrieved from www.imgur.com: <https://imgur.com/mA2nnTt>
114. *NATURAL LINEN FABRIC 150 G/M2*. (sd). Retrieved from www.linetales.com: <https://www.linetales.com/en/fabrics/natural/natural-linen-fabric-150-g-m2.html>
115. *NEW Piab piGRIP FLI-F Foam Suction Cup*. (sd). Retrieved from www.pneumatics.com.au: <http://www.pneumatics.com.au/index.php/news-sp-1901875887/pneumatic-products-enews/205-pneumatic-products-australia-enews-august-2012>
116. *Octopus vulgaris*. (2011, October 18). Retrieved from jumbhoanimal.blogspot.nl: <http://jumbhoanimal.blogspot.nl/2011/10/octopus-vulgaris.html>
117. *O-Ring, 4,00x1,80 mm, NBR (70A)*. (sd). Retrieved from www.landefeld.de: <https://www.landefeld.de/artikel/de/o-ring-400x180-mm-nbr-70a-/OR+4X1,8+N>
118. Palchesko, R., Zhang, L., Sun, Y., & Feinberg, A. (2012). Development of Polydimethylsiloxane Substrates with Tunable Elastic Modulus to Study Cell Mechanobiology in Muscle and Nerve. *PLoS ONE* 7 (12), e51499.
119. *Panda Garra for Sale*. (sd). Retrieved from www.aquariumfish.net: http://www.aquariumfish.net/catalog_pages/wild/panda_garra_for_sale.htm
120. Paskewicz, J., & Fathalla, F. (2007). Effectiveness of a manual furniture handling device in reducing low back disorders risk factors. *International Journal of Industrial Ergonomics* 37, 93-102.
121. Patkin, M. (2001). A Check-List for Handle Design. *Ergonomics Australia On-Line*, 15.
122. Piab. (sd). *piSAVE sense*. Retrieved from www.piab.com: <https://www.piab.com/Products/system-accessories/energy-saving/pisave-sense/>
123. Piab. (sd). *Suction cups*. Retrieved from www.piab.com: <https://www.piab.com/Products/suction-cups/>
124. *piGRIP®*. (sd). Retrieved from www.piab.com: <https://www.piab.com/en-US/products/suction-cups/shape/flat-concave/pigrip-configurable-suction-cups/pigrip/>
125. *piSAVE™ sense*. (sd). Retrieved from www.piab.com: <https://www.piab.com/Products/suction-cups/suction-cup-accessories/suction-cup-valves/pisave-sense/>
126. Poling, B., Prausnitz, J., & O'Connell, J. (2000). *The Properties of Gases and Liquids 5th edition*. McGraw-Hill Education.
127. *Pollards Removals*. (sd). Retrieved from www.yellowpages.com.au: <https://www.yellowpages.com.au/nsw/goulburn/pollards-removals-15767667-listing.html>
128. Pro Suction Hooks. (sd). *Instructions*. Retrieved from www.prosuctionhooks.com: <http://www.prosuctionhooks.com/instructions.html>
129. *Product overview*. (sd). Retrieved from www.uk.farnell.com: <http://uk.farnell.com/atmel/atmega328p-mcu-8bit-atmega-20mhz-qfn-32/dp/1748522>
130. Quintanilla, J. (1999). Microstructure and Properties of Random Heterogeneous Materials: a Review of Theoretical Results. *Polymer Engineering and Science* 39 (3), 559-585.
131. R., K. (2005, February 25). *The accelerating power of technology*. Retrieved from www.ted.com: http://www.ted.com/talks/ray_kurzweil_on_how_technology_will_transform_us?language=en
132. Raghaven, V. (2014, August 1). *Acrylics on Plastics*. Retrieved from www.justpaint.org: <http://www.justpaint.org/acrylics-on-plastics/>
133. *Reacher Grabber by VIVE - Suction Cup Grip - 32" Heavy Duty Mobility Aid - Tool for Light Bulb Remover, iPad Pick Up, Litter Picker, Trash / Garbage, Garden Nabber, Long Extender*. (sd). Retrieved from www.amazon.com: <https://www.amazon.com/Reacher-Grabber-VIVE-Mobility-Extender/dp/B00047ILVA>
134. Reuss, B. (2011, July 14). *Convert Durometer to Young's Modulus*. Retrieved from www.3dvision.com:

References

- <https://www.3dvision.com/blog/entry/2011/07/14/convert-durometer-to-youngs-modulus.html>
135. Rich, S. (2015, December 17). *How to find the adhesion of a gecko using JKR Theory*. Retrieved from [www.youtube.com: https://www.youtube.com/watch?v=c3q3RrTVE00](http://www.youtube.com/watch?v=c3q3RrTVE00)
136. Rutkowski, G. (2014). Numerical analysis of the contact forces generated on a "Hiload DP1" prototype attachment system at calm sea. *TransNav 8 (4)*, 505-512.
137. Rutkowski, G. (2014). Numerical analysis of the contact forces generated on a "Hiload DP1" prototype attachment system at calm sea. *TransNav 8 (4)*, 505-512.
138. Sandberg, M., Sattari, A., & Mattsson, M. (2013). Plaster finishes in historical buildings - measurements of surface structure, roughness parameters and air flow characteristics. *European Workshop on Cultural Heritage Preservation*, (pp. 69-76).
139. SANO. (sd). *The extremely fast and light powered stairclimber for loads up to 170 kg*. Retrieved from [www.sano-stairclimbers.com: http://www.sano-stairclimbers.com/en/liftkar-sal](http://www.sano-stairclimbers.com/en/liftkar-sal)
140. Scandinavian pulp, paper and board committee. (2002). *Air permeance*.
141. Shoulder Dolly. (sd). *Shoulder Dolly*. Retrieved from <http://www.shoulderdolly.com/>: <http://www.shoulderdolly.com/shop/shoulder-dolly-moving-straps/>
142. Sickler, D. (sd). *Water-based Alchemy*. Retrieved from www.dundean.com: http://www.dundean.com/tips_what_is_latex_paint.shtml
143. *siliconen schuim 12mm (100cm)*. (sd). Retrieved from www.rubbermagazijn.nl: http://www.rubbermagazijn.nl/collectie/celrubber/siliconen-schuimplaat/6723_wit_siliconen-schuim-12mm-100cm.html
144. Silva, G., Cauwenberghs, G., & Khraiche, M. (sd). *Validation testing of polyimide prototypes*. Retrieved from [www.beweb.ucsd.edu](http://beweb.ucsd.edu): http://beweb.ucsd.edu/courses/senior-design/projects/2011/project_12/Preliminary_Results.html
145. Silverstein, B., & Adams, D. (2007). *Work-related Musculoskeletal Disorders of the Neck, Back, and Upper Extremity in Washington State, 1997-2005*. Washington State Department of Labor and Industries.
146. Smith, A. (1996). Cephalopod sucker design and the physical limits to negative pressure. *The Journal of Experimental Biology*, 949-958.
147. Snakenborg, D., & Kutter, J. (2004). Microstructure fabrication with a CO2 laser system. *Journal of Micromechanics and Microengineering 14*, 182-189.
148. Stairmobil. (sd). *De Stairmobil, de krachtigste en veelzijdigste in zijn soort*. Retrieved from www.stairmobil.nl: http://www.stairmobil.nl/?page_id=6
149. *Standard PCB*. (sd). Retrieved from www.pcbcart.com: <http://www.pcbcart.com/quote>
150. *Store:Shenzhen Yanhua Faith Technology Co., Ltd.* (sd). Retrieved from www.nl.aliexpress.com: <https://nl.aliexpress.com/store/508843>
151. *THINGS WE LIKE TO DO IN HERMANUS: ABAGOLD – ABALONE FARM*. (2014, February 19). Retrieved from www.burgundyhermanusblog.wordpress.com: <https://burgundyhermanusblog.wordpress.com/2014/02/19/things-we-like-to-do-in-hermanus-abagold-abalone-farm/>
152. Tietbohl, M. (2014). *Fishes that suck: comparison of the adhesive discs of three fishes of the Pacific Northwest*. Friday Harbor Laboratories Student Research Papers.
153. Tiller. (sd). *LM75 Hefmobiel Original 09*. Retrieved from www.tiller.eu: <http://www.tiller.eu/lm75.html>
154. Tramacere, F., Follador, M., Pugno, N., & Mazzolai, B. (2015). Octopus-like suction cups: from natural to artificial solutions. *Bioinspiration & Biomimetics 10*, 035004.
155. Tramacere, F., Follador, M., Pugno, N., & Mazzolai, B. (2015). Octopus-like suction cups: from natural to artificial solutions. *Bioinspiration & Biomimetics 10*, 035004.
156. Tramacere, F., Kovalev, A., Kleintech, T., Gorb, S., & Mazzolai, B. (2013). Structure and mechanical properties of Octopus vulgaris suckers. *Journal of Royal Society Interface 11*, 20130816.
157. Tramacere, F., Pugno, N., Kuba, M., & Mazzolai, B. (2015). Unveiling the morphology of the acetabulum in octopus suckers and its role in attachment. *Interface focus 5*, 20140050.
158. *Tri-base Suction Cup Mount*. (sd). Retrieved from <http://freedom360.us/>: <http://freedom360.us/shop/tri-base-suction-cup-mount/>
159. Umrath, W. (2007, June). *Fundamental of Vacuum Technology*. Cologne.
160. *Un pez escalador*. (sd). Retrieved from www.ciprogress.wordpress.com: <https://ciprogress.wordpress.com/2014/04/22/un-pezes-escalador/>
161. Upcart. (sd). *The UpCart is a stair climbing folding hand cart like no other*. Retrieved from upcart.com: <https://upcart.com/>
162. Wagner, W. (2012). *Strömung und Druckverlust (Kamprath-Reihe)*. Vogel Business Media.
163. Wainwright, D., Kleintech, T., Kleintech, A., Gorb, S., & Summers, A. (2013). Stick tight: suction adhesion on irregular surfaces in the northern clingfish. *Biology Letters 9*, 2130234.
164. Wang, Z. (2011). *Polydimethylsiloxane Mechanical Properties Measured by Macroscopic Compression and Nanoindentation Techniques*. Tampa: University of South Florida.
165. Weisburger, J. (2016, April 6). *Abalone diving season is off to a hazardous start in California*. Retrieved from [www.boingboing.net](http://boingboing.net): <http://boingboing.net/2016/04/06/dangerous-start-to-california.html>
166. Wu, N. (sd). *Welcome*. Retrieved from www.norbertwu.com: http://www.norbertwu.com/nwp/subjects/octopus_bonniers/gallery-01.html
167. *XLf*. (sd). Retrieved from www.piab.com: <https://www.piab.com/en-US/products/suction-cups/application/glass-handling/xlf---extra-large-flat-150-300-mm5.9-11.8/xlf/>